Oxidative Stress Biomarkers in Dementia

By

Stuart James Bennett

A thesis submitted to the
School of Sport and Exercise Sciences
The University of Birmingham
For the degree of
DOCTOR OF PHILOSOPHY

School of Sport and Exercise Sciences
The University of Birmingham
United Kingdom
October 2010

Abstract

Alzheimer's disease (AD) is a devastating neurodegenerative disorder which is thought to affect 26.6 million individuals worldwide. There is growing concern over a worldwide dementia epidemic that is predicted to develop over the coming decades. The evidence thus far suggests that increased levels of oxidative stress and vascular risk factors are two major contributors, amongst others, to AD development.

The thesis aimed to investigate markers of oxidative stress in AD plasma. Moreover, the oxidative status of specific proteins was investigated using both hypothesis driven and proteomic approaches. Results presented in this thesis suggest that global plasma protein oxidation levels are not different when AD and control subjects are compared, but that individual plasma proteins are specific targets for oxidative modification in AD. The thesis explores different methodologies to assess oxidative changes in AD. In addition it demonstrates that emerging novel and powerful mass spectrometry techniques can be employed successfully to identify several proteins modified by oxidation, providing an initial starting point for further investigation.

Acknowledgements

I would like to begin my acknowledgements by thanking my Mum, Dad, brother Paul and family, whom without their constant love and support I would not have been in the privileged position to undertake and complete my PhD research, as well as achieve what I have so far in my life.

To my supervisors Sarah and Mel, the last three years have been a challenging but enjoyable learning experience for me and I thank you for your expert advice, guidance and help during this time.

I would also like to thank my fellow PhD students and friends especially Andrew Cooke, Leigh Breen, James Turner, Pete Rouse, Mark Holland and the Birmingham University Triathlon Club members who made this period of study most enjoyable. Also my thanks go to Dr Andrew Creese and Mr Andrew Jones for their technical assistance on some of the studies.

List of publications

Published original articles (Thesis)

Bennett,S., Grant,M.M., and Aldred,S. (2009). Oxidative Stress in Vascular Dementia and Alzheimer's Disease: A Common Pathology. J. Alzheimers Dis. Jun; 17(2):245-57.

Aldred,S., **Bennett,S.,** and Mecocci,P. (2010). Increased low-density lipoprotein oxidation, but not total plasma protein oxidation, in Alzheimer's disease. Clin. Biochem. Feb;43(3):267-71.

Conference proceedings

Aldred,S., **Bennett,S.,** and Mecocci,P. Increased low-density lipoprotein oxidation, but not total plasma protein oxidation, in Alzheimer's disease. Biochemical Society Focussed Meeting: Bioanalysis of Oxidative Stress.

Bennett,S., and Aldred,S. Plasma proteins are specifically oxidized in Alzheimer's disease. The 3rd International Symposium of Nutrition, Oxygen Biology and Medicine, Paris, France.

List of Abbreviations

µg	microgram/s
µl	micro litre/s
µmol	micromole/s
1-DE	One dimensional gel electrophoresis
2-DE	Two dimensional gel electrophoresis
2-DG	Two dimensional gel
AAPH	azo-bis dihydrochloride
AD	Alzheimer's disease
ATP	Adenosine triphosphate
BCA	Bicinchoninic acid
BSA	Bovine serum albumin
ddH_2O	Double distilled water
DNA	Deoxyribonucleic acid
DNP	Dinitrophenyl
DNPH	Dinitrophenylhydrazine
DTT	Dithiothreitol
ECL	Enhanced chemiluminescence
EDTA	Ethylenediaminetetraacetic acid
ELISA	Enzyme linked immunosorbent assay
FRAP	Ferric reducing ability of plasma
HPLC	High performance liquid chromatography
HRP	Horseradish peroxidase
IEF	Isoelectric focusing
IgG	Immunoglobulin G
IP	Immunoprecipitation
IPG	Immobilized pH gradient
LC	Liquid chromatography
mA	milliamp
mg	milligram/s
ml	milli litre/s

mmol	millimole/s
MnSOD	Manganese Superoxide Dismutase
MS	Mass spectrometry
MS/MS	Tandem mass spectrometry
n	number of participants
nmol	nanomole/s
NED	*N*-(1-naphthyl) ethylendiamine dihydrochloride
OPD	O-phenylenediamine
OSA	octanesulfonic acid
PAGE	Polyacrylamide gel electrophoresis
PVDF	Polyvinylidene fluoride
RNA	Ribonucleic acid
RPM	Revolutions per minute
SCX	Strong cation chromatography
SD	Standard deviation
SDS	Sodium dodecyl sulfate
TAC	Total antioxidant capacity
TBS	Tris buffed saline
TBST	Tris buffed saline with Tween 20
TCA	Trichloroacetic acid
TG	Tris-glycine
TGS	Tris-glycine SDS
TPZ	Tris (2-pyridyl)-S-triazine
V	Voltage

Table of Contents

List of tables

List of figures

Chapter 1

General Introduction

1.1 Alzheimer's disease

The most common form of dementia is Alzheimer's disease (AD): a devastating neurodegenerative disorder which affects the brain. This devastating disease typically leaves sufferers exhibiting severe memory deficits and having difficulty performing everyday tasks. As people are living longer, and the population is becoming more elderly, the prevalence of AD is predicted to increase dramatically, thus causing an increased burden to society. Alarmingly, in 2006 it was reported that 26.6 million individuals were suffering from AD worldwide, and predicted that this figure would increase to 106.2 million by 2050 worldwide (Brookmeyer et al., 2007).

1.2 Neuropathological hallmarks of AD

It has been over 100 years since the first case of AD was reported in 1907 (Alzheimer, 1907; Alzheimer et al., 1995; Burns et al., 2002), yet it still remains true that definitive AD diagnosis is only possible by assessing the neuropathological hallmarks post-mortem. Extracellular senile plaques, which comprise mainly amyloid-β (Aβ) peptide, and intracellular hyper-phosphorylated tau (τ) are the two major brain pathologies associated with AD (Katzman and Saitoh, 1991; Selkoe, 2001). In general, Aβ is considered to play an important role in the development of AD and this is mainly based on early genetic experiments which pointed to abnormal mutations in the amyloid precursor protein (APP) as being responsible for the increased deposition of Aβ in AD brain (Hardy and Selkoe, 2002; Butterfield et al., 2001).

The toxic Aβ peptide evident in AD is generated during the abnormal proteolytic processing of the APP; this is commonly referred to as the amyloidogenic pathway (see figure 1.1) and

two major forms of the peptide are produced, Aβ40 and Aβ42, the latter being the most toxic form (Cole and Vassar, 2008). During this process APP is cleaved by the β-secretase enzyme (BACE1) to produce a N terminal Aβ fragment, APPsβ and a C terminal fragment named C99 (Cole and Vassar, 2008). Cleavage of this C99 fragment by the γ-secretase enzyme produces an APP intracellular domain (AICD) and Aβ peptides of various lengths, which include Aβ40 and Aβ42. On the other hand, APP processing can follow a non-amyloidogenic pathway (see figure 1.1) where it is cleaved by the enzyme α-secretase to produce an APPsα and C terminal fragment of 83 residues, as subsequent γ-secretase processing generates a p3 fragment and an AICD (Cole and Vassar, 2008). It is likely that Aβ serves an important physiological role under normal conditions, given that the peptide is produced by various cell types and is conserved between species (Moreira et al., 2007). Indeed, secreted forms of APP (APPs) have been shown to promote neuronal cell survival, aid the migration and differentiation of neurons, and protect neurons against oxidative challenges (Araki et al., 1991; Goodman and Mattson, 1994; Mattson, 1997).

The second characteristic neuropathology associated with AD is the presence of paired helical filaments which are formed mainly of the hyperphosphorylated form of the microtubule associated protein τ, and commonly referred to as neurofibrillary tangles. Early work revealed levels of abnormally phosphorylated τ to be elevated in AD brain tissue compared to normally aged controls (Khatoon et al., 1992), with this increase being a likely cause of microtubule breakdown evident in AD (Alonso et al., 1994) leading to this 'tangle' like pathology. The microtubule system is an important network along which material can be transported within nerve cells, impairment or damage to this system can ultimately lead to cell death.

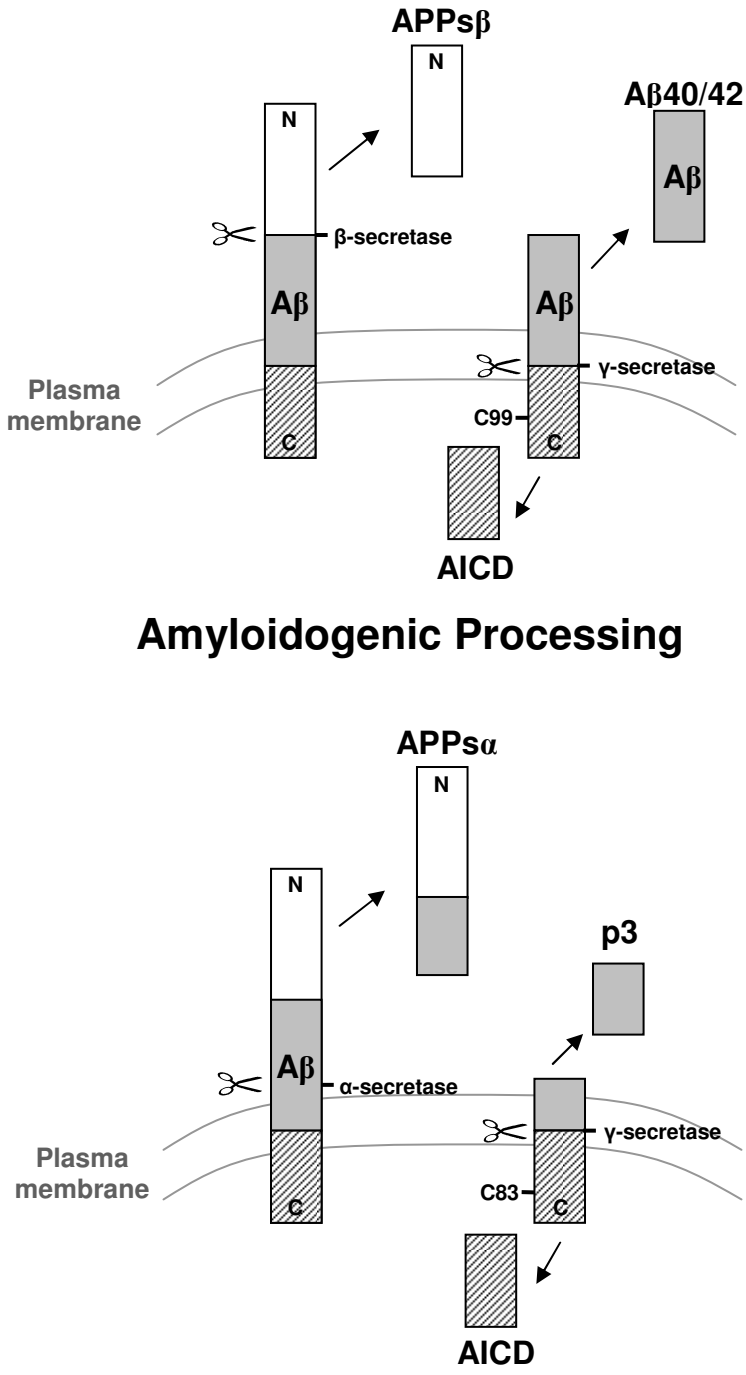

Figure 1.1. Proteolytic processing of APP. Diagram is based on that of Mattson (2004) and Cole and Vassar (2008) and describes the amyloidogenic (top) and non-amyloidogenic (bottom) pathways of APP processing.

Several hypotheses have been proposed to contribute to AD and these include the amyloid (Hardy and Selkoe, 2002), vascular (de la Torre, 2002), inflammatory (Akiyama et al., 2000) and oxidative stress hypotheses (Markesbery, 1997). The oxidative stress hypothesis will be the focus of this thesis.

1.3 Reactive Oxygen Species (ROS), Antioxidants and Oxidative stress

Free radicals (FR) are molecules which possess at least one unpaired electron in their outer shell, and therefore they are highly reactive as they desire further electrons from other molecules for their stability. Reactive oxygen species (ROS) is a term used to describe reactive forms of oxygen, as well as FR which are derived from oxygen. Examples of ROS include the superoxide anion ($O_2^{\bullet -}$), hydroxyl radical ($OH^{\bullet}$), peroxynitrite ($ONOO^-$) and hydrogen peroxide (H_2O_2). H_2O_2 is classed as a reactive form of oxygen and not a FR as it does not possess an unpaired electron (Finaud et al., 2006).

Production of ROS occurs during energy metabolism reactions which routinely take place in the cell. Specific sites for ROS generation include the mitochondria and peroxisomes (Beckman and Ames, 1998). In addition they are produced by neutrophils and macrophages as a protective mechanism against foreign material, which is commonly referred to as the respiratory or oxidative burst (Bedard and Krause, 2007). Historically, these unstable and highly reactive biological molecules were believed to have a detrimental effect on cellular components. However, it has become apparent that they also have an important role in cell signalling as they can induce various biological processes (e.g., cell growth and cell apoptosis) by acting as secondary messengers and through stimulation of protein phosphorylation and transcription factors (Suzuki et al., 1997).

Antioxidants were elegantly defined by Barry Halliwell and John Gutteridge, as 'a substance, that when present at low concentrations compared to those of an oxidizable substrate, significantly delays, or prevents oxidation of that substrate' (Halliwell and Gutteridge, 1989). The body has an extensive and complex enzymatic antioxidant defence system in place to neutralise ROS. The enzymatic antioxidant system includes superoxide dismutase (SOD), catalase (CAT) and glutathione peroxidase (GPx). These proteins provide a means of breaking down radical species into less harmful products. SOD promotes the dismutation of the superoxide radical to hydrogen peroxide which can then be converted to water by either CAT or GPx (Finkel and Holbrook, 2000). In addition to this, non-enzymatic antioxidants derived from fruit and vegetables can add to these defences (Sies, 1997; Beckman and Ames, 1998). They are able to scavenge free radicals and can be divided into lipid soluble (e.g., α-tocopherol, carotenoids and flavonoids) and water soluble based molecules (e.g., glutathione, uric acid and ascorbic acid). In situations where these antioxidant defences become depleted or overwhelmed by ROS a state of 'oxidative stress' can occur (Sies, 1997), and if prolonged and sustained, oxidative damage to proteins, lipids and DNA can ensue.

1.4 General indices of oxidative stress

1.4.1 Protein oxidation

Proteins are highly susceptible to free radical insults, and such events can lead to irreversible oxidative modification. However, mildly oxidized proteins are degraded and removed from cells via the proteasome, and enzymes (e.g., methionine sulfoxide reductases, thioredoxin and glutathione reductases) have evolved which reduce oxidized methionine and cysteine returning them to their native state (Berlett and Stadtman, 1997). Free radicals can oxidize a protein's backbone and the side chains of particular amino acids (e.g., lysine, arginine,

proline, tyrosine, tryptophan and threonine), as well as induce protein fragmentation. In all of these instances carbonyl groups (C=O) may be introduced into the protein's structure. In addition the reaction of proteins with aldehyde compounds produced by lipid peroxidation (e.g., 4-hydroxynonenal (4-HNE) and malonaldehyde (MDA)) can lead to carbonyl formation (Berlett and Stadtman, 1997). As a consequence protein carbonyl groups are considered to be an index of protein oxidation. Since Levine and colleagues (1994) demonstrated that protein carbonyl groups could be derivatized with 2, 4-dinitrophenylhydrazine (2, 4-DNPH) to form a 2,4-dinitrophenyl group, which could be detected by the use of a specific antibody (i.e. anti-DNP), enzyme-linked immunosorbent assay (ELISA) and Western blotting has been used to provide a quantitative and qualitative measurement of protein oxidation respectively (Shacter et al., 1994; Aldred et al., 2004).

1.4.2 Protein nitration

Peroxynitrite ($ONOO^-$) is a highly potent reactive nitrogen species (RNS) formed during the reaction between nitric oxide ($NO^\bullet$) and $O_2^{\bullet-}$. In addition to oxidizing proteins $ONOO^-$ has the ability to nitrate proteins: a nitro group ($-NO_2$) replaces a hydrogen atom at the 3' position of a tyrosine residue, forming a 3-nitrotyrosine adduct (Souza et al., 2008). This post translational modification can impact protein function; in renal allografts the enzyme MnSOD exhibits increased nitration in parallel with a reduction in its activity (Millan-Crow et al., 1996). Additionally, the presence of 3-nitrotyrosine on tyrosine residues prevents their phosphorylation by tyrosine kinases. This has an impact on signalling pathways mediated by tyrosine kinases, such as brain derived neurotrophic factor (BDNF) and nerve growth factor (NGF) resulting in possible cell apoptosis (Berlett and Stadtman, 1997; Mangialasche et al., 2009). Quantification of this modification is typically measured using high performance

liquid chromatography with electrochemical detection (HPLC-ECD), although ELISA and Western blotting using a 3-nitrotyrosine antibody is also frequently used (Duncan, 2003).

1.4.3 Lipid peroxidation

Polyunsaturated fatty acids (PUFA) are components of cell membranes which are highly susceptible to oxidative damage by free radicals: such damage is referred to as free radical-mediated lipid peroxidation (LPO) (Buettner, 1993; Niki, 2009). The initial step of LPO involves the free radical-mediated abstraction of hydrogen atoms from PUFA to form lipid radicals which react with molecular oxygen to form the highly reactive peroxyl radical. This extremely unstable species can further oxidize lipids to produce new lipid radicals and thereby propagate a chain reaction (Buettner, 1993; Niki, 2009). LPO can be terminated if lipid radicals (e.g., lipid peroxides) react with themselves to form stable lipid peroxide products, or if lipid-soluble antioxidants (e.g., vitamin E) are available to reduce peroxyl radicals to lipid hydroperoxides, albeit these can be cleaved by reduced metals to form harmful alkoxyl radical species which may initiate further lipid peroxidation reactions (Buettner, 1993).

MDA, 4-HNE and F_2-isoprostanes are three products which are routinely used as an index of lipid peroxidation. In a recent study, Spickett and co-workers (2010) assessed the reproducibility of these measures in fifteen different laboratories, from plasma samples exposed to varying degrees of UVA irradiation. The authors reported that the measurement of MDA by HPLC was the most sensitive and reproducible measure of the three lipid peroxidation products (Breusing et al., 2010). In addition, a widely used index of lipid peroxidation is the thiobarbituric acid reactive substances assay (TBARS) which measures

the reaction between MDA, the breakdown product of lipid peroxides, and thiobarbituric acid (TBA) (Esterbauer et al., 1991; Sayre et al., 2001). A simple spectrophotometric method has been described by El-Saadani et al. (1989) which measures total lipid peroxide levels in tissues, such as plasma.

1.4.4 Antioxidants

Measurement of endogenous and exogenous antioxidants such as various vitamins, polyphenols and carotenoids, activities of enzymatic antioxidants and total antioxidant capacity (TAC) of biological samples are routinely used as an index of the body's antioxidant defences. The Ferric Reducing Ability in Plasma (FRAP), as a measure of antioxidant power, is a common measure of TAC which includes all endogenous and exogenous antioxidants. In addition, the balance between levels of the small antioxidant molecule glutathione (GSH), and its oxidized counterpart (GSSG), provide an indication of cellular levels of oxidative stress. Under oxidative stress GSH levels are reduced and GSSG levels are increased (Sies, 1999; Bermejo et al., 2008).

1.5 Ageing and Oxidative stress

In 1956, Harman published The Free Radical Theory of Ageing. He suggested that free radical species, formed predominately as a by-product of cellular redox reactions, could contribute to oxidative damage to bio-molecules and accelerate ageing (Harman, 1956). A decade ago Beckman and Ames (1998) comprehensively reviewed the free radical theory and highlighted that ROS indeed play a role in the functional changes characteristic of ageing. However, they suggested that the theory should be broadened to encompass

oxidative stress as a phenomenon not just involved in events concerning determination of lifespan but associated with the whole process of ageing.

Later studies in animals and humans are in agreement with these theories. For example liver and brain tissue from aged Fisher male rat exhibited increased oxidative damage to proteins when compared to young rats. Furthermore, some antioxidant activities show an age dependent decrease (Tian et al., 1998) and in human plasma it has been reported that there is a linear increase in oxidative markers with respect to age and a decline in antioxidant defences after 45 years of age (Jones et al., 2002). Levels of plasma MDA and protein carbonyls have also been observed as increased in elderly compared to young subjects in parallel with a decrease in antioxidant capacity (Mutlu-Turkoglu et al., 2003). Moreover, in transgenic *Drosophila melanogaster* fruit flies which over express genes encoding for cytosolic and mitochondrial SOD, lifespan has been shown to be increased (Parkes et al., 1998; Sun et al., 2002). Taken together these data provide evidence to suggest oxidative stress should be considered as a contributor of ageing.

1.6 Oxidative stress is increased in AD

AD is an age-related disease and extensive data comprehensively show that there are increased levels of oxidative damage in brain tissue from AD sufferers (Markesbery, 1997; Aksenov et al., 2001), above that of healthily aged individuals, and thus it is now considered that increased levels of oxidative stress are associated with AD. These increased levels appear to be brain region specific; for example an early study revealed no differences in protein oxidation between AD and age matched controls in the frontal and occipital lobe brain regions (Smith et al., 1991). Lyras and colleagues (1997) comprehensively investigated

oxidative damage to proteins, lipids and DNA in various brain regions. They found a tentative increase in protein oxidation in several brain regions and a significant increase in protein and DNA oxidation in the parietal lobe brain region in AD compared to controls. In contrast they found no change in lipid peroxidation levels. Aksenov et al. (2001) later demonstrated that protein oxidation was increased in the hippocampus and superior temporal middle gyrus brain regions in AD compared to age matched controls, but not in the cerebellum. Interestingly, increased levels of protein oxidation were reported in AD brain regions dense in Aβ plaques, such as the hippocampus and inferior parietal lobule, when compared to the cerebellum, a region virtually devoid of this pathology (Hensley et al., 1995). Similarly, protein nitration is increased in AD and is region specific with the hippocampus, inferior parietal lobule (IPL) and superior/middle temporal gyri most affected, while the cerebellum and cerebral cortex remain unaffected (Smith et al., 1997b; Hensley et al., 1998). Furthermore, 4HNE, an aldehyde product of lipid peroxidation, is increased in the amygala, hippocampus and parahippocampal gyrus regions of AD brain compared to controls (Markesbery and Lovell, 1998).

It has also emerged that specific proteins in AD brain tissue are targets for oxidative modification. In the IPL brain region, cytoskeletal proteins, such as β-actin, and proteins involved in energy metabolism and proteolytic degradation, such as α-enolase and ubiquitin carboxyl-terminal hydrolase L-1 respectively, are targets of oxidation and nitration in AD (Castegna et al., 2002a; Castegna et al., 2002b; Castegna et al., 2003). Pamplona and colleagues (2005) have also shown that a small number of cytoskeletal proteins in the brain cortex and proteins involved in energy metabolism exhibit increased lipoxidation. Furthermore, in the entorhinal cortex, a brain region involved in the earliest stages of AD,

the α-mitochondrial ATP synthase subunit is modified by 4-HNE concurrent with a decrease in its activity (Terni et al., 2009). These specific oxidative alterations may have a detrimental impact on protein function, for example in the hippocampus, Pin1, a protein which regulates phosphorylation and dephosphorylation of tau, exhibits increased oxidation in parallel with reduced activity in AD (Sultana et al., 2006a). Pin1 has been shown to be downregulated in AD and could be crucial in neurofibrillary tangle formation (Sultana et al., 2006a).

1.7 Oxidative stress is an early event in AD development

It is thought that oxidative stress is an early event in AD, and this was elegantly demonstrated in a study undertaken by Nunomura and colleagues (2001) which set out to determine the stage of AD at which oxidative damage occurs. The study assessed neuronal oxidative damage from subjects who had suffered with AD for various durations, with their primary outcome measurement of oxidative damage being modifications to RNA. The authors suggested that this modification does not accumulate as seen with modifications to proteins, and as such, provides a better measure of the steady state balance of oxidative damage (Nunomura et al., 2001). The authors reported that levels of oxidative damage were inversely correlated to both disease duration and deposition of Aβ, and thus concluded that oxidative damage is an early event in AD (Nunomura et al., 2001). Later studies have assessed markers of oxidative damage in mild cognitive impairment (MCI). MCI is considered a transitional disease state which occurs between normal healthy aging and mild dementia. In 10-15% of cases, individuals affected by MCI will convert to AD, which is in contrast to the normally aged population which progress to AD at a 1-2% rate (Petersen et al., 2001). Studies in MCI brain demonstrate increased protein carbonylation, lipid

peroxidation and 3-nitrotyrosine (Keller et al., 2005; Butterfield et al., 2007) and are in agreement with the concept that oxidative stress is an early event in this disease.

1.8 Aβ is central feature of oxidative stress in AD

It is commonly perceived that Aβ has pro-oxidant properties which contribute to the elevated levels of oxidative stress evident in AD. For example, Mattson and co-workers (1997) reported that in hippocampal neurons Aβ induced the production of 4-HNE which led to their degeneration. However, studies have shown that Aβ has antioxidant capacity. Within its sequence, a methionine residue exists at position 35, and as well as being responsible for reducing transition metals to their highly active form and thus increasing radical production, it also functions as a free radical scavenger (Kontush, 2001; Moreira et al., 2007).

It appears that Aβ is anti-oxidant in diffuse plaques, then as Aβ becomes more fibrillar it becomes pro-oxidant. For example Nunomura et al. (1999) reported reduced oxidative damage in the brain cortex in parallel with the deposition of early diffuse Aβ plaques, which indicates that the presence of these early diffuse plaques maybe a compensatory response to reduce oxidative damage (Moreira et al., 2007). For Aβ to be a pro-oxidant a high concentration of fibrillar Aβ, the presence of transition metals and a methionine at residue 35 are required (Moreira et al., 2007). Due to the observed antioxidant nature of Aβ it has been suggested that it may become a pro-oxidant from an antioxidant if the aforementioned conditions are satisfied (Kontush, 2001). Further evidence is supplied by Tamagno and colleagues who have demonstrated that oxidative stressors promoted the amyloidogenic processing of the amyloid precursor protein leading to increased Aβ production (Tamagno et al., 2002; Tamagno et al., 2003).

1.9 Vascular nature of AD

There are several data, from population based studies, which associate an increased incidence of AD with various vascular risk factors, suggesting that AD may not just be a disease confined to the brain. The report that AD is associated with atherosclerosis (Hofman et al., 1997), further substantiated by a recent follow-up study (van et al., 2007) is suggestive of this. Furthermore, diabetes and peripheral vascular disease (Ott et al., 1996; Newman et al., 2005) have also been associated with AD. Moreover, in a review, Launer (2002) discussed existing data which links vascular disease with AD and concluded from this commentary that there are clinical, experimental and epidemiological data supporting a role for vascular risk factors in AD. More recently Dede and colleagues (2007) reported that endothelial function was impaired in AD patients when compared to healthy controls, providing further evidence that vascular factors have a role in the pathogenesis of AD. It has also been suggested that over 30% of AD cases exhibit cerebrovascular pathology, and that cerebrovascular disease worsens cognitive function in the early stages of AD subjects (Esiri et al., 1999; Kalaria and Ballard, 1999), where levels of oxidative stress are thought to be increased. In addition clinically diagnosed AD patients at post-mortem examination have significant lesion formation present in the main artery to brain (Roher et al., 2003).

1.9.1 Nitric oxide is instrumental to vascular changes

The free radical nitric oxide ($NO^{\bullet}$) is synthesised by the enzyme nitric oxide synthase (NOS), of which three isoforms have been identified and these include neuronal (nNOS) inducible (iNOS) and endothelial (eNOS). In AD brain, altered $NO^{\bullet}$ regulation is evident with increased NOS activity being demonstrated in brain micro vessels compared to control subjects (Dorheim et al., 1994). Changes to $NO^{\bullet}$ status may also in part contribute to elevated

levels of oxidative stress present in AD brain tissue. Lűth and colleagues (2002) reported that iNOS and eNOS are highly expressed in astrocytes and that nNOS was co-localised with 3-nitrotyrosine in pyramidal cells in AD. The authors suggested that increased expression of all NOS isoforms in astrocytes and neurons contribute to peroxyntitrite synthesis and likely 3-nitrotyrosine formation.

In blood vessels $NO^{\bullet}$ impacts on vascular disease such as atherosclerosis, a risk factor for AD (Hofman et al., 1997). In endothelial and smooth muscle cells, $NO^{\bullet}$ is produced at relatively low levels and acts in response to various stimuli to maintain blood vessel architecture and homeostasis. It possesses anti-atherosclerotic properties which are attributed to its ability to reduce intracellular levels of oxidative stress and prevent signalling processes integral to atherosclerosis development (Maxwell, 2002). It is well recognized that high blood pressure or hypertension increases the vascular production of ROS, which can result in the loss of endothelium-derived $NO^{\bullet}$ by reaction with radicals (e.g., superoxide anion) and thus ROS in the vasculature are firmly established as initiators of atherosclerosis and cardiovascular disease (Taniyama and Griendling, 2003; Landmesser et al., 2003). In general reported plasma and serum levels of $NO^{\bullet}$ in AD are reduced compared with control subjects (Selley, 2003; Corzo et al., 2007).

1.9.2 Specific oxidative vascular changes in AD

It is hardly surprising that increased oxidative damage is evident in AD brain tissue if oxidative stress is indeed part of AD pathology. However peripheral tissue oxidative changes have also been identified in AD. These changes may reflect processes which occur in the brain, but equally they could represent whole body changes which accompany, or contribute

to, this disease. Given the strong link between vascular risk factors and AD these whole body changes seen in the AD periphery are highly likely to involve vascular pathology.

For example, the oxidative modification of alpha 1-antitrypsin (α1-AT) in the vasculature may contribute to AD. α1-AT is a protease inhibitor responsible for preventing tissue damage by inactivating proteinases released during inflammation, and in its oxidized form (Ox α1-AT) has been shown to activate primary monocytes and induce pro-inflammatory cytokine expression (Moraga and Janciauskiene, 2000). It is also considered a marker of oxidative stress (Ueda et al., 2002). Increased levels of plasma Ox α1-AT have been reported in AD (Choi et al., 2002; Yu et al., 2003) and hence such modifications may contribute to inflammatory processes associated with this neurodegenerative disease (Akiyama et al., 2000). Indeed, a role for α1-AT in AD has been previously suggested given that elevated levels are found localised to neuropathologies associated with AD (Gollin et al., 1992).

A further finding reported by Choi et al. (2002) was the increased oxidation to fibrinogen in AD subjects compared to controls. The authors suggested that this modification may result in increased activation of plasminogen and therefore contribute to fibrinolysis and proteolysis at sites of inflammation (Choi et al., 2002). Several molecules of the coagulation and fibrinolysis system have been detected in AD brain and Aβ plaques. The observation that heparin enhances the actions of these proteins, coupled to the presence of heparin sulphate glycoprotein in Aβ plaques and neurofibrillary tangles has led to the suggestion that these proteins maybe actively involved in AD neuroinflammation (Strohmeyer and Rogers, 2001). The observed increase in fibrinogen oxidation in AD is also interesting from the viewpoint

that the oxidized form of fibrinogen has been shown in particular to play an important role in the development of atherosclerosis (Azizova et al., 2007).

A further example of an oxidative vascular pathology associated with AD is low density lipoprotein (LDL) oxidation. LDL is responsible for the transport of triglycerides and cholesterol from the blood and surrounding tissues to the liver and is highly susceptible to oxidation (Steinberg et al., 1989). In this oxidized state, LDL has been shown to facilitate the loading of cholesterol into macrophages and promote smooth muscle cell proliferation, platelet adhesion and foam cell formation (Holvoet et al., 2001; Parthasarathy et al., 1989; Witztum and Steinberg, 1991), indicative of early atherosclerosis. The demonstration that LDL susceptibility to oxidation is increased in cerebrospinal fluid (CSF) and plasma from AD subjects, in parallel with reduced levels of antioxidants, further indicates a role for LDL oxidation in AD (Schippling et al., 2000). More recently Aβ (peptides Aβ40 and Aβ42) has also been shown to bind modified forms of LDL *in vitro*, including oxidized LDL, and increase foam cell formation in vascular lesions (Schulz et al., 2007).

1.10 Peripheral oxidative stress may contribute to AD biomarkers

Vascular oxidative changes may represent a potential cause of AD and therefore assessing such changes enables greater understanding of underlying vascular pathologies which may contribute to this dementia. On the other hand, such changes may also be present in peripheral tissue as a consequence of AD itself, and hence could be viewed as potential biomarkers. There is an increased urgency to develop a biomarker, or series of biomarkers for AD given that the only definitive way to diagnose AD at present is at post-mortem (Mattson, 2004). The challenge remains to be able to diagnose AD at a much earlier stage,

ideally earlier than the onset of clinical symptoms so that treatment, therapies or interventions can be deployed and consequently symptoms can be alleviated or delayed.

A consensus report published in 1998 by the Ronald and Nancy Reagan Research Institute of the Alzheimer's Association and the National Institute on Aging Working Group recommended that a biomarker for AD should be characteristic of AD pathology, reliable, cheap, non-invasive and simple to undertake and analyse (1998). Additionally, in a recent review by Aluise at al. (2008) the authors described a biomarker as a change or abnormal signal that occurs in tissue or fluid excreted or secreted in the body which is distinguishable in a patient population.

The two bodily fluids used for biomarker discovery in AD are cerebrospinal fluid (CSF) and plasma. CSF is acquired via lumbar puncture which is an invasive process, nonetheless it provides an ideal bodily fluid to assess changes which occur in the brain as it is in direct contact with the brain extracellular space (Davidsson et al., 2002; Davidsson and Sjogren, 2006). Plasma on the other hand provides a less invasive, accessible route to investigate processes which take place in the body. It is often regarded as the 'dustbin' for the human body, and as such, hallmarks of processes and reactions which take place in the body, such as the brain, can be exported in the plasma. Plasma contains proteins from the periphery that may affect the brain (Aluise et al., 2008), and it has been suggested that approximately half a litre of CSF is absorbed into plasma on a daily basis (Hye et al., 2006).

1.10.1 Broad markers

1.10.1.1 Protein oxidation

Existing studies assessing the extent of plasma protein carbonylation in AD continue to present an unclear picture (see Table 1.1). For example, no change in plasma protein oxidation between AD and age matched controls subjects has been reported when analysing a specific product of protein oxidation in plasma (Pulido et al., 2005), which is in contrast to work by Conrad and colleagues (2000) and Bermejo et al. (2008) who showed that plasma protein oxidation was increased in AD by Western blotting and a spectrophotometric assay respectively. There is the potential possibility that the disease time course may influence plasma protein oxidation levels as oxidative stress is most prevalent in the earliest stages of the disease (Nunomura et al., 2001). Indeed, Greilberger et al. (2008) reported increased protein oxidation in a patient group consisting of both MCI and AD subjects and Bermejo et al. (2008) revealed a severity dependent increase in plasma protein oxidation. However no differences were reported in mild to moderate, and advanced AD (Zafrilla et al., 2006) or in mild AD patients (Baldeiras et al., 2008) in two separate studies. Evidently further investigation into CSF and plasma protein oxidation levels is warranted.

Authors	Participants	Parameters measures	Changes compared to control	Comments
Padurarin *et al*. (2009)	15AD, 15MCI and 15 Controls	MDA SOD GPx	↑ AD, ↑ MCI ($p<0.0005$) ↓ AD, ↓ MCI ($p<0.0004$) ↓ AD, ↓ MCI ($p<0.0001$)	Show correlation between ↓ AOx defences and ↑ MDA, Similar changes between AD and MCI
Martin-Aragón *et al.* (2009)	45 AD, 34 MCI and 28 Controls	MDA Total GPx activity GR activity	↑ AD ($p<0.05$), ↔ MCI ↔ AD, ↔ MCI ↔ AD, ↔ MCI	Levels of MDA increased in MCI but fail to reach statistical significance
Greilberger *et al.* (2008)	16 NDD and 15 Controls	Protein oxidation MDA Oxidized Human Albumin	↑ ($p<0.05$) ↑ ($p<0.05$) ↑ ($p<0.05$)	Authors suggest these are useful markers for neurodegenerative diseases
Bermejo *et al.* (2008)	45 AD, 34 MCI and 28 Controls	Protein oxidation GSH/GSSG levels in erythrocytes GPx activity GR activity	↑ AD ($p<0.05$) ,↑ MCI ($p<0.05$) ↓ AD ($p<0.05$), ↓ MCI ($p<0.05$) ↓ AD ($p<0.05$), ↔ MCI ↔ AD, ↔ MCI	Increased oxidation not just restricted to the brain in these diseases
Balderias *et al*. (2008)	42 mild AD, 85 MCI and 37 Controls	Plasma; protein oxidation, MDA, TAS, GSH, GSSG. Erythrocytes; MDA,GSH, GSSG	Plasma: Protein oxidation, MDA, GSH; ↔ Mild AD, ↔ MCI. GSSG: ↑ AD ($p<0.005$), ↑ MCI ($p<0.05$). Erythrocytes: GSH, GSSG, GPx and GR; ↔ AD, ↔ MCI. MDA: ↑ AD ($p<0.05$), ↑ MCI ($p<0.05$)	The majority of oxidative changes in mild AD are already present in MCI
Zafrilla *et al*. (2006)	36 Moderate AD, 30 Advanced AD and 27 Controls	Protein oxidation TBARS TAS	↔ Mod AD, ↔ Adv AD ↑ Mod AD, ↑ Adv AD ($p<0.05$) ↔ Mod AD, ↓ Adv AD ($p<0.05$)	TAS reduced in moderate AD but not significant. No differences between severity of disease for protein and lipid oxidation
Calabrese *et al*. (2006)	18 AD and 18 Controls	Protein Oxidation 3-nitrotyrosine 4-HNE	↑ ↑ ↑	All parameters were assessed by Western blotting. No statistical data provided.

Table 1.1. Markers of oxidative stress in AD peripheral tissues.

Authors	Participants	Parameters measures	Changes compared to control	Comments
Pulido *et al*. (2005)	20AD and 22 Control	Protein Oxidation TAC	↔ ↔	2-AAS product measured for protein oxidation. FRAP and ABTS+ assay used
Migliore *et al* (2005).	20AD, 15MCI and 15 healthy controls	DNA strand breaks DNA oxidized pyrimidines DNA oxidized purines	↑ AD ($p<0.001$), ↑ MCI ($p<0.001$) ↑ AD ($p<0.002$), ↑ MCI ($p<0.002$) ↑ AD ($p<0.001$), ↑ MCI ($p<0.001$)	Oxidative damage is present at the peripheral level in AD
Rinaldi *et al.* (2003)	63AD, 25MCI and 56 Control	Plasma antioxidants SOD GPx SOD RBC	↓ several antioxidants ($p<0.001$) ↔ lycopene and β-carotene in AD ↓ SOD, GPx and SOD RBC in AD	Peripheral antioxidant levels are depleted in AD
Mecocci *et al*. (2002)	40AD and 39 Control	8-OHdG in lymphocytes Antioxidants in plasma	↑ ($p<0.001$) ↓ ($p<0.001$)	↓Vitamins A, C, E, carotenoids. Only lutein was same between AD and control
M^{c}Grath *et al.* (2001)	29AD and 46Control	Protein Oxidation MDA 4-HNE	↔ ↔ ↑ ($p<0.001$)	Oxidative stress involved in AD
Bourdel-Marchasson *et al*. (2001)	20AD and 23 Control	Antioxidants, enzyme activity and MDA in plasma and erythrocytes	↓ plasma α-tocopherol and retinol ($p<0.014$) ↑ MDA in plasma ($p=0.036$)	Antioxidants consumed as increased free radical production
Repetto *et al*. (1999)	18 Probable AD and 18 Control	TAC *Tert*-butyl hydroperoxide-initiated chemiluminescence	↓24% ($p=0.036$) ↑ 56% ($p=0.006$)	Increased oxidative stress in blood from AD patients

Abbreviations: AD, Alzheimer's disease; **MCI**, Mild Cognitive Impairment; **MDA**, Malonaldehyde; **GPx**, Glutathione Peroxidase; **GR**, Glutathione Reductase; **NDD**, Neurodegenerative disease; **GSH**, Glutathione; **GSSG**, Oxidized Glutathione; **TAS**, Total Antioxidant Status; **TBARS**, Thiobarbituric acid reactive substances; **4-HNE**, 4-hydroxy -2-nonenal; **TAC**, Total Antioxidant Capacity; **2-AAS**, 2-amino-adipic semialdehyde; **FRAP**, Ferric reducing ability of plasma ; **8-OHdG**, 8-hydroxy-2'-de-oxyguanosine; **RBC**, Red blood cells; **AOx**, antioxidants.

1.10.1.2 Protein nitration

From the limited studies which investigate CSF protein nitration levels in AD it is apparent that generally levels are increased in AD subjects compared to controls, with two groups reporting this finding. However Ryberg et al. (2004) have shown there is no difference in Free 3-nitrotyrosine levels between AD and control subjects. Studies of protein nitration in plasma are extremely limited. One study used Western blotting to show an increase in plasma protein nitration, but the authors did not include any statistical analysis (Calabrese et al., 2006). A more recent comprehensive study by Korolainen and Pirttilä (2009) revealed no differences in plasma protein nitration between AD and control subjects. Further investigations into peripheral protein nitration levels are therefore required.

1.10.1.3 Antioxidant status

In general, measurements of antioxidant defences are reduced in AD patient populations compared with control groups. TAC, as measured by FRAP, has been reported to be reduced in AD (Sekler et al., 2008). Further, a 24% decrease in TAC in plasma from probable AD compared to controls (Repetto et al., 1999) has been reported using *tert*-butyl hydroperoxide chemiluminescence. It has been suggested that reduction of antioxidant defences occurs in only the most advanced cases of AD as these reductions are evident in severe, but not in moderate cases (Zafrilla et al., 2006; Sekler et al., 2008). In contrast to these studies other groups have reported no differences (Sinclair et al., 1998; Pulido et al., 2005; Baldeiras et al., 2008). Additional antioxidant defence measures are in support of antioxidants being reduced in AD: one study showed that the activity of superoxide dismutase (SOD) and glutathione peroxidase (GPx) were reduced in plasma (Rinaldi et al., 2003). Furthermore, studies which assessed levels of specific antioxidants in AD plasma revealed a depletion in several

compounds compared to control, these include: vitamins A, C and E; Zeaxanthin; β-Cryptoxanthin; Lycopene; and α and β-carotene (Mecocci et al., 2002; Polidori et al., 2004; Rinaldi et al., 2003).

1.10.1.4 Lipid oxidation

Studies assessing oxidative damage to lipids in plasma suggest that there is increased damage in AD compared to control subjects. One study reports comparable levels of lipid peroxidation, from AD and control plasma, and a further study supports these findings, albeit 4-HNE is shown to be increased (McGrath et al., 2001; Polidori et al., 2004). In contrast, studies have reported increased plasma levels of MDA in light to moderate cases of AD, and in AD (Greilberger et al., 2008; Martin-Aragon et al., 2009; Zafrilla et al., 2006). MDA is also found to be increased in red blood cells in AD compared to control subjects (Baldeiras et al., 2008).

1.11 Methodologies used to identify specific plasma proteins modified by oxidation

There are a number of ways to assess the oxidation status of specific proteins. For example a protein of interest can be isolated (e.g., immunoprecipitation) and then assessed for a particular oxidative adducts for example by Western blotting or ELISA. This approach allows hypothesis driven research. In contrast, 2-DE is commonly used to assess the whole proteome of a particular biological sample at a given moment in time. It may then be coupled to Western blotting and mass spectrometry (MS) in order to identify which proteins are oxidized.

1.11.1 2-DE and Western blotting

During 2-DE proteins are initially separated according to their charge by isoelectric focussing and then based on their mass by polyacrylamide gel electrophoresis (Aldred et al., 2004). Separated proteins are then either stained (e.g., Coomassie staining and silver staining) and their expression assessed, or they are transferred to membrane (e.g., PVDF or nitrocellulose) where Western blotting can then be employed to identify specific proteins which contain oxidation adducts. Proteins whose degree of expression or oxidation is significantly altered are then excised from 2-DG gels and identified by MS.

1.11.2 Mass Spectrometry

Mass spectrometry is an analytical technique which is typically used to determine the molecular mass of proteins within a particular sample. Protein samples are firstly digested into peptides enzymatically using trypsin, a serine protease which cleaves peptides at the carboxyl end of arginine and lysine amino acid residues. They are then ionised, separated according to their mass to charge (*m/z*) ratio in a MS analyzer and detected. The m/z ratios for all detected ions are represented in the form of a mass spectrum.

MS using multiple analyzers is referred to as tandem mass spectrometry (MS/MS) and allows for the generation of structural information from a particular biological sample. It is therefore used for protein identification purposes (Wysocki et al., 2005). During MS/MS specific precursor ions (e.g., the most abundant) from initial MS are selected and fragmented to form product ions which are analysed by a separate analyzer. As shown in figure 1.2 there are several sites along the peptide backbone which are cleaved during fragmentation. The major site of cleavage is at the peptide bond (CO-NH), and this gives rise to either ‘b’ or ‘y’

ions, which is dependent on whether charge is retained on the amino or carboxyl fragment respectively. Further fragment ions can also be formed by cleavage at the CH-CO (e.g., 'a' and 'x') and NH-CH (e.g., 'c' and 'z') bond. This information is particularly useful as the mass difference between adjacent 'b' or 'y' ions can be used to deduce the amino acid sequence of a particular peptide (see figure 1.3), and in theory these ion fragmentation patterns can therefore be assembled to form an original peptide sequence (Wysocki et al., 2005).

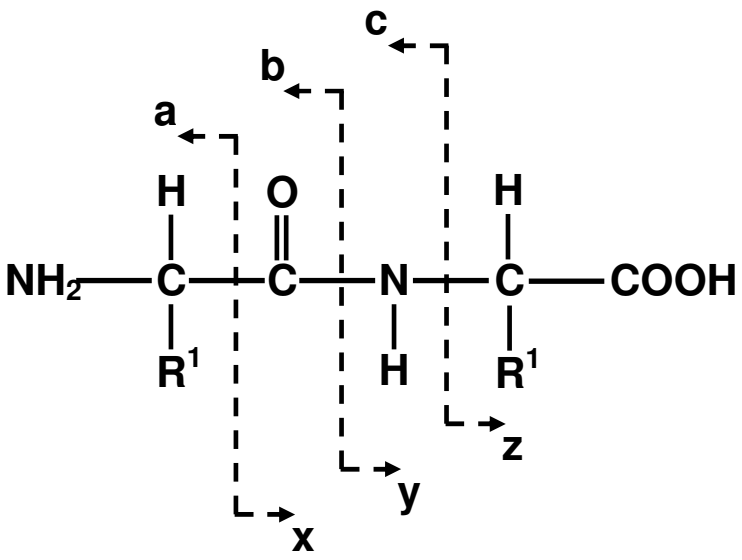

Figure 1.2 Nomenclature for peptide backbone fragmentation. Peptide backbone fragmentation typically occurs at the peptide bond to produces 'b' and 'y' ions. If the charge remains at the amino (NH_2) end 'b' ions are produced and if the charge remains at the carboxyl end (COOH) 'y' ions are produced. Other ions can also be observed during fragmentation and these include a, c, x and z ions.

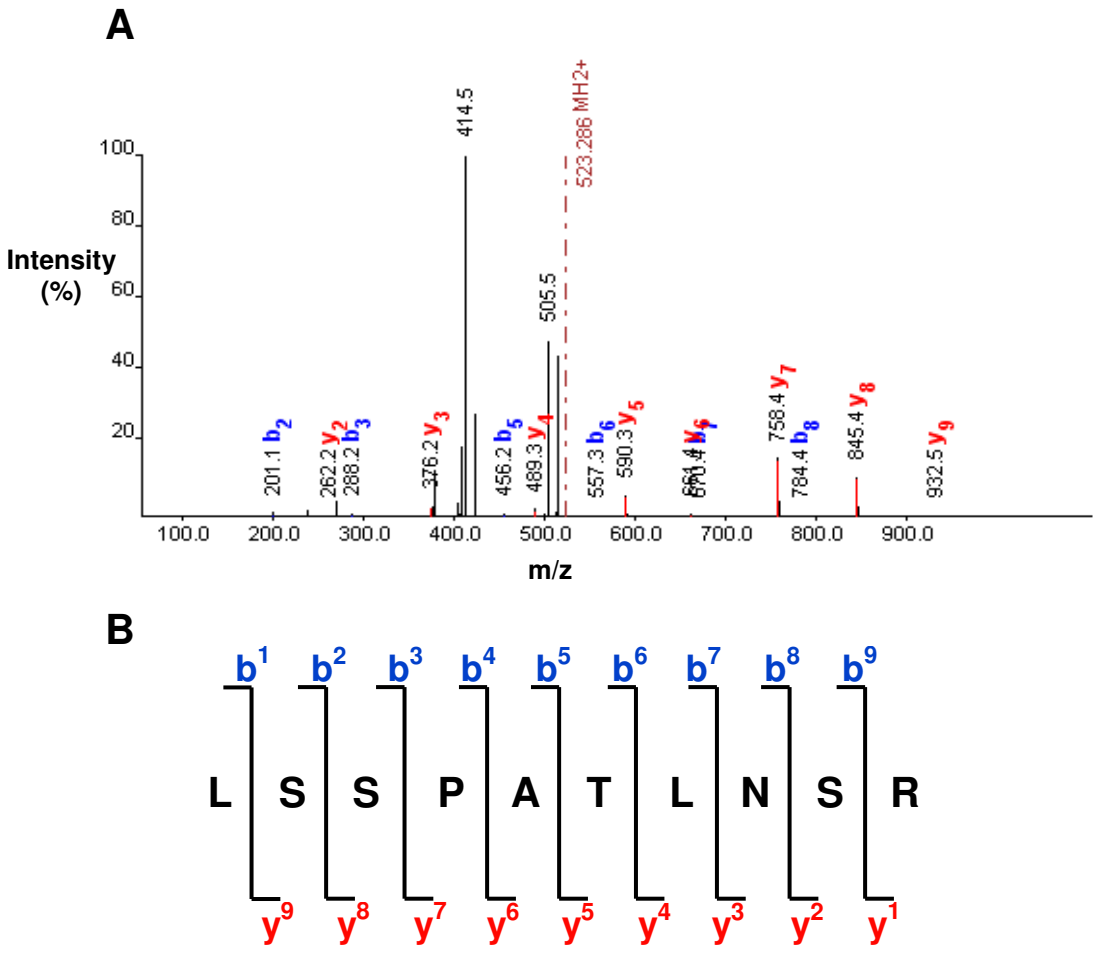

Figure 1.3. Peptide sequencing from MS/MS spectra. Most abundant precursor ions generated from a survey MS scan are taken forward for CID fragmentation. (A) Example of spectra for peptide LSSPATLNSR, produced from fragmentation of one selected precursor ion. (B) The mass difference between adjacent fragments of a series can be calculated to deduce a peptide sequence, for example $b^7 – b^6$ = 670.4 – 557.3 = 113.10Da corresponds to the amino acid residue Leucine (L) and $y^7 - y^6$ = 758.4 – 661.4 = 97Da corresponds to the amino acid residue Proline (P). This peptide sequence covers part of the amino acid sequence for trypsin precursor protein P00761/136429.

1.12 Specific markers using redox proteomics

The use of 2-DE coupled to Western blotting to enable the identification of specific proteins modified by oxidation was termed 'redox' proteomics by Butterfield and colleagues (Butterfield et al., 2006). This group and others have used this approach extensively (Korolainen et al., 2002; Pamplona et al., 2005; see table 1.2) to identify proteins that are specific targets of oxidation in AD brain and thus the group has increased knowledge of the possible molecular mechanisms underlying AD development and progression. For example, as the brain is a metabolically active tissue, with glucose being its primary fuel source, disturbances or problems with metabolizing glucose may lead to cognitive decline associated with AD (Costantini et al., 2008). Enolase is an enzyme responsible for the interconversion of 2-phosphoglycerate and phosphoenolpyruvate in the glycolytic pathway and consists of α, β and γ subunits. It has been shown that the α-subunit is oxidized and nitrated, and the γ subunit lipoxidized in AD brain (Castegna et al., 2002b; Castegna et al., 2003; Pamplona et al., 2005). In light of these observations impairment of glycolytic enzymes maybe linked to the decreased glucose metabolism seen in AD (Castegna et al., 2002b; Costantini et al., 2008).

In peripheral tissue such studies are limited (see table 1.2). In a recent pilot study Korolainen et al. (2007) demonstrated that the CSF protein λ chain precursor and an unidentified CSF protein exhibited increased oxidation in AD compared to control patients. In plasma Choi and colleagues (2002) identified two oxidized proteins: fibrinogen γ-chain precursor protein and α-1-antitrypsin precursor protein. The authors suggested that in their oxidized state these two proteins may contribute to increased inflammation in AD (Choi et al., 2002). Increased oxidation to the proteins transferrin and hemopexin has also been reported, with both being

Authors	Participants	Parameters measures	Changes compared to control	Comments
Perez-Gracia *et al.* (2009)	27AD brain tissue from CP at various stages of the disease	CEL adducts CML adducts	↑ CEL; tyrosine 3/tryptophan 5-monooxygenase activation protein, zeta polypeptide and tropomyosin 3 isoform 2 in advanced AD. ↑ CML; apolipoprotein A-II with advanced stages of AD.	Specific proteins are oxidized during the advanced stages of AD in the CP, this may alter protein interactions and folding
Terni *et al.* (2009)	6 early stage AD and 6 Control from entorhinal cortex brain tissue	4-HNE adducts	↑ α-subunit of mitochondria ATP-synthase	Entorhinal cortex is area of brain first affected by NFT pathology
Korolainen *et al.* (2007)	11 probable AD and 8 control lumbar CSF early stage samples	Carbonyl adducts	↑ λ chain precursor ($p<0.05$) ↓ unidentified protein ($p<0.05$)	Further studies are required in CSF measuring carbonylated proteins
Sultana *et al.* (2006a)	Hippocampus brain samples from 6 AD and 6 age -matched control subjects	Carbonyl adducts	↑ Pin1	Oxidative modification reduces Pin1 activity and maybe an initial event in tangle formation evident in AD
Sultana *et al.* (2006b)	Hippocampus brain samples from 6 AD and 6 age -matched control subjects	Carbonyl adducts	↑ phosphoglycerate mutase 1,ubiquitin carboxyl terminal hydrolase 1, DRP-2, carbonic anhydrase II, triose phosphate isomerase, α -enolase and γ-SNAP	Similar proteins are specifically oxidized in hippocampus brain tissue in comparison with IPL region.
Pamplona *et al.* (2005)	8 AD and 5 Control from brain cortex tissue	MDAL	↑ cytoskeletal proteins (i.e. Neurofilament triplet L) . ↑ proteins involved in energy metabolism (i.e. ATP synthase)	Lipoxidative damage to specific proteins involved in energy metabolism have a pathogenic role in AD
Yu *et al.* (2003)	Plasma from control (n=9) and AD (n=10)	Carbonyl adducts	↑ human transferrin and hemopexin	Possible to detect specific glycoproteins which are targets for oxidation in AD plasma

Table 1.2. Proteomic studies in AD subjects

Authors	Participants	Parameters measures	Changes compared to control	Comments
Castegna *et al*. (2003)	5 AD and 5 Control samples from IPL brain tissue	3-nitrotyrosine	↑α-enolase, triosephosphate isomerase and neuropolypeptide h3.	Specific proteins are targets for nitration in IPL
Castegna *et al.* (2002a)	5 AD and 5 Control samples from Inferior parietal lobule brain tissue	Carbonyl adducts	↑Creatine kinase BB, Glutamine synthase, Ubiquitin carboxyl-terminal hydrolase L-1	
Castegna *et al.* (2002b)	5 AD and 5 Control samples from Inferior parietal lobule brain tissue	Carbonyl adducts	↑Dihydropyrimidinase related protein-2, α-enolase and heat shock cognate-71	Specific oxidation events occur to proteins in IPL from AD subjects
Choi *et al.* (2002)	9 AD and 9 Control plasma samples	Carbonyl adducts	↑fibrinogen γ-chain precursor protein and α-1-antitrypsin precursor protein	Possible to detect specific proteins which are targets for oxidation in AD plasma

Abbreviations: AD, Alzheimer's disease; **MDAL**, malonaldehyde lysine; **ATP**, adenosine triphosphate; **CP**, choroid plexus; **IPL**, inferior parietal lobule; **CEL, N**carboxyethyl-lysine; **CML,** carboxymethyl-lysine; **4-HNE**, 4-hydroylnonenal.

involved in iron/redox homeostasis (Yu et al., 2003). Peripheral redox proteomics remains in its infancy in AD research, but warrants further investigation in order for the role of oxidative metabolism in AD to be further understood.

1.13 Aims and Overview of thesis

The main aims of this thesis were to measure peripheral oxidative and nitrative stress of AD and more specifically identify plasma proteins which are specific targets for oxidative modification in AD. Broad measures of oxidative and nitrative stress were assessed and subjective and non-subjective experimental approaches used to determine the oxidative status of specific plasma proteins in AD.

The value and importance of this work are as follows 1) existing studies which have assessed plasma protein carbonylation levels in AD present an unclear picture. Several studies report levels to be increased in AD compared to control subjects in contrast to others which observe no change. Therefore further studies are required to clarify plasma protein oxidation levels in these groups; 2) at the time of undertaking the work for this thesis investigation of plasma protein nitration in peripheral tissue was extremely limited. One study had assessed protein nitration levels in AD by Western blotting and reported an increase compared to controls. However, the data presented was minimal and no statistical analysis was provided for this reported finding. For this reason, studies which compare plasma protein nitration in AD and control subjects were required. The work in this thesis will firstly clarify protein nitration levels between disease and control and secondly further current understanding of peripheral nitrative stress in AD; and 3) only two studies have employed redox proteomics to investigate oxidized plasma proteins in AD. Therefore further investigation is required to add

to, and build on these studies to determine whether these particular proteins and others are oxidized in a different cohort of AD samples.

Given the association of cardiovascular disease and atherosclerosis with AD, low density lipoprotein was a specifically chosen plasma protein whose oxidation status was determined. Additionally total levels of plasma protein oxidation and total antioxidant capacity were measured by ELISA and spectrophotometric assay respectively. This is described in **Chapter 3**. In light of the limited studies which have assessed nitrative stress in AD, a further outcome of this thesis was to develop and provide a quantitative measure for 3-nitrotyrosine. The attempted use of HPLC-ECD and development of an in-house 3-nitrotyrosine ELISA is described in **Chapter 4.** The validation of the Griess Assay to measure nitric oxide metabolites and the use of SDS-PAGE and Western blotting to provide a measure of total protein nitration, in addition to the identification of plasma proteins altered by nitration is the focus of **Chapter 5**. Gel based redox proteomics was undertaken in **Chapter 6** to assess specific plasma proteins modified by oxidation in AD. The use of a non-gel based proteomic method, which utilized isobaric labelling, was employed to explore plasma proteins modified by oxidation and nitration and is presented in **Chapter 7**.

Chapter 2

General Methods

2.1 Materials

2.1.1 Chemicals and reagents

Electrode wicks, Mineral oil, ReadyStrip™ IPG strips, bio-lytes (100x), micro-spin® 6 chromatography columns, Pre-cast Criterion™ gels, Kaleidoscope® pre-stained standards, Readyprep™ TBP reducing agent, TGS, TG, thin blot filter paper and Aurum™ Affi-Gel® Blue columns was purchased from BioRad, UK. Destreak™ rehydration solution, Hybond™- P PVDF membrane, ECL + Western blotting detection system, Amersham™ tracker tape, and High performance chemiluminescent film Amersham hyperfilm™ was purchased from GE Healthcare, Amersham, UK. HPLC grade methanol, acetonitrile, acetone, ethanol, OSA acid, EDTA, sulphuric acid, sodium hydrogen carbonate was purchased from Fisher Scientific, UK. Dialysis membrane was purchased from Medicell International Limited, UK. Sequencing grade trypsin was purchased from Promega, USA. Rat anti-mouse IgE conjugated horseradish peroxidase antibody was purchased from AdB Serotec, UK. Goat anti-mouse IgG conjugated horseradish peroxidase was purchased from Cell Signalling, UK. Pronase from *Streptomyces griseus* was purchased from Biochemika. C18 ZipTip™ and mouse monoclonal anti-nitrotyrosine IgG antibody was purchased from Millipore, UK and mouse monoclonal α-2 macroglobulin and Complement 4A IgG antibodies waspurchased from AbCam Limited, Cambridge, UK. Film developer and fixer were purchased from Ilford, UK. All other chemicals and reagents were purchased from Sigma Aldrich, UK.

2.1.2 Plasma samples

Samples collected for this thesis are part of an ongoing collaboration between Professor Patrizia Mecocci at the University hospital Perugia, Italy and Dr Sarah Aldred. Patients

attended the dementia clinic of the department of gerontology and geriatrics, University hospital Perugia, Italy in a fasted state and blood samples were collected. Ethical approval for sample collection and processing is held in Italy.

All samples acquired conformed to the principles outlined in the Declaration of Helsinki. Patients with diagnosis of dementia made on the basis of scores obtained to a full battery of cognitive, functional and behavioural tests were divided into two groups according to NINDS-AIREN (Wetterling et al., 1996) and NINCDS-ADRDA (1985) criteria as follows: Neuropsychological and functional assessment tests were administered by a trained physician, who was blind to the operative procedure, in a quiet environment in the hospital. The battery of tests included the mini mental state examination (MMSE) as measure of global cognitive function and tests evaluating the following cognitive domains: a) memory: Babcock Story Recall test and Rey's Auditory Verbal Learning test immediate (Rey-IR) and delayed recall (Rey-DR) to assess episodic memory, and verbal fluency with semantic cues (Category Naming Test, CNT) to estimate semantic abilities; b) attention and executive functions: Trail-Making test part A (TMT-A) and B (TMT-B) to evaluate selective and divided attention, respectively, and Controlled Oral Word Association test (COWA) to estimate executive functioning; c) visuospatial and constructional abilities: Copy Drawing test (CD). Details on administration procedures and Italian normative data for score adjustment for age and education, and normality cut-off scores (95% of the lower tolerance limit of the normal population distribution) were used for each test. Patients diagnosed as having AD were compared to healthy controls. After obtaining informed consent from subjects or their relatives, patients and controls underwent blood drawing. Blood was immediately centrifuged and plasma stored frozen at -80°C until analysis.

In this thesis it was necessary to use two separate sample sets of Alzheimer's disease (AD) and age matched control plasma to investigate oxidative stress biomarkers in dementia. Plasma from an initial sample set, which consisted of 144 plasma samples (72 AD and 72 aged matched controls), was used in chapters 3, 4 and 6 (see table 2.1).

Subject Group	Age (yrs)	MMSE (mean ± SD)
Alzheimer's disease	**80 ± 4**	**19 ± 4**
Control	**75 ± 6**	**27 ± 2**

Table 2.1. Subject characteristics for first group of samples.

A separate sample set of plasma was obtained (25 AD and 25 aged matched controls) and analysed in chapters 5 and 7 (see table 2.2).

Subject Group	Age (yrs)	MMSE (mean ± SD)
Alzheimer's disease	**74 ± 4**	**13 ± 10***
Control	**74 ± 6**	**28 ± 2****

Table 2.2. Subject characteristics for second group of samples. *MMSE scores available for 17 out of 25 samples. **MMSE scores available for 18 out of 25 samples

2.2 Methods

2.2.1 Bicinchoninic acid assay

The bicinchoninic acid (BCA) assay based on method described by Smith et al. (1985) was used to assess plasma protein concentration. A stock solution of 1mg/ml Bovine Serum Albumin (BSA) was prepared and diluted to form a six point standard curve. Standards were kept at -80ºC until required. BCA working solution was prepared by adding 250 µl of copper sulphate solution (4% w/v) to 12.5 ml BCA solution (Sigma, UK). Standard (10 µl) or sample (10 µl) was added to 96 well microtitre plates and BCA working solution (200 µl) was added to each well for 30 minutes at 37ºC. Absorbance values were measured at 490 nm (Lab system Multiskan MS). Samples were assayed in triplicate and protein concentration expressed as mg/ml.

2.2.2 Measurement of Protein oxidation using ELISA

2.2.2.1 Preparing BSA standards

Dialysis membrane was boiled in sodium bicarbonate (2%) and EDTA (1 mM, pH 8), washed thoroughly in distilled water and boiled for a further 10 minutes in EDTA (1 mM, pH 8). After cooling to room temperature, tubing was stored in ethanol at 4ºC. Before use, tubing was washed thoroughly in distilled water.

Reduced and oxidized BSA was prepared as described by Carty et al. (2000). BSA, (10 mg/ml) dissolved in TBS (Tris-HCl 6 g/l, 9 g/l NaCl, pH 7.4), was reduced with sodium borohydride (1 g) overnight at 4ºC. Excess foam was removed by the drop wise addition of 100% acetone and the solution adjusted to a neutral pH using concentrated hydrochloric acid. BSA (10 mg/ml) was oxidized by exposure to 2, 2′-Azobis (2-methylpropionamidine)

dihydrochloride (AAPH, 500 mM) for one hour at 37ºC, in a water bath. To remove residual oxidizing and reducing agents solutions were dialyzed against TBS, over a 24 hour period with six buffer changes. Reduced and oxidized BSA were adjusted to 2 mg/ml (Carty et al., 2000), mixed at different oxidized ratios (0-100%) and stored at -80ºC until further use.

The method used by Carty et al. (2000) to quantify the degree of protein oxidation to known BSA standards was undertaken. Standards (500 µl) were mixed with 2, 4 – DNPH (500 µl) and left at room temperature for one hour with gentle agitation. TCA (20% w/v; 500 µl) was added to each to precipitate protein solution and thoroughly mixed. Solutions were centrifuged for 3 minutes at 13,000 xg and protein pellets were washed vigorously three times with ethanol: ethyl acetate (ratio 1:1) and redissolved in 6 M guanidine hydrochloride (1 ml) for 30 minutes at 37ºC. Solutions were centrifuged at 13,000 xg for a further minute, the supernatant was removed and the absorbance of solutions was measured at 360 nm. Molarity of solutions was determined using a molar co-efficient value (ε_{360} = 22000 $M^{-1}cm^{-1}$). Protein carbonylation levels were expressed as nmol/ per milligram of protein.

2.2.2.2 Protein carbonyl ELISA

Protein carbonyl ELISA was undertaken in accordance with Carty et al. (2000). Samples (50 µl) diluted in coating buffer (50mM Sodium carbonate, pH 9.2) to a final concentration of 0.05 mg/ml were applied to 96 well NUNC microtitre plates, for one hour at 37ºC. To each well 50µl of 2, 4-dinitrophenylhydrazine (DNPH) in 2 M HCl was added and left for one hour at room temperature. Wells were blocked with TBST (Tween 20, 0.1%) for 1 hour at 37ºC and monoclonal mouse anti-DNP antibody diluted at 1:1000 was added for two hours at 37ºC. Wells were incubated with peroxidase conjugated rat anti-mouse IgE conjugated

HRP diluted at 1:5000 for 1 hour at 37ºC. Between each step wells were washed four times with TBS-Tween 20 (0.05%). Substrate (0.5 M Citrate phosphate buffer (10 mls), hydrogen peroxide (8 µl) and OPD tablet (2 mg); 50µl) was added to each well and the reaction was stopped after fifteen minutes with 2 M sulphuric acid. Absorbance values were measured at 490 nm (Multiscan MS, Labsystems, Finland).

2.2.3 Total antioxidant capacity

Total antioxidant capacity was measured using a slight modification to the FRAP assay described by Benzie and Strain (1999) and McAnulty et al. (2005). Freshly prepared FRAP reagent (300 µl; 300 mM sodium acetate, pH 3.6, 10 mM 2, 4, 6-tris (2-pyridyl)-S-triazine in 40 mM HCl and 20mM Ferric Chloride ($FeCl_3$) in ddH_2O in ratio 10:1:1) was added to plasma (10 µl) or standard samples (10 µl) in triplicate at room temperature. The absorbance was then measured at 650nm after an eight minute reaction period and FRAP values were expressed as FRAP (µM) as determined by linear regression using a range of ascorbic acid standards (0-1000 µM). An ascorbic acid standard of 1000 µM is equivalent to 2000 µM of antioxidant power as measured by FRAP. This is because the direct reaction of ascorbic acid gives a change in absorbance double that of Fe (II) (Benzie and Strain, 1999).

2.2.4 Lipid peroxide assay

A spectrophotometric assay based on that described by el-Saadani et al. (1989) was used for the measurement of lipid peroxide levels in plasma. Samples and a blank standard (10 µl) were assayed in duplicate or triplicate and added to a 96 well microtitre plate. Each well was incubated with 100 µl of reagent mix (see table 2.3) for 30 minutes at 25°C and protected from light. The plate was read at 340 nm (Multiscan MS, Labsystems, Finland).

Reagent mix	Concentration
Potassium Phosphate	0.2 M, pH 6.2
Potassium Iodide	0.12 M
Sodium Azide	0.15 µM
Triton X	2 g/l
Alkylbenzyldimethylammonium Chloride	0.1 g/ml
Ammonium Molybdate	10 µM

Table 2.3. Reagent mix used for lipid peroxide assay

The concentration of lipid peroxides in plasma was determined using the Beer- Lambert Law (extinction co-efficient $\varepsilon_{340} = 24600\ M^{-1}cm^{-1}$). Values were expressed as µmol/l.

2.2.5 One dimensional gel electrophoresis (1-DE)

Plasma was added to an equal volume of Laemmli buffer (4% SDS, 20% glycerol, 10% 2-mercaptoethanol, 0.004% bromophenol blue and 0.125 Tris HCl, pH 6.8) and boiled for 5 minutes at 100°C. For separation, Pre-cast Criterion™ 4-15% gradient Tris-HCl gels and running buffer (25 mM Tris, 192 mM glycine and 0.1% SDS (w/v)) were used and plasma protein were run at 150 V (unlimited amps) for 85 minutes, or until dye front reached the bottom of the gel. Samples were assayed in duplicate or triplicate. Subsequently gels were Western blotted or silver stained.

2.2.6 Two dimensional gel electrophoresis (2-DE)

2.2.6.1 Isoelectric focussing

Electrode wicks were soaked in an ample amount of ddH_2O, blotted to remove excess liquid and then placed over electrode wires in an 11 cm IEF Protean tray (BioRad). Rehydration buffer and bio-lytes (0.5%) were added to plasma samples (100-150 µg). Samples (200 µl) were then applied to individual wells of IEF tray and 11 cm IPG ReadyStrip™ strips inserted. The strips were covered with 2-3 mls mineral oil prior to isoelectric focussing to prevent dehydration during separation. Gels were focussed using a Protean IEF cell (BioRad) and were passively rehydrated for 12 hours at 20 ºC, they were subsequently run at 250 V for 15 minutes, followed by linear ramp 250-8000 V for 3500 Vh and maintained at 8000 V for 90 kVh. Gels were held at 500 V to prevent over focussing until stopped and stored at -20ºC.

2.2.6.2 Gel electrophoresis

Gels were equilibrated for 20 minutes in equilibration buffer (6 M Urea, 375 mM Tris HCl pH 8.8, 2% SDS, 20% Glycerol, Tributyl Phosphine (2mM) and a spatula tip of bromophenol blue) on a rotary mixer at room temperature prior to use. Individual IPG strips were inserted into wells of Pre-cast Criterion™ 4-15 % Tris-HCl gels and overlaid with hot agarose (1 %) to prevent movement when running. Once set the system was run at 150 V (unlimited amps) for 85 minutes, or until dye front reached the bottom of the gel.

2.2.7 Western blotting

Hybond-P™ membrane was equilibrated in 100% methanol for two minutes followed by transfer buffer (25 mM Tris, 192 mM glycine and 20% v/v methanol) for 10 minutes. Proteins were transferred from electrophoresis gels to Hybond-P™ membrane by applying

170 mA with unlimited voltage for two hours. After transfer of proteins Western blotting was undertaken as described in table 2.4. After the final washing step, signal was visualised using an ECL+ detection system and captured on ECL plus hyper film at various exposure times. Film was developed using film developer and fixer. Blots were scanned using a GS-800 densitometer (BioRad).

Step	Solution	Time
Washing	TBST (0.05%)	Three ten minute washes
Blocking	Non fat milk (5%) in TBST (0.1%)	Overnight at 4ºC
Washing	TBST (0.05%)	Three ten minute washes
Antibody incubation	Primary antibody in TBST (0.1%)	Two hours at room temperature
Washing	TBST (0.05%)	Three ten minute washes
Antibody incubation	Secondary antibody in TBST (0.1%)	One hour at room temperature
Washing	TBST (0.05%)	Two ten minute washes
Washing	TBS with no Tween 20	Two ten minute washes

Table 2.4. Outline of Western blotting protocol.

2.2.8 Silver staining

Silver staining was undertaken based on a method described by Yan et al. (2000). Gels were washed in acetic acid (10% v/w), methanol (40% v/w) for 15 minutes twice to fix proteins, and sensitized with methanol (30% v/w), sodium thiosulphate (0.2% v/w) and 0.83 M sodium acetate for 30 minutes. After three, five minute washes with HPLC grade water, gels were incubated for 20 minutes with silver nitrate (0.25% v/w). Gels were washed a further two times for five minutes and developed in freshly made sodium carbonate (0.24 M) and formaldehyde (0.04% v/v). To arrest reactions, gels were incubated with EDTA (0.05 M) for

ten minutes and then washed in HPLC grade water. Gels were scanned using a GS-800 densitometer (BioRad).

2.2.9. Identification of plasma protein bands and spots

2.2.9.1 In-gel digestion

Destaining of samples was undertaken according to the method described by Gharahdaghi et al. (1999). Silver stained gel pieces of interest proteins were thawed and destained using potassium ferricyanide (30 mM) and sodium thiosulphate (100 mM) at a 1:1 ratio and rinsed three times with double distilled water (ddH_2O). Destained gel pieces were then washed in ammonium bicarbonate (200 mM) for 20 minutes, rinsed with 3 changes of ddH_2O and dehydrated repeatedly with acetonitrile. In gel digestion of samples was performed based on methods described by Rosenfield et al. (1992) and Hellman et al. (1995). Acetonitrile dehydrated gel pieces were rehydrated in a vacuum centrifuge for 5 minutes. The gel pieces were rehydrated with 10 mM DTT in 25 mM ammonium bicarbonate and incubated at 56ºC, for 45 minutes. DDT was removed and replaced with 55 mM iodoacetamide in 25 mM ammonium bicarbonate for 45 minutes at room temperature, samples were protected from light. The liquid was removed and gel pieces were incubated with shaking for 10 minutes in ammonium bicarbonate (25 mM) and twice with 50% acetonitrile in ammonium bicarbonate (25 mM). Destained gel pieces were then dehydrated in a vacuum centrifuge for 5 minutes. Gel pieces were covered with 12.5 ng/µl of trypsin in 25 mM ammonium bicarbonate, and rehydrated on ice for 10 minutes. Excess trypsin was removed, and gel pieces were covered in 25 mM ammonium bicarbonate and incubated at 37ºC overnight (~ 18 hours). Digest solutions were transferred to a fresh eppendorf tube (1.5 ml) and gel pieces covered with 50% acetonitrile and 5% formic acid and vortexed for 30 minutes, this was repeated twice.

All digest solutions were pooled together and stored at -80ºC. Samples were desalted using a Michrom MacroTrap C_8 cartridge and dried to 10 µl by vacuum centrifugation.

2.2.9.2 LC-MS

On-line liquid chromatography was performed by use of a Micro AS autosampler and Surveyor MS pump (Thermo Fisher Scientific, Bremen, Germany). Peptides were loaded onto a 75 µm (internal diameter) Integrafrit (New Objective) C_8 resolving column (length, 10 cm) and separated over a 40 min gradient from 0 to 40% acetonitrile (J. T. Baker Inc.). Peptides eluted directly (~350 nl/min) via a Triversa nanospray source (Advion Biosciences) into a 7 Tesla LTQ FT mass spectrometer (Thermo Fisher Scientific) where they were subjected to data-dependent CID.

2.2.9.3 Data-dependent CID

The mass spectrometer alternated between a full FT-MS scan (*m*/*z* 400-1600) and subsequent CID MS/MS scans of the five most abundant ions above a threshold of 40,000. Survey scans were acquired in the ICR cell with a resolution of 100,000 at *m*/*z* 400. Precursor ions were isolated and subjected to CID in the linear ion trap in parallel with the completion of the full FT-MS scan. The width of the precursor isolation window was *m*/*z* 3. Only multiple charged precursor ions were selected for MS/MS. CID was performed with helium gas at a normalized collision energy of 35%. Automated gain control was used to accumulate sufficient precursor ions (target value, 5×10^4; maximum fill time, 0.2 s). Precursor ions were activated for 30 ms. Data acquisition was controlled by Xcalibur 2.0 and Tune 2.2 software (Thermo Fisher Scientific).

2.2.9.4 Data Analysis

DTA (data) files were created from the raw data using Bioworks 3.3.1 (Thermo Fisher Scientific). The DTA files were searched directly using OMSSA Browser 2.1.1 against the human subset of the IPI database. N-terminus acetylation, Cysteine, Phenylalanine, Histidine, Methionine, Proline, Tryptophan and Tyrosine oxidation were specified as variable modifications, with carboxymethylation of cysteine as a static modification. The data were searched with a peptide m/z tolerance of ± 0.02 and a MS/MS m/z tolerance of ± 0.8. The search results were scored and filtered with an E-value cut-off, so that the searches could be repeated exactly in the future (E-value cut-off is statistical confidence generated from the OSSMA algorithm when completing the search, and the value used is the suggested threshold). A probability score (*p*-Score) was generated (any *p*-Score > 0 was rejected) and OMSSA results were filtered to allow only the top scoring identification per DTA.

2.2.10 General statistics

For comparison of values between AD and control subjects, data from each group was checked for normality using the Shapiro-Wilk statistical test, and if this assumption was violated, log transformation was applied. A parametric independent samples t-test, or a non parametric Mann Whitney U statistical test, was subsequently used on normally and non-normally distributed data respectively. Significance was accepted if $p < 0.05$.

Chapter 3

Increased LDL oxidation, but not total plasma oxidation in AD

3.1 Abstract

It is becoming increasingly clear that oxidative stress and vascular risk factors (e.g., atherosclerosis) play an important part in Alzheimer's disease (AD) pathology. The established link between increased LDL oxidation and atherosclerosis, coupled to the demonstration, in AD peripheral tissue, that the rate of LDL oxidation is increased, may suggest a role for oxidized LDL in this neurodegenerative disease. This study assessed oxidative damage in total plasma proteins, and isolated LDL in AD patients and age matched controls. In addition total antioxidant capacity (TAC) and lipid peroxide levels were measured. Significantly higher LDL protein carbonylation was observed in AD compared to age matched controls (Control: 3.85 ± 0.86 Vs. AD: 4.17 ± 0.73 nmol/mg LDL; $p = 0.05$, 2 tailed Mann-Whitney), in addition reduced TAC was found (Control: 1078.536 ± 252.633 Vs. AD: 924.708 ± 174.429µM FRAP; $p = 0.001$, 2 tailed Mann-Whitney). No differences were seen in total plasma protein carbonyl content (Control: 3.98 ± 0.48 Vs. AD: 3.88 ± 0.31nmol/mg protein, 2 tailed Mann-Whitney) or lipid peroxide levels (Control: 15.51 ± 19.41 Vs. AD: 14.21 ± 15.06 nmol/mg protein, independent samples t-test). These data further support the view that oxidation events in AD may be specific in nature, and represent functional changes to proteins, rather than random global events.

3.2 Introduction

In recent years it has become clear that there are considerable overlaps between AD and vascular pathologies. Vascular dementia (VaD) is caused by damage to the vascular system leading to reduced supply of blood to the brain and loss of cognitive function (Roman, 2003). The role that vascular diseases, and indeed that may play in AD has received an increasing amount of attention. VaD and AD have been considered two separate diseases, but it is now becoming increasingly clear that vascular factors are an important part of AD (Launer, 2002). A possible mechanism believed to contribute to both vascular pathologies and AD involves oxidative stress (for review see Bennett et al., 2009). Oxidative stress has been implicated in a number of diseases including Alzheimer's disease, vascular dementia, cardiovascular disease, rheumatoid arthritis and diabetes (Telci et al., 2000; Markesbery, 1997; Harrison et al., 2003; Casado et al., 2008; Taysi et al., 2002).

ROS can increase to high levels in some disease processes or where there is antioxidant deficiency, and may react with cellular constituents to cause damage, disruption of function, or degradation. An increase in oxidation products has been identified in Alzheimer's pathology including DNA damage seen as an increase in 8-oxo-dG in cortical tissue and lymphocytes (Mecocci et al., 2002). Markers of protein oxidation including protein carbonyl formation have been identified in AD brain tissue (Korolainen et al., 2002) and plasma proteins of Alzheimer's sufferers have been identified as altered (Korolainen et al., 2007).

Unfavourable lipoprotein profiles are associated with chronic vascular disease including heart disease and atherosclerosis, and are often associated with ageing. Decreased levels of high density lipoprotein (HDL) cholesterol and increased levels of low density lipoprotein

(LDL) cholesterol are strong markers for risk of disease (Fuster et al., 1992; Poulter, 2003). LDL transports cholesterol from the liver to the circulation, and is susceptible to oxidation by ROS. In addition, oxidative damage to LDL by ROS is a contributing factor in atherosclerosis (Raitakari et al., 1997). In LDL oxidation, damage is seen both to the lipid and to the protein moiety. A number of studies have suggested that protein oxidation of the lipoprotein molecule can occur as a direct result of free radical action and as a secondary result of the free radical cascade brought about by initial lipid peroxidation (Berlett and Stadtman, 1997). Although the majority of lipoprotein oxidation research has been done on the lipid moiety, protein oxidation has a number of functional consequences as Apolipoprotein B oxidation (the protein moiety associated with LDL) is pivotal to the modulation of LDL uptake and accumulation. Elevated levels of circulating oxidized LDL are reported in individuals suffering from cardiovascular disease (Holvoet et al., 2001; Kita et al., 2001), and, as previously mentioned, oxidative damage to LDL is a contributing factor in atherosclerosis (Raitakari et al., 1997). Atherosclerosis has also been linked to an increased incidence of AD and VaD (Hofman et al., 1997; van et al., 2007) and therefore risk factors for atherosclerosis may also represent risk factors for AD and VaD. Indeed, increased levels of LDL in AD serum (Kuo et al., 1998), in addition to an increased rate of lipoprotein oxidation in AD cerebrospinal fluid and plasma has been reported (Bassett et al., 1999; Schippling et al., 2000), which may suggest increased LDL oxidation is present in circulation of AD sufferers. However none of these studies actually assess levels of oxidized LDL *in vivo*. The primary aim of this study, therefore, was to identify increased oxidative damage to key plasma proteins in AD when compared to age matched controls; specifically LDL protein.

3.3 Methods

3.3.1 Sample population

AD samples and age matched control samples were obtained as described in general methods **section 2.1.4.** In total, 144 patients and control volunteers were recruited into the study (72 in each group), dependent on availability of blood samples, and the success of LDL preparation subsets were used for endpoint analysis.

3.3.2 BCA assay

Total protein concentration was determined by the BCA assay as described in general methods **section 2.2.1.**

3.3.3 Isolation of LDL

LDL from all plasma samples was isolated by density gradient centrifugation in a Beckman TL-100 based on the method of Chung et al. (1980). Each plasma sample (1 ml) was adjusted to a three-step gradient using Sodium Chloride (0.04, 0.08 and 0.32 g/ml) and overlaid with isotonic saline (0.9% NaCl, B Braun, Sheffield, UK). Adjusted plasma was centrifuged for 4 hours, at 100,000 xg using a Beckman TL-100 ultracentrifuge and LDL was obtained and kept at –80°C until required.

3.3.4 Protein carbonyl ELISA, FRAP and lipid peroxide assay

Protein carbonyl ELISA, FRAP and lipid peroxide assays were undertaken as described in general methods **section 2.2.2.2, 2.2.3 and 2.2.4.** A subset of 50 AD and 59 control samples were used for lipid peroxide analysis and a subset of 47 AD and 56 control samples were used for FRAP analysis, this was based on sample availability.

3.3.5 Statistics

Statistical analysis was undertaken as described in general methods section **2.2.10**. Significance was accepted if $p \leq 0.05$.

3.4 Results

3.4.1 Subject Information

The age ranges for both AD and control groups can be seen in table 2.1 (general methods), along with the average MMSE score for each group. At the time of this analysis, the mean time since diagnosis was 1.3 yrs +/- 0.8 in the AD group. Table 2.1 summarizes patient characteristics for the samples. They are not significantly different from each other in terms of age.

3.4.2 Protein oxidation

As shown in figure 3.1, there was no observed difference in total plasma protein oxidation between the control and AD groups (Control 3.98 ± 0.48 nmol/mg Vs. AD: 3.88 ± 0.31 nmol/mg; $p = 0.197$, 2 tailed Mann-Whitney). It is interesting to note that the spread of AD values compared to that of the controls is much greater.

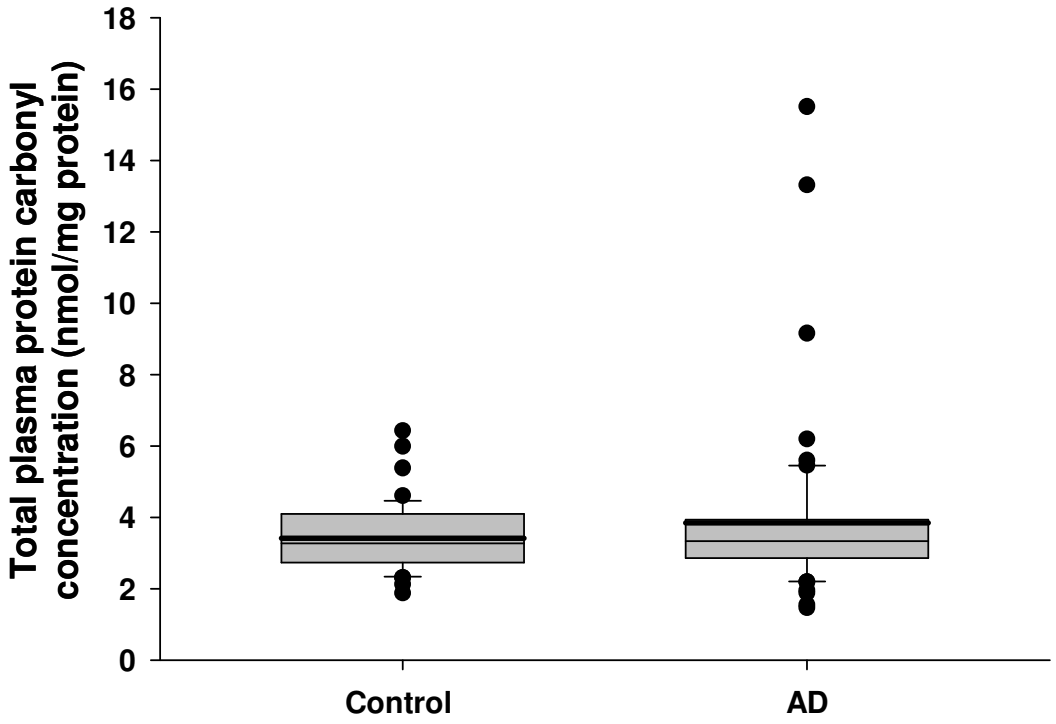

Figure 3.1. Total plasma protein carbonyl levels. Protein oxidation was measured by carbonyl ELISA. Data (Control n = 72 and AD n = 72) are presented as a box plot. Percentiles are represented by the box (25^{th} and 75^{th}) and whisker (10^{th} and 90^{th}) with thick and thin lines corresponding to mean and median values respectively. Filled circles represent outliers.

3.4.3 LDL oxidation

A significantly greater level of LDL oxidation was evident in AD compared to control subjects (Control 3.85 ± 0.86 nmol/mg Vs. AD: 4.17 ± 0.73 nmol/mg LDL; $p = 0.05$, 2 tailed Mann-Whitney), as shown in figure 3.2.

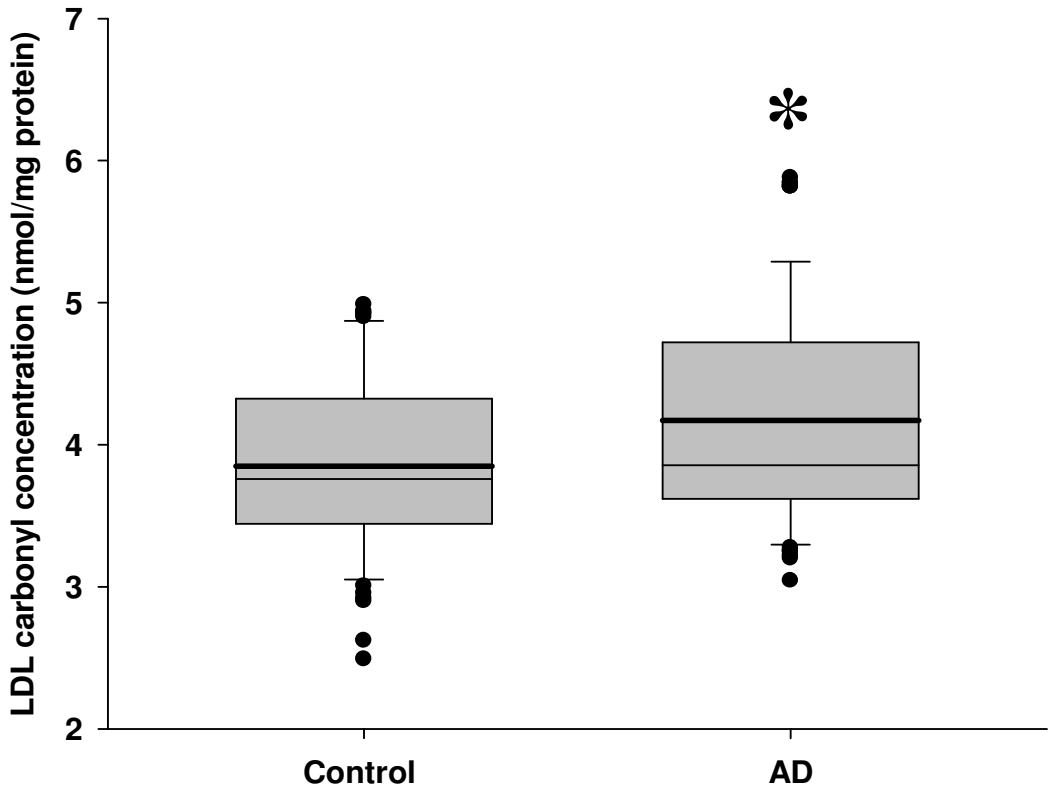

Figure 3.2. LDL carbonylation levels. LDL oxidation was measured by carbonyl ELISA. Data (Control n = 70 and AD n = 69) are presented as a box plot. Percentiles are represented by the box (25^{th} and 75^{th}) and whisker (10^{th} and 90^{th}) with thick and thin lines corresponding to mean and median values respectively. *Significant difference between the control and AD group (*$p = 0.05$). Filled circles represent outliers.

3.4.4 Total antioxidant capacity

As evident in figure 3.3, there was a significant decrease in total antioxidant capacity, as measured by FRAP (section 3.3.4), in the AD group compared to the control group (Control: 1078.536 ± 252. 633 Vs. AD: 924.708 ± 174.429 µM FRAP; p = 0.001, 2 tailed Mann-Whitney).

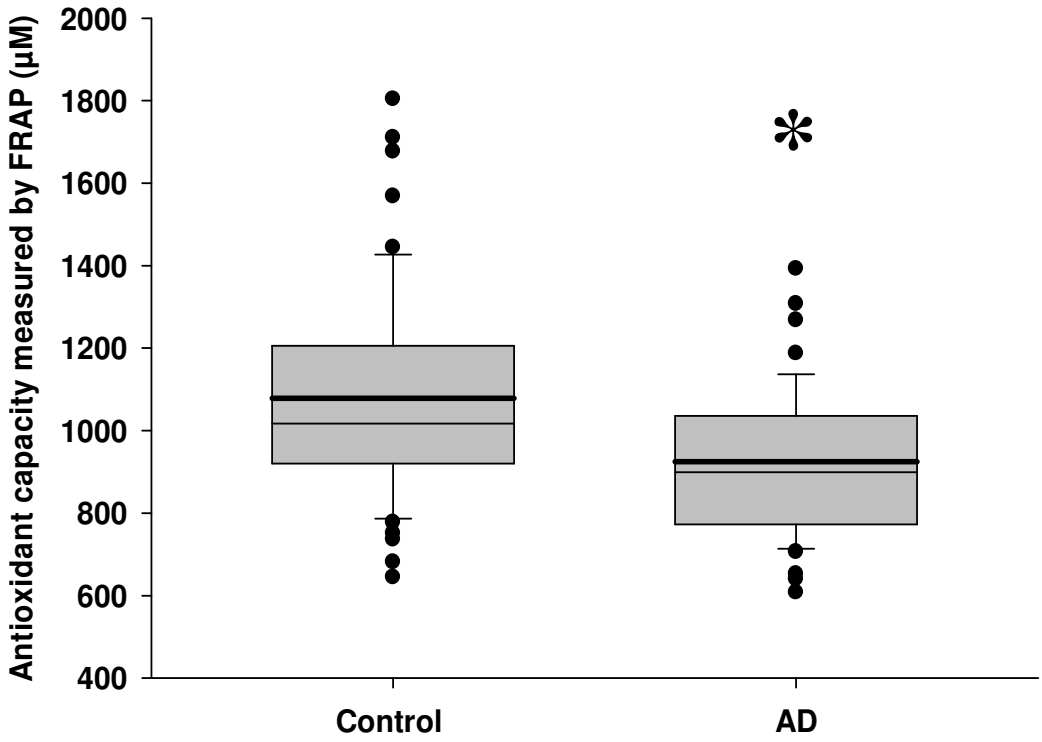

Figure 3.3. Total antioxidant capacity. TAC was measured by FRAP. Data (Control n = 59 and AD = 50) are presented as a box plot. Percentiles are represented by the box (25th and 75th) and whisker (10th and 90th) with thick and thin lines corresponding to mean and median values respectively. *Significant difference between the control and AD group (*p = 0.001). Filled circles represent outliers.

3.4.5 Plasma lipid peroxide levels

One AD sample and 4 control samples were omitted from analysis as their lipid peroxide levels were below the limit of detection of this assay (1nmol/ml). As shown in figure 3.4, there was no change in levels of lipid peroxides between the control and AD group subjects (Control 15.51 ± 19.41 Vs. AD: 14.21 ± 15.06 nmol/ml lipid peroxides, $p > 0.05$; independent samples t-test).

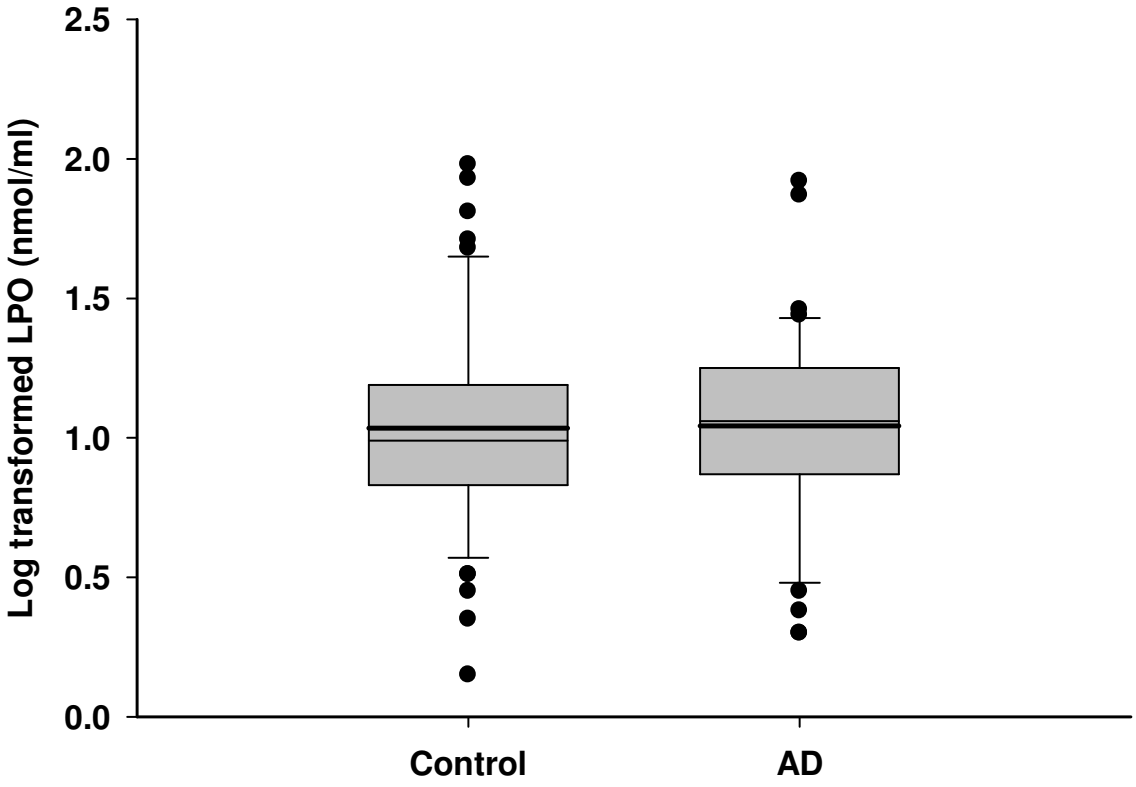

Figure 3.4. Lipid peroxide levels. Lipid peroxide levels were measured by lipid peroxide assay. Data (control n = 56 and AD n = 47) are presented as a box plot. Percentiles are represented by the box (25th and 75th) and whisker (10th and 90th) with thick and thin lines corresponding to mean and median values respectively. Filled circles represent outliers.

3.5 Discussion

The study demonstrated increased LDL protein carbonylation in patients with AD. Studies suggest that levels of oxidative stress are elevated during the earliest stages of AD (Nunomura et al., 2001). The demonstration in this work that LDL undergoes oxidation in AD, coupled to existing studies which have demonstrated that the rate of LDL oxidation increases with age and that this susceptibility to oxidation is elevated further in AD (Khalil et al., 1996; Schippling et al., 2000), may indicate that vascular change should considered as a relatively early event in AD pathology. Indeed LDL oxidation is a pathological hallmark of atherosclerosis and atherosclerosis is an associated risk factor for AD.

In contrast to LDL carbonylation, there was no difference in total plasma protein carbonylation between the AD and control groups. Existing studies assessing plasma protein oxidation in Alzheimer's disease are equivocal, with several studies reporting no change but with others reporting increased levels in AD. For example, Greilberger et al. (2008) and Bermejo and colleagues (2008), in separate studies reported increased plasma protein oxidation in a group consisting of mild cognitive impairment (MCI) and AD patients. These studies are in contrast to no differences reported in mild to moderate and advanced AD (Zafrilla et al., 2006), or in mild AD patients (Baldeiras et al., 2008). All of the studies use similar spectrophotometric methodology to assess plasma protein oxidation so differences in methodology are unlikely to account for the disparity between studies. It is possible that the severity of the disease would influence protein oxidation levels, as it has been suggested oxidative stress is prevalent in the earliest stages of the disease (Nunomura et al., 2001); however, the studies mentioned above measure plasma protein oxidation in both MCI and early AD sufferers and in advanced AD.

There was also an appreciable variation in the degree of protein oxidation within the AD group of the present study. An explanation for the discrepancy in reported protein carbonylation and the observed range of values is the multi factorial nature of AD. For example, the rate of cognitive decline between individuals suffering from AD varies considerably. In some patients cognition deteriorates rapidly, where as in others very little change or no decline is experienced (Holmes and Lovestone, 2003). Differences in the rate of cognitive decline has been shown to influence peripheral proteins levels in AD subjects (Guntert et al., 2010). These subject characteristics may therefore contribute to the individual variation in protein oxidation levels seen in this study. Other subject characteristics (e.g., physical activity pattern, diet and vitamin use) may have also influenced some of the indices measured in this study. However these were not known, and as such are an acknowledged limitation of the presented work.

Additionally, the absence of an increased plasma protein oxidation in AD in the current study may add to the evidence that suggests that oxidation events within AD are specific and critical events which take place to alter the function of certain proteins, and this may contribute to the pathology of AD, rather than oxidative damage occurring in a non specific and random manner. Previous studies assessing oxidative changes in AD brain have found similar specific protein oxidation events (Castegna et al., 2002a; Castegna et al., 2002b).

In this study we observed a significant reduction in total antioxidant TAC in an AD group compared to a control group, as measured by FRAP. Various methodologies (e.g., and total antioxidant status (TAS)) have been employed to measure total antioxidant capacity (TAC) in AD compared to control plasma. Although these methods are not identical to each other,

they all provide a quantitative indication of the levels of total antioxidant components over time, or at a given time point in plasma. The results presented here are in agreement to a recent study by Sekler et al. (2008) who used the same methodology to measure TAC and reported a significant reduction of FRAP in an AD group compared to a control group, albeit only in the most severe cases (the authors also suggested that the stage of the disease may influence TAC). Indeed, further studies have demonstrated a significant decrease of total antioxidant status (TAS) in advanced AD, but not in moderate AD (Zafrilla et al., 2006) as well as a trend for decreased TAS in MCI and AD (Baldeiras et al., 2008). In addition, a 24% decrease in TAC in plasma from probable AD compared to controls (Repetto et al., 1999) has been reported. Studies which assess levels of individual antioxidants in plasma from AD subjects report a depletion of several vitamins compared to control subjects (Bourdel-Marchasson et al., 2001; Rinaldi et al., 2003) and a reduction in an extensive range of vitamins and carotenoids has more recently been reported in AD and VaD patients (Polidori et al., 2004). It maybe that the vascular or degenerative severity of the disease accounts for the depletion of particular antioxidants, and thus contributes to the varied data reported by different groups regarding total antioxidant capacity in AD.

The physiological levels of lipid peroxides reported in this work are in agreement with other studies. For example in normal healthy individuals, levels are of low micromolar concentrations (Ferretti et al., 2008) and in patients with non-insulin dependent diabetes mellitus and metabolic disorders levels are increased to approximately 8 nmol/ml (Sodergren et al., 1998). However, no change in lipid peroxide levels was observed between control and AD subjects; this finding is in accordance with other groups who have reported no differences in MDA levels between these two groups (Polidori et al., 2004; Baldeiras et al.,

2008). On the other hand, MDA and TBARS have been reported to be increased in AD serum and plasma (Zafrilla et al., 2006; Martin-Aragon et al., 2009; Padurariu et al., 2009).

It is becoming increasingly accepted that patients with AD, more often than not, will have a vascular element to their disease pathology (Launer, 2002). The observed higher LDL oxidation level in this study concurs with this perception. Almost all healthy elderly individuals will have atherosclerotic plaque formation, and associated increased circulating oxidized LDL, if compared to younger controls (Khalil et al., 1996). However, this study presented healthy aged individuals as controls, and thus the finding that LDL oxidation was significantly higher in AD, when compared to age matched controls, goes some way to demonstrating increased LDL oxidation is part of AD pathology.

Chapter 4

Development of a 3-nitrotyrosine ELISA

4.1 Abstract

The increased production of reactive oxygen and nitrogen species contributes to oxidative stress. The reaction between nitric oxide ($NO^{\bullet}$) and superoxide ($O_2^{\bullet-}$) leads to the production of peroxynitrite ($ONOO^-$), a highly reactive molecule which has the ability to oxidize and nitrate proteins. Protein nitration is important as it can impact protein function, and is therefore of particular interest in diseases associated with increased levels oxidative stress, such as Alzheimer's disease (AD). $NO^{\bullet}$ is clearly involved in vascular function and it is sensible to suggest that there may potential link between $NO^{\bullet}$ and 3-nitrotyrosine levels in AD, given the reaction $NO^{\bullet}$ and $O_2^{\bullet-}$ to form $ONOO^-$. Plasma $NO^{\bullet}$ levels have been successfully measured in AD. In contrast, although a wide range of studies have assessed protein nitration in AD brain tissue, limited studies exist which assess levels in plasma. There is a need to develop a high throughput method to measure 3-nitrotyrosine in AD plasma, to enable the potential link between $NO^{\bullet}$ and 3-nitrotyrosine levels to be investigated in this disease. ELISA is one method which has been successfully employed to measure plasma 3-nitrotyrosine levels in individuals suffering from Diabetes Mellitus and Behçet disease, conditions both associated with increased oxidative stress. In contrast, at the time of undertaking this work, no study had previously reported the use of ELISA to measure plasma 3-nitrotyrosine levels in AD. In the study presented here, attempts were made to develop an ELISA for the high throughput measurement of 3-nitrotyrosine in AD plasma, in order to investigate the potential link between $NO^{\bullet}$ and 3-nitrotyrosine levels. Levels of 3-nitrotyrosine levels could only be detected in a minority of plasma samples when employing ELISA, suggesting that currently ELISA is not sensitive enough to detect 3-nitrotyrosine in all AD and control plasma samples.

4.2 Introduction

The increased production of reactive oxygen and nitrogen species (ROS/RNS) is a contributory factor of oxidative stress. Peroxynitrite ($ONOO^-$), a RNS produced during the reaction between $NO^\bullet$ and $O_2^{\bullet-}$ nitrates proteins in *vivo*. Protein nitration occurs when a nitro group ($-NO_2$) is substituted for a hydrogen atom on the aromatic ring of a tyrosine residue at the 3 prime position; the adduct formed is named 3-nitrotyrosine (Souza et al., 2008). At physiological pH $ONOO^-$ is rapidly protonated to form peroxynitrous acid (ONOOH), which can be homolytically cleaved to form nitrogen dioxide ($NO_2^\bullet$) and $OH^\bullet$. ONOOH may also react with CO_2 to form $NO_2^\bullet$ and the carbonate radical ($CO_3^\bullet$) (Halliwell, 2006; Souza et al., 2008), with $NO_2^\bullet$ possessing the ability to react with and nitrate tyrosine residues. Additional nitrating agents which account for *in vivo* nitration include haemoperoxidases such as myeloperoxidase and eosinophil peroxidase (Souza et al., 2008). The predominant source of protein nitration *in vivo* is from $ONOO^-$, and as such 3-nitrotyrosine is considered by many as an indirect marker for $ONOO^-$ (Beckman and Koppenol, 1996; Oldreive and Rice-Evans, 2001). However, it is appreciated that other nitrating agents may also exist *in vivo* (Oldreive and Rice-Evans, 2001).

Increased protein nitration is associated with AD brain pathology (Smith et al., 1997b; Hensley et al., 1998) and in addition, specific brain proteins have been shown to be nitrated in early AD and AD (Castegna et al., 2003; Reed et al., 2008). In contrast, limited studies have measured nitration in AD plasma. Calabrese and colleagues (2006) demonstrated that plasma proteins exhibited increased nitration in AD, however they only provided evidence for a minority of subjects using Western blotting and no statistical information was reported, hence further investigation is required. Limited information on nitration status is somewhat

surprising as a global measure of 3-nitrotyrosine in AD would be desirable for a number of reasons: firstly the current understanding of the role oxidative stress in the disease pathology would be furthered. For example there may be an additional link to vascular pathology (e.g., $NO^{\bullet}$ is clearly involved in vascular function and hence it is sensible to suggest that $NO^{\bullet}$ and $O_2^{\bullet-}$ may react); and secondly such studies would contribute to biomarker discovery.

To date several methods have been used to quantify 3-nitrotyrosine levels in healthy human plasma. A number of methodologies have been mass spectrometry based, including GC-tandem MS, GC-MS and LC-tandem MS. Non-mass spectrometry based techniques include various high performance liquid chromatography (HPLC) methods and ELISA (Tsikas and Caidahl, 2005). Reported levels of 3-nitrotyrosine from mass spectrometry based, and HPLC methods, range from approximately 1-60 nM (Tsikas and Caidahl, 2005). In addition, groups have attempted to develop a robust, reproducible and reliable 3-nitrotyrosine ELISA (see table 4.1), with the premise that it has a higher throughput, does not require specialist equipment and is less time consuming than other established techniques (i.e. GC-tandem MS, GC-MS and LC tandem MS and HPLC-ECD). There are a wide range of reported values from such assays, levels range between undetectable to 0.1 µM for healthy subjects, and are increased further in diseased subjects. These data also suggest that when assessing 3-nitrotyrosine levels in plasma by ELISA, from diseased subjects, levels are elevated and typically of high nM or low µM concentrations.

At the time of commencing this work, no studies had measured 3-nitrotyrosine in AD plasma, therefore the primary aim of this work was to attempt to develop an ELISA in order to measure total levels of 3-nitrotyrosine in AD.

Authors	Participants	ELISA	Plasma levels
Khan *et al*. (1998)	4 healthy non-smoking subjects	Competitive ELISA	0.12 ± 0.02µM
Ter Steege *et al.* (1998)	12 Control and 19 Celiac disease subjects	In house sandwich ELISA	Control s: undetectable Celiac disease:1.27 ± 1.03µM
Ceriello *et al.* (2001)	40 type II diabetics and 35 control subjects	Indirect ELISA	Controls: undetectable Diabetic Type II: 0.251 ± 0.141µM
Sun *et al.* (2007)	70 healthy individuals and subjects with various inflammatory conditions	In house sandwich ELISA	Males: 8.3 ± 8.6nM Females: 7.5 ± 5.3nM
Sakano *et al*. (2009)	68 healthy subjects	Commercially available ELISA	Controls: 93.3 ± 3.2nM In individuals who exercised ≥ 6 times a week levels elevated to 460 ± 207.4nM

Table 4.1. Measurement of plasma 3-nitrotyrosine by ELISA

4.3 Methods

4.3.1 Sample Population

Pooled AD and age matched control plasma from a subset of samples were obtained as described in general methods **section 2.1.4, table 2.1**. Individual AD and age matched control samples from a second subset of samples were obtained as described in general methods **section 2.1.4, table 2.2**.

4.3.2 BCA assay

Total protein concentration was determined by the BCA assay as described in general methods **section 2.2.1.**

4.3.3 HPLC-ECD

4.3.3.1 Sample Preparation

For measurement of total 3-nitrotyrosine samples were diluted to 1 mg/ml in Calcium Chloride (10 mM) and hydrolysed with Pronase (20 µg/ml) at 37ºC overnight and analysed by HPLC-ECD. For measurement of bound 3-nitrotyrosine samples (1 mg/ml) containing Pronase (20 µg/ml) and Calcium Chloride (10 mM) were incubated at 37ºC overnight. Samples were washed with ice cold methanol (300 µl), mixed thoroughly and centrifuged at 3,500 xg for 10 minutes. The supernatant was discarded and this procedure was repeated. The resultant protein pellet was re-suspended in mobile phase (100 µl) and analysed by HPLC-ECD. Samples were assayed in duplicate or triplicate.

4.3.3.1 Detection and quantification of 3-nitrotyrosine

A modified high performance liquid chromatography with electrochemical detection (HPLC-ECD) method, from that described by Maruyama et al. (1996) was undertaken for the detection of plasma 3-nitrotyrosine and nitrated BSA. Synthetic 3-nitrotyrosine was used to calibrate the HPLC and produce a series of known standards for subsequent sample analysis (see figure 4.1). Samples were spiked with a known concentration of synthetic 3-nitrotyrosine (10 µM) and loaded (10 µl) onto the column (Phenomenex, Luna 3 µM, C18 (2) 100_A, 150 x 4.60 mm). Mobile phase (Phosphoric Acid (50 mM), Citric Acid (50 mM, pH 5.0), EDTA (40 mg/l), Octane Sulphonic Acid (100 mg/l) and methanol (5%)) was set at a flow rate of 1.5 ml/min. An applied voltage was set at 990 mV as optimized from preliminary experiments (See Appendix I). Standard curves were constructed on a regular basis, and the limit of detection for this technique was consistently 1 µM. Levels of 3-nitrotyrosine were calculated from a standard curve of peak areas (mV*min) from known concentrations of 3-nitrotyrosine using linear regression. The peak area of 3-nitrotyrosine (10 µM) was taken away from peak areas measured for spiked samples prior to this calculation.

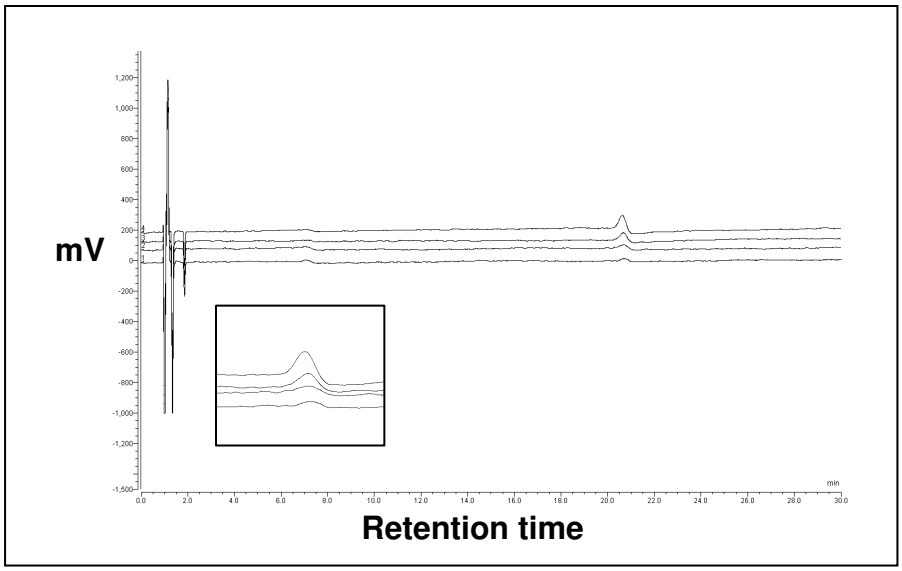

Figure 4.1. Chromatogram of 3-nitrotyrosine synthetic standards. Peaks from top to bottom correspond to 20 µM, 10 µM, 5 µM, 2.5 µM and 1.25 µM. Area of chromatogram where 3-nitrotyrosine peaks reside is enlarged in boxed area.

.

4.3.4 Preparation of nitrated BSA using various reagents

4.3.4.1 Sodium nitrite

BSA (5 mg/ml) was dissolved in ddH_2O and adjusted to pH 3.5 with glacial acetic acid. Sodium nitrite (200 mM) was then added to a final concentration of 1 mM (ter Steege et al., 1998).

4.3.4.2 Peroxynitrite

Synthesis of peroxynitrite was based on a method described by Packer and Murphy (1994). Acidified hydrogen peroxide (0.6 M HCl + 0.7 M hydrogen peroxide) and sodium nitrite (0.6M) were mixed thoroughly and dropped into rapidly stirred sodium hydroxide (2 M) to arrest the reaction. Solutions of synthesised peroxynitrite were quantified using a molar absorbance co-efficient value ($\varepsilon_{302\ nm}$ = 1670 M^{-1} cm^{-1}(Packer and Murphy, 1994)) and were used immediately to nitrate BSA. BSA (1mg/ml) was dissolved in phosphate buffer (250 mM K_2HPO_4-KH_2PO_4, pH 7.4) and exposed to peroxynitrite (1 mM). The solution was incubated for one hour in a water bath set at 37ºC and dialyzed against double distilled water for 24 hours, with six changes, to remove any nitrate or nitrate produced from peroxynitrite decomposition (Whiteman and Halliwell, 1999).

4.3.5 1-DE, silver staining and Western blotting

Nitrated BSA (5µg) was separated on a 1D gel, silver stained and blotted for 3-nitrotyrosine as described in general methods **section 2.2.5, 2.2.7** and **2.2.8.** For Western blotting, mouse monoclonal anti-nitrotyrosine antibody was used at 1:500 with an appropriate horseradish peroxidase conjugated secondary antibody (1: 2,000).

4.3.6 3-nitrotyrosine ELISA

4.3.6.1 Preparation of 3-nitrotyrosine standards

To prepare 3-nitrotyrosine standards for use in ELISA, serial dilutions of a known concentration of nitrated BSA stock (12.2 M) in coating buffer (50 mM Sodium carbonate, pH 9.2) was undertaken.

4.3.6.2 ELISA

A modified indirect ELISA protocol, based on that described by Ceriello et al. (2001) was undertaken. Samples (50 µl) diluted in coating buffer (50 mM Sodium carbonate, pH 9.2) were applied to a microtitre plate, for one hour at 37ºC. Wells were blocked overnight at 4ºC with 1% BSA in PBST (0.1%), incubated for 2 hours at 37ºC with mouse monoclonal anti-nitrotyrosine antibody (1:500) and incubated with a horseradish peroxidase conjugated goat anti-mouse IgG secondary antibody (1:4000). The horseradish peroxidase reaction product was produced using citrate phosphate buffer 0.15 M (pH 5), O-phenylenediamine (2 mg) and hydrogen peroxide (1:125). The reaction was arrested with 2M H_2SO_4 and absorbance measured at 490nm using a microtitre plate reader. Background was accounted for by taking away blank absorbance values from all wells. The concentrations of nitrated proteins present in samples were compared to the standard curve nitrated BSA standards of known concentrations. They were expressed as µM BSA equivalents (i.e. an equivalent concentration of nitrotyrosine in BSA).

4.3.7 In-solution digestion

An in-solution digestion protocol based on that described by Kinter and Sherman (2000) was used to digest samples. Bovine serum albumin (BSA) was evaporated and re-suspended in

6M urea, 100mM Tris buffer to a concentration of 10mg/ml. Standards (100µl containing 1mg of protein) were diluted with 775µl ddH_2O (to reduce concentration of urea and retain trypsin activity). Trypsin (20 ng/µl) was added to digested standards (1:100 substrate to protease ratio), and ddH_2O was used as a substitute for controls, all standards were incubated overnight at 37ºC. Reactions were stopped by adjusting pH to < 6 with concentrated acetic acid. Standards were concentrated to approximately 100µl and total protein levels were determined using the BCA assay. Zip tips were used to remove urea from standards. They were prepared by wetting with 50% HPLC grade acetonitrile twice and then equilibrated with 0.1% trifluoroacetic acid twice. Digests were prepared by adding 1µl of 1% trifluoroacetic acid to 10µl of the digest. Once peptides were bound to the zip tip, they were washed with 0.1% trifluoroacetic acid twice and then eluted into 5µl of 50% acetonitrile solution. Acetonitrile was subsequently removed by vacuum centrifugation. Peptides were then resuspended in appropriate buffer for downstream applications.

4.4 Results

4.4.1 Measurement of 3-nitrotyrosine using HPLC-ECD

Quantification of plasma levels of 3-nitrotyrosine was undertaken in a small group of AD (n=4) and age-matched control plasma (n=3) in order to establish whether, 3-nitrotyrosine levels were detectable, and whether these levels were distinguishable between AD and control subjects. As shown in figure 4.2, levels of 3-nitrotyrosine in half of the samples analyzed are negligible and fall on or below the limit of detection. However, in three subjects 3-nitrotyrosine was detected in the micromolar range (3 to 8 μM). Based on these results, in order to detect significant differences in 3-nitrotyrosine between AD and control samples, assessment of a large cohort would be necessary (sample size calculation estimated > 300). HPLC is an extremely time consuming and expensive technique and in order to assess 3-nitrotyrosine in a large cohort of AD and age-matched control samples, ELISA was attempted.

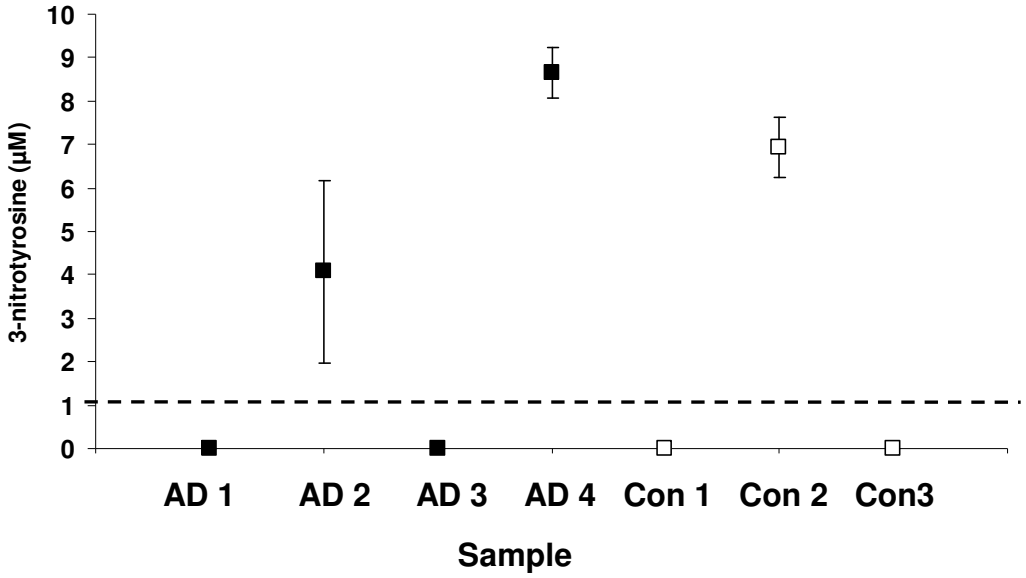

Figure 4.2. Plasma levels of 3-nitrotyrosine from AD and controls using HPLC-ECD. Plasma from AD (n=4) and age-matched control subjects (n=3) was analysed for 3-nitrotyrosine using HPLC-ECD. Error bars represented as standard error of the mean and samples were assayed in duplicate. Limit of detection (1 µM) shown by dotted line.

4.4.2 Measurement of 3-nitrotyrosine using ELISA

4.4.2.1 Preparation of nitrated standards using sodium nitrite

For preparation of nitrated standards, BSA was nitrated with sodium nitrite (BSA-$NaNO_2$). A noticeable colour change from colourless to yellow was observed after BSA solutions were incubated with sodium nitrite. This colour change may account for synthesis of $ONOO^-$, but is likely to indicate the presence of 3-nitrotyrosine (ter Steege et al., 1998). Levels of nitrated BSA were calculated as 8.87 ± 1.95 µM by HPLC-ECD. However, as shown in figure 4.3, when levels of nitrated BSA were assessed by ELISA no signal was evident.

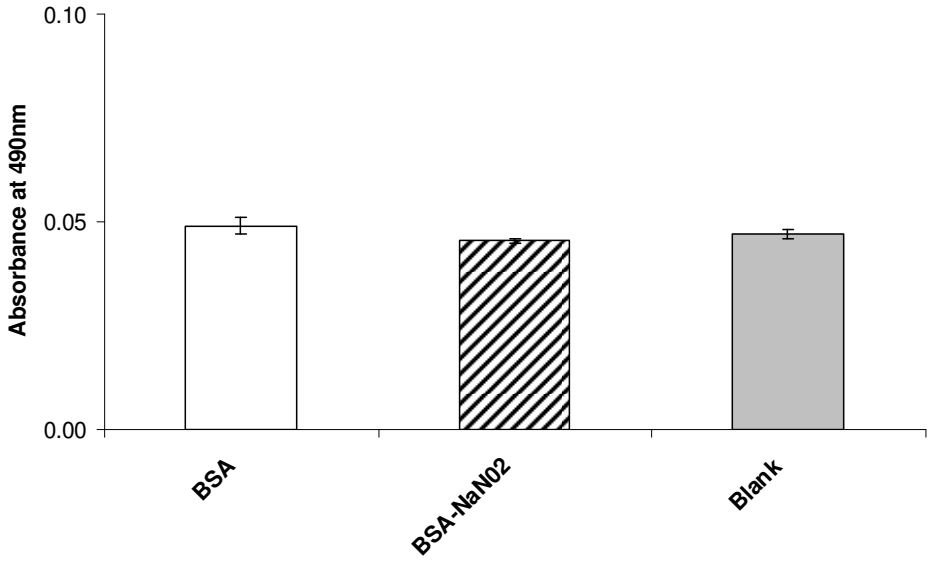

Figure 4.3. ELISA to assess nitration to BSA using sodium nitrite. Samples (5 mg/ml) were assessed for nitration by ELISA (see section 4.3.4). Error bars are displayed as SEM. Samples were run in triplicate.

4.4.2.2 Western blotting to assess antibody binding

The results of the ELISA suggested that nitration of BSA was unsuccessful. To confirm this Western blotting was undertaken. In addition, to confirm presence of BSA, 1-DE and silver staining was run in parallel. As shown in figure 4.4a (lanes 1 and 2), BSA and BSA-$NaNO_2$ are present on a 1D gel as evidenced by distinct bands at approximately 70 kDa. In contrast, no band is present in the region of 70 kDa on a Western blot for nitrated BSA (Figure 4.4b, lane 2).

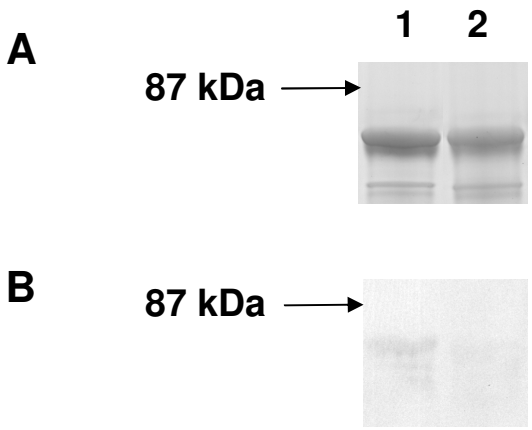

Figure 4.4. BSA nitration using sodium nitrite. Lane 1, BSA (5 µg); Lane 2, BSA treated with $NaNO_2$ (5 µg). A) Silver stained 1D gel B) Western blot for 3-nitrotyrosine.

To explain these disparities between quantification of 3-nitrotyrosine, using HPLC-ECD, and validation with 3-nitrotyrosine antibody, bound 3-nitrotyrosine was measured using HPLC-ECD. Levels of 'bound' 3-nitrotyrosine were below the detection limit, and hence it was considered that free 3-nitrotyrosine was formed. Together these data suggested that nitration of BSA using this particular nitrating agent was ineffective.

4.4.2.3 Preparation of nitrated standards using peroxynitrite

Peroxynitrite is a further agent commonly used to nitrate proteins. As a consequence peroxynitrite was employed as a nitrating agent as a consequence of the ineffective nitration of BSA using sodium nitrite. The concentration of prepared peroxynitrite solutions ranged between 20-30mM. BSA treated with $ONOO^-$ was assayed for bound and total 3-nitrotyrosine levels by HPLC-ECD. Levels were found to be 2.56 ± 0.22 nmol/mg and 12.14 ± 0.77 μM respectively. From these data bound 3-nitrotyrosine is evident; suggesting that BSA nitration using peroxynitrite had been successful.

4.4.2.4 Confirmation of BSA nitration using $ONOO^-$

To confirm that BSA had been successfully nitrated, Western blotting was undertaken. In addition, to confirm presence of BSA, 1-DE and silver staining was run in parallel. As shown in figure 4.5a (lanes 1 and 2), BSA and BSA-$ONOO^-$ are present on a 1D gel as evidenced by distinct bands at approximately 70 kDa. In addition, the Western blot presented in figure 4.5b demonstrates the successful nitration of BSA using peroxynitrite. This is demonstrated by the presence of a distinct band present at approximately 70 kDa for BSA treated with $ONOO^-$, but not for BSA (Figure 4.5b, lanes 1 and 2).

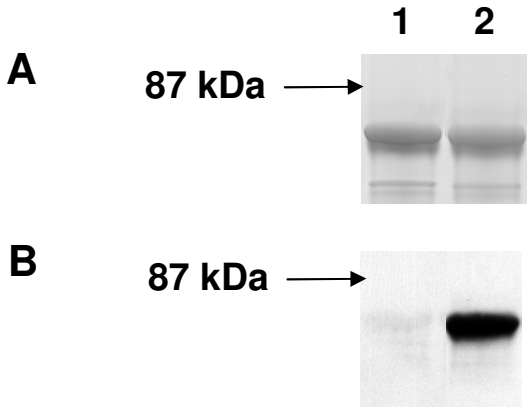

Figure 4.5. BSA nitration using peroxynitrite. Lane 1, BSA (5 µg); Lane 2, BSA treated with $ONOO^-$ (5 µg). A) Silver stained 1D gel B) Western blot for 3-nitrotyrosine.

4.4.2.5 Construction of five point 3-nitrotyrosine standard curve for ELISA

A standard curve of known nitrated BSA concentrations was constructed and assessed using ELISA (see methods section 4.3.6.1). As shown in Figure 4.6a, nitrated BSA concentrations ranging between 5 and 400 nM are detectable with the linear region of the standard curve evident between 5 and 100 nM nitrated BSA equivalents. A plateau at concentrations greater than approximately 150 nM nitrated BSA equivalents was observed. Figure 4.6b shows a 5 point standard curve, for the linear region of the standard curve, for three separate experiments.

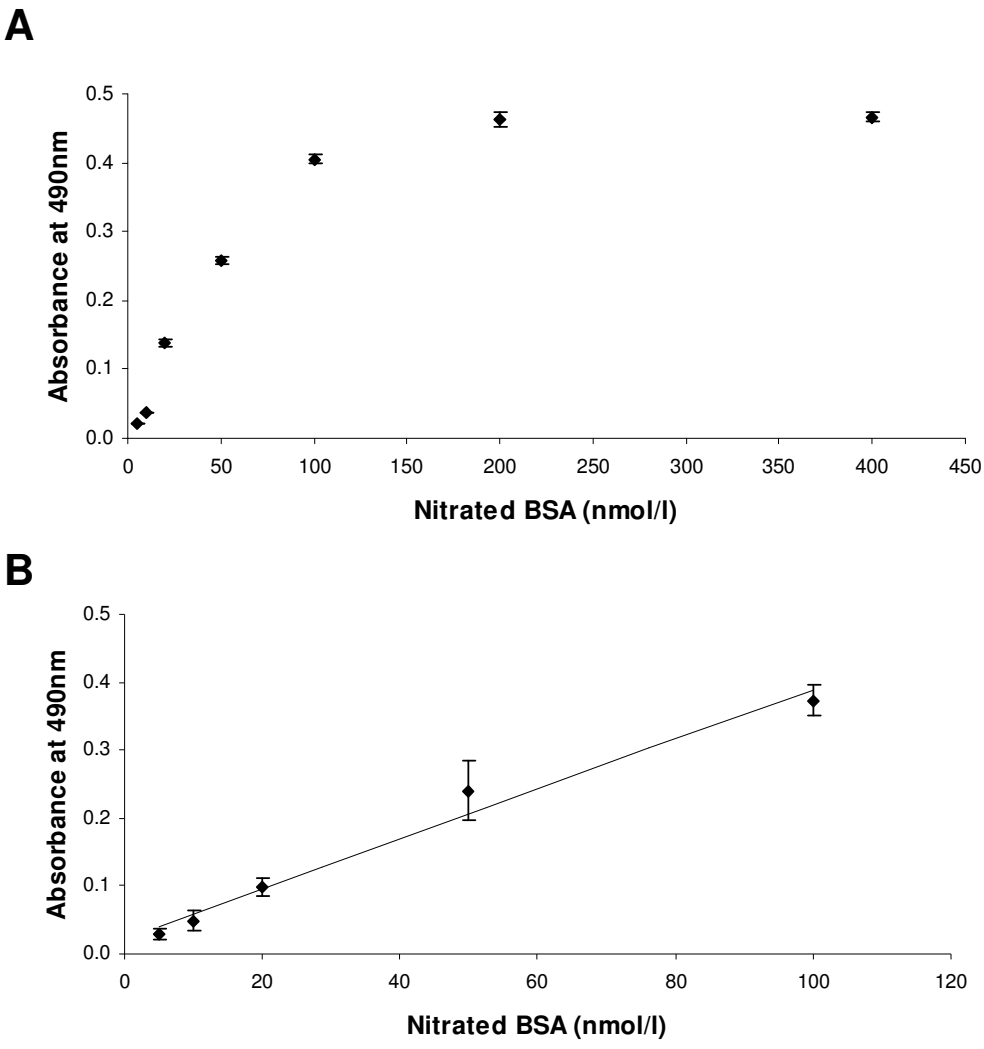

Figure 4.6. 3-nitrotyrosine standard curve. A) Levels of 3-nitrotyrosine plateau at approximately 150-200 nmol/l nitrated BSA B) A linear 5 point standard curve ranging from 5 (lowest detectable nitrated BSA standard) to 100 nmol/l nitrated BSA (n=3). Error bars displayed as SEM.

4.4.2.6 Levels of 3-nitrotyrosine in AD and age matched control plasma

4.4.2.6.1 Pooled samples

Due to the availability of AD and control plasma, initial experiments assessed 3-nitrotyrosine levels using pooled samples (n=3). Figure 4.7 shows that detectable levels of 3-nitrotyrosine were present in these pooled sample sets.

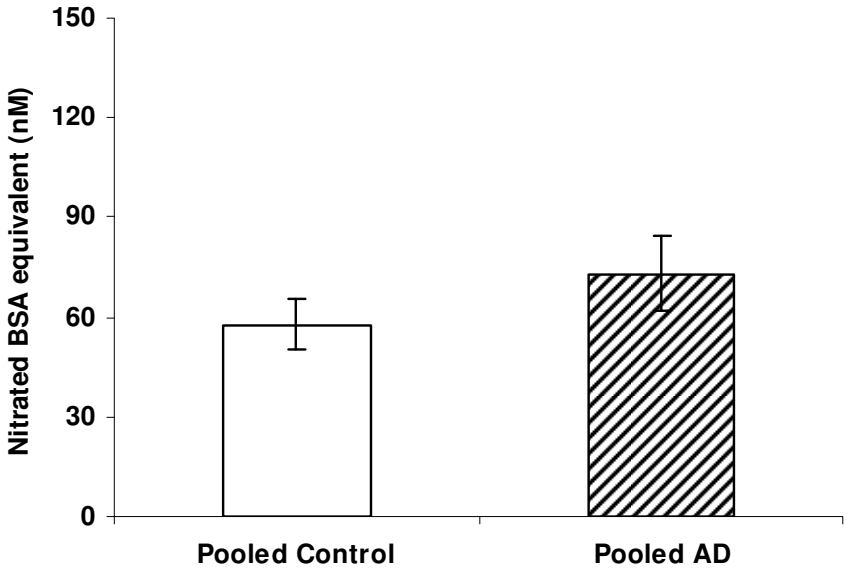

Figure 4.7. Pooled plasma 3-nitrotyrosine levels. Level of nitration expressed as nitrated BSA equivalents calculated by linear regression Pooled samples diluted 1 in 5 and error bars displayed as SEM.

4.4.2.6.2 Individual samples

A small subset of samples (7 AD and 7 age matched control) from a second cohort were assayed for 3-nitrotyrosine at a 1 in 5 dilution. This was to confirm further that 3-nitrotyrosine is detectable in individual plasma samples from this population, and to determine whether a difference is detectable using this methodology. As shown in figure 4.8a, detectable levels of nitration were variable between individual samples, with some samples above but others below the lowest detectable nitrotyrosine standard (5 nM nitrated BSA equivalent). Hence a larger subset of individual samples (12 AD and 12 control subjects) was assessed at a greater concentration. Samples were diluted 1 in 2. In agreement with the previous experiment, figure 4.8b demonstrates that a minority of samples are above the lowest detectable nitrotyrosine standard (5 nM nitrated BSA equivalent) with most below this point.

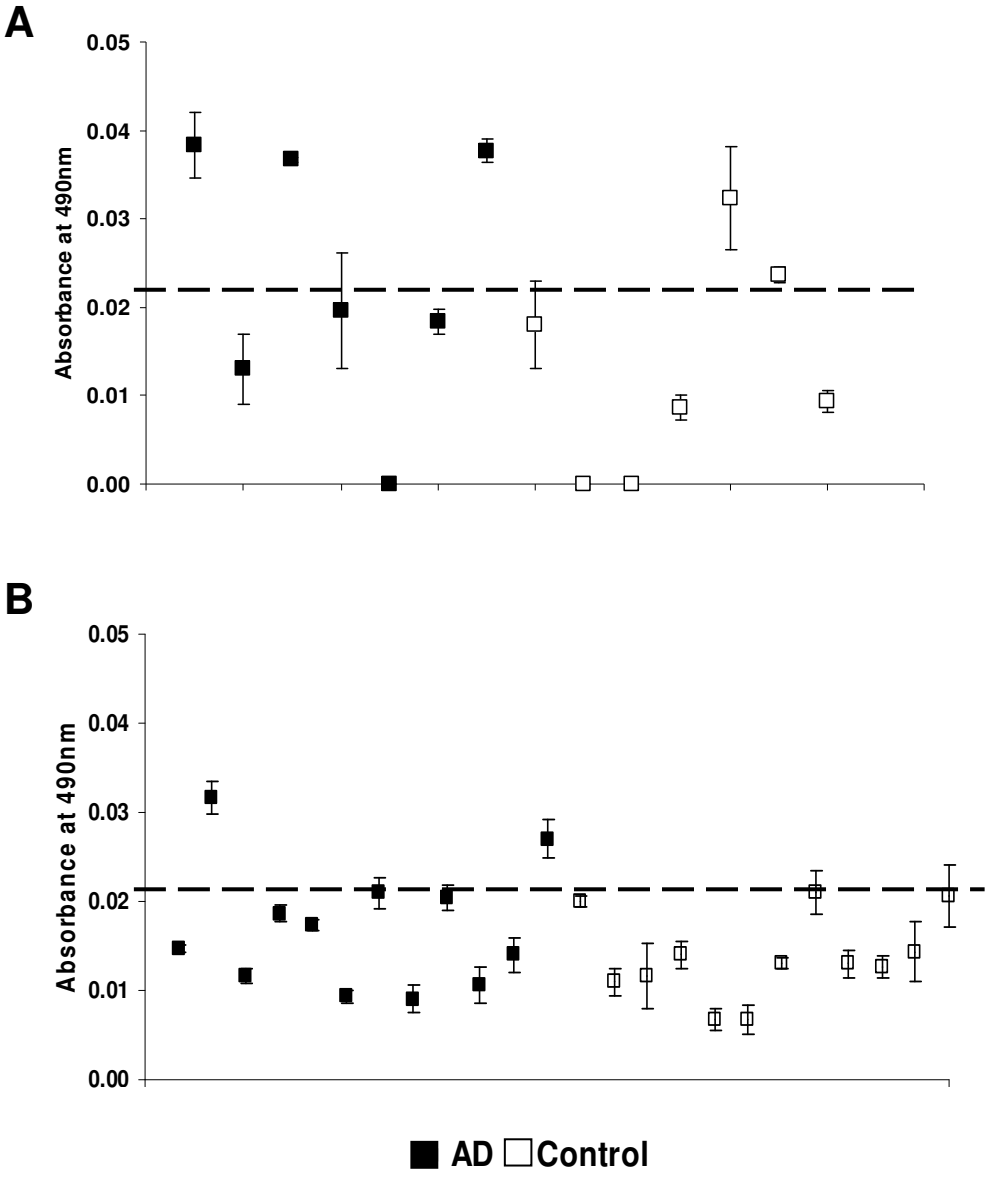

Figure 4.8. Plasma levels of 3-nitrotyrosine in AD and control samples. Levels 3-nitrotyrosine as determined by ELISA. A) Subset of 7 AD and 7 control plasma samples diluted 1 in 5. B) Subset of 12 AD and 12 control plasma samples diluted 1 in 2. The lowest detectable nitrated BSA standard for this assay was 5 nM (Indicated by dotted line). Error bars represented as SEM and samples were assayed in triplicate.

4.4.2.7 Increasing detectable levels of 3-nitrotyrosine by trypsin digestion

In order to improve the sensitivity of the ELISA, tryptic digestion of nitrated BSA to peptides was attempted. It was hypothesised that by cleaving proteins into smaller peptides nitrated tyrosine residues, that preferentially reside in the interior of proteins, would be exposed, and that this would allow binding of an antibody specific for the 3-nitrotyrosine adduct.

BSA and BSA-$ONOO^-$ were compared to BSA and BSA-$ONOO^-$ digests using indirect ELISA. All samples were plated as the same protein concentration to ensure nitration levels were comparable. As shown in Figure 4.9, an expected increase in signal for BSA-$ONOO^-$ compared to BSA is apparent. Surprisingly, the BSA-$ONOO^-$ digest exhibits lower signal compared to BSA-$ONOO^-$, and the same observation is evident for the BSA digest compared to BSA. These data showed that detectable levels of nitration are reduced using this approach. One possible reason for this observation may be that peptides do not adhere to, or are less likely to adhere to the microtitre plate when compared with proteins. The stringent washing steps employed during ELISA may also remove peptides from the surface of the microtitre plate. Peptides containing a 3-nitrotyrosine adduct may not therefore be recognized by an antibody specific for the 3-nitrotyrosine epitope.

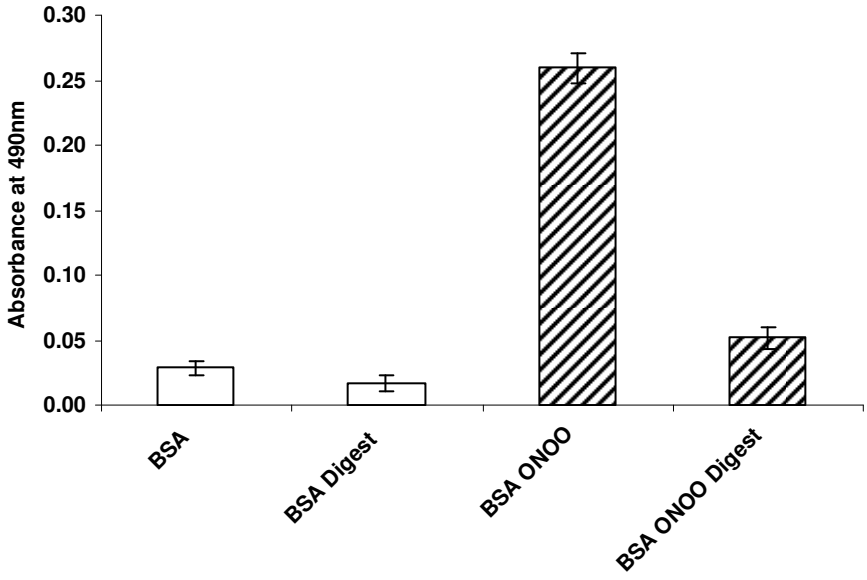

Figure 4.9. In-solution trypsin digestion of BSA and BSA-ONOO- samples. Comparison of nitration levels between digested and non-digested BSA samples and BSA-$ONOO^-$. All samples plated at the same protein concentration (2.5 µg/ml), assayed in duplicate and values are represented as mean ± SEM.

4.5 Discussion

It is firmly established that heightened levels of oxidative stress contribute to development and progression of Alzheimer's disease (AD) (Markesbery, 1997). In regions of the brain most affected by AD pathologies increased levels of protein nitration are evident, suggesting a link between increased protein nitration and AD (Smith et al., 1997b; Hensley et al., 1998). Moreover, specific proteins in the IPL are targets of nitration and this modification may potentially alter their normal function, in AD (Castegna et al., 2003). Although markers of oxidative stress in plasma are increasingly being assessed for their application as a biomarker, and to contribute to current understanding as to their role in AD (Zafrilla et al., 2006; Baldeiras et al., 2008), few studies have assessed global levels of protein nitration in peripheral tissues in AD (Calabrese et al., 2006; Korolainen and Pirttila, 2009).

This work attempted to measure total levels of protein nitration in AD plasma. HPLC-ECD was initially used to measure 3-nitrotyrosine in AD plasma as it is considered one of the most sensitive and specific methods for 3-nitrotyrosine measurement in biological fluids (Hensley et al., 1999; Duncan, 2003). After establishing the optimal applied voltage to use (see Appendix I), a detection limit of 1 µM was observed. In a small subset of AD and age matched control subjects analysed, levels of 3-nitrotyrosine were on or below the limit of detection. Hence, in order to gain a valid measure of 3-nitrotyrosine it was evident that a large sample set would be necessary. Thus attempts were made to develop an in-house ELISA.

In order to prepare a series of known nitrated standards for use in ELISA initial experiments used sodium nitrite to nitrate BSA. Sodium nitrite was used as work by Onshima and

colleagues (1990) had previously demonstrated that approximately 2nmol of 3-nitroytrosine are produced per milligram of protein when exposed to this agent under acidic conditions. The phenolic hydroxyl group of protein bound tyrosine residues has a pK_a of 10-10.3. Upon nitration this is lowered by three pH units to 7.2-7.5 and causes the phenolate ion to be formed at a lower pH (Souza et al., 2008). The phenolate ion produces an intense yellow colour indicating 3-nitrotyrosine formation (ter Steege et al., 1998). After initially observing a notable colour change in BSA treated with $NaNO_2$ and detecting levels of total 3-nitrotyrosine by HPLC, no signal was evident using ELISA or Western blotting. Having shown that levels of bound 3-nitrotyrosine were below the limit of detection it was considered that free 3-nitrotyrosine was potentially formed in solution when synthesising the nitrated protein.

However, $ONOO^-$ is relatively stable in alkaline solution, but rapidly decomposes under acidic conditions (Beckman et al., 1994), and hence it was not known in this work whether $ONOO^-$ was actually formed during the sodium nitrite treatment. Additionally, it was not known whether Pronase successfully cleaved protein at every possible site, which may account for levels not being able to be detected. A further possibility is that other modifications to the may have occurred. For example, the modification 3-chlorotyrosine produces a peak at the same retention time as 3-nitrotyrosine using HPLC-ECD (Hensley et al., 1999). Although these two modifications are distinguishable by their electrical potential, in the work presented this was not investigated, and so this may have contributed to the peaks seen on chromatograms. Consequently peroxynitrite was used to nitrate BSA for preparation of standards for ELISA. This was successful and confirmed by HPLC-ECD and

Western blotting, Approximately 2.5nmol 3-nitrotyrosine per milligram of protein was found to be nitrated which is comparable to a study by Whiteman and Halliwell (1999).

The resulting ELISA was able to detect 5nM BSA 3-nitrotyrosine (the lowest standard), with saturation of antibody binding at concentrations greater then approximately 150nM BSA 3-nitrotyrosine. These observations are in agreement with other 3-nitrotyrosine ELISA's presented in existing literature: Ceriello and colleagues (2001) reported that the limit of detection of their assay was 10 nM and that there was an evident flattening of the standard curve at concentrations greater than 400 nM. In addition, Sun et al. (2007) reported saturation of antibody binding at 3-nitrotyrosine concentrations exceeding 200 nM using a commercial competitive ELISA.

Using a subset of pooled samples initial results suggested that a detectable difference in 3-nitrotyrosine levels was evident between AD and control. However, when individual samples were assayed the majority fell below, or were near the limit of detection. These observations indicate that only a minority of plasma samples exhibit measurable levels of 3-nitrotyrosine when assessed by ELISA. The detectable levels evident in pooled samples presented in this study can be explained by at least one individual sample present in the pool having detectable levels of 3-nitrotyrosine, and substantiate this assumption. Moreover, these data are comparable to those reported in a recent study which used commercial ELISA to assess total levels of 3-nitrotyrosine in plasma from 17AD and 18 control subjects. Within this data set only three AD, and four control samples had measurable levels of 3-nitrotyrosine (above detection limit of the assay: 2 nM) (Korolainen and Pirttila, 2009).

It was hypothesised that the signal in these plasma samples could be increased by digesting plasma proteins into peptides. The rationale being that 3-nitrotyrosine adducts within the protein structure would be exposed and be recognized by an anti-nitrotyrosine antibody which would otherwise not be able to be detected. It was observed that detectable signal was markedly reduced in standard samples which had been digested with trypsin. Potential reasons for these observations maybe that non-specific binding sites are removed, or peptides adhere less well to the microtitre surface as they are too small to bind sufficiently. Consequently peptides with the 3-nitrotyrosine adduct would not then be recognized by an antibody specific for this particular epitope.

In conclusion, these data suggest that, the measurement of 3-nitrotyrosine in order to distinguish detectable differences between AD and age matched control is difficult using HPLC-ECD. It was observed that concentrations of 3-nitrotyrosine in AD samples were on the limit of detection of the HPLC-ECD system. Secondly the measurement of 3-nitrotyrosine using an indirect ELISA was found to be equally challenging. Increasing the sample size did not improve the ability to detect differences in 3-nitrotyrosine between AD and age matched controls. Although measurement of 3-nitrotyrosine using ELISA in this population is in its infancy, one may speculate that the current sensitivity of ELISA cannot cope with the individual variation of 3-nitrotyrosine levels within this sample population. Thirdly, the hypothesis that 3-nitrotyrosine signal could be increased by digesting proteins into peptides, thereby exposing 3-nitrotyrosine adducts and increasing antibody binding, is unproven.

Chapter 5

Peripheral markers of nitrative and oxidative stress in Alzheimer's disease

5.1 Abstract

It is well established that increased levels of oxidative and nitrative stress, in the brain, are part of Alzheimer's disease (AD) pathology. In contrast, levels require further clarification in plasma. To extend previous work presented in Chapter 3, analysis of markers of oxidative stress were undertaken in a further AD (n=25) and control plasma (n=25) sample set. In addition, further measures to assess protein nitration and nitric oxide metabolites (NO_x) were employed. No differences in total protein oxidation and antioxidant capacity ($p > 0.05$) were found. In contrast, plasma NO_2^-/ NO_3^- levels were significantly reduced ($p < 0.001$) and one plasma protein of approximately 170 kDa exhibited increased nitration in the AD group ($p = 0.001$). When assessed by 1-DE, Western blotting and mass spectrometry (MS) this plasma protein was identified as alpha-2-macroglobulin (α-2M).

5.2 Introduction

It is widely considered that increased oxidative stress, in the brain, is part of AD pathology. This view is based on extensive studies in brain tissue which have reported increased protein oxidation, lipid oxidation and protein nitration in AD (Smith et al., 1997b; Markesbery and Lovell, 1998; Aksenov et al., 2001; Butterfield et al., 2007). In contrast, levels of plasma protein nitration have been reported in only two studies involving AD sufferers (Calabrese et al., 2006; Korolainen and Pirttila, 2009), and levels of protein oxidation remain unclear in this tissue.

Central to protein nitration *in vivo* is the nitrating agent peroxynitrite ($ONOO^-$) (Souza et al., 2008), produced during the reaction between nitric oxide ($NO^\bullet$) and superoxide ($O_2^{\bullet-}$) (Souza et al., 2008). Therefore, $NO^\bullet$ and $O_2^{\bullet-}$ can be considered as important molecules involved in the process of protein nitration. $NO^\bullet$ possesses several important functions in the body. It is a potent vasodilator and regulates blood pressure, inhibits platelet and leukocyte adhesion, and thus has anti-atherosclerosis properties (Maxwell, 2002). *In vivo* $NO^\bullet$ production is typically assessed by measurement of the stable end products of $NO^\bullet$, nitrite (NO_2^-) and nitrate (NO_3^-) (Moshage et al., 1995; Zahedi et al., 2008). $NO^\bullet$ and $O_2^{\bullet-}$ are produced by several cells in the body and these include endothelial cells, macrophages and leukocytes, hence $ONOO^-$ production can occur within close proximity to these sites (Oldreive and Rice-Evans, 2001).

In one study, plasma protein nitration levels were shown to be increased in AD by Western blotting (Calabrese et al., 2006). However, only one Western blot representing a few plasma samples was shown, and no protein band analysis or statistical data was reported. In studies where it has been assessed, $NO^\bullet$ levels are reduced in AD serum and plasma (Selley, 2003;

Corzo et al., 2007). Given these observations, coupled to AD being a condition associated with increased oxidative stress, measurement of plasma protein nitration in AD is needed. Moreover, the relationship between plasma levels of $NO^{\bullet}$ and protein nitration requires investigation in this disease.

Plasma protein oxidation levels in AD compared to control patients have been investigated more extensively than protein nitration, but still require further clarification. The work presented in Chapter 3 of this thesis showed that plasma protein oxidation levels were comparable between AD and age-matched controls. These data are in agreement with some existing studies (Polidori et al., 2004; Zafrilla et al., 2006), but not with others (Greilberger et al., 2008; Baldeiras et al., 2008).

Given the extremely limited studies which measure protein nitration in AD, the principle aim of this work was to compare levels of plasma protein nitration between a group of AD and control subjects using Western blotting, as well as investigate the relationship between plasma protein nitration and nitric oxide levels. In addition, a broad range of oxidative indices were measured in a different sample set to that used in Chapter 3. More specifically, levels of plasma protein carbonylation were measured in order to confirm the comparable levels reported between AD and control subjects in Chapter 3.

5.3 Methods

5.3.1 Declaration of ownership

In this Chapter the advice of Mr Andrew Jones was sought in order to undertake LC-MS/MS and CID. Responsibility for the choosing of filtering parameters for data analysis, and decisions on sample preparation were made by the author. The author was also present for the running of this analytical technique and was also responsible for all further data analysis.

5.3.2 Sample Population

AD samples and age matched control samples were obtained as described in general methods **section 2.1.4.** In total, 50 patients and control volunteers were used for this study (25 in each group).

5.3.3 BCA assay

Total protein concentration was determined by the BCA assay as described in general methods **section 2.2.1.**

5.3.4 Measurement of total nitrite and nitrate levels in plasma

5.3.4.1 Principle of the Griess Assay

The Griess Assay was employed to assess total levels of the metabolites NO_2^- and NO_3^- in AD and control plasma samples. As shown in figure 5.1, plasma samples were deproteinized and the supernatant removed for analysis. Any NO_3^- present in the supernatant was reduced to NO_2^- by the addition of vanadium (III) chloride. Griess Reagent was subsequently added and a colour change which is directly proportional to the level of NO_2^- was observed. This colour change can be measured by a spectrophotometer set at 540 nm and the amount of

nitrite in samples can then be determined by comparison to a standard curve of known nitrite concentrations. Total nitrite and nitrate levels were represented as total nitric oxide metabolites (NO_x) and measurement of NO_x is considered a direct marker of *in vivo* $NO^{\bullet}$ production (Moshage et al., 1995; Miranda et al., 2001).

5.3.4.2 Measurement of NO_x using the Griess Assay

Measurement of NO_x was undertaken as described by Zahedi et al. (2008). Plasma samples (100 µl) were diluted fourfold with HPLC grade water (375 µl) and 25 µl zinc sulphate (300 mg/ml) added to give a final concentration of 15mg/ml (Moshage et al., 1995). Samples were centrifuged at 10,000 g for 10 minutes (Miranda et al., 2001; Zahedi et al., 2008) and supernatants (100 µl) were applied to a 96 well microtitre plate. To each well 100 µl vanadium (III) chloride (8mg/ml) was added and then. 50 µl sulphanilamide (2%) and 50 µl N-(1-naphthyl) ethylendiamine dihydrochloride (0.1%) was added immediately. Plates were incubated at 37^0C for 30 minutes and absorbance read at 540 nm (Multiscan MS, Labsystems, Finland) (Zahedi et al., 2008). Total nitric oxide metabolites were calculated from the linear standard curve of known nitrite concentrations ranging from 0-100 µM (Zahedi et al., 2008). All samples were assayed in triplicate.

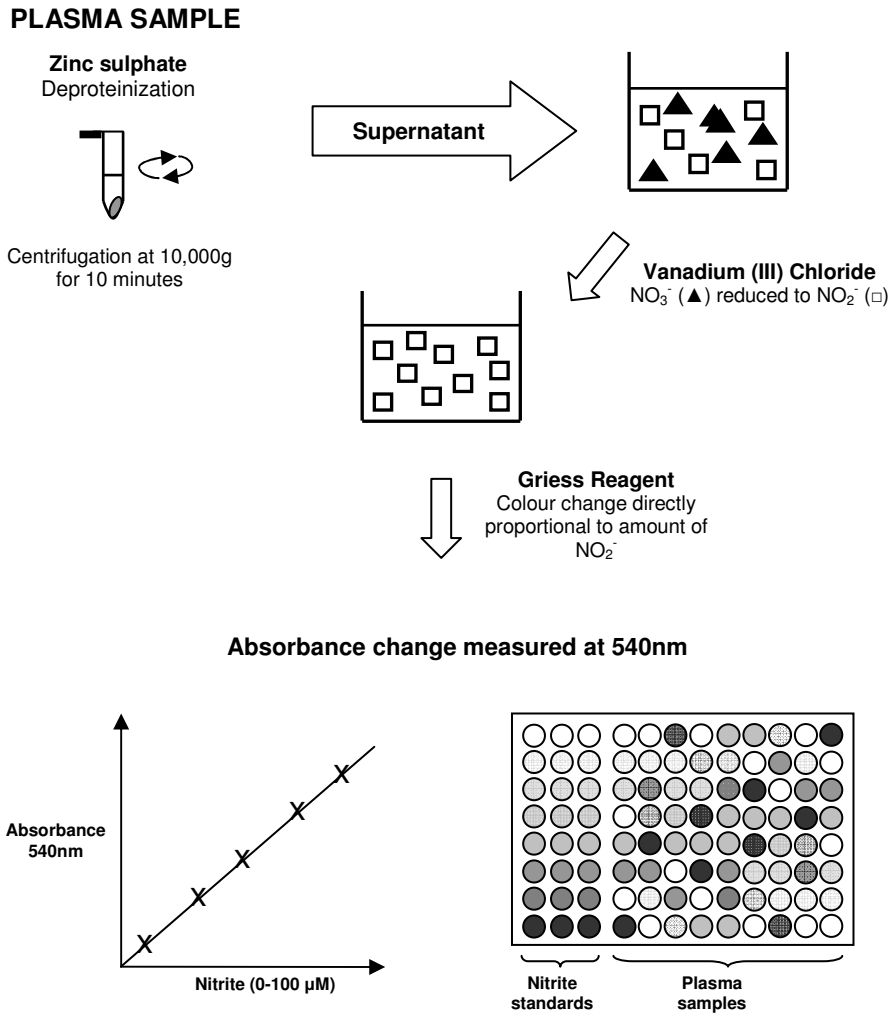

Figure 5.1. Determination of total nitrite and nitrate levels in plasma. Plasma samples are firstly deproteinized by the addition of zinc sulphate and centrifugation at 10,000 g for 10 minutes. The supernatants are then added to wells of a microtitre plate. Vanadium chloride is added to each well to reduce all NO_3^- to NO_2^- and then Griess Reagent is immediately added. A colour change which is directly proportional to the amount of NO_2^- present in the sample is observed after 30 minutes incubation, and can be measured at 540 nm using a spectrophotometer. The amount of nitrite present in the sample can be determined by comparison with a standard curve of known nitrite concentrations. The total amount of nitrite and nitrate levels is represented as total nitric oxide metabolites (NO_x).

5.3.5 Measurement of protein nitration

To evaluate nitration to plasma proteins, samples (30 µg) were separated by 1D electrophoresis and protein expression and nitration were assessed by silver staining and Western blotting as described in general methods **sections 2.2.5, 2.2.7 and 2.2.8**. For Western blotting, mouse monoclonal anti-nitrotyrosine antibody was used at 1:500 with an appropriate horseradish peroxidase conjugated secondary antibody (1: 2,000). The optical densities of bands present on 1D gels and/or Western blots corresponding to nitrated plasma proteins and plasma proteins respectively, were evaluated using Quantity One™ software (BioRad) by user defined volume integration. An equal number of control and AD samples were assessed on each 1D gels and/or Western blot to ensure that ECL and silver stain development were identical between the two groups. Optical densities for protein nitration values were normalised against optical densities for total protein values. Blots with samples considered of poor quality were repeated. Samples were run in duplicate.

5.3.6 Broad measures of oxidative stress

Plasma protein oxidation, total antioxidant capacity (TAC) and lipid peroxides were carried out as stated in the general methods **sections 2.2.2, 2.2.3 and 2.2.4**.

5.3.7 Mass Spectrometry analysis

Protein band excision, LC-MS/MS, data dependent CID and analysis were undertaken as described in general methods (general methods **section 2.2.9.2**).

5.3.8 Statistics

Statistical analysis was undertaken as described in general methods section **2.2.10**.

5.4 Results

5.4.1 Nitric oxide metabolites

As shown in figure 5.2, plasma NO_x levels as measured by the Griess Assay were significantly reduced in the AD group compared to age matched control subjects (Control: 60.50 ± 25.00 µM Vs. AD: 30.34 ± 29.88 µM; $p < 0.001$, Mann-Whitney U test).

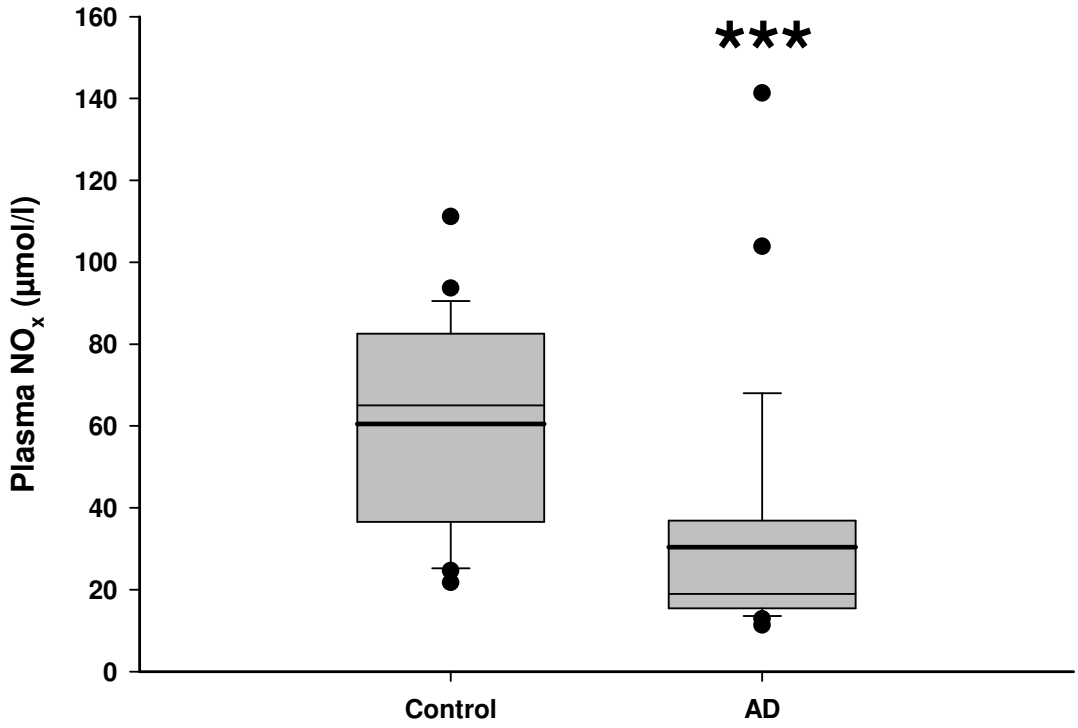

Figure 5.2. Total nitric oxide metabolite levels. Data (n=25; AD and control) are presented as a box plot. Nitric oxide metabolites were measured by Griess Assay (section 5.3.4).Percentiles are represented by the box (25^{th} and 75^{th}) and whisker (10^{th} and 90^{th}) with thick and thin lines corresponding to mean and median values respectively. Outliers are shown as filled circles. ***$p < 0.001$ Vs Control.

5.4.2 Plasma protein nitration

5.4.2.1 Optimization of antibody conditions

In order to identify nitrated plasma protein bands it was necessary to use relatively concentrated primary and secondary antibody solutions. As shown in Figure 5.3, for plasma proteins (30 µg) there are a greater amount of visible nitrated protein bands using mouse peroxidase conjugated goat anti-mouse secondary antibody at 1:2000, compared to 1:4000, when using mouse monoclonal anti-nitrotyrosine primary antibody at 1:500.

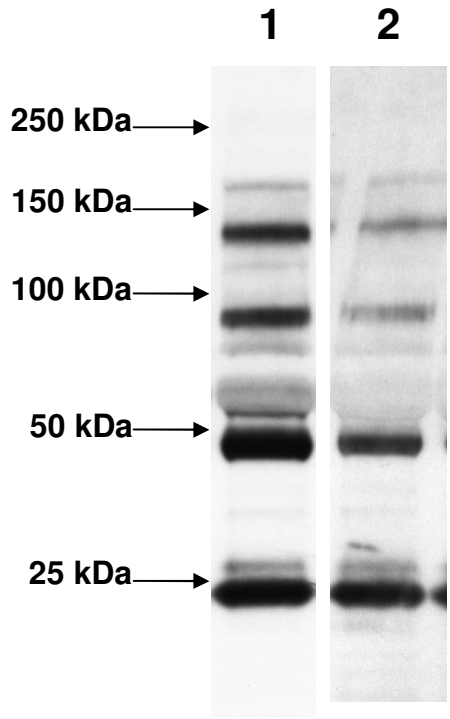

Figure 5.3. Optimizing antibody conditions. Mouse monoclonal anti-nitrotyrosine antibody used at 1:500 dilutions with peroxidase conjugated secondary antibody used at 1:2000 (lane 1) and 1:4000 (lane 2).

5.4.2.2 Specificity of peroxidase conjugated goat anti- mouse IgG antibody

The specificity of secondary antibody for the mouse monoclonal primary antibody was investigated. Due to the high concentration of secondary antibody required in order to detect nitrated plasma protein bands, some non-specific binding was expected and as demonstrated in figure 5.4, a degree of non-specific binding is evident. The non-specificity is likely to be cross reactivity to human immunoglobulin G which comprises of heavy chain (~150,000 Da) and light chains (~50,000 and 22,500 Da). The non-specific binding using the Sigma (A4416) antibody is more severe than the Cell Signalling antibody (#7076), however the intensity of bands which correspond to nitrated proteins are more visible and thus easier to quantify using a densitometer. Several protein bands corresponding to nitrated plasma proteins are present: bands are evident at approximately 250, 170, 120 and 80 kDa.

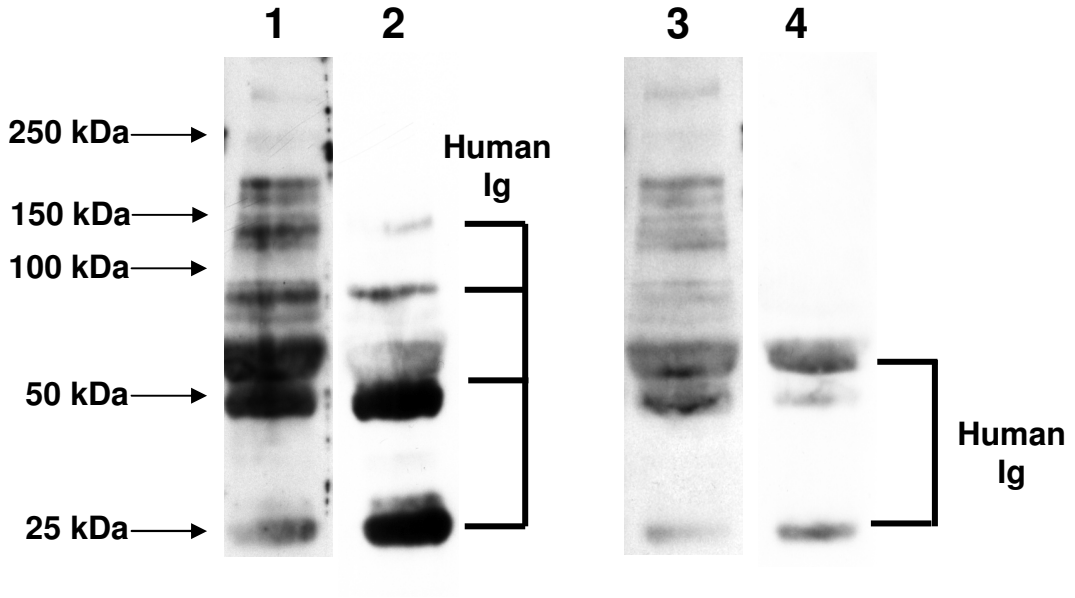

Figure 5.4. Assessing non-specificity of secondary antibody. Two secondary antibodies were used to assess specificity. Lane 1: Mouse monoclonal anti-nitrotyrosine antibody (1:500) with peroxidase conjugated goat anti-mouse secondary antibody (Sigma A4416) at 1:2000 dilution; lane 2: Peroxidase conjugated goat anti-mouse secondary antibody (Sigma A4416) at 1:2000 dilution; lane 3: Mouse monoclonal anti-nitrotyrosine antibody (1:500) with peroxidase conjugated goat anti-mouse secondary antibody (Cell Signalling #7076) at 1:2000 dilution; and lane 4: Peroxidase conjugated goat anti-mouse secondary antibody (Cell Signalling #7076) at 1:2000 dilution.

5.4.3 Plasma protein nitration

Bands corresponding to plasma protein nitration and protein expression were quantified by Quantity one software (BioRad) as shown in Figure 5.5. The prominent nitrated bands at approximately 170 kDa and 80 kDa, labelled as U7-10 and U31-34 (U refers to user defined parameters), were detectable and quantifiable in all plasma samples; the very faint nitrated band at approximately 250 kDa although visible to the naked eye, was not accurately quantifiable using a densitometer in all plasma samples; and the nitrated band at approximately 120 kDa was detectable and accurately quantifiable, but only in a minority of plasma samples.

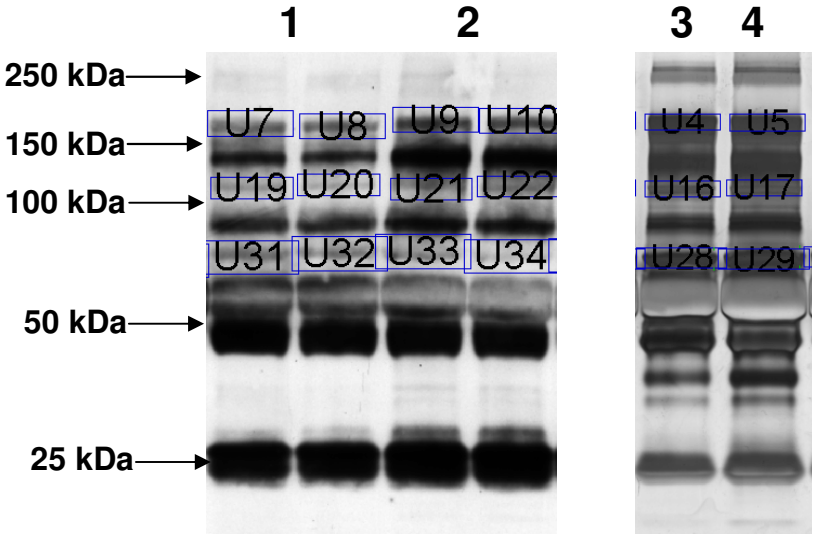

Figure 5.5. Quantification of protein expression and protein nitration. Quantity one® software (BioRad) was used to calculate optical density of three individual bands at approximately 170, 120 and 80 kDa using user defined volume integration (Boxed and labelled accordingly). For equivalent bands (U7-U10, U4 & U5; U19-22, U16 & U17; and U31-34, U28 and U29) analysed on Western blots and silver stained gels, user defined volumes were kept consistent and an equal amount of control and AD samples were assayed: Lane 1, Western blot for control sample assayed in duplicate; Lane 2, Western blot for AD sample assayed in duplicate; Lane 3, silver stained control; and Lane 4, silver stained AD sample.

5.4.3.1 Protein band exhibits increased nitration in AD plasma

As demonstrated in figure 5.6 the band at approximately 170 kDa exhibits significantly greater signal after normalisation against total protein levels (Control: 0.95 ± 0.45 OD units Vs. AD: 1.36 ± 0.62 OD units; p = 0.001, Mann-Whitney U test), suggesting its nitration status is increased in AD compared to control. No difference in signal and thus nitration status was observed for the band at approximately 80 kDa (Control: 0.97 ± 0.38 OD units Vs. AD: 1.12 ± 0.52 OD units; p = 0.27, independent samples t-test).

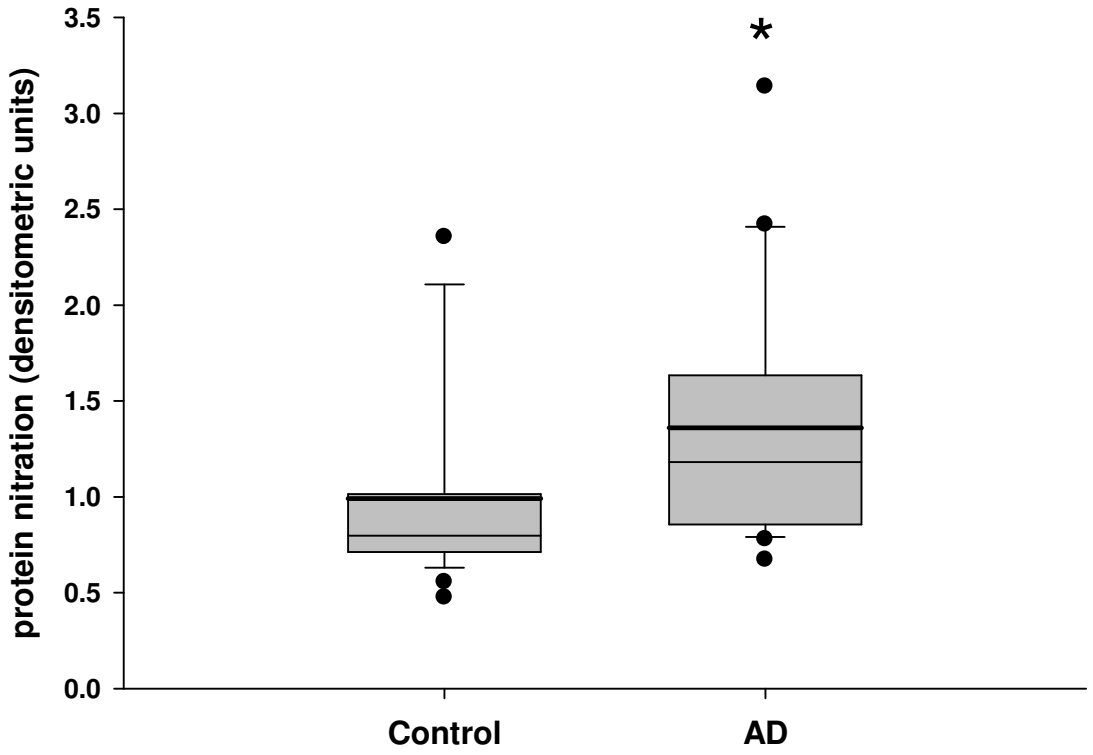

Figure 5.6. Increased nitration for unknown plasma protein band at ~170 kDa. Data (n=25; AD and control) are presented as a box plot. Percentiles are represented by the box (25th and 75th) and whisker (10th and 90th) with thick and thin lines corresponding to mean and median values respectively. Outliers are shown as filled circles. *p = 0.001 Vs. Control.

5.4.3.2 Identification of excised plasma protein band

In an attempt to identify the protein corresponding to the 170 kDa band, the protein band was excised from a silver stained gel. This particular band was very prominent on the Western blot and silver stained gel enabling its accurate excision. The protein band was digested and subjected to LC-MS and data dependent CID (as described in general methods 2.2.9). Data files created from the raw data produced by LC-MS and data-dependent CID for the excised gel band was searched against the human subset of the international protein index (IPI) database. As shown in table 5.1 a confident match for α-2 macroglobulin (α-2M) was obtained. The top match based on protein score had total peptide coverage of 28.29% (see figure 5.7).

Protein Band	Accession number/gi	Protein Score	Coverage (%)	Description	MW
~170kDa	P01023/112911	-837.53	28.29	α-2-macroglobulin	163.3
	Q5R4NB/75054706	-791.50	26.80	α-2-macroglobulin	163.3
	Q5NVH5/75054626	-586.60	45.32	Serum albumin	69.4
	P08603/159517847	-371.29	21.36	Complement Factor H	139.1
	P04264/238054406	-315.40	27.64	Keratin, Type II	66.0
	A5A6M6/215275331	-314.37	26.37	Keratin, Type II	65.5
	Q28522/2492797	-296.91	25.33	Serum albumin	67.9
	A2V9Z4/190358749	-296.58	25.00	Serum albumin	68.9
	P027069/1351907	-286.73	24.55	Serum albumin	69.3
	P01024/119370332	-280.10	10.82	Complement C3	187.1
	***P06238/119370261	-81.01	5.03	α-2-macroglobulin	163.8

Table 5.1. Protein identification for excised protein band using OSSMA. For positive identifications, the peptides are initially scored and filtered with an E-value threshold (this value is the statistical confidence generated from the OMSSA algorithm when running a search), and the value used is the suggested threshold. The peptide scores are then compared according to random chance using a second probability equation, and a Protein Score (*p*-Score) is calculated. Any *p*-Score >0 is discarded as a false identification. The lower the protein score the more confident the protein identification The greatest protein match from IPI database for excised protein band corresponded to α-2-macroglobulin with a highly confident *p*-Score of -837.53. *** A further protein match for α-2-macroglobulin from database search.

```
1     MGKNKLLHPS LVLLLLVLLP TDASVSGKPQ YMVLVPSLLH
41    TETTEKGCVL LSYLNETVTV SASLESVRGN RSLFTDLEAE
81    NDVLHCVAFA VPKSSSNEEV MFLTVQVKGP TQEFKKRTTV
121   MVKNEDSLVF VQTDKSIYKP GQTVKFRVVS MDENFHPLNE
161   LIPLVYIQDP KGNRIAQWQS FQLEGGLKQF SFPLSSEPFQ
201   GSYKVVVQKK SGGRTEHPFT VEEFVLPKFE VQVTVPKIIT
241   ILEEEMNVSV CGLYTYGKPV PGHVTVSICR KYSDASDCHG
281   EDSQAFCEKF SGQLNSHGCF YQQVKTKVFQ LKRKEYEMKL
321   HTEAQIQEEG TVVELTGRQS SEITRTITKL SFVKVDSHFR
361   QGIPFFGQVR LVDGKGVPIP NKVIFIRGNE ANYYSNATTD
401   EHGLVQFSIN TTNVMGTSLT VRVNYKDRSP CYGYQWVSEE
441   HEEAHHTAYL VFSPSKSFVH LEPMSHELPC GHTQTVQAHY
481   ILNGGTLLGL KKLSFYYLIM AKGGIVRTGT HGLLVKQEDM
521   KGHFSISIPV KSDIAPVARL LIYAVLPTGD VIGDSAKYDV
561   ENCLANKVDL SFSPSQSLPA SHAHLRVTAA PQSVCALRAV
601   DQSVLLMKPD AELSASSVYN LLPEKDLTGF PGPLNDQDDE
641   DCINRHNVYI NGITYTPVSS TNEKDMYSFL EDMGLKAFTN
681   SKIRKPKMCP QLQQYEMHGP EGLRVGFYES DVMGRGHARL
721   VHVEEPHTET VRKYFPETWI WDLVVVNSAG VAEVGVTVPD
761   TITEWKAGAF CLSEDAGLGI SSTASLRAFQ PFFVELTMPY
801   SVIRGEAFTL KATVLNYLPK CIRVSVQLEA SPAFLAVPVE
841   KEQAPHCICA NGRQTVSWAV TPKSLGNVNF TVSAEALESQ
881   ELCGTEVPSV PEHGRKDTVI KPLLVEPEGL EKETTFNSLL
921   CPSGGEVSEE LSLKLPPNVV EESARASVSV LGDILGSAMQ
961   NTQNLLQMPY GCGEQNMVLF APNIYVLDYL NETQQLTPEV
1001  KSKAIGYLNT GYQRQLNYKH YDGSYSTFGE RYGRNQGNTW
1041  LTAFVLKTFA QARAYIFIDE AHITQALIWL SQRQKDNGCF
1081  RSSGSLLNNA IKGGVEDEVT LSAYITIALL EIPLTVTHPV
1121  VRNALFCLES AWKTAQEGDH GSHVYTKALL AYAFALAGNQ
1161  DKRKEVLKSL NEEAVKKDNS VHWERPQKPK APVGHFYEPQ
1201  APSAEVEMTS YVLLAYLTAQ PAPTSEDLTS ATNIVKWITK
1241  QQNAQGGFSS TQDTVVALHA LSKYGAATFT RTGKAAQVTI
1281  QSSGTFSSKF QVDNNNRLLL QQVSLPELPG EYSMKVTGEG
1321  CVYLQTSLKY NILPEKEEFP FALGVQTLPQ TCDEPKAHTS
1361  FQISLSVSYT GSRSASNMAI VDVKMVSGFI PLKPTVKMLE
1401  RSNHVSRTEV SSNHVLIYLD KVSNQTLSLF FTVLQDVPVR
1441  DLKPAIVKVY DYYETDEFAI AEYNAPCSKD LGNA
```

Figure 5.7. Peptide coverage for α-2-macroglobulin (P01023/112911). The sequence information for α-2-macroglobulin is shown. Matched residues are highlighted in grey. A total peptide coverage of 28.29% (417 out of 1474) for this sequence was observed.

Three further possible matches for, serum albumin, complement and keratin type II proteins are also evident. When the molecular weights of each individual protein are taken into account the likely identity of the excised plasma protein is α-2 macroglobulin (α-2M). Multiple proteins present during 1-DG separation may explain the reason for several identifications. Although the protein was confidently identified as α-2M, no evidence that this plasma protein is actually nitrated was found. As shown in Figure 5.8, LC-MS/MS spectra for the three highest scoring peptide matches for the α-2M sequence demonstrate that no tyrosine residues present are nitrated.

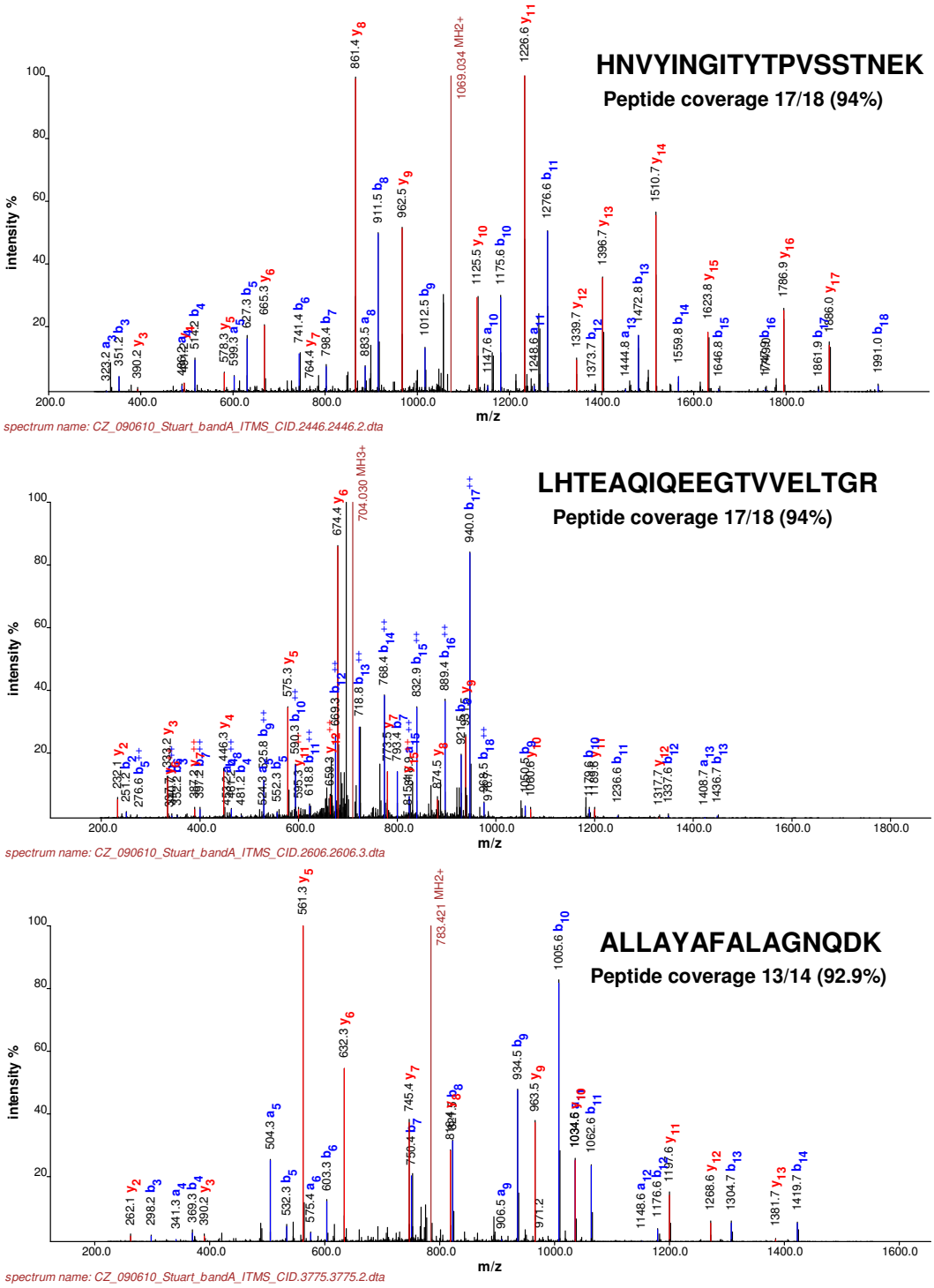

Figure 5.8. Mass spectra of top three peptide hits for α-2M sequence. The top three peptide matches for the α-2M sequence demonstrate that no tyrosine residues present are nitrated. Total amino acid coverage for each peptide is greater than 92.9%.

5.4.4 Protein oxidation

As shown in figure 5.9 no differences in total levels of protein carbonylation between AD and age matched control subjects, from the particular sample set used in this chapter (Control: 2.91 ± 0.26 nmol/mg Vs. AD: 2.89 ± 0.26 nmol/mg protein, $p = 0.8$ independent samples t-test).

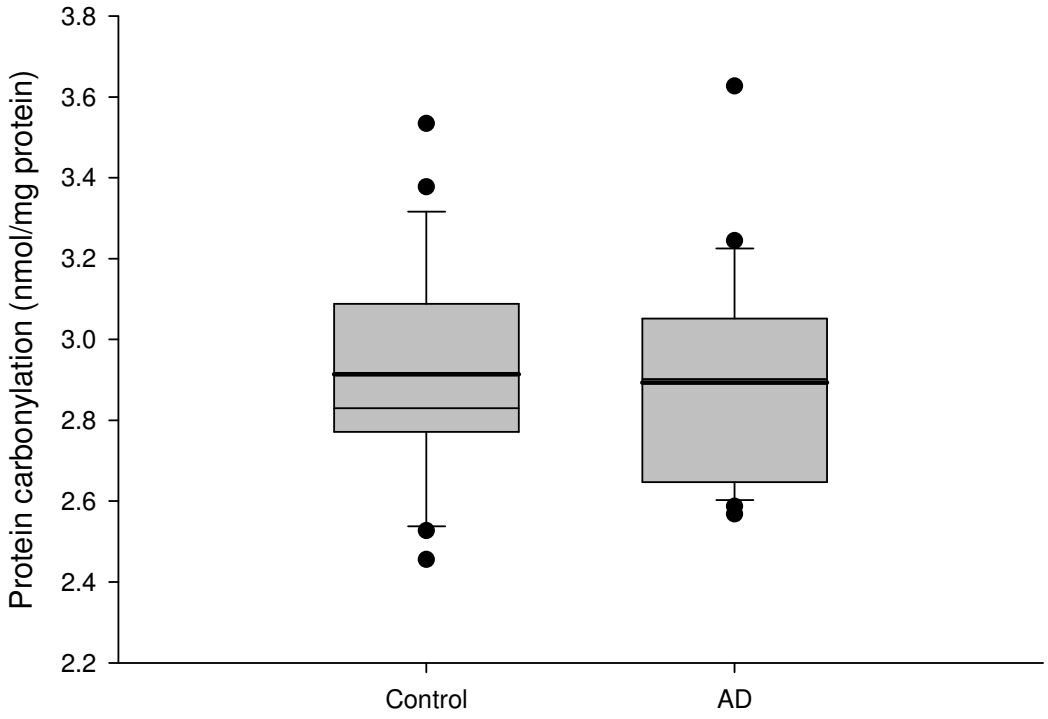

Figure 5.9. Total protein oxidation. Protein oxidation was measured by carbonyl ELISA. Data (n=25; AD and control) are presented as a box plot. Percentiles are represented by the box (25^{th} and 75^{th}) and whisker (10^{th} and 90^{th}) with thick and thin lines corresponding to mean and median values respectively. Filled circles represent outliers.

5.4.5 Total antioxidant capacity

No change in total antioxidant capacity was observed (figure 5.10), as measured by FRAP, between AD and age matched control subjects, from the particular sample set used in this chapter (Control: 910.800 ± 208.927µM Vs. AD: 992.933 ± 331.012µM, p = 0.4 independent samples t-test).

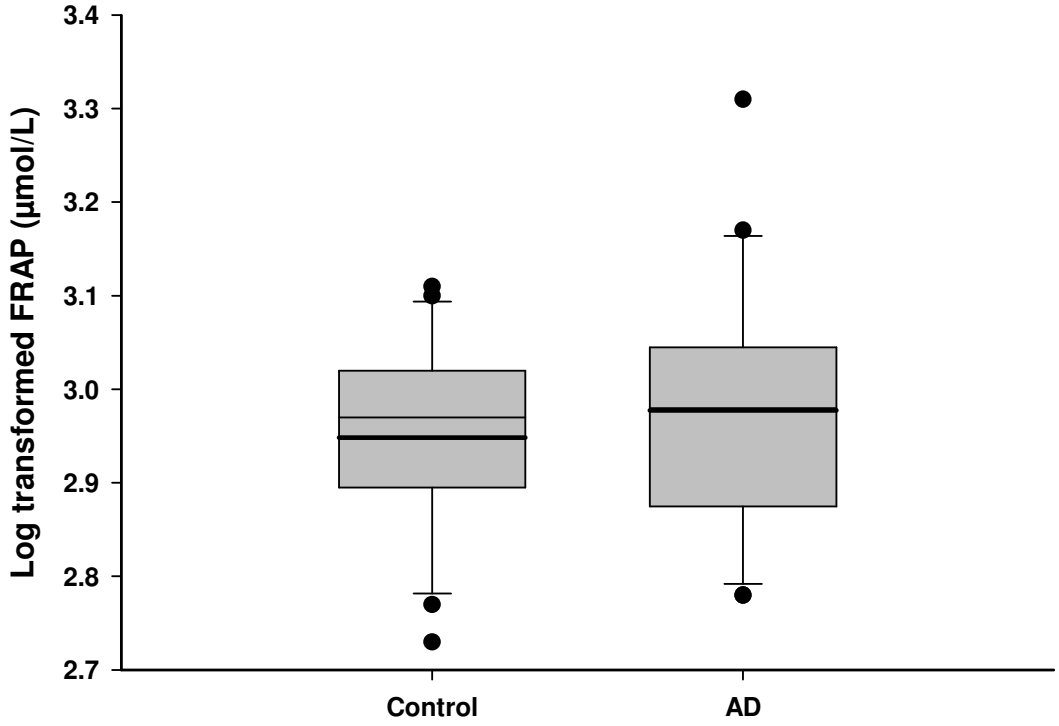

Figure 5.10. Total Antioxidant Capacity. TAC was measured by FRAP. Data (n=25; AD and control) are presented as a box plot. Percentiles are represented by the box (25^{th} and 75^{th}) and whisker (10^{th} and 90^{th}) with thick and thin lines corresponding to mean and median values respectively. Filled circles represent outliers.

5.4.6 Lipid peroxide levels

As shown in figure 5.11 no changes in lipid peroxide levels were observed in AD compared and age matched control samples, from the particular sample set used in this chapter (Control: 6.53 ± 5.23nmol/ml, Vs. AD: 10.26 ± 14.17nmol/ml, $p = 0.4$ independent samples t-test). Six AD and fourteen control samples were below the limit of detection of this assay (1nmol/ml).

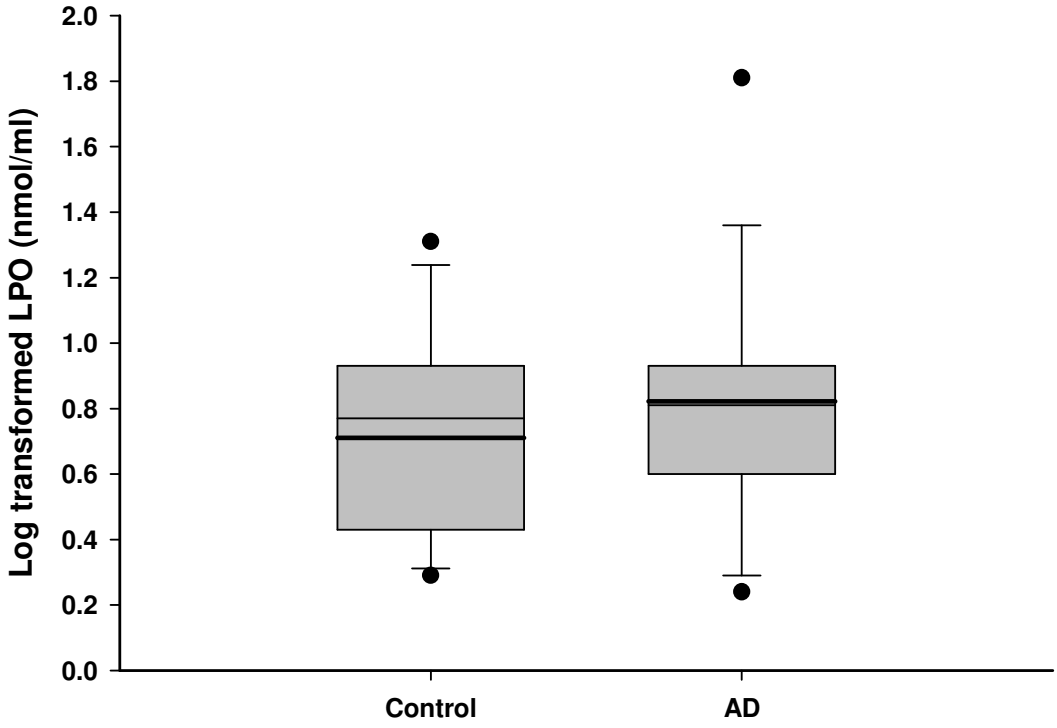

Figure 5.11. Lipid peroxide levels. Lipid peroxide levels were measured by lipid peroxide assay. Data (n=25; AD and control) are presented as a box plot. Percentiles are represented by the box (25^{th} and 75^{th}) and whisker (10^{th} and 90^{th}) with thick and thin lines corresponding to mean and median values respectively. Filled circles represent outliers.

5.5 Discussion

In view of the growing evidence supporting a role for nitrative stress in AD, this study aimed to evaluate $NO^{\bullet}$ and protein nitration levels in AD plasma in addition to other markers of oxidative stress. $NO^{\bullet}$ and levels of 3-nitrotyrosine were assessed as measurements which reflect nitrative stress.

It is widely accepted that levels of plasma NO_2^-/NO_3^- reflect *in vivo* production of $NO^{\bullet}$ (Moshage et al., 1995; Zahedi et al., 2008). In this study a remarkable decrease in NO_x levels was observed in AD compared to control subjects, a finding which is in agreement with existing studies in AD patients (Selley, 2003; Corzo et al., 2007). It is appreciated that diet can influence plasma NO_2^- and NO_3^- levels as certain foods (e.g., spinach, kale) are high in these metabolites (Dusse et al., 2005). With this in mind, it has been suggested that subjects should be fasted and their diet restricted two days prior to blood drawing (Dusse et al., 2005), however such measures are difficult to control for in this specific population. Therefore, caution is required when interpreting the results presented in this work.

Although it was not possible to accurately assess total protein nitration by Western blotting due to non-specific antibody binding, one specific plasma protein was successfully found to exhibit increased nitration in the AD group. Given this finding, one may suggest that decreased plasma NO_x levels maybe a result of their reaction and subsequent removal by $O_2^{\bullet-}$. Production of $ONOO^-$ may then subsequently nitrate specific plasma proteins. On the other hand, as suggested by Selley (2003) the reduction in $NO^{\bullet}$ maybe due to increased levels of homocysteine and asymmetric dimethylarginine and subsequent inhibition of the $NO^{\bullet}$ producing enzyme nitric oxide synthase.

In this study no difference in total protein oxidation or lipid peroxides was observed. These data are in agreement with results presented in Chapter 3, which were undertaken on a different set of plasma samples. In contrast, the reduction in TAC reported in AD compared to control subjects in Chapter 3 was not replicated in the sample set analysed in this study. It has been suggested that disease severity (e.g., mild, moderate or severe AD) may affect peripheral levels of antioxidants (Sekler et al., 2008) and hence using samples which include individuals across the full spectrum of AD severity may represent a reason for TAC levels to remain unchanged between the AD and control groups in this study. However, a significant reduction in TAC was demonstrated in Chapter 3 without different stages of the disease being taken into consideration. Moreover, there is also a study which reports of no correlation between the degree of cognitive impairment as quantified by MMSE, and TAC as measured by FRAP, when using large cohorts (Guidi et al., 2006). Interestingly the same study found a slight negative correlation between TAC, as measured by FRAP, and the duration of the disease (Guidi et al., 2006) suggesting that disease duration may affect TAC. The APOE genotype of AD subjects may also have an effect on TAC levels as measured by FRAP. A study undertaken by Pulido and colleagues (2005) reported that only AD subjects classified as APO 4/4 had a significant reduction in antioxidant capacity. A further factor which may contribute to the equivalent TAC demonstrated in this work is the number of subjects that were analysed. As with this study, groups who report no change in TAC between AD and control subjects typically assess a relatively small number of subjects (20 to 25 AD samples) (Sinclair et al., 1998; Pulido et al., 2005). Although not known, subject characteristics such as vitamin use, physical activity pattern and diet may have also influenced this measurement, and hence are a limitation of this work. Taken together these data may suggest that the conflicting TAC data presented in this study, and in Chapter 3,

may be in part due to subject APOE genotype, the duration of disease or the relatively small cohort of samples analysed.

The observation that total protein carbonylation remained unchanged between AD and control subjects is in agreement with other studies (Polidori et al., 2004; Zafrilla et al., 2006). Further, a recent study which assessed total levels of oxidized and nitrated proteins in various peripheral tissues, which included plasma, found no difference in levels between AD and controls (Korolainen and Pirttila, 2009). Based on these data the authors suggest that oxidative metabolism related to AD pathogenesis cannot be detected. One may suggest that as shown with previous studies in AD brain and plasma (Castegna et al., 2002a; Castegna et al., 2002b; Castegna et al., 2003; Choi et al., 2002), specific proteins which may be involved in disease pathology are targets of oxidative modification, rather than these events being a random, more global process.

Indeed, data presented in this chapter identified α-2M as one plasma protein that exhibited increased nitration in AD compared to age matched control subjects. These observations are also in agreement with a study by Mitrogianni et al. (2004); this group used the same methodology to identify specific proteins that exhibited increased plasma protein nitration in haemodialysis patients, a condition also associated with increased oxidative stress. α-2M was identified by its approximate molecular weight on a Western blot and by mass spectrometry and sequence data of the excised protein band.

One limitation of using 1-DE to evaluate plasma protein nitration is that given the vast dynamic range of plasma proteins (i.e. magnitude of different concentrations of proteins)

other proteins of similar molecular weights, which may account for the nitrated protein, may be masked by α-2M as it is highly abundant in plasma. However, nitration is selective and 1 to 10 residues of tyrosine per 100,000 are nitrated in conditions associated with inflammation and cardiovascular disease (Souza et al., 2008). Therefore it is very likely that only nitrated proteins which are highly abundant (e.g. α-2M) will be detected when employing 1-DE and Western blotting.

From the mass spectrometry data there was no evidence that α-2M was actually nitrated. Tyrosine and Tryptophan amino acid residues are targets for nitration by reactive oxygen species (Berlett and Stadtman, 1997; Souza et al., 2008), and of the peptides which accounted for 28.29% of the α-2M protein sequence, none of these residues were found to be nitrated. However, nitration of α-2M cannot be ruled out based on this assumption alone, as a further 72.71% of the protein sequence was not matched and therefore may well have contained nitrated tyrosine and tryptophan residues. Although likely to be modified, from the mass spectrometry data presented here α-2M cannot be confirmed as the nitrated plasma protein.

In AD altered levels of α-2M have been described previously. Its expression is increased in senile plaques and plasma from AD sufferers (Bauer et al., 1991; Hye et al., 2006). There is a selective and specific interaction between α-2M and the Aβ peptide and α-2M inhibits the fibrillization of Aβ peptide. Based on these observations it has been suggested α-2M may sequester and bind the Aβ peptide to provide its clearance from tissues brain (Du et al., 1997; Hughes et al., 1998). Increased nitration to α-2M as tentatively shown in this work may compromise this suggested function and thus result in greater Aβ load evident in the AD

brain. In addition this interaction may indicate that this particular protein is targeted for oxidative damage, more so than others. Moreover, the balance between proteases and protease inhibitors plays an important role in mediating inflammation associated tissue damage. As previously mentioned, α-2M is a protease inhibitor, and its modification by oxidation or nitration may impact on its function and thus play an important role during the inflammation process. For example, Wu et al. (1998) demonstrated that oxidation to α-2M affects its ability to bind cytokines and growth factors and thus proposed that such modification may act as a switch mechanism to help regulate acute inflammation and tissue repair. Further work by the same group reported that oxidized α-2M is greater in synovial fluid from Rheumatoid Arthritis patients when compared to control plasma, and that the degree of oxidation correlates to the observed reduction in its activity (Wu and Pizzo, 2001). One may speculate that nitration to α-2M would exert a similar effect and thus contribute to inflammatory processes associated with AD (Akiyama et al., 2000).

In summary, this study tentatively identified α-2M as a plasma protein which exhibits increased nitration in AD. Further work is required to definitively show and confirm this finding. In addition, no difference in total plasma protein oxidation between AD and control subjects was observed, providing further evidence that oxidative events in AD are specific, rather than global events. Further studies in a larger cohort of samples are required to further confirm these findings.

Chapter 6

Gel based Redox Proteomics for the study of Alzheimer's disease

6.1 Abstract

The recent emergence of 'redox' proteomics has allowed for the identification of proteins altered by oxidative modifications. Such investigations in Alzheimer's disease (AD) brain have advanced the existing understanding into the oxidative mechanisms which underlie the disease. Plasma is representative of processes and events which occur in the body and coupled to its easy accessibility and practicality provides an ideal source to monitor oxidative changes to proteins which may occur during AD. In this study, non-depleted pooled AD and pooled control plasma (n=25) were subjected to 2-DE with Western blotting for the detection of proteins which were specifically oxidized. One protein was shown to exhibit increased oxidation in AD. The use of narrow range IPG gels and excision of altered plasma proteins from multiple gels was undertaken to overcome encountered difficulties when attempting to obtain protein identification.

6.2 Introduction

Proteomics is the study of a group of proteins expressed at a particular snapshot in time (e.g., a disease state). In addition, proteomics can be used to assess post translational modifications (PTM) to proteins which may include phosphorylation, sulphation and glycosylation. These are important as they can determine activity, turnover and stability of a protein, which governs its function (Pandey and Mann, 2000). It has been assumed that oxidative events are damaging and harmful since early exercise studies in the late 1970's and early 1980's (Dillard et al., 1978; Davies et al., 1982). More recently, the notion that these events may actually be important regulatory PTMs is gaining credibility (Spickett et al., 2006).

Impairment of protein function and reduced activity are recognized consequences of protein oxidation (Friguet, 2006), and therefore proteins which are targets of such events are of particular interest. The emergence of a recent new division of proteomics named 'redox proteomics,' allows the identification of specific proteins modified by oxidation. By using 2-DE coupled with immunoblotting, oxidative modifications to proteins (e.g., oxidation, nitration, advanced glycation end products, advanced lipid end products) can be assessed. This has allowed the molecular mechanisms of diseases associated with oxidative stress, such as AD, to be further understood (Butterfield et al., 2006).

Increasingly, the focus of AD research has been to come up with approaches to slow or prevent the development of AD. As a consequence, recent redox proteomic studies have switched their focus to oxidative modifications that occur as AD progresses, by either comparing brain tissue from mild cognitive impairment (MCI) and early AD subjects, or by examining brain regions, such as the entorhinal cortex, which are affected at the earliest

stage of AD (Braak and Braak, 1995; Terni et al., 2009; Sultana et al., 2010). For example, Terni et al (2009) demonstrated that mitochondrial ATP synthase exhibited increased lipooxidation at the first stage of AD, when no clinical symptoms are evident.

Perhaps the largest drawback of such work is that brain tissue can only be obtained post mortem. Even though these aforementioned redox proteomic studies are vitally important in characterising oxidative changes which occur when AD progresses, brain tissue does not reveal specific peripheral oxidative changes that maybe significant in AD, and cannot be used as a biomarker in a living person to monitor interventions or therapies. Although AD originates in the brain, blood plasma does contain brain derived proteins (Aluise et al., 2008); and oxidative changes (e.g., protein carbonylation) in plasma provide a good indication of oxidative status in the body (Veskoukis et al., 2009). Studies which have investigated plasma protein oxidation in AD present an unclear picture, some have demonstrated increased plasma protein oxidation in AD, where as others have reported no change (Bermejo et al., 2008; Zafrilla et al., 2006). In agreement with studies undertaken by Zafrilla et al. (2006) and Balderias et al. (2008), results from Chapter 3 demonstrated that plasma protein oxidation levels are equivalent between AD and controls. However, TAC levels were shown to be reduced, and a specific plasma protein which was oxidized was also identified. These observations may suggest that oxidation to specific plasma proteins are more important than a global oxidative change, when investigating peripheral oxidative stress in AD.

To date, limited 'redox' proteomic AD research has been undertaken in plasma in order to identify proteins altered by oxidation, and only a few oxidized plasma proteins have so far

been identified. Conrad et al. (2000) used Western blotting to demonstrate that a 78 kDa plasma protein exhibited increased oxidation in AD compared to control patients. In two later studies specific plasma proteins and glycoproteins were shown to be targets of oxidation in AD (Choi et al., 2002; Yu et al., 2003). In this study 2-DE with Western blotting was undertaken to identify specific plasma proteins which undergo oxidation in AD compared to age-matched controls.

6.3 Methods

6.3.1 *Declaration of Ownership*

In this Chapter the advice of Mr Andrew Jones was sought in order to undertake LC-MS/MS and CID. Responsibility for the choosing of filtering parameters for data analysis, and decisions on sample preparation were made by the author. The author was also present for the running of this analytical technique and was responsible for all further data analysis.

6.3.2 Sample selection

A subset of 50 samples (25 AD and 25 control patients) were selected from the original 144 sample set (see **section 2.1.4** in general methods) based on the availability of plasma.

6.3.3 Desalting plasma samples

Twenty five control and AD samples were pooled together and desalted using Micro Bio-Spin™ 6 chromatography columns. Total protein concentration of the desalted samples was measured using the BCA assay (see general methods **section 2.2.1**).

6.3.4 IEF, 2-DE, silver staining and derivatization of protein carbonyls,

Desalted pooled plasma samples (100-150 µg) were separated by IEF and 2-DE (see general methods **2.2.6**). Total protein content was visualised by silver staining (general methods **2.2.8**) and protein carbonylation was determined by an anti-DNP Western blot. For anti-DNP Western blots plasma protein transfer was undertaken as described in general methods **section 2.2.7**. Hybond-P™ membrane (GE Healthcare, UK) was subsequently derivatized with 2, 4-DNPH (1mM 2, 4-DNPH in 2M HCl), washed three times in TBST (0.05%) for 10 minutes and then incubated with mouse monoclonal anti-DNP (1:200) for 2 hours at room

temperature. Hybond-P™ membrane (GE Healthcare, UK) was washed a further three times in TBST (0.05%) for 10 minutes, and then incubated with an appropriate horseradish peroxidase conjugated secondary antibody (1: 2,000) for 1 hour at room temperature. Oxidized protein spots were visualized using a chemiluminescent detection system (see general methods **section 2.2.7**). Modified protein spots were excised from silver stained gels under aseptic conditions with a sterile scalpel, placed into clean eppendorf tubes and kept overnight at -20ºC.

6.3.5 Plasma protein oxidation analysis and statistics

Pooled AD and control plasma samples were run concurrently to ensure that any detectable differences seen were truly representative of the disease state. Gaussian modelled protein spots were matched and their optical densities assessed using PD Quest image analysis software™ (BioRad). As employed in existing proteomic studies protein spots which exhibited a difference in signal intensity of $\geq$ 3-fold, with a p value of < 0.05 (independent samples t-test) was considered significant (Castegna et al., 2002b; Butterfield et al., 2006b). Protein expression of spots was accounted for by normalisation against total protein content.

6.3.6 Immunoprecipitation of oxidized proteins

Preparation of magnetic Dynabeads® (Invitrogen, UK), Dynabead- antibody binding and immunoprecipitation of target proteins was undertaken as described in the manufacturer's guidelines. Dynabeads® (Invitrogen, UK) were re-suspended by gentle inversion and washed three times with citrate phosphate buffer (pH 5). Mouse monoclonal anti-DNP antibody was diluted in citrate phosphate buffer, added to Dynabeads® at the desired ratio (Dynabeads: Antibody; 75:1) and rotated for 40 minutes, at 4ºC. Dynabead®-antibody

complexes were washed three times with citrate phosphate buffer (pH 5). Samples were diluted to desired concentration (Dynabead-Antibody complex: antigen; 1:10) in citrate phosphate buffer (pH 5) and incubated with Dynabead®-antibody complexes for one hour at 4ºC. For 2-DE gels immuno-precipitates were resuspended in rehydration buffer, boiled for 5 minutes and kept at -20ºC until they were analyzed. Optimal amounts of oxidized plasma proteins to use were deduced from preliminary experiments using oxidized BSA. The amount of plasma proteins used was governed by antibody availability.

6.3.7 Mass Spectrometry analysis

Protein spot excision, LC-MS/MS, data dependent CID and analysis were undertaken as described in general methods (**section 2.2.9.2**).

6.4 Results

6.4.1 Two dimensional gel electrophoresis and Western blotting for protein oxidation

Representative blots of a pooled AD and pooled control plasma sample assayed concurrently are shown in figure 6.1. As visualized on the Western blot there are numerous plasma proteins which are carbonylated within the 4-8 pH range in both the pooled AD and control samples. This is accompanied by minimal background signal.

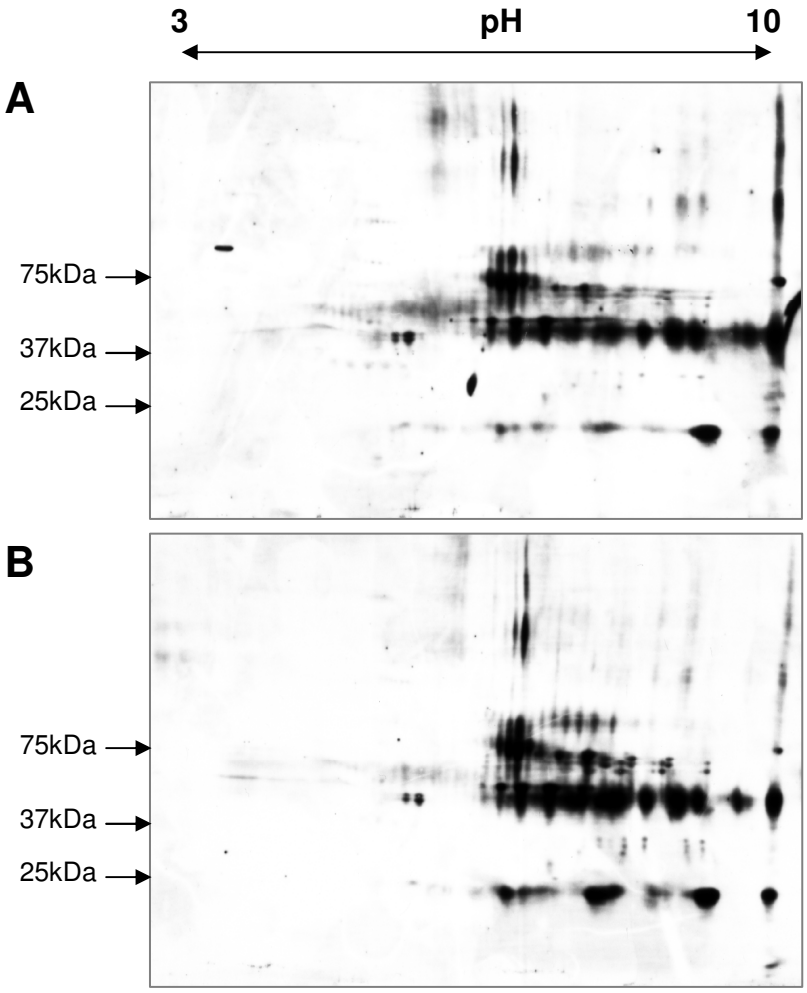

Figure 6.1. Protein oxidation in Pooled AD and Pooled Control sample. Plasma protein oxidation was assessed by an anti-DNP Western blot (see section 6.6.4). A representative blot for a pooled AD and pooled control plasma sample run concurrently is shown. (A) Pooled Control (100 µg) and (B) Pooled AD (100 µg).

6.4.2 Matching oxidized plasma proteins between groups

Forty seven carbonylated plasma proteins were successfully matched between all replicate Western blots (Pooled AD and control blots run in triplicate). Figure 6.2 shows an example of protein matching in pooled AD and control samples run in parallel for protein carbonylation using PD Quest™ software. The triangles represent landmark plasma protein spots which are well resolved and present in all replicate gels. These landmarks are used for gel alignment and accurate protein spot matching.

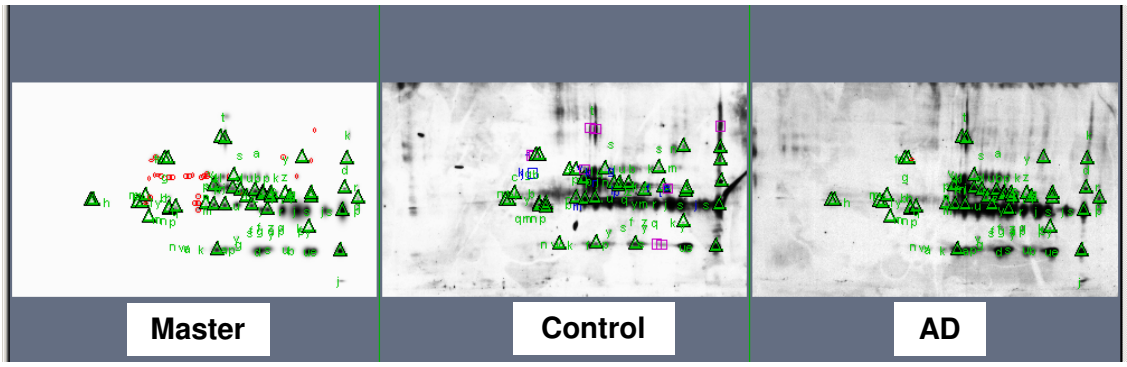

Figure 6.2. Protein spot matching using PD Quest software™. Representative blots for pooled control and pooled AD samples are shown. Blots were assayed in parallel to ensure identical experimental and developmental conditions. A reference blot (master) is created which contains protein spots from all pooled control and pooled AD blots; from this protein spots can be matched between all replicate blots and differences identified between control and AD groups.

6.4.3 Oxidation differences between AD and control subjects

Of all of the matched proteins, only one protein was identified as exhibiting increased oxidation AD compared to control subjects when ≥ 3 fold change was applied. Following normalisation for total protein concentration, this difference was still observed (Figure 6.3).

Parallel silver stained gels of the same samples were used for total protein content. Figure 6.3A shows the region of interest on a silver stained gel and Western blot. The protein exhibiting increased oxidation is circled. Figure 6.3B shows the optical densities for total protein content, amount of oxidation and degree of protein oxidation when AD and control samples were compared. The degree of protein oxidation was calculated by dividing the optical density of the amount of oxidation by total protein content.

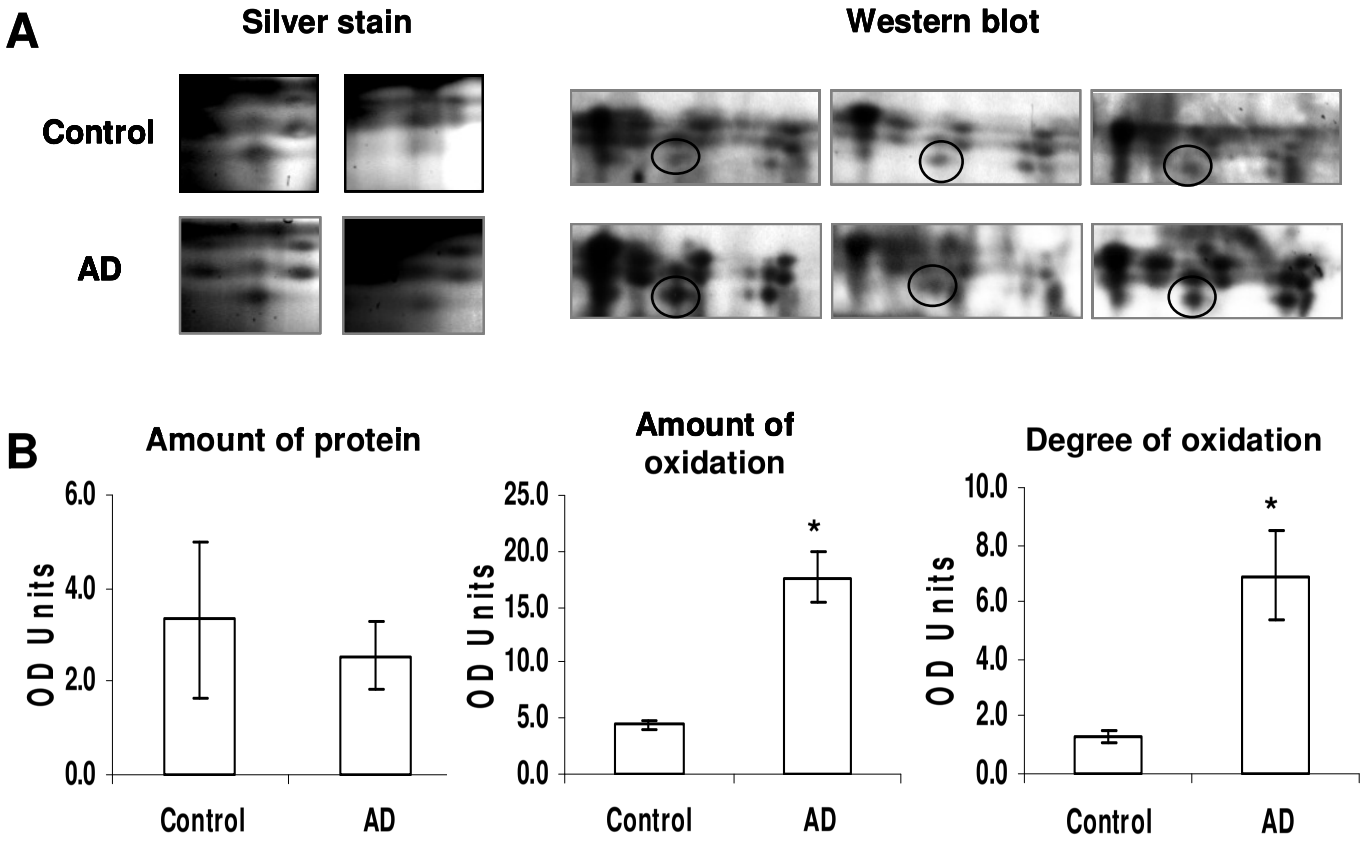

Figure 6.3. Plasma protein exhibiting increased oxidation in AD compared to Control. Silver stains run in duplicate (n=2) and anti-DNP Western blot run in triplicate (n=3). (A) Protein expression and degree of oxidation to plasma protein spot as assessed by silver stain and anti-DNP Western blot. (B) Optical density data for protein expression and oxidation of protein spot represented in the form of a bar chart. Optical density (OD) values represent means ± SEM for replicate silver stained gels and Western blots. The degree of oxidation of the protein spot is the amount of oxidation after normalisation against its expression. * $p < 0.05$ using student t-test.

6.4.4 The use of immunoprecipitation and verification of antibody suitability

Due to the low abundant nature of the oxidized plasma protein it was necessary to undertake immunoprecipitation (IP) in order to try to increase the chances of gaining a protein identity by mass spectrometry. Downstream applications of IP (e.g., SDS-PAGE and 2-DE) can result in co-elution of antibody and target protein due to the use of the reducing agents (e.g., 2-mercapthoethanol and destreak™). Therefore a preliminary experiment to ensure that the antibody used for IP was not of the same molecular weight and isoelectric point as the plasma protein of interest was undertaken. As shown in figure 6.4B (circled), the pooled AD plasma sample derivatized with 2, 4-DNPH and spiked with rat anti mouse IgE secondary antibody is accompanied with minimal streaking compared to the non-spiked pooled AD plasma sample in the gel region of interest (circled in figure 6.4A).

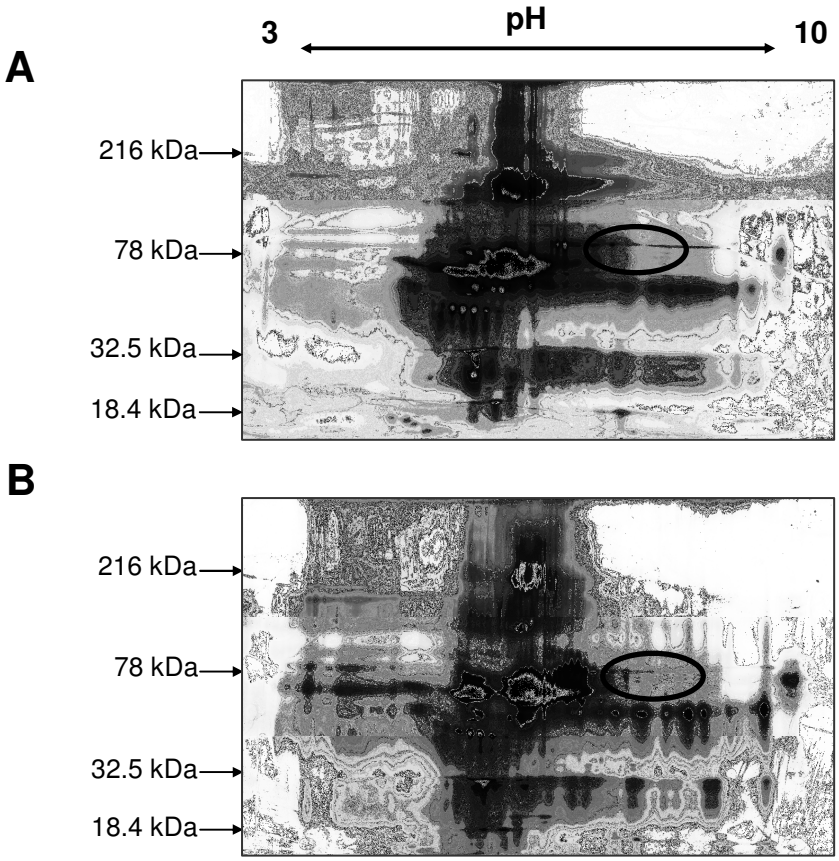

Figure 6.4. Characteristics of primary antibodies used for immunoprecipitation using 2-DE. (A) Silver stain of pooled AD plasma (100 µg); (B) derivatized with 2, 4 – DNPH and spiked with mouse monoclonal anti-DNP IgE (10 µg).

6.4.5 IP of oxidized proteins

6.4.5.1 Optimal antigen concentration

To ensure that optimal conditions were employed for IP of oxidized plasma proteins (e.g., Dynabead-antibody complexes were not over saturated with antigen) preliminary experiments were undertaking using oxidized BSA (see methods section for 2.2.2.1 for preparation). Figure 6.5 demonstrates that the optimal amount of antigen added to Dynabead-antibody complexes without over saturation was approximately 10-20 µg per 150 µg Dynabead-antibody complexes.

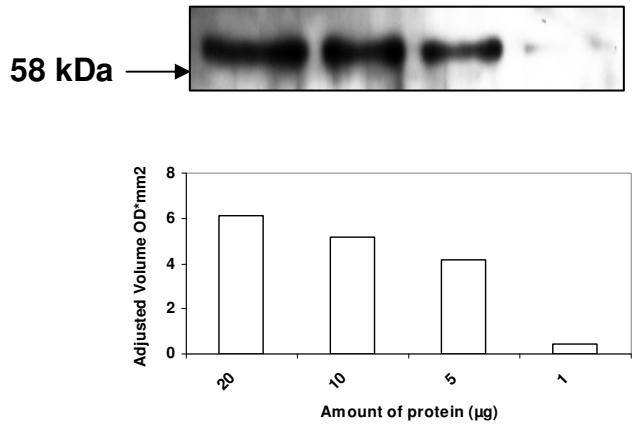

Figure 6.5. Optimization of amount of bead-antibody complex and antigen, using oxidized BSA. Dynabead® protein G, mouse monoclonal anti-DNP and various concentrations of oxidized BSA, derivatized with 2, 4 – DNPH.

6.4.5.2 IP of oxidized plasma proteins

IP of oxidized plasma proteins resulted in reduced background when they were separated by 2-DE and silver stained (figure 6.6A and 6.6B). The resolution of several highly abundant plasma proteins was also improved (See figures 6.6A and 6.6B). However the plasma protein spot of interest was barely visible and could not be detected by densitometry and the resolution was of poorer quality than the non IP sample (Figure 6.6, circled). This technique was considered a non-viable approach and not used further due to the antibody investment and cost.

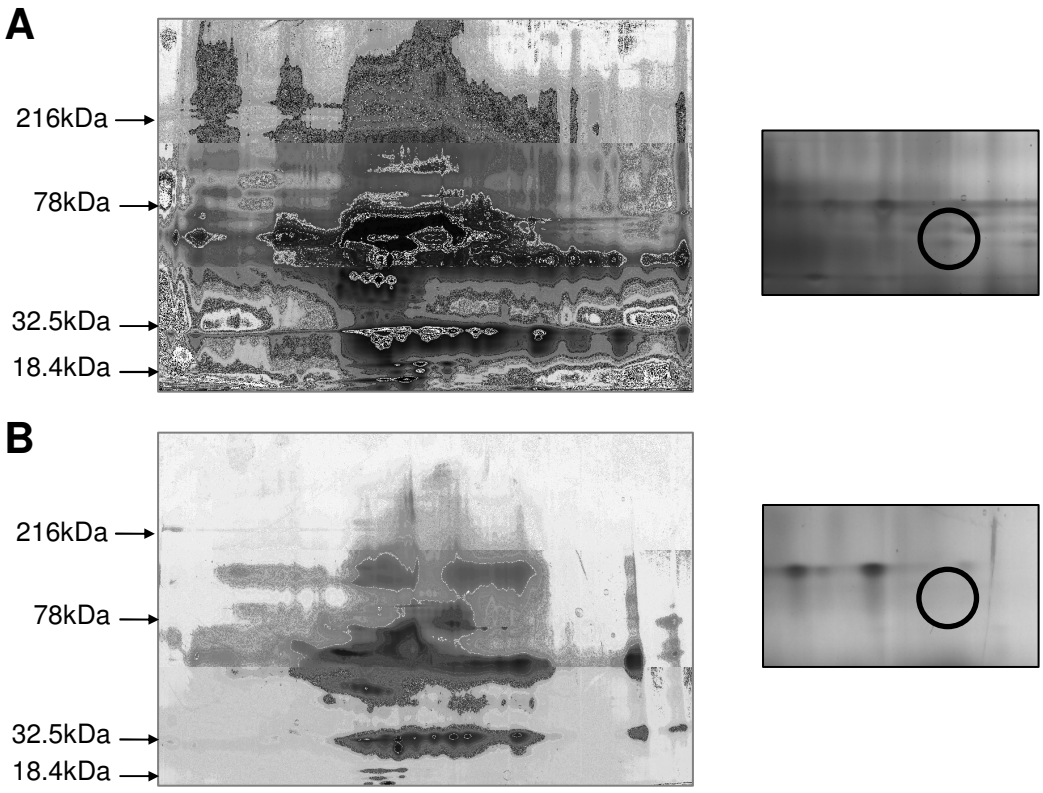

Figure 6.6. Comparison of oxidized plasma proteins and precipitated oxidized plasma proteins by silver staining. (A) Plasma proteins (200 µg) and (B) oxidized plasma proteins (225 µg). Part of gel which contains proteins of interest are boxed to the right of the gel.

6.4.6 Excision of protein spot from single and multiple 2D gels

Following unsuccessful use of IP, attempts were made to gain protein identification by simply excising the modified protein spot. LC-MS/MS and data dependent CID was used to gain protein identification. Figure 6.7 shows a representative gel of the plasma protein spot location and its excision.

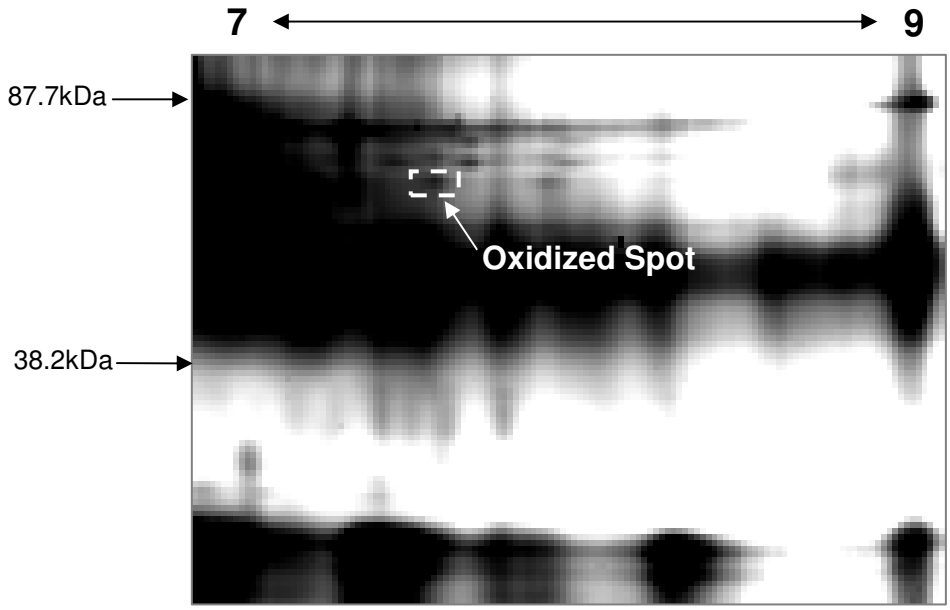

Figure 6.7. Excision of single plasma protein spot from a representative silver stained gel. Plasma proteins (100 µg) separated by 2DGE; Isoelectric focussing undertaken using pH 3-10 Readystrips™, SDS-PAGE was undertaken using 4-15% Tris-HCl criterion gels. Plasma proteins were visualised using silver staining. The oxidized protein is boxed.

Following MS analysis, the top two most confident matches comprised of trypsin and anionic trypsin (see Appendix III for data). Low protein concentration due to low protein abundance was considered the limiting factor of successful protein identification, potentially due to self digestion of trypsin precursor protein. Therefore the plasma protein spot was excised from two gels, in order to gain more protein quantity and pooled together. As shown in Table 6.1 (see Appendix III for full data), trypsin was the most confident match, with the greatest protein score and peptide coverage, for each sample. A further match included actin; however the molecular weight and isoelectric point for actin is not consistent with the region of the 2D gel from which the protein spot was excised.

	Accession number/gi	Protein Score	Coverage (%)	Description	MW	*pI
Unknown	P00761/136429	-129.62	17.32	Trypsin	24.4	7.00
oxidized	P10981/113258	-82.03	11.97	Actin-87E	41.8	5.30
protein	P84183/113258	-82.03	11.97	Actin, cytoplasmic	41.8	5.30

Table 6.1. Data for protein identification from LC-MS/MS for excision of two spots. Top protein hits listed for excised spots from silverstained 2D gels. *pI was predicted using ExPASY proteomics server from protein sequence data.

6.4.7 Identification of a highly abundant plasma protein

In order to confirm that the excision of protein spots and their subsequent identification was possible under these experimental conditions a very abundant protein spot in the neutral region of the 2D gel was excised as a control. The location of this plasma protein spot is displayed in figure 6.8. The protein spot was identified as Transthyretin as there are two hits in the top four matches and of these (see Appendix III for full data), there is a high protein score and high coverage for this particular protein. In addition the isoelectric point and molecular weight of this protein corresponds to the location of the protein spot on a 2D gel. These data confirmed that the excision of protein spots, their digestion and identification had been undertaken successfully, and that previous unsuccessful protein identification was due to low abundance.

A

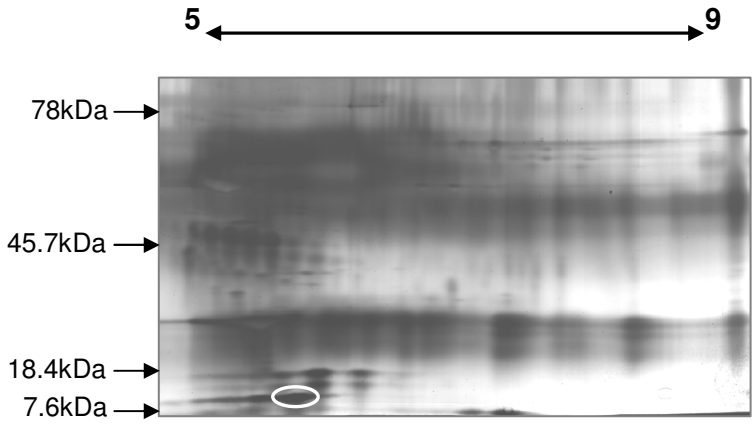

B

	Accession number/gi	Protein Score	Coverage (%)	Description	MW	*pI
Control spot	P02766/136464	-461.67	48.98	Transthyretin	15.9	5.52
	P04264/238054406	-278.59	25.00	Keratin	66.0	8.15
	A5A6M6/215275331	-263.85	23.70	Keratin	65.0	7.61
	Q5NVS2/75040810	-211.81	30.00	Transthyretin	15.8	5.38

Figure 6.8. Excision and identification of highly abundant protein. (A) Plasma proteins (100 µg) separated by 2-DE; Isoelectric focussing undertaken using pH 3-10 Readystrips , SDS-PAGE was undertaken using 4-15% Tris-HCl criterion gels. Plasma proteins were visualised using silver staining. High abundant protein (circled) excised from gel. (B) Top four protein hits listed for excised spot from silver stained gel. *pI was predicted using ExPASY proteomics server from protein sequence data.

6.4.8 Protein identification by pooling multiple spots from narrow range gels

To overcome the low levels of protein which had prevented protein identification in previous experiments application of more plasma protein to the IPG strip was necessary. However, the large range IPG strips previously used, clearly shows congestion and poor resolution of some proteins. The use of narrow range IPG strips allows a greater concentration of protein to be focussed, while maintaining good protein resolution and avoiding excessive spot congestion in the second dimension of separation (Yan et al., 2000) and thus was employed for further experiments. Figure 6.9 illustrates that protein spots were less congested on the gel and were better resolved, more intensely stained and visually more prominent having employed this approach (compare to figure 6.7). In addition this allowed greater accuracy when excising the modified plasma protein.

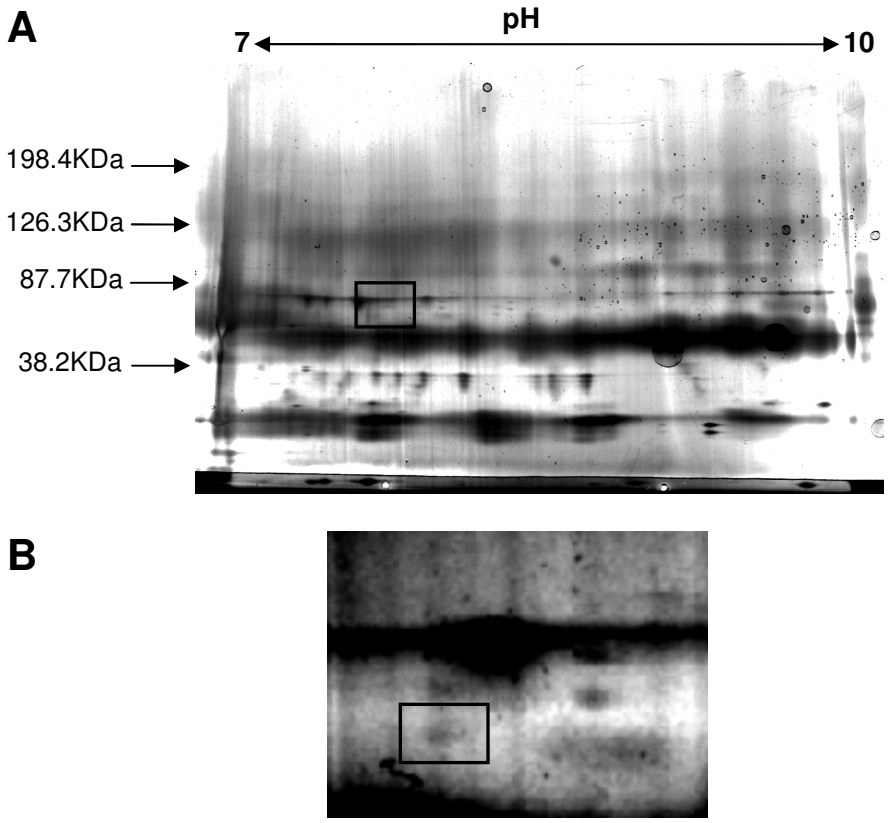

Figure 6.9. Representative narrow range gel of pooled AD plasma sample. Pooled AD plasma proteins (150 µg) focused in 1st dimension using narrow range pH 7-10 IPG Readystrip™ (BioRad) and separated in 2nd dimension using Tris-HCl Criterion 4-15% gels (BioRad). A) Silver stained gel. B) location of excised spot.

Following mass spectrometric analysis of the excised protein from the narrow range IPG strip experiment, protein identification for the plasma protein which exhibited increased oxidation in AD was still unsuccessful. As demonstrated in table 6.2 (see Appendix III) serum albumin precursor proteins accounted for five out of the six top matches for this unknown protein spot, but their isoelectric point and molecular weight was calculated to be approximately 5.9 and 69 kDa respectively, which is evidently inaccurate as the pI of the excised spot was estimated to be nearer 8 from its location on a 2D gel. Therefore serum albumin precursor protein cannot be the true identity of this particular excised spot.

	Accession number/gi	Protein Score	Coverage (%)	Description	MW	*pI
Unknown oxidized protein spot	Q5NVH5/75054626	-288.31	12.81	Serum Albumin	69.4	5.92
	Q28522/2492797	-145.26	4.67	Serum Albumin	67.9	5.85
	A2V9Z4/190358749	-145.24	4.61	Serum Albumin	68.9	5.91
	P08835/71152981	-138.33	2.14	Serum Albumin	69.7	6.08
	P00761/436129	-103.18	8.66	Trypsin	24.4	7.00
	P49065/44889024	-49.51	1.97	Serum Albumin	68.9	5.85

Table 6.2. Protein identification for oxidized plasma protein spot. Proteins listed in descending order according to best protein match. *pI was determined using pI/MW prediction software available on ExPASY proteomics server.

6.5 Discussion

Two-dimensional gel electrophoresis coupled to Western blotting highlighted one plasma protein which exhibited increased oxidation in AD compared to age matched control plasma. Numerous attempts, employing different gel techniques, to identify this protein by mass spectrometry failed. Protein identification could not be achieved because the sample was contaminated with albumin and the only hit obtained was to albumin. This identity was incorrect as the molecular weight and isoelectric point did not correspond to the location of the excised spot, as visualised on a 2-DG.

There are a number of gel based proteomic studies which combine 2-DE and Western blotting that have been successfully used to analyse protein modifications in AD brain (Korolainen et al., 2002; Castegna et al., 2002a; Castegna et al., 2002b; Castegna et al., 2003; Pamplona et al., 2005; Terni et al., 2009; Sultana et al., 2010). For example Korolainen and colleagues (2002) demonstrated that protein carbonylation status is altered in several proteins from the frontal cortex region of AD brain tissue and Castegna et al. (2002a) revealed creatine kinase BB, glutamine synthase and ubiquitin carboxy-terminal hydrolase L-1 as proteins, present in the inferior lobule region, which exhibit increased oxidation.

While in brain 2-DE and MS are enough to gain protein identification from an excised gel spot, it appears from data presented in this work and reports by others (Korolainen et al., 2007) that it is not sufficient when attempting to identify the low abundant peripheral proteins. Such proteomic work in AD plasma is very limited; to date only two studies have used this technique. Choi et al. (2002) showed that the fibrinogen γ-chain and α-1-antitrypsin

precursor protein are oxidized in AD plasma and Yu and colleagues (2003) reported a few plasma glycoproteins to be oxidized in AD.

Redox proteomic studies which have investigated protein modifications between AD and controls samples calculate the signal ratio between individual protein spots, and then look at differences above a particular threshold (Choi et al., 2002; Butterfield et al., 2006; Castegna et al., 2002b). In this study the same approach was employed to identify one altered plasma protein; a stringent 3 fold change was applied, and changes with a p-value < 0.05 were considered significant. A recognized limitation of this methodology is that the variability of each individual protein is not taken into account as the researcher is only looking at an average change, and hence any differences seen can only be assumed to be representative of a particular population. However, this approach does have a potential role in preliminary analysis, enabling altered proteins to be identified for further investigation (Karp and Lilley, 2007).

Albumin makes up a large proportion of the plasma proteome and has transport functions in human blood plasma, it binds to a wide range of compounds including lipoproteins, cytokines and hormones (Adkins et al., 2002). Its capacity to stick to a variety of compounds in human blood plasma may provide one possible explanation for its identification in the work presented here. Additionally, the presence of a prominent region of proteins representing albumin as visualised on a 2-DG (Anderson and Anderson, 1977), coupled to evidence of streaking, suggested that the identification of serum albumin could be artefactual and not the real identity of the oxidized protein. A large group of human plasma proteins corresponding to fibrinogen γ-chain fragments are located in the gel region where the protein

spot was excised from (Anderson and Anderson, 1977), and are therefore more likely to represent the protein spot identity, rather than human serum albumin.

The high abundance of albumin in plasma is a recognized problem in such work, and with this in mind one approach is to deplete plasma of albumin prior to analysis, to uncover the 'deeper' proteome (Righetti et al., 2005). Conversely, interesting proteins that may have been altered due the disease or condition may be depleted or excluded if depletion is employed (Hye et al., 2006), and there is always the possibility that serum albumin may be a disease altered protein. For example, in a recent study by Greilberger and colleagues (2008) the disulphide form of albumin was shown to be increased in plasma from individuals with neurodegenerative disorders; where cysteine 34 residue was oxidized compared to its native form. Additionally, plasma albumin is the predominant target of oxidation in other conditions associated with increased oxidative stress, such as Uraemia (Himmelfarb and McMonagle, 2001).

A further decision faced when employing gel-based proteomics in plasma, is whether to use individual samples or to pool samples together prior to analysis. Each approach has its merits and disadvantages. Availability of material to the researcher, and time and cost which may limit the amount of gels that can be processed, are acknowledged disadvantages of using individual samples (Horgan, 2007). Moreover, the efficiency of protein spot matching is reduced when analysing a large number of individual gels (Voss and Haberl, 2000).

Sample pooling is attractive as it can overcome these aforementioned limitations. The approach also reduces biological variation by forming an average sample (Karp et al., 2005),

which may allow differences and similarities between individual groups to be more easily identified. It may also prevent inaccurate conclusions based on information obtained from a limited number of individual samples. On the other hand, by forming an average protein distribution the pooling process may lead to the loss of information; individual proteins which are not present in all of the sample pool will go undetected (Zolg, 2006). In a recent study Diz et al. (2009) reported that volumes of protein spots in a sample pool matched that of the majority of individual samples for that particular pool. In addition the study found sample pooling led to a reduction in biological variation, thus providing reassuring evidence for some key aspects of the sample pooling approach. The use of multiple individual gels and sample pooling have been successfully implemented in studies which use gel based proteomics for biomarker discovery (Huang et al. 2006; Hye et al. 2006; Taneja et al. 2009). In this study the decision was made to pool individual samples together for proteomic analysis.

IP is a technique that can be used to concentrate a particular target protein from a biological sample. In this work it was initially employed to concentrate plasma proteins modified by oxidation to enhance the chances of obtaining positive protein identification. This was necessary because the modified plasma protein of interest was of low abundance, however this approach provided no improvement compared to a normally processed plasma sample. Initial mass spectrometry data for the excised plasma protein spot from single and multiple gels revealed high protein scores and peptide coverage for trypsin precursor protein. This observation suggested that self digestion of trypsin may have occurred, and hence that it was likely that low plasma protein concentration was a limiting factor. Indeed difficulty in detecting low abundant proteins has previously been reported in a study by Korolainen and

colleagues (2007) who were unable to identify such proteins by pooling spots from several gels. Moreover, at present there is no definitive answer as to how many low abundant protein spots from replicate gels should be pooled together to gain a positive protein identification. The use of narrow range IPG strips allowing for more plasma proteins to be focussed, improved spot clarity and reduced spot congestion in this study, but did not overcome this encountered problem.

In summary, one plasma protein was found to have altered oxidative status in AD compared to control. A positive identification for this protein could not be obtained because the sample was contaminated with albumin. The decision was taken, following unsuccessful use of IP and narrow range IPG strips, not to pursue the identity of this protein using gel based methods. If future studies were to employ 2-DG, a larger sample should be used with narrow range IPG strips to confirm and add to these findings. The use of non-gel based proteomic methods may complement gel based approaches, and may be more successful in identifying proteins altered due to disease.

Chapter 7

Non-gel based proteomics for the study of Alzheimer's disease

7.1 Abstract

The specific location and nature of oxidative modifications to proteins are of particular importance as they may impact on protein structure and function. The introduction of isobaric tagging for absolute and relative quantification (iTRAQ) has allowed for the comparison of protein expression levels between various sample populations. This technique, coupled to improvements in high resolution mass spectrometry may provide the potential for protein modification analysis. iTRAQ analysis was undertaken and identified eleven peptides which were altered in expression in plasma samples from AD sufferers when compared to control. Five peptides containing a nitration adduct were identified, with four displaying increased expression and one displaying decreased expression in AD compared to control samples. In addition, eleven peptides containing oxidized adducts were identified with ten showing increased expression and one showing decreased expression in AD compared to control samples. Furthermore, eleven plasma proteins were found to be differentially expressed between pooled AD and control plasma samples, which were considered of possible significance. The identity of alpha-2-Macroglobulin (α-2M) and Complement 4a protein (C4a) were validated by Western blotting. The modification data require further investigation but suggest that peptides are differentially oxidized and nitrated between AD and control subjects. Of particular interest are the presence of oxidation adducts to serum transferrin and haptoglobin, given their role in iron homeostasis and ability to sequester haemoglobin respectively and thus prevention of radical generation in plasma.

7.2 Introduction

The importance of oxidative modifications in relation to disease pathology has been elegantly demonstrated in studies assessing AD brain. Sultana and colleagues (2006a) conducted a study in AD and control hippocampus tissue and reported that the chaperone enzyme Pin1 exhibited increased oxidation and was down regulated in parallel with a reduction in habitual activity in AD. The authors suggested that as Pin1 binds to tau, a protein involved in microtubule assembly which is central to the formation of neurofibrillary tangle pathologies, one could speculate that such changes maybe involved in AD development.

Identifying the nature and location of post-translational modifications (PTMs), is potentially more important than assessing the global status of a protein. Oxidation and nitration events may now be thought of as PTMs in their own right (Spickett et al., 2006) and the location of specific oxidative modifications on the protein may aid understanding of how oxidative modifications lead to the altered function of a protein. A study undertaken by Ishii et al. (2003) is supportive of this concept. The group showed that incubation of the enzyme Glyceraldehyde-3-phosphate dehydrogenase (GAPDH) with HNE, resulted in 60% of amino acid bound HNE being in the form of Michael adducts, which possess carbonyl functionality. This was concurrent with a decrease in enzyme activity due to selective modification of amino acids located at the molecules surface. Moreover, Ji, Neverova and colleagues (2006) reported that in rat, peroxynitrite activation of microsomal glutathione S-transferase 1 is mediated by the nitration of a tyrosine residue located at position 92. From this observation the authors suggested that this activation is an important mechanism for cellular protection against nitrosative stress.

Classically, two dimensional gel electrophoresis (2-DE) based redox proteomic research has been used to identify specific proteins which are modified by oxidation in disease. In AD several proteins have been reported to be modified by oxidation or nitration in the inferior parietal lobule and hippocampus regions of the brain (Castegna et al., 2002a; Castegna et al., 2002b; Castegna et al., 2003; Sultana et al., 2006a). In contrast, very few studies have identified specific plasma proteins modified by oxidation (Choi et al., 2002; Yu et al., 2003), and no study has investigated nitration to specific plasma proteins in AD. In addition to this, in all of these aforementioned studies the location and nature of these oxidative modifications were not reported. One reason may be that more protein sample is required to determine specific sites of modification, rather than just obtaining a protein identity (Pandey and Mann, 2000). Moreover, previous experiments reported in Chapter 5 of this thesis (Bennett et al. unpublished) highlighted the difficulty in obtaining even a protein identity for a low abundant protein when using 2-DE, and in these experiments locating the site of modification was impossible. This limitation has also been reported in a recent study by Korolainen et al. (2007) when the authors attempted to identify modified cerebrospinal fluid (CSF) proteins from AD patients using 2-DE.

An innovative approach using iTRAQ (isobaric tagging for absolute and relative quantification) reagents coupled to mass spectrometry (MS), for quantitative measurement of protein expression levels in complex protein mixtures was first described in *Saccharomyces cerevisiae* by Ross and colleagues (2004). There are eight forms of iTRAQ reagent currently available with each reagent comprising of a reporter group, a balance group and an amine specific peptide reactive group. The reporter groups (114.1, 115.1, 116.1, 117.1, 118.1, 119.1, 120.1 and 121.1 Da) are balanced with a neutral group (31, 30, 29, 28, 27, 26, 25 and

24Da) such that after reacting with primary amino group of peptides they are isobaric (total mass of 145.1Da). When undertaking this methodology samples are labelled with one of the iTRAQ reagents and then mixed before MS analysis. In all samples, identical peptides will be visualised as one distinct peak on a mass spectrum, as they will be labelled with a different isobaric tag, and will therefore have the same mass and be chemically indistinguishable from each other. Upon fragmentation the neutral balance group is lost and the reporter groups can then be detected on the MS/MS spectrum (Ross et al., 2004; Chiappetta et al., 2009). Peptides can be identified by their fragmentation sequence, and the relative abundance of reporter group ions allows for the accurate comparison of a particular peptide between two or more experimental conditions (see figure 7.1). Since this landmark study by Ross and colleagues (2004) the technique has been successfully used to identify protein expression level differences, in peripheral tissue from AD patients (Abdi et al., 2006; Guntert et al., 2010).

More recently Amoresano and co-workers (2009) demonstrated that the iTRAQ labelling strategy could be used for the analysis of PTMs. The group coupled MS analysis with selective labelling of ortho-nitrotyrosine residues using iTRAQ reagents, and reported that the number and position of modified tyrosine residues in plasma from haemodialysis patients could be identified. Furthermore, given the recent introduction of the next generation ion trap Orbitrap instrument described by Olsen et al. (2009), possible improvements to PTM's analysis maybe possible due to greater resolution and accuracy provided by using this system (Olsen et al., 2009; Chiappetta et al., 2009)

In this study, iTRAQ labelling coupled to mass spectrometry using a LTQ Orbitrap Velos system was undertaken in order to identify plasma proteins altered by expression and more importantly proteins which were modified by oxidation or nitration in AD. At the time of undertaking this research, no previous study had investigated specific plasma proteins altered by nitration in AD. Moreover, plasma protein expression and the identification of specific sites of oxidative modifications in AD had not been explored using this non-gel based methodology.

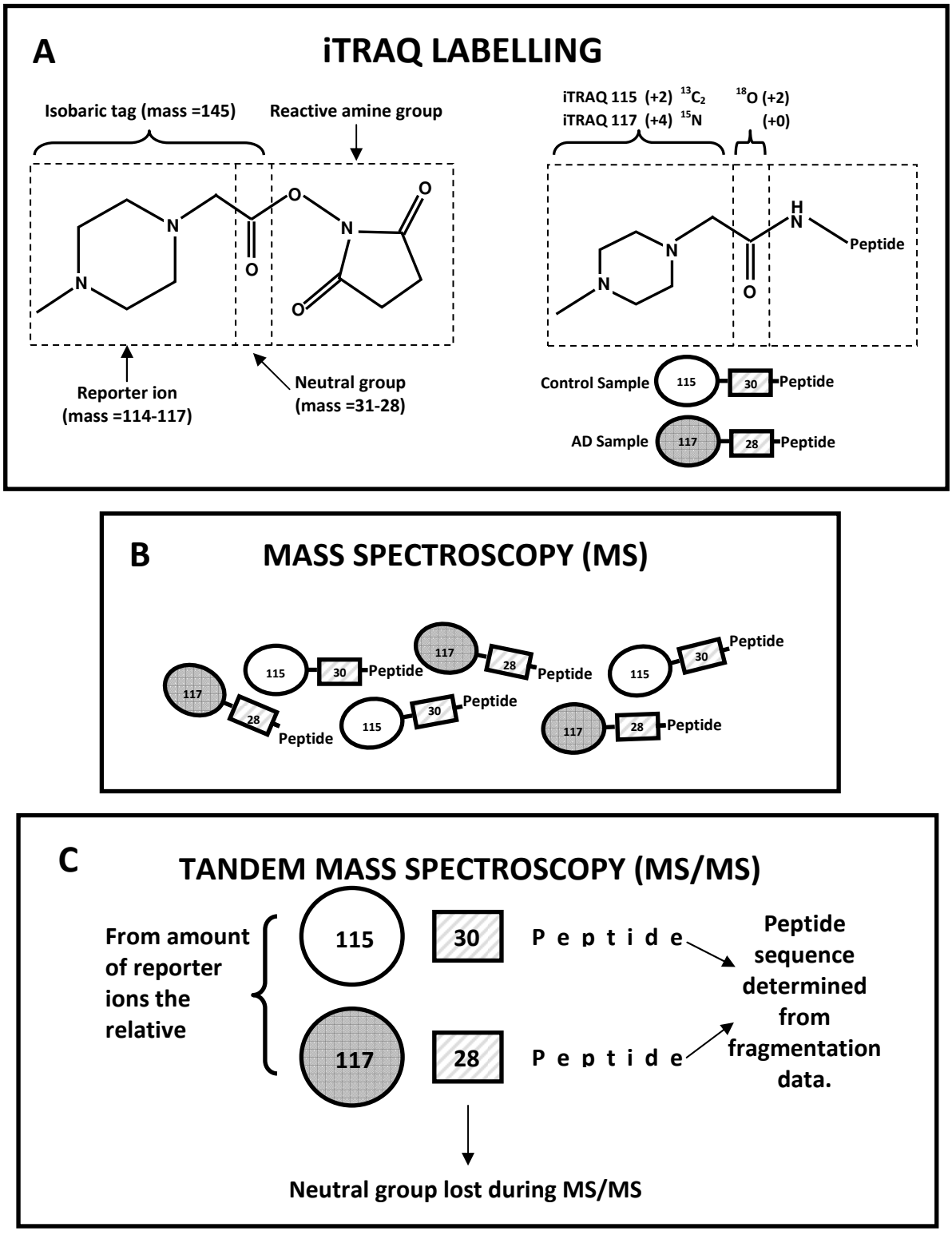

Figure 7.1. iTRAQ labelling and mass spectrometry. Diagram based on that of Ross et al. (2004). A) Isobaric tag consisting of a reporter ion, neutral group and a reactive amine group. Overall mass of reporter ion and balance group kept the same using ^{13}C, ^{15}N and ^{18}O atoms. AD and control samples are labelled with different iTRAQ tags and mixed. B) AD and control peptides are chemically indistinguishable on mass spectra and are visualised by one peak as have the same *m/z*. C) During MS/MS labelled peptides are fragmented; peptides are deduced from fragmentation data and relative amount of reporter ions allow the relative amounts of peptides to be determined.

7.3 Methods

7.3.1 Declaration of ownership

In this Chapter the expertise and advice of Dr Andrew Creese was sought in order to undertake the running of SCX chromatography and LC-MS/MS. Responsibility for the choosing of filtering parameters for data analysis, and decisions on pooling of fractionated samples and their depletion were made by the author. The author was also present for the running of these analytical techniques and was responsible for all further data analysis.

7.3.2 Sample selection

Twenty five control and twenty five AD plasma samples were pooled together for the experiment (see general methods **section 2.1.4**).

7.3.3 Albumin depletion

To increase the number of low abundant plasma proteins detected, pooled samples were depleted of the most abundant plasma protein (albumin) with an Aurum Affi-gel blue mini kit. Protein concentrations were determined by BCA assay (see general methods **section 2.2.1**). For assessment of albumin depletion, depleted and non depleted pooled plasma protein samples (50µg) were separated by 1-DE and visualized by silver staining (see general methods, **section 2.2.5** and **2.2.7**).

7.3.4 iTRAQ labelling

Two pooled samples were digested in parallel with trypsin and used for iTRAQ experiments. Samples (50 µl, 1 mg/ml) were diluted with ammonium bicarbonate (150 µl, 200 mM) and dithiothreitol (40 µl, 50 mM) was added and incubated at 60^{o}C for 45 minutes. The samples

were returned to room temperature before iodoacetamide (200 µl, 22 mM) was added and the samples incubated at room temperature for 25 minutes. To consume any remaining iodoacetamide, dithiothreitol (56 µl, 5 mM) was added and samples incubated for 15 minutes. The samples were digested overnight with sequencing grade modified trypsin (2 µg) at 37^{o}C. The samples were vacuum centrifuged to dryness, resuspended in trifluoroacetic acid (TFA, 0.5%, 200 µl) and desalted using a Michrom desalting Macrotrap (Michrom, USA). The trap was wetted using acetonitrile:water (50:50, 300 µl) and washed with TFA (0.1%, 200 µl). The sample was loaded onto the trap and washed with TFA (0.1%, 200 µl) and eluted in acetonitrile:water (70:30, 200 µl). Samples were vacuum centrifuged to dryness.

Samples were resuspended in dissolution buffer (0.5 M triethylammonium bicarbonate, 30 µl). Half the sample was taken forward for labelling and two samples were labelled in total, as follows. The iTRAQ 8-plex labels (Applied Biosystems, USA) were resuspended in isopropanol (50 µl), added to the 2 samples as below, vortexed for 1 minute and incubated at room temperature for 2 hours. The labels were applied in the following order (condition, sample ID): Control, 115; Alzheimer's disease, 117. The two labelled samples were combined and vacuum centrifuged dry. The pooled sample was desalted as above and resuspended in mobile phase A (see below, 200 µl).

7.3.5 Strong cation HPLC

The dynamic range of plasma protein concentrations are in the region of nine to ten orders of magnitude, resulting in more abundant proteins masking proteins of lower abundance during proteomic analysis (Righetti et al., 2005). Therefore, the sample was separated using strong cation exchange high performance liquid chromatography (SCX-HPLC) and fractions collected in order to obtain a more detailed proteomic analysis. The chromatography was performed on an Ettan LC (GE Healthcare Life Science, UK) with a Frac-950 fraction collection system. The sample was separated on a polysulfoethyl A column (100 mm x 2.1 mm, 5 µm particle size, 200 Å pore size. PolyLC, USA) with a javelin guard cartridge (10 mm x 2.1 mm, 5 um particle size, 200 Å pore size. PolyLC, USA). Mobile phase A was potassium dihydrogen orthophosphate (10 mM, pH 3) dissolved in water:acetonitrile (80:20). Mobile phase B was potassium dihydrogen orthophosphate (10 mM), potassium chloride (500 mM, pH 3) dissolved in water:acetonitrile (80:20). The LC gradient ran from 0 to 80% mobile phase B over 73 minutes. Half of the sample was loaded into column and eighteen fractions were collected in eppendorf tubes (1.5 ml). Fractions were combined to give a total of 5 fractions (fractions 5, 16 and 17 were combined; 6, 14 and 15 combined; 3, 7 and 13 combined; 4, 8 and 12 combined; 9, 10 and 11 combined). The combinations gave rise to a minimum number of fractions with similar peptide quantities. The five fractions were vacuum centrifuged to dryness and desalted as above. The fractions were resuspended in formic acid (0.1%, 50 µl). Each sample was analysed in triplicate with 5 µl used for mass spectrometric analysis.

7.3.6 LC-MS/MS

On-line liquid chromatography was performed by use of a Dionex Ultimate 3000 autosampler and Surveyor MS pump (Thermo Fisher Scientific, Bremen, Germany). Peptides were loaded onto a 75 µm (internal diameter) Integrafrit (New Objective, USA) C18 resolving column (length 10 cm) and separated over a 30 minute gradient from 3.2% to 40% acetonitrile (Baker, Holland). Peptides were eluted directly (≈350 nL/min) via a Triversa nanospray source (Advion Biosciences, NY, USA) into a LTQ Orbitrap Velos ETD mass spectrometer (Thermo Fisher Scientific), where they were subjected to data-dependent MS/MS.

7.3.7 Data-dependent MS/MS

The mass spectrometer alternated between a full FT-MS scan (m/z 380-1600) and subsequent higher collision dissociation (HCD) and CID MS/MS scans of the three most abundant ions above a threshold of 5,000. HCD was used solely for quantification and CID for identification. Survey scans were acquired in the Orbitrap with a resolution of 60,000 at m/z 400. Precursor ions were subjected to HCD in the HCD collision cell. The width of the precursor isolation window was 3 m/z. Only multiply-charged precursor ions were selected for MS/MS. HCD was performed with nitrogen gas at a normalized collision energy of 55% and activation time 100 ms. Automated gain control was used to accumulate sufficient precursor ions (target value $10x10^5$, maximum fill time 100 ms). Precursor ions were subjected to CID in the linear ion trap. The width of the precursor isolation window was 2 m/z. CID was performed with helium gas at a normalized collision energy of 35%, activation Q 0.25 and activation time 10 ms. Automated gain control was used to accumulate sufficient precursor ions (target value $10x10^5$, maximum fill time 50 ms).

Dynamic exclusion was used with a repeat count of 1 and exclusion duration of 180 s. Data acquisition was controlled by Xcalibur software V2.1.0 (Thermo Fisher Scientific Inc.).

7.3.8 Data analysis

The MS/MS spectra were searched against a concatenated forward and reverse IPI human database v3.72 (173046 entries) using the SEQUEST algorithm in Proteome Discoverer sp 1.0 (Thermo Fisher Scientific). iTRAQ labels, tyrosine and tryptophan nitration and methionine oxidation were specified as variable modifications, with carboxyamidomethylation of cysteine as a static modification. The data were searched with a precursor mass error of 10 ppm and a fragment mass error of 0.5 Da. The search results were filtered using XCorr vs charge state (peptides reporting XCorr values <2.5 for 2+ ions, <3.0 for 3+ ions and <3.5 for 4+ or greater ions are rejected) resulting in a false discovery rate of 2 protein in 49 proteins identified (See figure 7.2 for overview of iTRAQ procedure).

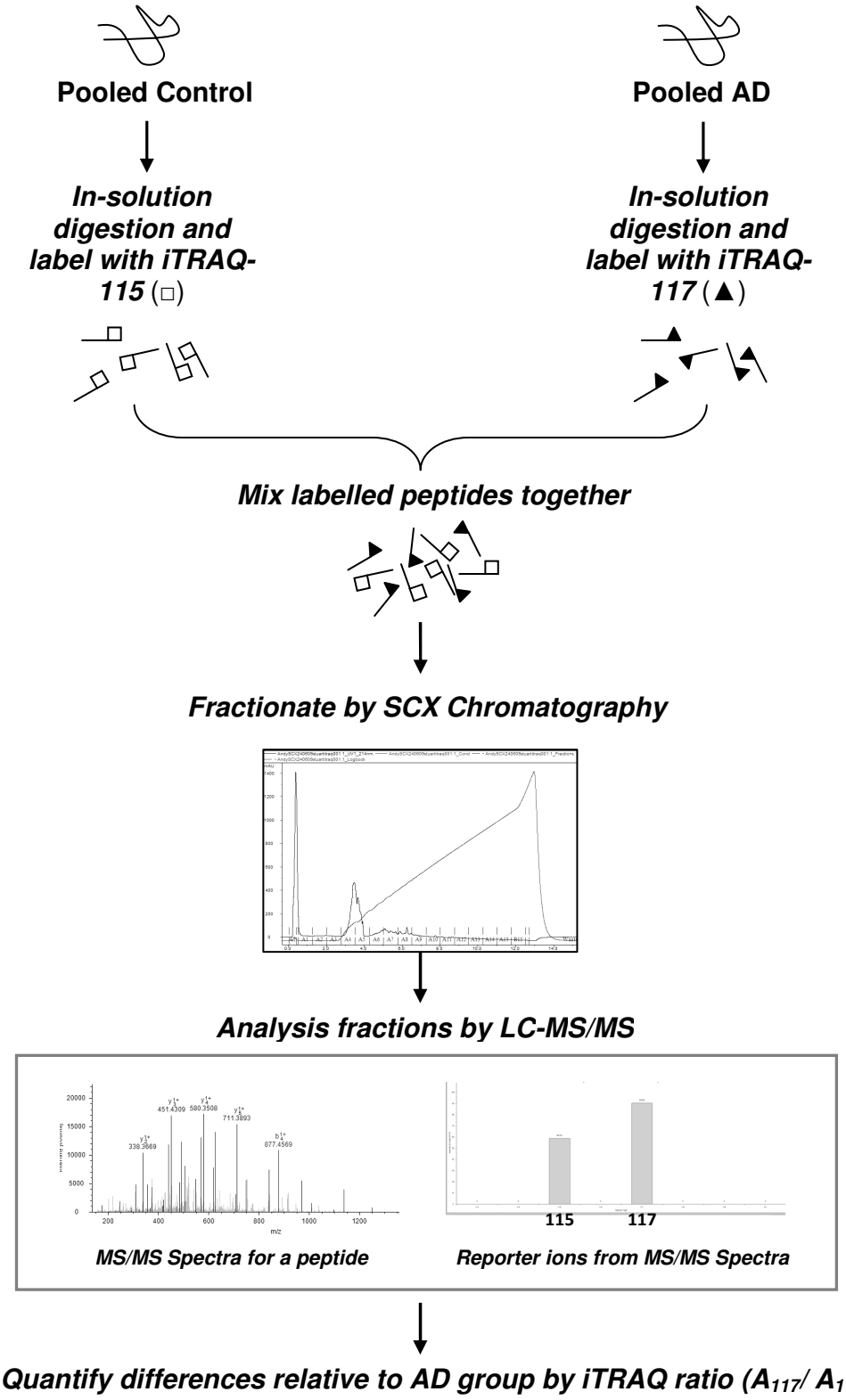

Figure 7.2. Overview of iTRAQ experiment. Further detail provided in methods section.

7.3.9 Quantification of protein expression differences between groups

Protein quantification was achieved by averaging the iTRAQ ratio of individual peptides for a particular protein; ratios were obtained for individual peptides by dividing the intensity count of the iTRAQ label 117 (Pooled AD sample) by label 115 (Pooled Control sample). After iTRAQ ratios were calculated, normalisation against the mean value of all iTRAQ ratios, when all peptides were considered, was enforced, such that the data was normally distributed with the mean and median values equal to 1. A slight modification to the approach used by Abdi et al. (2006) to define changes in protein expression was employed; changes of more than 50% were considered significant. Changes which were <15% and ≥15% were defined as having unlikely and uncertain significance respectively.

7.3.10 Western blot analysis and statistics

Western blotting was undertaken as described in **section 2.2.7**. Mouse monoclonal anti-α-2M (AbCam Ltd, Cambridge, UK) was used at 1:10,000 with an appropriate horseradish peroxidase conjugated secondary antibody (1: 50,000). Mouse monoclonal anti-C4a antibody (AbCam Ltd, Cambridge, UK) was used at 1:200 with an appropriate horseradish peroxidase conjugated secondary antibody (1: 2,000). Pooled AD and control samples (10 µg) were assayed in duplicate or triplicate. Optical densities of bands were analysed by user defined volume integration using Quantity One software™ (BioRad). Statistical analysis was undertaken as described in section **2.2.10**.

7.4 Results

7.4.1 Albumin depletion

Figure 7.3 shows pooled control and AD plasma samples were successfully depleted of albumin using Aurum™ Affi-Gel® Blue columns. A very prominent protein band at approximately 66 kDa is present in non-depleted pooled control plasma as visualised on a silver stained gel (Figure 3a, lanes 1 and 2). This band corresponds to Human Serum Albumin. The intensity and size of this band is decreased in the depleted pooled control plasma sample (Figure 3a, lanes 3 and 4). This difference is also observed between non-depleted and depleted pooled AD plasma (Figure 3b, lanes 1 to 4).

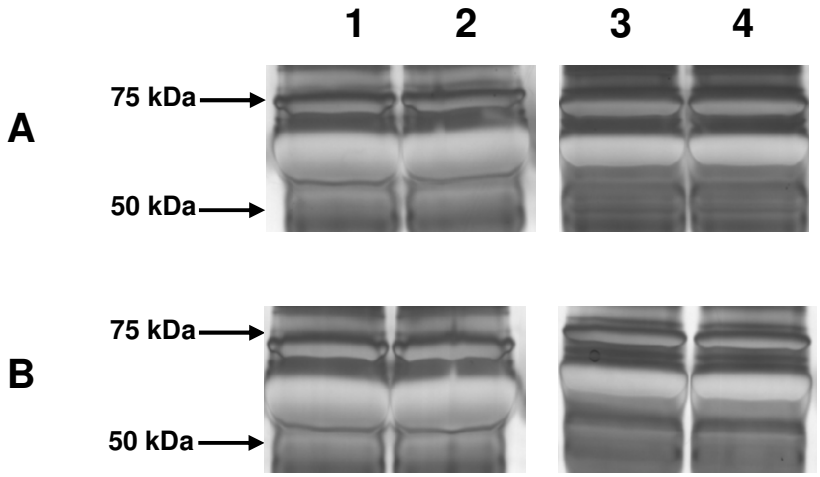

Figure 7.3. Albumin depletion of Pooled plasma samples. A) Non-depleted pooled control sample (lanes 1 and 2) and depleted pooled control sample (lanes 3 and 4). B) Non-depleted pooled AD sample (lanes 1 and 2) and depleted pooled AD sample (lanes 3 and 4). All plasma samples (20 µg) were loaded in duplicate.

7.4.2 Fractionation of peptides by SCX-HPLC

Figure 7.4 shows the iTRAQ labelled sample was separated into several fractions (A1-B15) using SCX-chromatography. The line with several peaks represents absorption of UV at 214nm for the sample as it passes through the column. The initial peak corresponds to the solvent front, which represents any chemicals which do not bind to the column; subsequent peaks correspond to peptides in the sample. Further peaks correspond to the amount of peptides present; peaks visible later on the chromatogram correspond to peptides which have a higher affinity for the column and bind for longer based on their charge. As demonstrated in figure 7.4 a large quantity of peptides are present in fractions A4 and A5 in contrast to fractions A15 and B15 which have little peptide abundance. Conductance increased linearly as the sample was passed through the column suggesting the gradient had been successful (diagonal line).

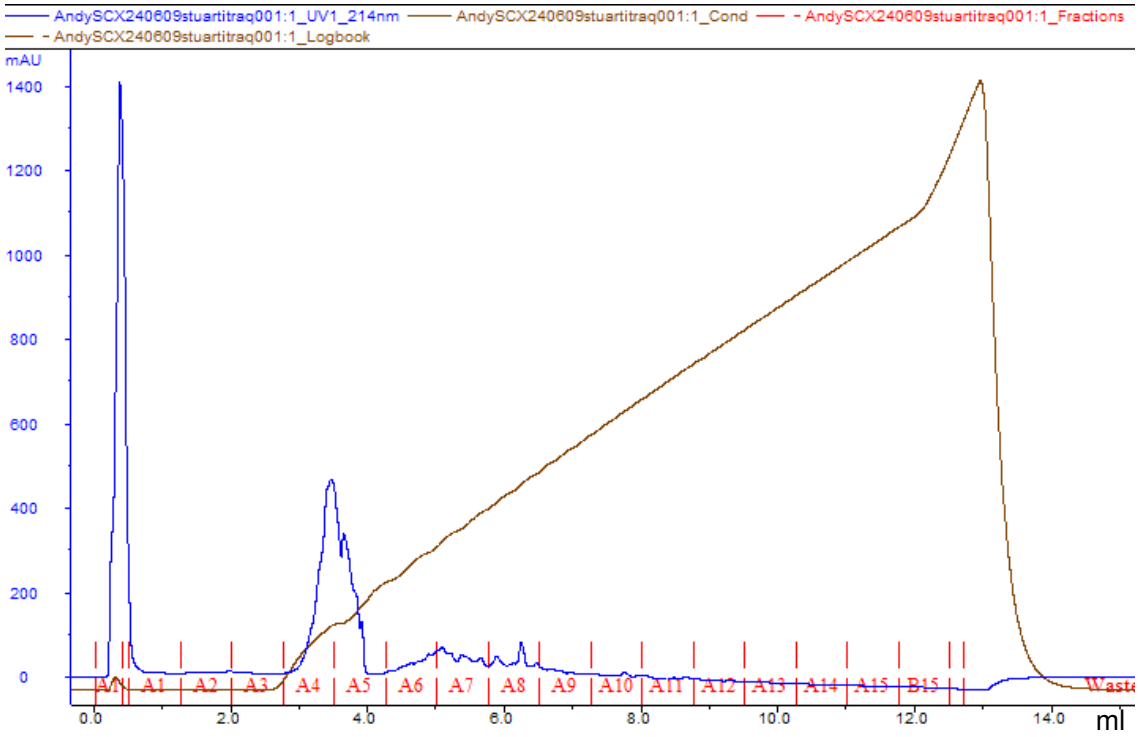

Figure 7.4. SCX chromatogram for iTRAQ labelled sample. SCX elution profile of sample: UV absorption at 214nm is represented by line with several peaks, fractions are represented along the x-axis (Labelled A1-B15) and conductance demonstrating a successful linear gradient is shown by the diagonal line running from bottom left to top right of chromatogram.

7.4.3 Protein expression differences between AD and Control

Forty nine proteins present in both AD and control groups were successfully detected using iTRAQ and LC-MS/MS. Of this initial group of proteins two were reverse sequences and six were keratin type precursor proteins. Thirty six of the remaining 41 proteins had > 2 unique peptides and were taken forward for analysis. It was also noted that there was some redundant data. For example 245 peptides were identified for serum albumin precursor protein, of which several different peptides were detected multiple times. As shown in Table 7.1, proteins exhibited variable protein expression between the AD and control group. More specifically no proteins were identified as having significantly altered expression between the two groups. Eleven proteins were found to have altered expression which was considered to be of possible significance; 6 proteins were increased and 5 were decreased in the AD group compared to the control group. Protein expression differences in the remaining twenty five proteins were considered unlikely to be significant.

Protein	IPI#	No. of peptides	Coverage (%)	iTRAQ ratio	SEQUEST Score
Isoform 1 of Serum albumin precursor	00745872.2	245	32.51	1.06 (↔)	2680.81
42 kDa protein	00942787.1	106	26.44	0.93 (↔)	621.52
Serotransferrin	00022463.1	81	23.35	1.03 (↔)	576.59
Alpha-2-macroglobulin	00478003.2	34	6.11	0.89 (↔)	393.51
Ig gamma-3 chain C region	00827754.3	32	14.32	1.00 (↔)	289.06
Complement C3 (Fragment)	00783987.2	31	7.10	1.01 (↔)	223.28
Apolipoprotein A1	00853525.1	31	26.12	1.12 (↔)	188.09
Isoform 2 of Fibrinogen alpha chain	00029717.1	24	9.47	0.90 (↔)	170.65
Conserved hypothetical protein	00644497.4	24	10.58	0.77 (↓)	156.98
Apolipoprotein A-IV	00304273.2	21	18.94	0.81 (↓)	99.94
Putative uncharacterized protein	0084758.1	21	6.21	0.79 (↓)	135.12
cDNA FLJ58075, highly similar to Ceruloplasmin	00947307.1	20	6.45	1.01 (↔)	88.28

Protein	IPI#	No. of peptides	Coverage (%)	iTRAQ ratio	SEQUEST Score
Alpha-1-acid glycoprotein 2	00020091.1	19	13.93	0.86 (↔)	137.41
Hemoglobin subunit beta	IPI00654755.3	18	23.81	1.35 (↑)	88.30
Isoform 2 of Alpha-1-antitrypsin	00790784.2	15	7.24	0.78 (↓)	199.97
C4A protein	00889723.2	14	2.89	1.15 (↑)	80.68
Isoform 1 of Alpha-1-antichymotrypsin	00847635.1	13	8.51	1.06 (↔)	74.78
Fibrinogen beta chain	00298497.3	13	10.59	0.96 (↔)	82.22
Isoform 1 of Gelsolin	00026314.1	13	3.84	1.17 (↑)	51.41
Hemopexin	00022488.1	11	6.49	1.16 (↑)	84.15
Full-length cDNA clone CS0DD006YL02 of Neuroblastoma of Homo sapiens	00479708.6	10	6.13	1.13 (↔)	62.87
Hemoglobin subunit alpha	00410714.5	9	10.56	1.23 (↑)	44.50
Isoform Gamma-A of Fibrinogen gamma chain	00219713.1	8	5.49	0.95 (↔)	50.82
Apolipoprotein B-100	00022229.1	7	0.85	1.08 (↔)	35.42

Protein	IPI#	No. of peptides	Coverage (%)	iTRAQ ratio	SEQUEST Score
25 kDa protein	00940069.1	6	10.68	1.05 (↔)	41.84
Alpha-1B-glycoprotein	00022895.7	6	2.42	0.74 (↓)	24.03
IGL@ protein	00829877.1	5	13.36	0.98 (↔)	65.71
Isoform 2 of Vitamin D-binding protein	00954102.1	5	3.43	0.91 (↔)	21.15
Prothrombin (Fragment)	00019568.1	5	5.14	1.04 (↔)	27.13
Isoform 2 of Nipped-B-like protein	00026466.9	5	0.78	0.97(↔)	23.37
Isoform 1 of Zinc finger CCCH domain-containing protein 13	00329547.3	4	0.42	0.90 (↔)	18.66
SERPINC1 protein	00844156.2	4	8.49	1.19 (↑)	20.71
13 kDa protein	00646384.1	4	11.02	0.89 (↔)	12.92
Serum paraoxonase/arylesterase 1	00218732.3	3	3.10	0.98 (↔)	18.80
Isoform GTBP-alt of DNA mismatch repair protein Msh6	00106847.3	3	1.03	0.87 (↔)	13.67
CLU	00795633.1	3	2.68	1.03 (↔)	16.67

Table 7.1. Differential plasma protein expression between AD and age-matched control subjects. A slight modification to the approach used by Abdi et al. (2006) to define changes in protein expression was employed; changes of more than 50% were considered significant (↑↑). Changes which were <15% and ≥15% were defined as having unlikely (↔) and possible significance (↑) respectively. Only greater than 2 peptides were considered for differential protein expression between AD and control groups.

7.4.4 Validation of protein expression data

Plasma proteins α-2M and C4a protein were chosen to validate protein expression data acquired from LC-MS/MS. α-2M was used as a control (i.e. no change in protein expression between groups) and C4a was used as a positive control as it was one of six proteins found to be increased in AD with possible significance.

7.4.4.1 α-2-Macroglobulin

When visualised on a Western blot α-2M forms a band at 173kDa. As shown in figure 7.5, in both pooled AD and control samples there is a distinct band at approximately 170 kDa which corresponds to α-2M. Consistent with LC-MS/MS data (section 7.4.3, table 7.1) there is no difference (Control: 170.76 ± 38.47 OD Vs AD: 188.54 ± 1.79 OD units; p = 0.63, independent samples t-test) in α-2-Macroglobulin levels as assessed by Western blotting.

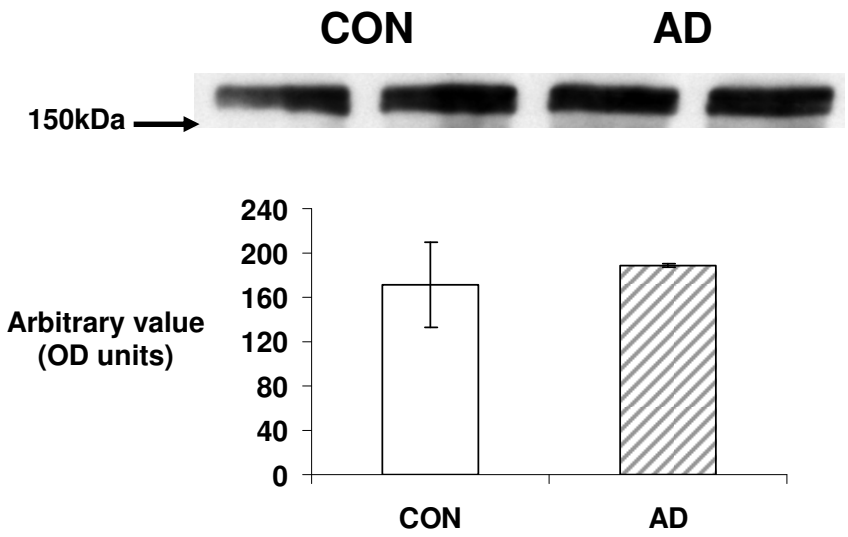

Figure 7.5. α-2M protein expression in control and AD subjects. A band at approximately 170 kDa corresponding to α-2M is evident on a Western blot for control and AD plasma samples. Primary mouse monoclonal anti-α-2M (1:10,000; AbCam, Cambridge, UK) antibody and an appropriate peroxidase conjugated goat anti-mouse secondary (1:50,000; Sigma, UK) were used.

7.4.4.2 Complement 4a protein

Complement 4 is an inflammatory protein which is broken down to form C4a protein which has a molecular weight of 193 kDa. As shown in figure 7.6, a band is present in both pooled AD and control samples at approximately 190 kDa. Consistent with LC-MS/MS data (section 7.4.3, table 7.1) there was a significant increase in C4a protein expression in the pooled AD compared to pooled control sample when assessed by densitometry (Control: 43.78 ± 3.62 OD Vs AD: 69.46 ± 10.21 OD units; $p = 0.02$, independent samples t-test).

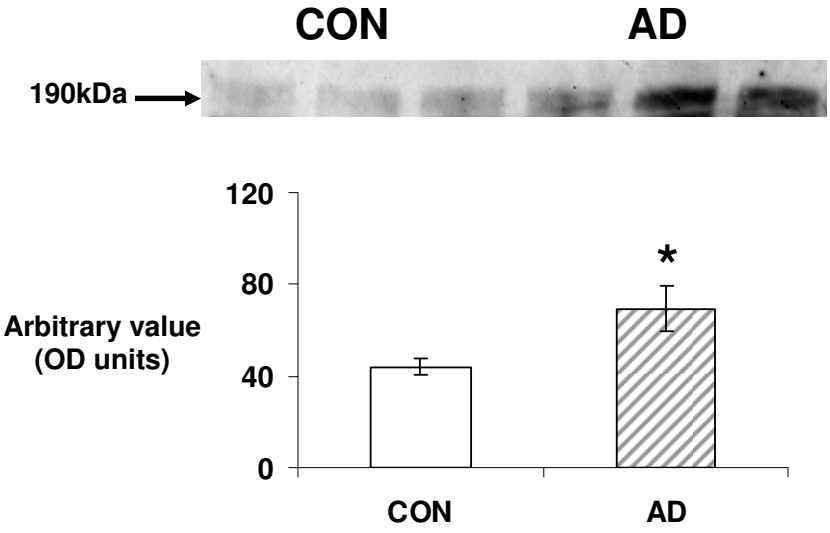

Figure 7.6. C4a protein expression in control and AD subjects. A band at approximately 190 kDa corresponding to C4a protein is evident on a Western blot for control and AD plasma samples. Primary mouse monoclonal anti-C4a (1:250; AbCam, Cambridge, UK) antibody and an appropriate peroxidase conjugated goat anti-mouse secondary (1:2000; Sigma, UK) were used. * $p = 0.02$.

7.4.5 Modified peptides in AD and control plasma

Forty four peptides were identified as exhibiting an oxidative modification, with twelve of these representing reverse sequences. As shown in Table 7.2, five peptides present in both AD and control plasma were found to contain nitrated tyrosine or tryptophan residues (a schematic diagram of nitrated tyrosine and tryptophan residues are shown in figure 7.7). These peptides correspond to Alkaline Phosphatase, Dynein heavy chain 1 and 11, Glycolipid transfer protein and Thyroid Receptor Interacting Protein 11. In addition, several peptides were shown to be oxidized in both AD and control plasma populations. These peptides are named in Table 7.2, and include Serotransferrin, Fibrinogen β-chain, Isoforms 1, 2 of fibrinogen α-chain, α-2M, Vitronectin, DNA mismatch repair protein, Serum amyloid A-4 protein, serum albumin (Isoforms 1 and 2) and Haptoglobin. They all contained oxidized adducts.

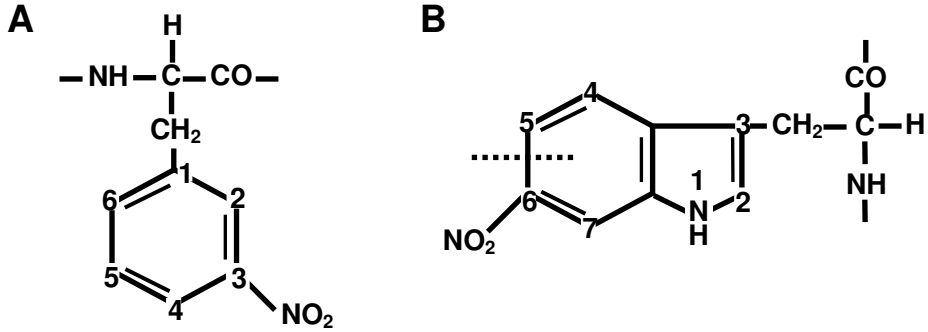

Figure 7.7. Nitrated Tryptophan and Tyrosine residues. 3-nitrotyrosine (A) is formed by the reaction of RNS and tyrosine residues in proteins. Tryptophan has several sites which can be nitrated or oxidized. These include ring positions 2,4,5,7 and the indole imino group (dotted line). 6-NO_2Trp (B) is the most abundant nitrated product formed by the reaction of RNS and tryptophan in proteins (B), although 4-NO_2Trp and 5-NO_2Trp has also been reported (Yamakura and Ikeda, 2006).

Protein	Amino acid sequence (peptide)	Oxidative Modification	117/115 Ratio	XCorr Score
Alkaline Phosphatase	VQHASPAGAyAHTVNR	Y10 [N]	↓	2.55
Dynein heavy chain	EwMKGIPERLVGLEER	W2 [N]	↑	2.71
Thyroid receptor interacting protein 11	AMySAELEKQK	Y3[N]	↑	2.58
Glycolipid transfer protein	KyHGWIVQK	Y2[N]	↑	3.04
Dynein heavy chain 11	ASSITEIwSLNK	W8[N]	↑	2.80
Fibrinogen β-chain	IESDVSAQmEYcR	M9[O] C12 [Carbomidomethyl]	↑	4.99
α-2-Macroglobulin	VGFYESDVmGR	M9[O]	↑	4.57
Serum amyloid A-4 protein	EALQGVGDmGR	M9[O]	↑	3.00
Serum Transferrin (Serotransferrin)	KDSGFQmNQLR DSGFQmNQLR	M7[O] M6[O]	↑	3.29 3.89
54, 52, 66, 53 kDa protein	YVTSAPmPEPQAPGR	M7[O]	↑	3.36
Unknown protein	ILmTVESAK	M3[O]	↑	2.72

Protein	Amino acid sequence (peptide)	Oxidative Modification	117/115 Ratio	XCorr Score
Vitronectin	DWHGVPGQVDAAmAGR	M13[O]	↑	3.09
Fibrinogen α-chain	DSHSLTTNImEILR	M10 [O]	↑	3.71
Isoform 1 of serum albumin	ETYGEmADccAK	M6[O], C9,C10[Carbamidomethyl]	↑	3.00
Haptoglobin	YVmLPVADQDQcIR	M3[O], C12[Carbamidomethyl]	↓	5.25
Isoform 2 of serum albumin	AVmDDFAAFVEK	M3[O]	↑	3.93
DNA mismatch repair Msh6 protein	RmVTGNGSLKR	M2[O]	↑	2.60

Table 7.2. Levels of peptides containing oxidatively modified residues in AD and age-matched control plasma. Modified peptides were present in both AD and control plasma protein, as assessed by iTRAQ and LC-MS/MS. Levels of modified peptides were altered between groups and are indicated by arrows relative to AD. The letters in the modification column refer to the amino acid which is modified and [N] or [O] refers to whether they are modified by nitration or oxidation respectively.

A

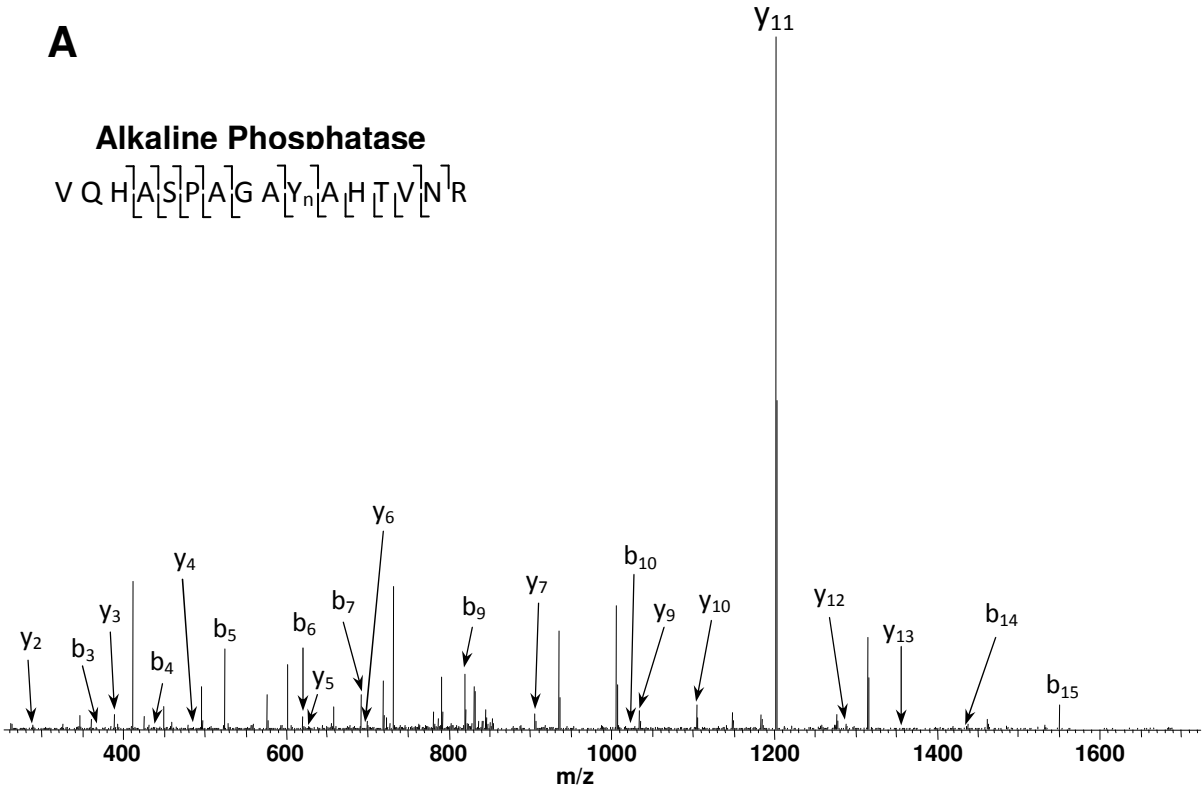

Number	Acid	B [M+H]+		Y [M+H]+		Number
1	V	---		---		16
2	Q	228.134		1624.76		15
3	H	365.193	**365.18**	1496.7		14
4	A	436.23	**436.25**	1359.64	**1359.56**	13
5	S	523.262	**523.2**	1288.6	**1288.64**	12
6	P	620.315	**620.31**	1201.57	**1201.53**	11
7	A	691.352	**691.38**	1104.52	**1104.54**	10
8	G	748.374		1033.48	**1033.39**	9
9	A	819.411	**819.39**	976.46		8
10	Y(Nitration)	1027.46	**1027.65**	905.422	**905.41**	7
11	A	1098.5		697.374	**697.85**	6
12	H	1235.56		626.337	**626.4**	5
13	T	1336.6		489.278	**489.01**	4
14	V	1435.67	**1435.99**	388.23	**388.25**	3
15	N	1549.71	**1549.65**	289.162	**289.36**	2
16	R	---		175.119		1

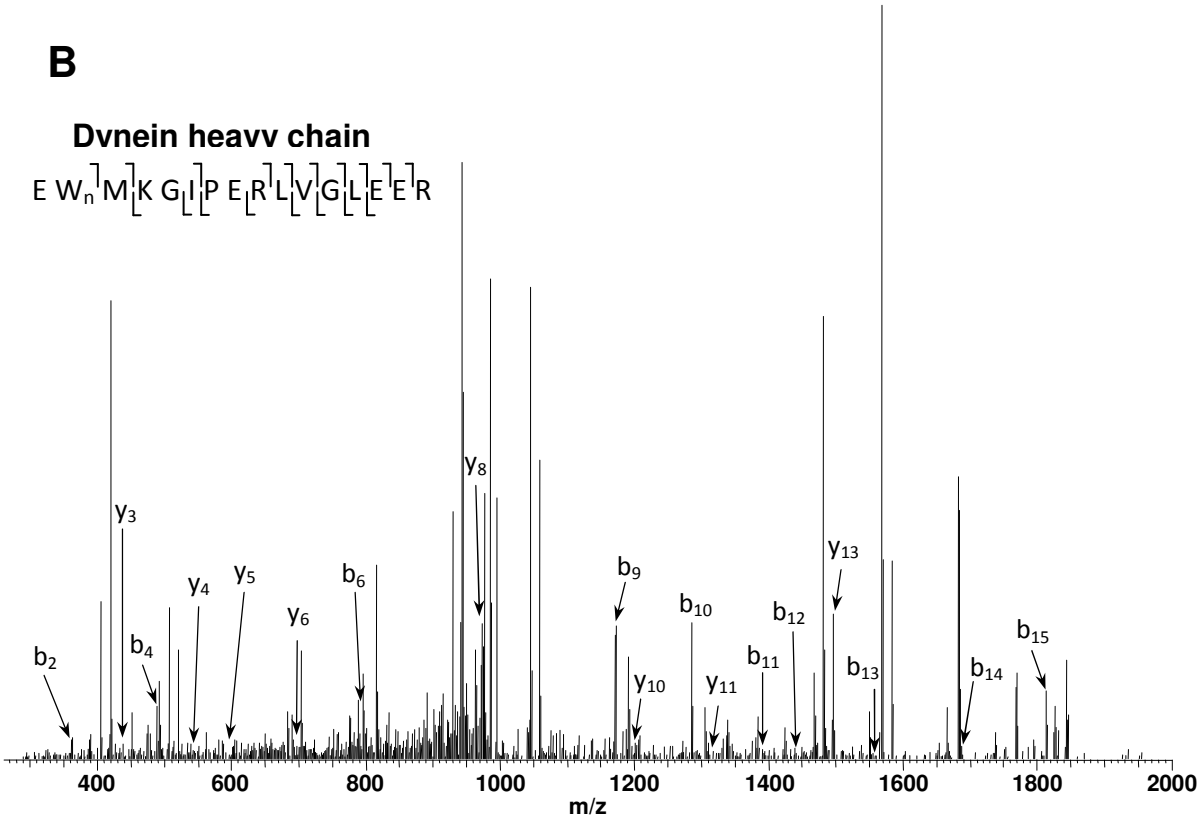

Number	Acid	B [M+H]+		Y [M+H]+		Number
1	**E**	---		---		16
2	**W(Nitration)**	361.109	**361.28**	1857.96		15
3	**M**	492.15	**492.33**	1626.9		14
4	**K**	620.245		1495.86	**1495.6**	13
5	**G**	677.266		1367.76		12
6	**I**	790.35	**790.56**	1310.74	**1310.7**	11
7	**P**	887.403		1197.66	**1197.59**	10
8	**E**	1016.45		1100.61		9
9	**R**	1172.55	**1172.45**	971.563	**971.9**	8
10	**L**	1285.63	**1285.56**	815.462		7
11	**V**	1384.7	**1384.7**	702.378	**702.42**	6
12	**G**	1441.72	**1441.62**	603.31	**603.32**	5
13	**L**	1554.8	**1554.87**	546.288	**546.44**	4
14	**E**	1683.85	**1685.72**	433.204	**433.26**	3
15	**E**	1812.89	**1812.85**	304.162		2
16	**R**	---		175.119		1

C

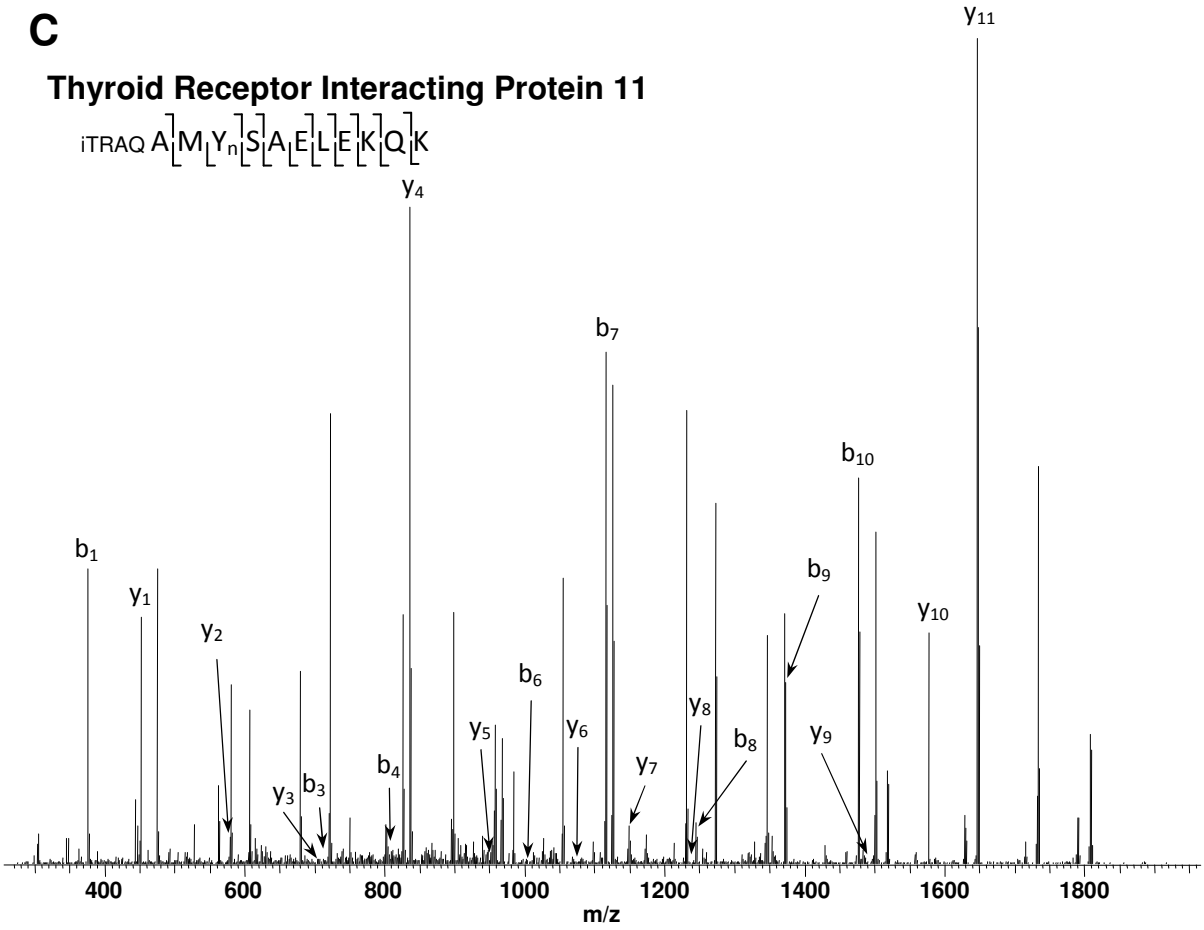

Number	Acid	B [M+H]+		Y [M+H]+		Number
	iTRAQ8plex					
1	**A**	376.2497	**376.39**	1646.836	**1646.81**	11
2	**M**	507.2902		1575.799	**1575.8**	10
3	**Y(Nitration)**	715.3386	**715.5**	1444.759	**1444.86**	9
4	**S**	802.3707	**802.53**	1236.71	**1236.65**	8
5	**A**	873.4078		1149.678	**1149.49**	7
6	**E**	1002.45	**1002.45**	1078.641	**1078.38**	6
7	**L**	1115.534	**1115.66**	949.5984	**949.52**	5
8	**E**	1244.577	**1244.71**	836.5143	**836.51**	4
9	**K**	1372.672	**1372.66**	707.4717	**707.41**	3
10	**Q**	1500.731	**1500.68**	579.3767	**579.41**	2
11	**K(iTRAQ8plex)**	---		451.3182	**451.41**	1

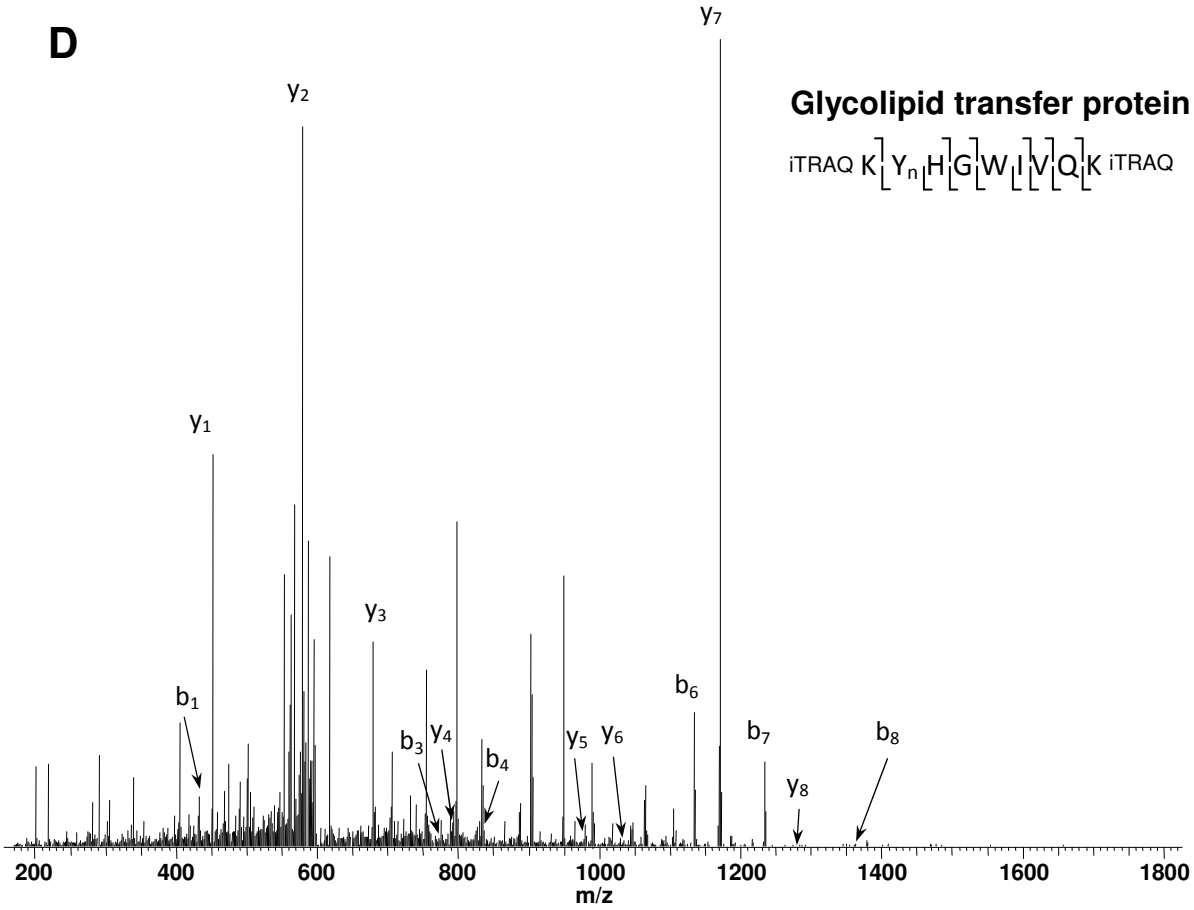

Number	Acid	B [M+H]+		Y [M+H]+		Number
	iTRAQ8plex					
1	**K**	433.308	**432.94**	1507.83		9
2	**Y(NITRO)**	641.356		1379.74	**1378.72**	8
3	**H**	778.415	**778.74**	1171.69	**1171.56**	7
4	**G**	835.436	**835.59**	1034.63	**1034.58**	6
5	**W**	1021.52		977.609	**978.5**	5
6	**I**	1134.6	**1134.54**	791.529	**791.45**	4
7	**V**	1233.67	**1233.62**	678.445	**678.49**	3
8	**Q**	1361.73	**1362.19**	579.377	**579.37**	2
9	**K(iTRAQ8plex)**	---		451.318	**451.5**	1

E

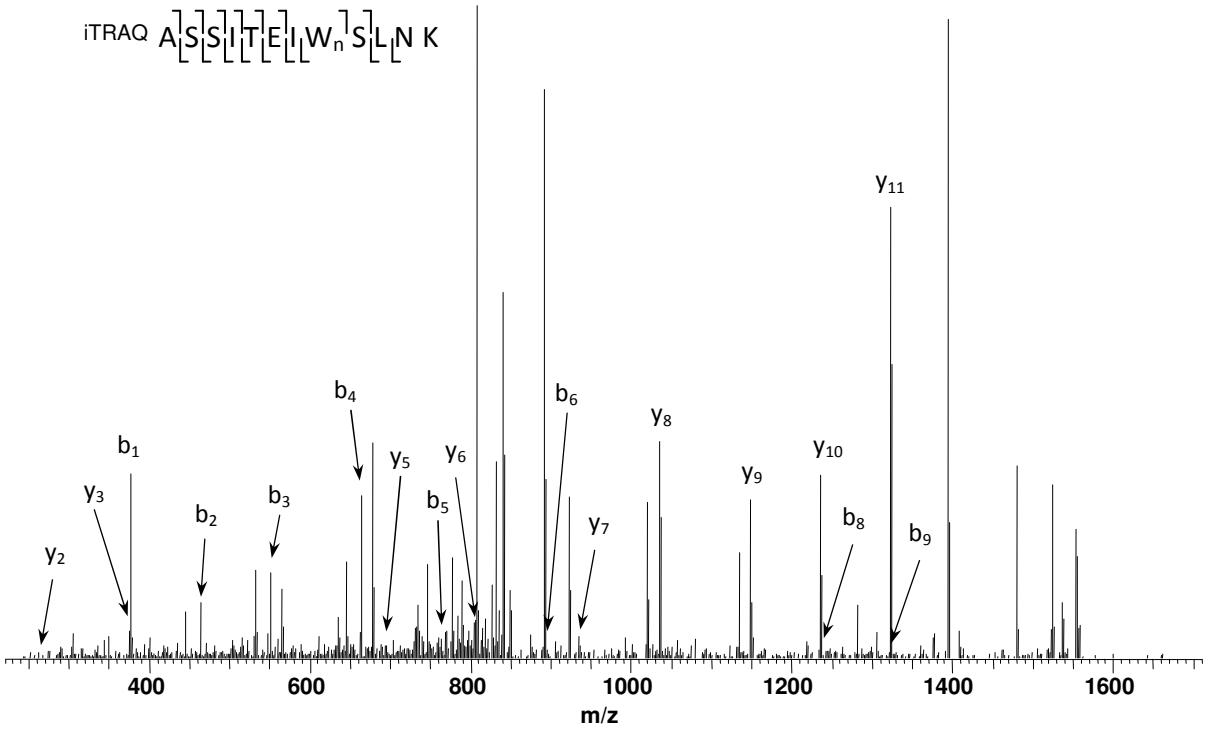

Number	Acid	B [M+H]+		Y [M+H]+		Number
	iTRAQ8plex					
1	A	376.25	**376.34**	-		12
2	S	463.28	**463.21**	1322.66	**1322.58**	11
3	S	550.31	**550.28**	1235.63	**1235.61**	10
4	I	663.4	**663.46**	1148.59	**1148.62**	9
5	T	764.45	**764.45**	1035.51	**1035.55**	8
6	E	893.49	**893.56**	934.46	**934.52**	7
7	I	1006.57		805.42	**805.42**	6
8	W(Nitration)	1237.64	**1237.63**	692.34	**692.32**	5
9	S	1324.67	**1324.52**	461.27		4
10	L	1437.75		374.24	**374.27**	3
11	N	1551.8		261.16	**261.2**	2
12	K	-		147.11		1

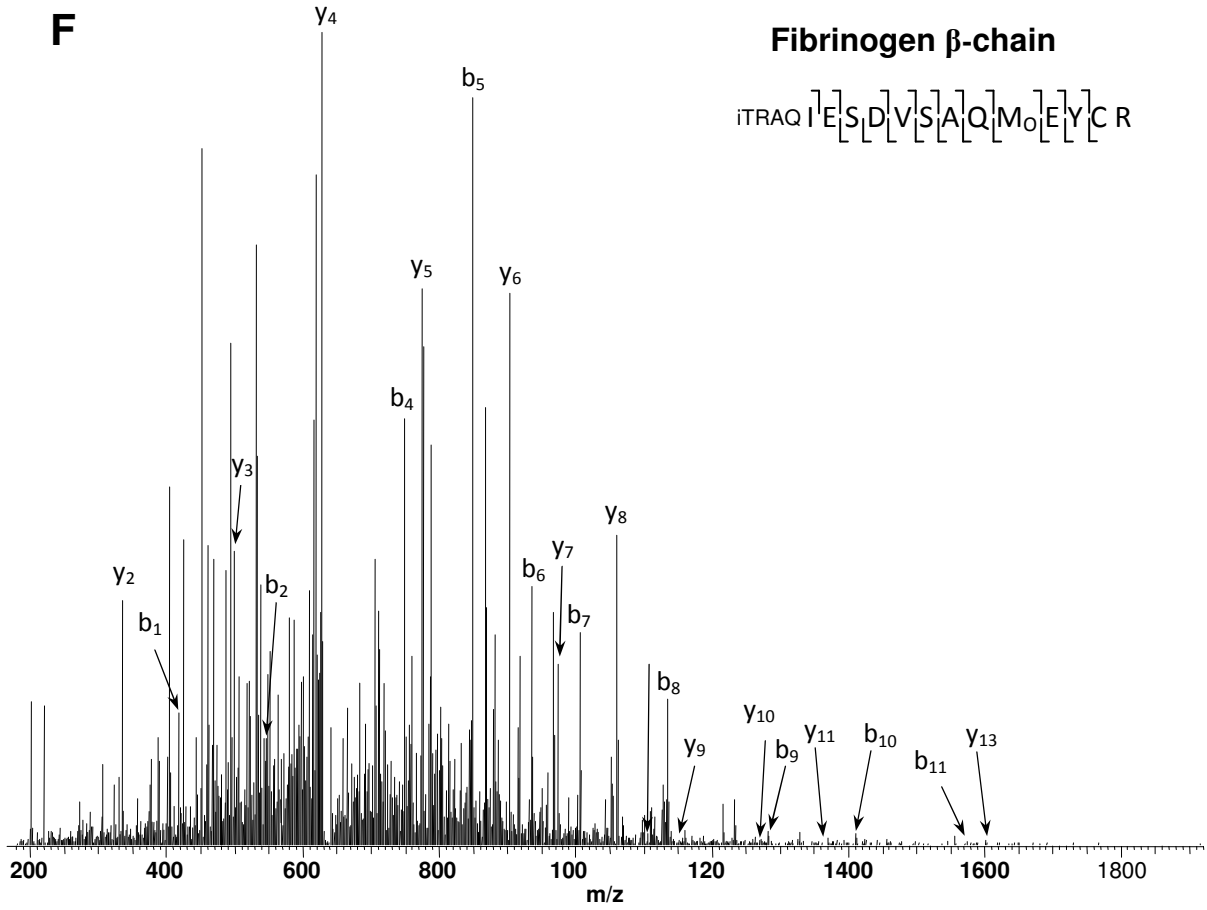

Number	Acid	B [M+H]+		Y [M+H]+		Number
	iTRAQ8plex					
1	I	418.297	**418.44**	1603.67	**1603.72**	13
2	E	547.339	**547.35**	1490.59		12
3	S	634.371		1361.55	**1361.43**	11
4	D	749.398	**749.45**	1274.51	**1274.47**	10
5	V	848.467	**848.5**	1159.49	**1159.26**	9
6	S	935.499	**935.49**	1060.42	**1060.38**	8
7	A	1006.54	**1006.52**	973.387	**973.33**	7
8	Q	1134.59	**1134.53**	902.35	**902.37**	6
9	M(Oxidation)	1281.63	**1281.61**	774.291	**774.34**	5
10	E	1410.67	**1410.69**	627.256	**627.29**	4
11	Y	1573.74	**1573.67**	498.213	**498.27**	3
12	C(Carbamidomethyl)	1733.77		335.15	**335.39**	2
13	R	---		175.119		1

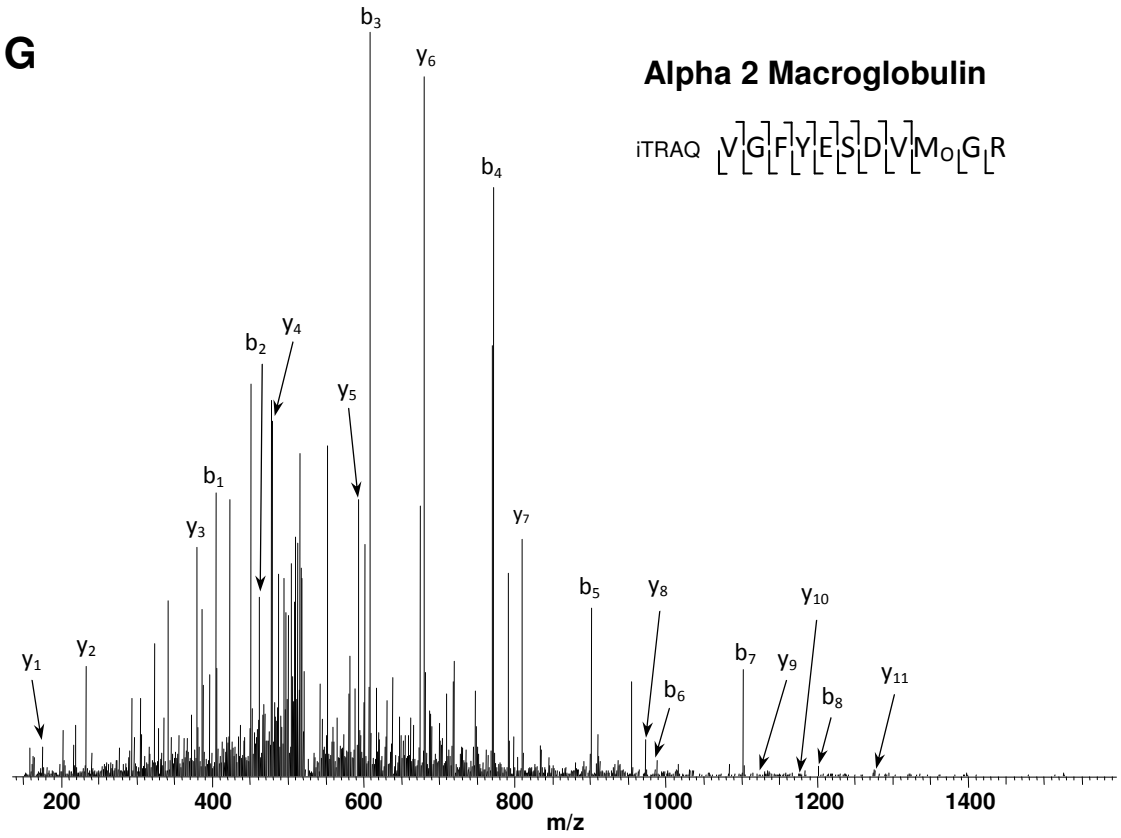

Number	Acid	B [M+H]+		Y [M+H]+		Number
	iTRAQ8plex					
1	V	404.281	**404.42**	1275.57	**1275.81**	11
2	G	461.303	**461.41**	1176.5	**1176.65**	10
3	F	608.371	**608.39**	1119.48	**1119.77**	9
4	Y	771.434	**771.3**	972.409	**972.42**	8
5	E	900.477	**900.5**	809.346	**809.37**	7
6	S	987.509	**987.59**	680.303	**680.32**	6
7	D	1102.54	**1102.45**	593.271	**593.29**	5
8	V	1201.6	**1201.56**	478.244	**478.32**	4
9	M(Oxidation)	1348.64		379.176	**379.38**	3
10	G	1405.66		232.14	**232.24**	2
11	R	---		175.119	**175.15**	1

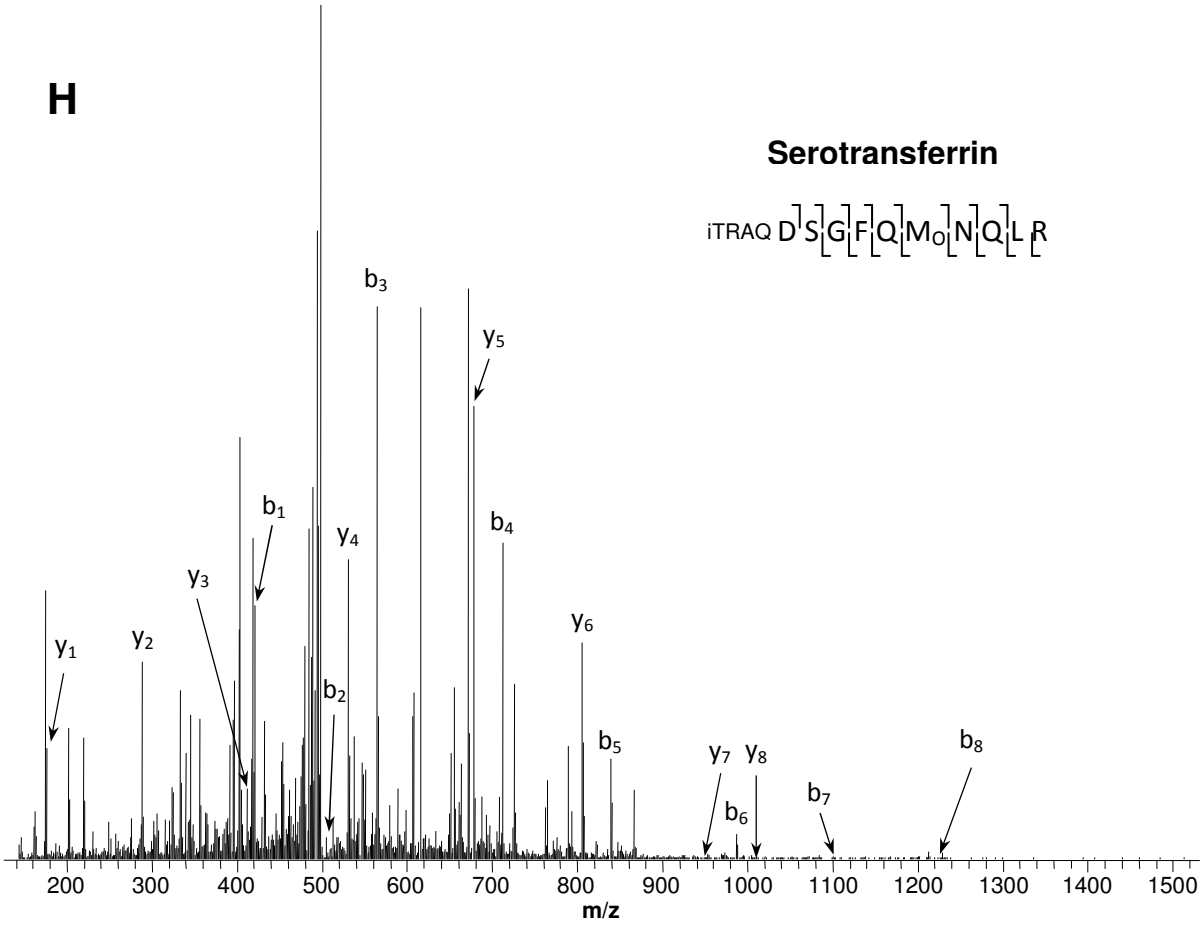

Number	Acid	B [M+H]+		Y [M+H]+		Number
	iTRAQ8plex					
1	**D**	420.24	**420.47**	1211.55		10
2	**S**	507.272	**507.41**	1096.52		9
3	**G**	564.293	**564.33**	1009.49	**1009.4**	8
4	**F**	711.362	**711.43**	952.467	**952.64**	7
5	**Q**	839.42	**839.46**	805.399	**805.4**	6
6	**M(Oxidation)**	986.456	**986.42**	677.34	**677.46**	5
7	**N**	1100.5	**1100.56**	530.305	**530.36**	4
8	**Q**	1228.56	**1228.48**	416.262	**416.47**	3
9	**L**	1341.64		288.203	**288.48**	2
10	**R**	---		175.119	**175.31**	1

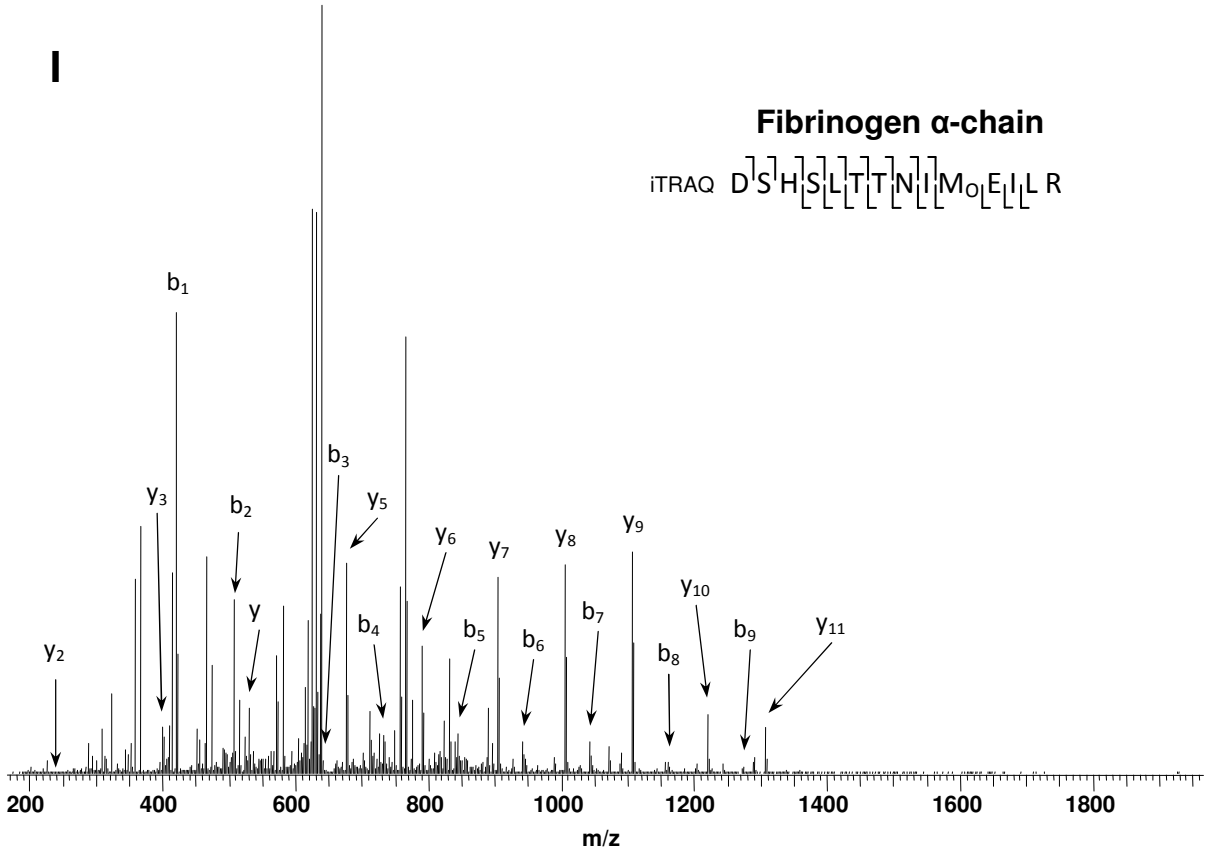

Number	Acid	B [M+H]+		Y [M+H]+		Number
	iTRAQ8plex					
1	D	420.24	**420.54**	-		14
2	S	507.28	**507.43**	1530.79		13
3	H	644.34	**644.49**	1443.76		12
4	S	731.37	**731.48**	1306.7	**1306.62**	11
5	L	844.45	**844.55**	1219.67	**1219.6**	10
6	T	945.5	**945.55**	1106.59	**1106.57**	9
7	T	1046.55	**1046.61**	1005.54	**1005.54**	8
8	N	1160.59	**1160.56**	904.49	**904.61**	7
9	I	1273.67	**1273.58**	790.45	**790.58**	6
10	M(Oxidation)	1420.71		677.37	**677.51**	5
11	E	1549.75		530.33	**530.5**	4
12	I	1662.84		401.29	**401.73**	3
13	L	1775.92		288.2	**288.7**	2
14	R	-		175.12		1

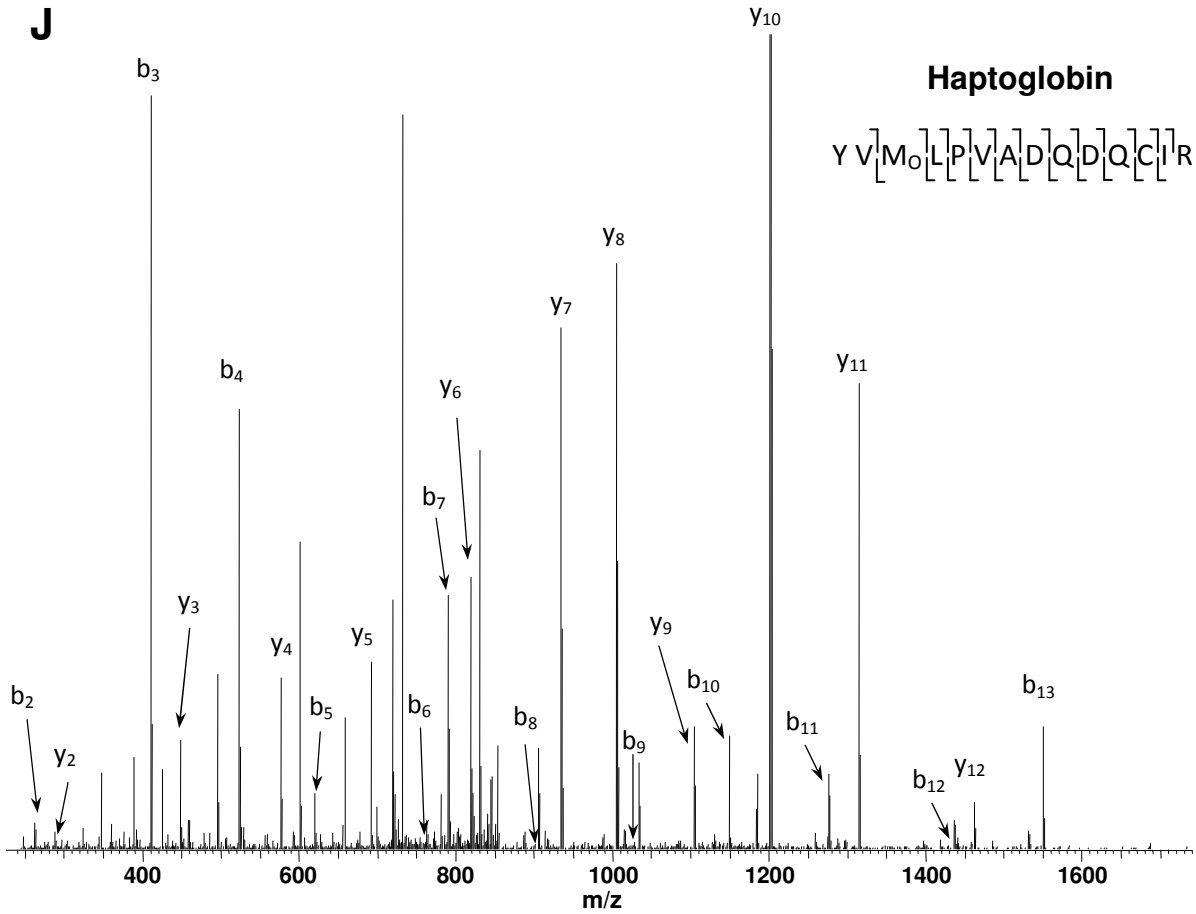

Number	Acid	B [M+H]+		Y [M+H]+		Number
1	Y	---		---		14
2	V	263.139	**263.27**	1560.75		13
3	M(Oxidation)	410.174	**410.29**	1461.68	**1461.59**	12
4	L	523.259	**523.2**	1314.65	**1314.57**	11
5	P	620.311	**620.32**	1201.56	**1201.53**	10
6	V	719.38	**719.4**	1104.51	**1104.52**	9
7	A	790.417	**790.5**	1005.44	**1005.48**	8
8	D	905.444	**905.47**	934.405	**934.46**	7
9	Q	1033.5	**1033.55**	819.378	**819.43**	6
10	D	1148.53	**1148.47**	691.319	**691.39**	5
11	Q	1276.59	**1276.49**	576.292	**576.31**	4
12	C(Carbamidomethyl)	1436.62	**1436.53**	448.234	**448.31**	3
13	I	1549.7	**1549.59**	288.203	**288.34**	2
14	R	---		175.119		1

Figure 7.8. Raw MS sequencing data for oxidative modifications. Representative raw MS spectra are displayed for tryptophan and tyrosine nitration, and oxidized methionine modifications. The peptide sequence and 'b' and 'y' ion fragmentation are shown for each individual chromatogram (relative abundance and m/z values on y and x-axis respectively). Representative raw MS chromatograms for: **A)** Alkaline phosphatase; **C)** Thyroid receptor interacting protein 11; and **D)** Glycolipid transfer protein represent examples of tyrosine nitration. Representative raw MS chromatograms for: **B)** Dynein heavy chain; and **E)** Dynein heavy chain 11 represent examples of tryptophan nitration. Representative raw MS chromatograms for: **F)** Fibrinogen β-chain; **G)** Alpha 2-Macroglobulin; **H)** Serotransferrin; **I)** Fibrinogen α-chain; and **J)** Haptoglobin represent examples of methionine oxidation.

7.5 Discussion

The main outcome of this study was the identification of a small number of peptides which were observed to carry either carbonylation or nitration adducts in disease and control samples. In addition several plasma proteins were identified as having altered expression in AD compared to controls. It is not practical to discuss exhaustively all of the altered proteins in detail; thus the discussion will focus on peptides demonstrated to contain oxidized adducts, considered to be particularly interesting in relation to AD. Moreover, discussion of protein expression changes from the presented iTRAQ work will be limited to those proteins validated by Western blotting.

Transition metals have the capacity to undergo reduction and oxidation reactions and as such have the potential to be involved in free radical reactions. The most abundant transition metal in the body is iron (Fe). Fe always exists in a bound state, normally with a protein, and when stored or transported is chelated by the specific iron binding proteins ferritin and transferrin (Tf) respectively (McCord, 2004). In AD brain it has been shown that iron and iron binding proteins are altered, with accumulation of iron in AD hippocampal tissue a source of free radicals which likely contributes towards oxidative damage evident in this disease (Connor et al., 1992; Smith et al., 1997a). In addition it has also been suggested that changes to iron binding protein levels in serum may indicate that these changes manifest themselves as peripheral markers (Smith et al., 1997a).

In this work it was observed that there was a greater amount of individual peptides in AD plasma compared to control subjects corresponding to Serotransferrin (serum Tf) which contained an oxidized methionine. This finding is of particular interest as a previous study by

Yu and colleagues (2003) also identified that serum Tf exhibits increased oxidation in AD compared to control patients. One may speculate that such modifications to serum Tf may alter iron homeostasis and thereby play a role in AD by increasing FR induced bio molecular damage (e.g., lipid peroxidation). However, whether oxidative modification to serum Tf contributes to AD development, or is a secondary event of this disease remains unclear.

A further finding of the work presented in this chapter was the identification of a peptide altered by oxidation which corresponded to Haptoglobin (Hp). Hp is a glycoprotein present in human plasma which functions to sequester free-haemoglobin (Hb) released from erythrocytes into the blood. Due to the oxidative nature of the iron containing heme group present in Free-Hb, free radicals can be readily formed. Consequently, Hp is considered to provide a crucial protective effect against oxidant damage induced by Hb (Kato, 2009). In a recent study Tseng et al. (2004) demonstrated that Hp was a potent antioxidant in LDL oxidation. This result coupled to previous experiments by the group which showed that the antioxidant potency of Hp exceeded that of Probucol (a drug commonly used to treat atherosclerosis), led the authors to suggest that theoretically, at the cellular level, Hp could play an important role as a natural antioxidant in protection against atherosclerosis (Tseng et al., 2004). Protein oxidation can alter how a protein functions; the altered levels of peptides containing oxidation adducts identified in this work may therefore potentially impact on the natural antioxidant function of Hp. Although further investigation is warranted to confirm this finding, altered antioxidant function of Hp may have implications in AD, given its strong association with vascular disease (Hofman et al., 1997; Ott et al., 1996).

The thyroid hormone receptor (TR) belongs to the nuclear receptor superfamily and is a ligand activated transcription factor that controls multiple biological functions. The main ligand for TR is 3, 5, 3'-triiodothyronine (T3), which results from the deiodination of thyroxine (T4) (Flamant et al., 2006). Upon binding, T3 induces a conformational change to TR which results in transcriptional activation of the receptor, by allowing and preventing coactivator and corepressor interactions respectively (Flamant et al., 2006). In this study thyroid receptor interacting protein 11 (TRIP11) was found to contain a nitrated tyrosine residue, of which there was a greater amount present in AD compared to control plasma. Although there appears to be no direct literature concerning TRIP11, the role of a 230 KDa protein named TRIP230, which corresponds to the C-terminal region of TRIP11, has been investigated (Chang et al., 1997). TRIP230 is a coactivator which binds the thyroid receptor in a T3 dependent manner and enhances transcription of the activated receptor (Chang et al., 1997). Although its biological function has yet to be fully elucidated, it has been suggested that it may have coactivator functions related to the cell cycle and be regulated at the post-translational level (Chen et al., 1999). A link between thyroid hormones and AD neuropathology does exist, with high levels of these demonstrated to regulate gene expression and decrease APP expression in adult mouse brain (O'Barr et al., 2006). One may speculate that the presence of a nitration adduct, as identified here, may have implications for such processes in AD. For example the nitration of TRIP11 may alter its interaction with the TR and prevent transcription of specific target genes.

These specific modifications to the aforementioned plasma proteins provide an initial point of interest that warrants further investigation. First, they require validation by a different

technique and secondly functional tests should be employed to determine their biological relevance.

iTRAQ coupled to MS analysis identified several plasma proteins that were differentially expressed between AD and control samples, as assessed by iTRAQ coupled to MS analysis. In order to validate these protein expression data two plasma proteins were selected for Western blotting; α-2M was chosen as its expression, as measured by iTRAQ remained unchanged, and C4a protein was chosen as its expression, as measured by iTRAQ was increased by 15% in the pooled AD sample compared to the pooled control sample. Western blotting studies validated and verified these findings.

This work demonstrated that plasma α-2M levels are equivalent between AD and control samples which is in agreement with a number of previous studies in peripheral tissue (Blennow et al., 2000; Scacchi et al., 2002). The finding is however, in contrast to one recent study by Hye et al. (2006) who reported increased α-2M plasma levels in AD compared to controls patients using 2-DE, which was validated by Western blotting using a separate cohort of samples. A further result of this work was the demonstration that α-2M contained an oxidized adduct in AD and control plasma. It has been shown that oxidation at physiologically relevant concentrations can inactivate α-2M (Wu and Pizzo, 1999). Moreover, in Rheumatoid Arthritis, an inflammatory disease associated with increased tissue destruction, levels of oxidized α-2M are increased (Wu and Pizzo, 2001). The authors of both of these studies suggested that oxidative modification to α-2M may affect its binding affinity for inflammatory proteins and enhance tissue damage during inflammation (Wu and Pizzo, 2001; Wu and Pizzo, 1999).

Although the oxidative modification data for α-2M requires further investigation, in the context of AD this finding is of particular interest. One may speculate that oxidation to this specific plasma protein (e.g., α-2M) in AD may partially contribute to the disease by enhancing tissue damage and stimulating inflammation (Akiyama et al., 2000). In addition, this work builds on that presented in Chapter 5, where α-2M was tentatively shown to be nitrated in AD, validating that nitration was increased and not protein expression.

This study also showed increased C4a protein expression in AD compared to control plasma by LC-MS/MS analysis, which was further validated by Western blotting. C4a acts as a weak mediator of inflammation and is produced on cleavage of Complement 4 protein. Indeed a strong link between inflammation and the functional changes evident in AD has been made, which has been discussed comprehensively in a review by Akiyama et al. (2000). In brain tissue a role for the complement 4 proteins in AD has been suggested. In early studies Complement 4 and its cleavage products were reported to be present in close proximity to senile plaques and neurofibrillary tangles (Eikelenboom and Stam, 1982; McGeer et al., 1989). In addition, the expression of five plasma proteins was shown to be reduced in AD, with these changes being of possible significance. The data presented in this study showed that α-1-glycoprotein plasma protein expression was markedly reduced; interestingly its expression has also been shown to be decreased in CSF from AD patients (Puchades et al., 2003), although its biological function remains unknown.

One important issue that requires discussion is the consideration of sample preparation when undertaking proteomic analysis. In this work the decision was made to use pooled samples instead of individual samples, which may be considered a limitation. This decision was

based on two recent studies which suggested that the use of pooled samples, rather than individual samples, was more productive when employing proteomics to analyse the AD CSF proteome (Zhang et al., 2005; Abdi et al., 2006). The main disadvantage of using individual samples is the inability to distinguish whether a change observed in a sample is due to the nature of that particular individual or the disease itself (Zhang et al., 2005; Abdi et al., 2006). The use of pooled samples removes this problem and effectively creates a representative disease sample. A further consideration when undertaking proteomic analysis in plasma is the presence of highly abundant proteins such as albumin. These proteins may cloud or mask the presence of low abundant proteins (Righetti et al., 2005). As a consequence pooled samples were depleted of albumin and then fractionated to enable a more detailed analysis of the AD and control plasma proteomes.

In summary this study successfully used iTRAQ coupled to MS/MS analysis to identify peptides which contained nitration and oxidation adducts in AD and control plasma. These initial data require further investigation by firstly selecting and validating proteins of interest and then determining the effect of oxidative modifications at these particular sites on their function.

Chapter 8

General Discussion

8.1 Introduction

The main aim of the studies presented in this thesis was to evaluate oxidative stress in Alzheimer's disease (AD) plasma and more specifically to assess oxidative modifications to individual plasma proteins. It is widely accepted that oxidative stress increases with ageing, and in recent years it has become apparent that in age-related diseases such as AD, these levels are further increased above what is considered normal healthy ageing (Markesbery, 1997). Oxidative damage to proteins (e.g., carbonylation, nitration) maybe of particular importance as it impacts upon how a protein functions (Friguet, 2006). In AD this may be of particular relevance when considering disease pathology, for example glycolytic enzymes, modified by oxidation, may be linked to the decreased glucose metabolism associated with AD (Castegna et al., 2002b; Costantini et al., 2008). In this work it was hypothesised that specific plasma proteins, likely to be vascular, would be targets for oxidative modification in AD, and that such changes would be potentially important when considering and understanding peripheral oxidative stress in AD.

Within AD research, studies using brain tissue are still of primary importance when assessing disease pathology, however one drawback is that these studies are conducted post-mortem. As a consequence, determining oxidative changes during the progression of the disease is near impossible using such methodologies. Further, the monitoring of interventions such as antioxidant supplementation is not possible. Peripheral tissues such as plasma and cerebrospinal fluid (CSF) provide a means of undertaking such work. The acquisition of plasma is less invasive than CSF collection (Hye et al., 2006) and contains proteins reflective of processes which occur in the body (Veskoukis et al., 2009). In addition, 500mls of CSF, which is in direct contact with the brain and is reflective of processes which

occur in the brain, is turned over into plasma each day (Davidsson and Sjogren, 2006; Hye et al., 2006). Therefore changes in plasma represent global and vascular changes in oxidative stress which occur in AD, and may also present potential biomarkers for this disease. The results presented here suggest that overall plasma protein oxidation levels are not different when AD and normally aged individuals are compared, and that individual plasma proteins are specific targets for oxidative modification in AD. This thesis explores different methodologies to assess oxidative changes in AD. Importantly, it highlights some of the difficulties encountered when attempting to identify particular modified proteins using classical gel based proteomics. In addition it demonstrates that emerging novel and powerful mass spectrometry techniques can be employed to identify several proteins modified by oxidation, providing an initial starting point for further investigation.

8.2 Main findings

In **Chapter 3** broad based oxidative stress markers were evaluated in addition to the oxidation status of low density lipoprotein (LDL). Due to the strong association between atherosclerosis and AD from population based studies (Hofman et al., 1997), coupled with the demonstration that the susceptibility of LDL to oxidation in plasma and CSF is increased in AD (Bassett et al., 1999; Schippling et al., 2000), it was hypothesised that plasma LDL oxidation would be increased in AD. The results from this study demonstrated that oxidized LDL was increased in AD and confirmed this hypothesis. This observation suggests that vascular changes such as oxidized LDL may partly contribute to AD pathology as the increased levels were significantly higher in AD sufferers, over and above the normal increased levels of oxidized LDL expected with age. Indeed, although patients with cardiovascular disease were excluded from this work, all subjects are still likely to have a

degree of atherosclerosis, given that hardening of arteries is an early event in life which progresses with age. To see levels of oxidized LDL in AD over and above that of controls, suggested that this change was related to disease.

Total levels of plasma lipid peroxides and plasma protein oxidation were unchanged in AD compared to control subjects. These results support the majority of reports in the current literature. One possible argument is that severity of the disease may influence protein oxidation levels (Bermejo et al., 2008; Ansari and Scheff, 2010) and therefore no significant difference in levels may be evident when comparing AD and control subjects which involve sufferers of differing disease severity. Results presented in **Chapter 3** support substantial evidence which suggests that specific plasma proteins are targets of oxidation (e.g., LDL). A global change in protein oxidation may therefore not be the important issue that requires investigation. Moreover, establishing a group of proteins that are altered, in the quest to further understand peripheral oxidative changes and develop a biomarker, is of more importance.

A high throughput measure of protein nitration is of particular interest as it may represent a footprint of the potent peroxynitrite radical ($ONOO^-$), and may contribute to further understanding disease pathology. On this premise the main focus of **Chapter 4** was to develop an ELISA for the semi-quantification of total protein nitration. This approach had been previously used successfully in other diseases associated with oxidative stress (Ceriello et al., 2001; Bekpinar et al., 2005). However, the data presented in this thesis suggests that most samples were below the detection limit of HPLC-ECD (1 µM) and an indirect ELISA (5 nM), and therefore that this approach lacked the sensitivity required for this measurement.

In a comprehensive study recently undertaken by Korolainen and Pirttilä (Korolainen and Pirttila, 2009) 3-nitrotyrosine levels in AD CSF, plasma and serum were assessed by commercial ELISA. In agreement with the findings produced in this thesis, levels of nitration from samples analysed in this aforementioned study were below the detection limit of the assay (2 nmol/l).

Following on from work in **Chapter 4**, a different strategy was employed in **Chapter 5** in an attempt to obtain a semi-quantitative measure of protein nitration. The Griess Assay and 1-DE coupled to Western blotting were employed to measure nitric oxide ($NO^{\bullet}$) levels and plasma protein nitration respectively. Results showed that plasma nitric oxide metabolites (NO_2^-/ NO_3^-) were reduced in AD, which is in agreement with several recent studies and adds weight to the observation that endothelial dysfunction is a characteristic of AD pathology (Selley, 2003). From the outset this work aimed to look at the association of nitric oxide levels and total plasma protein nitration, and it was proposed that 3-nitrotyrosine may be increased concurrently with a decrease in nitric oxide levels. This was based on the concept that $NO^{\bullet}$ would react with superoxide anions to form $ONOO^-$ and nitration of proteins. However, the results were inconclusive as problems with antibody non-specificity prevented accurate quantification of total nitration levels. That said, several nitrated proteins were observed and one of these, which corresponded to α-2 Macroglobulin (α-2M), was increased in AD compared to control subjects. Although one cannot rule out a change in global levels of nitration from these data, it does demonstrate that a specific protein is a target for oxidative modification (e.g., nitration) which is in agreement with the observations from **Chapter 3**. Moreover total protein carbonylation levels were consistent between groups confirming initial data from **Chapter 3** in a separate cohort of plasma samples.

The use of redox proteomics to identify specific plasma proteins which undergo oxidation was the main focus of **Chapter 6**. One plasma protein was found to undergo oxidation in AD compared to control subjects, although accurate identification of this protein could not be achieved due to low abundance, despite efforts using further techniques to do so. Work in this chapter used non-depleted samples which may be considered a limitation due to presence of high abundant proteins.

Following the inability to gain a protein identity in **Chapter 6**, non-gel based proteomics was employed to assess protein expression and modification in AD compared to control. The use of non-gel based proteomics is emerging as a powerful technique which can be utilized to discovery plasma based biomarkers and complement existing 2-DE based methods. The results presented in **Chapter 7** show several site specific oxidative modifications to proteins in both AD and control plasma. These oxidative modifications presented in both populations warrant further investigation. In addition the altered expression of several plasma proteins which were of possible significance was investigated. The expression of one of these plasma proteins, Complement 4a, was shown to be significantly increased in AD compared to control subjects. In contrast, the expression levels of α-2M were shown to be equivalent between AD and control subjects. Taken together, the results presented in **Chapter 5** and **Chapter 7** suggest that α-2M plasma protein expression remains unchanged, but that its nitration status is increased in AD.

8.3 Findings in context of existing literature

8.3.1 Equivalent plasma protein oxidation

When considering all broad measurements of oxidative stress presented in this thesis, it is apparent that total protein oxidation levels are unchanged in AD compared to control subjects. Despite some conflicting reports, this is in agreement with the majority of recent studies which assess this generic marker of oxidative stress (Baldeiras et al., 2008; Polidori et al., 2004; Pulido et al., 2005; Zafrilla et al., 2006). A potential explanation for equivalent protein oxidation levels is that disease severity may affect oxidative stress levels. There are studies which agree (Bermejo et al., 2008; Ansari and Scheff, 2010) and disagree (Zafrilla et al., 2006) with this idea as previously discussed.

The data from this thesis demonstrate that at least two plasma proteins (i.e. LDL and an unknown plasma protein) exhibit increased oxidation in AD, but that total protein oxidation remains equivalent when assessing total protein carbonylation (Aldred et al., 2009). As the plasma proteome is composed of thousands of proteins at any one given time, the oxidation of a few specific proteins may not be enough to cause a global change. This would support studies in AD brain tissue, where specific proteins have been shown to be oxidized, nitrated and lipoxidized (Castegna et al., 2002b; Castegna et al., 2003; Pamplona et al., 2005). It may well be the case that investigating particular plasma proteins which are targets of oxidative modification may provide more information on disease process, rather than a measurement of oxidative stress in whole plasma in AD.

8.3.2 Complementing gel based proteomics with non-gel based proteomics

Classically gel-based proteomics has been used to assess protein expression changes to the plasma proteome in disease states, and to a lesser extent oxidative modifications which occur. However more recently it appears that proteomics is moving away from classical gel-based methods to non-gel based methods when assessing the plasma proteome for protein expression changes in AD (Abdi et al., 2006; Choe et al., 2007). For example Lovestone and co-workers have used gel based methods to successfully identify plasma proteins which are altered in expression in AD (Hye et al., 2006), but have more recently used iTRAQ labelling coupled to mass spectrometry to complement this early work and discover several more proteins which have altered expression (Guntert et al., 2010). Given the recent improvement of isobaric labelling strategies coupled to mass spectrometry (Chiappetta et al., 2009) a non gel-based redox proteomic approach may also complement gel based redox proteomics. Work presented in this thesis suggests such an approach can be undertaken as non-gel based proteomics was employed to successfully identify specific sites of oxidative modification to plasma proteins in AD and control subjects. Where the technology perhaps still lacks, is in identifying modifications which are unique to the disease process.

8.3.3 Measurement of plasma 3-nitrotyrosine in AD

In this thesis two analytical techniques were employed to analyse 3-nitrotyrosine levels in biological fluids which included HPLC-ECD and antibody based methods. The actual physiological levels of 3-nitrotyrosine in normal and diseased subject's plasma remain open for debate, with conflicting data available in the literature. Basal levels of 3-nitrotyrosine using all of the analytical techniques mentioned are quite varied and range from undetectable to between 1 and 64 nM (Tsikas and Caidahl, 2005). The general consensus is that under

normal conditions, levels of free and bound 3-nitrotyrosine are low, but levels become elevated in conditions associated with increased oxidative stress (Souza et al., 2008).

In this work ELISA with a detection limit of 5 nM was used in order to provide a high throughput semi-quantitative measure of 3-nitrotyrosine in AD and age-matched control plasma. Levels of 3-nitrotyrosine were only detectable in a minority of plasma samples by HPLC-ECD (detection limit 1 μM) and only two out of 24 plasma samples were detectable by ELISA (detection limit 5 nM). Indeed in a recent study Korolainen and Pirttilä (2009) were unable to detect nitration using a commercial ELISA with a detection limit of 1nM in the majority of large cohort of AD CSF and plasma samples. In AD peripheral tissue 3-nitrotyrosine levels have been reported as 0.44 ± 0.031 nM and 11.4 ± 5.4 nM in studies by two separate groups using HPLC with electrochemical detection and gas chromatography-tandem mass spectrometry (Tohgi et al., 1999; Ryberg et al., 2004). From the data presented in this thesis and the aforementioned studies it is highly likely that plasma levels of 3-nitrotyrosine in AD are in the low nanomolar range. Therefore more sensitive analytical techniques need to be used to detect this analyte and determine whether total levels of free and bound 3-nitrotyrosine are actually altered in AD plasma.

8.4 Future directions

8.4.1 Oxidative stress in vascular dementia

There is a requirement to distinguish between different types of dementia to enable more suitable and directed therapies. Understanding the role of oxidative stress in different types of dementia will enable further characterisation of dementia and may contribute to biomarker discovery. Although several studies have compared markers of oxidative stress between Mild

Cognitive Impairment and AD, limited work has focussed on oxidative changes between vascular dementia (VaD) and AD. A link does exist between oxidative stress and VaD given that increased free radical production is associated with cerebral ischemia (Zini et al., 1992), a risk factor for vascular type dementias.

There are studies supporting a role for oxidative stress in VaD, with most to date investigating the lipid peroxidation product MDA. For example, MDA levels have been shown to be increased in AD and VaD patients over the ages of 65 (Casado et al., 2008), and in a very recent study Gustaw-Rothenberg et al. (2010) reported MDA levels to be increased in VaD and AD compared to controls. Interestingly this study highlighted a significant 3.4 fold increase in levels in VaD compared to AD. Notably there are only limited or in fact no measurements of protein carbonylation and nitration in VaD and AD comparison studies (Polidori et al., 2004).

Further investigations which compare a wide range of oxidative stress measurements are warranted in order to clarify the role of oxidative stress in VaD, and more specifically oxidative differences between AD and VaD. An extension of existing studies may be to undertake redox proteomic research to identify specific plasma proteins which are differentially altered between these two types of dementia.

8.4.2 Exercise as a therapeutic intervention for AD

A future direction and an extension of the work presented in this thesis would be to evaluate the effect of exercise on markers of oxidative stress in AD, with plasma being an ideal source due to the non-invasive nature of its collection. The benefits of exercise in AD are

well documented: Larson et al. (2006) reported that regular exercise is associated with delayed the onset of Alzheimer's type dementia. Further studies have shown exercise training resulted in improved cognition in fifteen patients with senile dementia (Palleschi et al., 1996); and improved capacity to perform everyday tasks in addition to improving muscle strength and flexibility in AD patients (Santana-Sosa et al., 2008). Given the recent demonstration by Donnelly and co-workers (2008) that cardiovascular fitness is comparable between demented and non-demented patients, in addition to oxidative stress being an early event in AD (Nunomura et al., 2001), a walking exercise test in this elderly population in the earliest stages of this disease is most definitely plausible.

When considering oxidative stress as an AD pathology, then exercise may be used to explore the AD disease process. Oxidative stress and free radical production during exercise has been well studied. Early work by Davies et al. (1982) suggested that exercise may be detrimental as it was demonstrated that free radicals were produced in rat skeletal muscle after running to exhaustion, and more recently increased free radical generation in rat skeletal muscle, after an acute bout of exhaustive exercise, was shown to be accompanied by increased oxidative stress (Bejma and Ji, 1999). However, Vina and co-workers (2000) found that oxidative stress occurred during exercise, but only when it was exhaustive.

Additionally, more recent research has shown exercise induced radical production to be essential for adaptation and signalling processes, thus suggesting that the production of ROS, during moderate intensity exercise, may be beneficial. Work by Navarro et al. (2004) demonstrated that moderate exercise in ageing mice reduced markers of oxidative damage (e.g., protein carbonyls and TBARS) in the sub mitochondrial fractions from organs

including the brain. Exercise also increased the activities of antioxidant enzymes (e.g., Mn-SOD, Cu, Zn-SOD and catalase) in these organs (Navarro et al., 2004; Boveris and Navarro, 2008), and this was paralleled with improvements in behavioural tests. A more recent study by Gomez-Cabrera et al. (2005) showed that ROS generated during exercise activates NFκB, which results in increased expression of important antioxidant enzymes such as Mn-SOD and GPx. This study highlights the importance of ROS produced during exercise for their role in cellular adaptations. Such studies have led to a growing opinion amongst exercise physiologists that moderate intensity exercise may itself be an antioxidant (Gomez-Cabrera et al., 2008).

In AD specifically, animal studies have shown that exercise can reduce Aβ42 peptide and improve behavioural function in transgenic mice (Um et al., 2008). Moreover, increases in neurotrophins (e.g., BDNF), heat shock protein 70 and antioxidant enzymes (e.g., SOD-1 and catalase) were also observed in exercised compared to sedentary transgenic mice (Um et al., 2008). These data support a role for exercise as a therapeutic strategy for the treatment of AD (Um et al., 2008) and may suggest that an improvement to the antioxidant defence system is one underlying mechanism by which exercise may exert its effect.

8.5 Conclusions

In conclusion, the series of studies conducted throughout this thesis suggest that particular plasma proteins are targets for oxidation, rather than oxidation events being random in nature. When considering LDL, it is likely that it is specifically oxidized in AD plasma as a result of its intimate involvement in the development of atherosclerosis, an established risk factor for this disease, instead of occurring as a consequence of AD. In contrast, other plasma proteins such as α-2M, which was found to exhibit an oxidized adduct, may be specifically targeted for oxidation due to the impact this modification has on their function. It has been proposed that oxidation to α-2M acts as a switch mechanism by down regulating acute inflammation and up-regulating tissue repair by sequestering cytokines and releasing growth factors respectively. This may be relevant in AD, a condition which is strongly linked with inflammation.

In addition, questions still remain as to whether free or bound 3-nitrotyrosine plasma levels are altered in AD, given the difficulties encountered during this thesis when assessing plasma protein nitration. Further experiments are therefore required which use analytical methods sensitive enough to accurately measure global 3-nitrotyrosine in plasma. Finally, the use of gel based and non-gel based proteomics identified plasma proteins which are targets for oxidative modification. This work requires further exploration to identify significant modifications which may be implicit in AD pathology.

Chapter 9

References

Reference List

(1985). Criteria for the clinical diagnosis of Alzheimer's disease. Excerpts from the NINCDS-ADRDA Workgroup report. J. Am. Geriatr. Soc. *33*, 2-3.

(1998). Consensus report of the Working Group on: "Molecular and Biochemical Markers of Alzheimer's Disease". The Ronald and Nancy Reagan Research Institute of the Alzheimer's Association and the National Institute on Aging Working Group. Neurobiol. Aging *19*, 109-116.

Abdi,F., Quinn,J.F., Jankovic,J., McIntosh,M., Leverenz,J.B., Peskind,E., Nixon,R., Nutt,J., Chung,K., Zabetian,C., Samii,A., Lin,M., Hattan,S., Pan,C., Wang,Y., Jin,J., Zhu,D., Li,G.J., Liu,Y., Waichunas,D., Montine,T.J., and Zhang,J. (2006). Detection of biomarkers with a multiplex quantitative proteomic platform in cerebrospinal fluid of patients with neurodegenerative disorders. J. Alzheimers. Dis. *9*, 293-348.

Adkins,J.N., Varnum,S.M., Auberry,K.J., Moore,R.J., Angell,N.H., Smith,R.D., Springer,D.L., and Pounds,J.G. (2002). Toward a human blood serum proteome: analysis by multidimensional separation coupled with mass spectrometry. Mol. Cell Proteomics. *1*, 947-955.

Akiyama,H., Barger,S., Barnum,S., Bradt,B., Bauer,J., Cole,G.M., Cooper,N.R., Eikelenboom,P., Emmerling,M., Fiebich,B.L., Finch,C.E., Frautschy,S., Griffin,W.S., Hampel,H., Hull,M., Landreth,G., Lue,L., Mrak,R., Mackenzie,I.R., McGeer,P.L., O'Banion,M.K., Pachter,J., Pasinetti,G., Plata-Salaman,C., Rogers,J., Rydel,R., Shen,Y., Streit,W., Strohmeyer,R., Tooyoma,I., Van Muiswinkel,F.L., Veerhuis,R., Walker,D., Webster,S., Wegrzyniak,B., Wenk,G., and Wyss-Coray,T. (2000). Inflammation and Alzheimer's disease. Neurobiol. Aging *21*, 383-421.

Aksenov,M.Y., Aksenova,M.V., Butterfield,D.A., Geddes,J.W., and Markesbery,W.R. (2001). Protein oxidation in the brain in Alzheimer's disease. Neuroscience *103*, 373-383.

Aldred,S., Bennett,S., and Mecocci,P. (2009). Increased low-density lipoprotein oxidation, but not total plasma protein oxidation, in Alzheimer's disease. Clin. Biochem.

Aldred,S., Grant,M.M., and Griffiths,H.R. (2004). The use of proteomics for the assessment of clinical samples in research. Clin. Biochem. *37*, 943-952.

Alonso,A.C., Zaidi,T., Grundke-Iqbal,I., and Iqbal,K. (1994). Role of abnormally phosphorylated tau in the breakdown of microtubules in Alzheimer disease. Proc. Natl. Acad. Sci. U. S. A *91*, 5562-5566.

Aluise,C.D., Sowell,R.A., and Butterfield,D.A. (2008). Peptides and proteins in plasma and cerebrospinal fluid as biomarkers for the prediction, diagnosis, and monitoring of therapeutic efficacy of Alzheimer's disease. Biochim. Biophys. Acta *1782*, 549-558.

Alzheimer,A. (1907). Uber einen eigenartige Erkranung der Hirnrinde. Allgemeine Zeitschrift fur Psychiatrie und Psychisch-Gerichtisch. Medizin *64*, 146-148.

Alzheimer,A., Stelzmann,R.A., Schnitzlein,H.N., and Murtagh,F.R. (1995). An English translation of Alzheimer's 1907 paper, "Uber eine eigenartige Erkankung der Hirnrinde". Clin. Anat. *8*, 429-431.

Anderson,L. and Anderson,N.G. (1977). High resolution two-dimensional electrophoresis of human plasma proteins. Proc. Natl. Acad. Sci. U. S. A *74*, 5421-5425.

Ansari,M.A. and Scheff,S.W. (2010). Oxidative stress in the progression of Alzheimer disease in the frontal cortex. J. Neuropathol. Exp. Neurol. *69*, 155-167.

Araki,W., Kitaguchi,N., Tokushima,Y., Ishii,H., Aratake,S., Shimohama,S., Nakamura,S., and Kimura,J. (1991). Trophic effect of beta-amyloid precursor protein on cerebral cortical neurons in culture. Biochem. Biophys. Res. Commun. *181*, 265-271.

Azizova,O.A., Aseichev,A.V., Piryazev,A.P., Roitman,E.V., and Shcheglovitova,O.N. (2007). Effects of oxidized fibrinogen on the functions of blood cells, blood clotting, and rheology. Bull. Exp. Biol. Med. *144*, 397-407.

Baldeiras,I., Santana,I., Proenca,M.T., Garrucho,M.H., Pascoal,R., Rodrigues,A., Duro,D., and Oliveira,C.R. (2008). Peripheral oxidative damage in mild cognitive impairment and mild Alzheimer's disease. J. Alzheimers Dis. *15*, 117-128.

Bassett,C.N., Neely,M.D., Sidell,K.R., Markesbery,W.R., Swift,L.L., and Montine,T.J. (1999). Cerebrospinal fluid lipoproteins are more vulnerable to oxidation in Alzheimer's disease and are neurotoxic when oxidized ex vivo. Lipids *34*, 1273-1280.

Bauer,J., Strauss,S., Schreiter-Gasser,U., Ganter,U., Schlegel,P., Witt,I., Yolk,B., and Berger,M. (1991). Interleukin-6 and alpha-2-macroglobulin indicate an acute-phase state in Alzheimer's disease cortices. FEBS Lett. *285*, 111-114.

Beckman,J.S., Chen,J., Ischiropoulos,H., and Crow,J.P. (1994). Oxidative Chemistry of Peroxynitrite. Methods Enzymol. *233*, 229-240.

Beckman,J.S. and Koppenol,W.H. (1996). Nitric oxide, superoxide and peroxynitrite:the good, the bad, and ugly. Am. J. Physiol *271*, C1424-C1437.

Beckman,K.B. and Ames,B.N. (1998). The free radical theory of aging matures. Physiol Rev. *78*, 547-581.

Bedard,K. and Krause,K.H. (2007). The NOX family of ROS-generating NADPH oxidases: physiology and pathophysiology. Physiol Rev. *87*, 245-313.

Bejma,J. and Ji,L.L. (1999). Aging and acute exercise enhance free radical generation in rat skeletal muscle. J. Appl. Physiol *87*, 465-470.

Bekpinar,S., Kilic,N., Unlucerci,Y., kdag-Kose,A., Azizlerli,G., and Ozbek-Kir,Z. (2005). Evaluation of nitrosative and oxidative stress in Behcet disease. J. Eur. Acad. Dermatol. Venereol. *19*, 167-171.

Bennett,S., Grant,M.M., and Aldred,S. (2009). Oxidative Stress in Vascular Dementia and Alzheimer's Disease: A Common Pathology. J. Alzheimers Dis.

Benzie,I.F. and Strain,J.J. (1999). Ferric reducing/antioxidant power assay: direct measure of total antioxidant activity of biological fluids and modified version for simultaneous measurement of total antioxidant power and ascorbic acid concentration. Methods Enzymol. *299*, 15-27.

Berlett,B.S. and Stadtman,E.R. (1997). Protein oxidation in aging, disease, and oxidative stress. J. Biol. Chem. *272*, 20313-20316.

Bermejo,P., Martin-Aragon,S., Benedi,J., Susin,C., Felici,E., Gil,P., Ribera,J.M., and Villar,A.M. (2008). Peripheral levels of glutathione and protein oxidation as markers in the development of Alzheimer's disease from Mild Cognitive Impairment. Free Radic. Res. *42*, 162-170.

Blennow,K., Ricksten,A., Prince,J.A., Brookes,A.J., Emahazion,T., Wasslavik,C., Bogdanovic,N., Andreasen,N., Batsman,S., Marcusson,J., Nagga,K., Wallin,A., Regland,B., Olofsson,H., Hesse,C., Davidsson,P., Minthon,L., Jansson,A., Palmqvist,L., and Rymo,L. (2000). No association between the alpha2-macroglobulin (A2M) deletion and Alzheimer's disease, and no change in A2M mRNA, protein, or protein expression. J. Neural Transm. *107*, 1065-1079.

Bourdel-Marchasson,I., mas-Beauvieux,M.C., Peuchant,E., Richard-Harston,S., Decamps,A., Reignier,B., Emeriau,J.P., and Rainfray,M. (2001). Antioxidant defences and oxidative stress markers in erythrocytes and plasma from normally nourished elderly Alzheimer patients. Age Ageing *30*, 235-241.

Boveris,A. and Navarro,A. (2008). Systemic and mitochondrial adaptive responses to moderate exercise in rodents. Free Radic. Biol. Med. *44*, 224-229.

Braak,H. and Braak,E. (1995). Staging of Alzheimer's disease-related neurofibrillary changes. Neurobiol. Aging *16*, 271-278.

Breusing,N., Grune,T., Andrisic,L., Atalay,M., Bartosz,G., Biasi,F., Borovic,S., Bravo,L., Casals,I., Casillas,R., Dinischiotu,A., Drzewinska,J., Faber,H., Fauzi,N.M., Gajewska,A., Gambini,J., Gradinaru,D., Kokkola,T., Lojek,A., Luczaj,W., Margina,D., Mascia,C., Mateos,R., Meinitzer,A., Mitjavila,M.T., Mrakovcic,L., Munteanu,M.C., Podborska,M., Poli,G., Sicinska,P., Skrzydlewska,E., Vina,J., Wiswedel,I., Zarkovic,N., Zelzer,S., and Spickett,C.M. (2010). An inter-laboratory validation of methods of lipid peroxidation measurement in UVA-treated human plasma samples. Free Radic. Res. *44*, 1203-1215.

Brookmeyer,R., Johnson,E., Ziegler-Graham,K., and Arrighi,H.M. (2007). Forecasting the global burden of Alzheimer's disease. Alzheimers & Dementia *3*, 186-191.

Buettner,G.R. (1993). The pecking order of free radicals and antioxidants: lipid peroxidation, alpha-tocopherol, and ascorbate. Arch. Biochem. Biophys. *300*, 535-543.

Burns,A., Byrne,E.J., and Maurer,K. (2002). Alzheimer's disease. Lancet *360*, 163-165.

Burns,J.M., Mayo,M.S., Anderson,H.S., Smith,H.J., and Donnelly,J.E. (2008). Cardiorespiratory fitness in early-stage Alzheimer disease. Alzheimer Dis. Assoc. Disord. *22*, 39-46.

Butterfield,D.A., Drake,J., Pocernich,C., and Castegna,A. (2001). Evidence of oxidative damage in Alzheimer's disease brain: central role for amyloid beta-peptide. Trends Mol. Med. *7*, 548-554.

Butterfield,D.A., Perluigi,M., and Sultana,R. (2006). Oxidative stress in Alzheimer's disease brain: new insights from redox proteomics. Eur. J. Pharmacol. *545*, 39-50.

Butterfield,D.A., Reed,T.T., Perluigi,M., De,M.C., Coccia,R., Keller,J.N., Markesbery,W.R., and Sultana,R. (2007). Elevated levels of 3-nitrotyrosine in brain from subjects with amnestic mild cognitive impairment: implications for the role of nitration in the progression of Alzheimer's disease. Brain Res. *1148*, 243-248.

Calabrese,V., Sultana,R., Scapagnini,G., Guagliano,E., Sapienza,M., Bella,R., Kanski,J., Pennisi,G., Mancuso,C., Stella,A.M., and Butterfield,D.A. (2006). Nitrosative stress, cellular stress response, and thiol homeostasis in patients with Alzheimer's disease. Antioxid. Redox. Signal. *8*, 1975-1986.

Carty,J.L., Bevan,R., Waller,H., Mistry,N., Cooke,M., Lunec,J., and Griffiths,H.R. (2000). The effects of vitamin C supplementation on protein oxidation in healthy volunteers. Biochem. Biophys. Res. Commun. *273*, 729-735.

Casado,A., Encarnacion Lopez-Fernandez,M., Concepcion,C.M., and de La,T.R. (2008). Lipid peroxidation and antioxidant enzyme activities in vascular and Alzheimer dementias. Neurochem. Res. *33*, 450-458.

Castegna,A., Aksenov,M., Aksenova,M., Thongboonkerd,V., Klein,J.B., Pierce,W.M., Booze,R., Markesbery,W.R., and Butterfield,D.A. (2002a). Proteomic identification of oxidatively modified proteins in Alzheimer's disease brain. Part I: creatine kinase BB, glutamine synthase, and ubiquitin carboxy-terminal hydrolase L-1. Free Radic. Biol. Med. *33*, 562-571.

Castegna,A., Aksenov,M., Thongboonkerd,V., Klein,J.B., Pierce,W.M., Booze,R., Markesbery,W.R., and Butterfield,D.A. (2002b). Proteomic identification of oxidatively modified proteins in Alzheimer's disease brain. Part II: dihydropyrimidinase-related protein 2, alpha-enolase and heat shock cognate 71. J. Neurochem. *82*, 1524-1532.

Castegna,A., Thongboonkerd,V., Klein,J.B., Lynn,B., Markesbery,W.R., and Butterfield,D.A. (2003). Proteomic identification of nitrated proteins in Alzheimer's disease brain. J. Neurochem. *85*, 1394-1401.

Ceriello,A., Mercuri,F., Quagliaro,L., Assaloni,R., Motz,E., Tonutti,L., and Taboga,C. (2001). Detection of nitrotyrosine in the diabetic plasma: evidence of oxidative stress. Diabetologia *44*, 834-838.

Chang,K.H., Chen,Y., Chen,T.T., Chou,W.H., Chen,P.L., Ma,Y.Y., Yang-Feng,T.L., Leng,X., Tsai,M.J., O'Malley,B.W., and Lee,W.H. (1997). A thyroid hormone receptor

coactivator negatively regulated by the retinoblastoma protein. Proc. Natl. Acad. Sci. U. S. A *94*, 9040-9045.

Chen,Y., Chen,P.-L., Chen,C.-F., Sharp,Z.D., and Lee,H.-W. (1999). Thyroid hormone, T3-dependent phosphorylation and translocation of Trip230 from the golgi complex to the nucleus. Proc. Natl. Acad. Sci. U. S. A *96*, 4443-4448.

Chiappetta,G., Corbo,C., Palmese,A., Galli,F., Piroddi,M., Marino,G., and Amoresano,A. (2009). Quantitative identification of protein nitration sites. Proteomics. *9*, 1524-1537.

Choe,L., D'Ascenzo,M., Relkin,N.R., Pappin,D., Ross,P., Williamson,B., Guertin,S., Pribil,P., and Lee,K.H. (2007). 8-plex quantitation of changes in cerebrospinal fluid protein expression in subjects undergoing intravenous immunoglobulin treatment for Alzheimer's disease. Proteomics. *7*, 3651-3660.

Choi,J., Malakowsky,C.A., Talent,J.M., Conrad,C.C., and Gracy,R.W. (2002). Identification of oxidized plasma proteins in Alzheimer's disease. Biochem. Biophys. Res. Commun. *293*, 1566-1570.

Chung,B.H., Wilkinson,T., Geer,J.C., and Segrest,J.P. (1980). Preparative and quantitative isolation of plasma lipoproteins: rapid, single discontinuous density gradient ultracentrifugation in a vertical rotor. J. Lipid Res. *21*, 284-291.

Cole,S.L. and Vassar,R. (2008). The role of amyloid precursor protein processing by BACE1, the beta-secretase, in Alzheimer disease pathophysiology. J. Biol. Chem. *283*, 29621-29625.

Connor,J.R., Menzies,S.L., St.Martin,S.M., and Mufson,E.J. (1992). A histochemical study of iron,transferrin,and ferritin in Alzhiemer's diseased brains. J. Neurosci. Res. *31*, 75-83.

Conrad,C.C., Marshall,P.L., Talent,J.M., Malakowsky,C.A., Choi,J., and Gracy,R.W. (2000). Oxidized proteins in Alzheimer's plasma. Biochem. Biophys. Res. Commun. *275*, 678-681.

Corzo,L., Zas,R., Rodriguez,S., Fernandez-Novoa,L., and Cacabelos,R. (2007). Decreased levels of serum nitric oxide in different forms of dementia. Neurosci. Lett. *420*, 263-267.

Costantini,L.C., Barr,L.J., Vogel,J.L., and Henderson,S.T. (2008). Hypometabolism as a therapeutic target in Alzheimer's disease. BMC Neuroscience 9(Suppl 2):S16.

Davidsson,P. and Sjogren,M. (2006). Proteome studies of CSF in AD patients. Mech. Ageing Dev. *127*, 133-137.

Davidsson,P., Westman-Brinkmalm,A., Nilsson,C.L., Lindbjer,M., Paulson,L., Andreasen,N., Sjogren,M., and Blennow,K. (2002). Proteome analysis of cerebrospinal fluid proteins in Alzheimer patients. Neuroreport *13*, 611-615.

Davies,K.J., Quintanilha,A.T., Brooks,G.A., and Packer,L. (1982). Free radicals and tissue damage produced by exercise. Biochem. Biophys. Res. Commun. *107*, 1198-1205.

de la Torre,J.C. (2002). Alzheimer disease as a vascular disorder: nosological evidence. Stroke *33*, 1152-1162.

Dede,D.S., Yavuz,B., Yavuz,B.B., Cankurtaran,M., Halil,M., Ulger,Z., Cankurtaran,E.S., Aytermir,K., Kabakci,G., and Ariogul,S. (2007). Assessment of Endothelial Function in Alzheimer's Disease:Is Alzheimer's Disease a Vascular Disease? JAGS *55*, 1613-1617.

Dillard,C.J., Litov,R.E., Savin,W.M., Dumelin,E.E., and Tappel,A.L. (1978). Effects of exercise, vitamin E, and ozone on pulmonary function and lipid peroxidation. J. Appl. Physiol *45*, 927-932.

Diz,A.P., Truebano,M., and Skinbinski,D.O.F. (2009). The consequences of sample pooling in proteomics: An empirical study. Electrophoresis *30*, 2967-2975.

Dorheim,M.A., Tracey,W.R., Pollock,J.S., and Grammas,P. (1994). Nitric oxide synthase activity is elevated in brain microvessels in Alzheimer's disease. Biochem. Biophys. Res. Commun. *205*, 659-665.

Du,Y., Ni,B., Glinn,M., Dodel,R.C., Bales,K.R., Zhang,Z., Hyslop,P.A., and Paul,S.M. (1997). alpha2-Macroglobulin as a beta-amyloid peptide-binding plasma protein. J. Neurochem. *69*, 299-305.

Duncan,M.W. (2003). A review of approaches to the analysis of 3-nitrotyrosine. Amino. Acids *25*, 351-361.

Dusse,L.M., Silva,R.M., Vieira,L.M., and das Gracas,C.M. (2005). Does plasma nitrite determination by the Griess reaction reflect nitric oxide synthesis? Clin. Chim. Acta *362*, 195-197.

Eikelenboom,P. and Stam,F.C. (1982). Immunoglobulins and Complement Factors in Senile Plaques. Acta Neuropathol. *57*, 239-242.

el-Saadani,M., Esterbauer,H., el-Sayed,M., Goher,M., Nassar,A.Y., and Jurgens,G. (1989). A spectrophotometric assay for lipid peroxides in serum lipoproteins using a commercially available reagent. J. Lipid Res. *30*, 627-630.

Esiri,M.M., Nagy,Z., Smith,M.Z., Barnetson,L., and Smith,A.D. (1999). Cerebrovascular disease and threshold for dementia in the early stages of Alzheimer's disease. Lancet *354*, 919-920.

Esterbauer,H., Schaur,R.J., and Zollner,H. (1991). Chemistry and biochemistry of 4-hydroxynonenal, malonaldehyde and related aldehydes. Free Radic. Biol. Med. *11*, 81-128.

Ferretti,G., Bacchetti,T., Masciangelo,S., and Pallotta,G. (2008). Lipid peroxidation in hemodialysis patients: effect of vitamin C supplementation. Clin. Biochem. *41*, 381-386.

Finaud,J., Lac,G., and Filaire,E. (2006). Oxidative stress : relationship with exercise and training. Sports Med. *36*, 327-358.

Finkel,T. and Holbrook,N.J. (2000). Oxidants, oxidative stress and the biology of ageing. Nature *408*, 239-247.

Flamant,F., Baxter,J.D., Forrest,D., Refetoff,S., Samuels,H., Scanlan,T.S., Vennström,B., and Samarut,J. (2006). International Uinon of Pharmacology.LIX.The Pharmacology and Classification of the Nuclear Receptor Superfamily:Thyroid Hormone Receptors. Pharmacol Rev *58*, 705-711.

Friguet,B. (2006). Oxidized protein degradation and repair in ageing and oxidative stress. FEBS Lett. *580*, 2910-2916.

Fuster,V., Badimon,J.J., and Badimon,L. (1992). Clinical-pathological correlations of coronary disease progression and regression. Circulation *86*, III1-11.

Gharahdaghi,F., Weinberg,C.R., Meagher,D.A., Imai,B.S., and Mische,S.M. (1999). Mass spectrometric identification of proteins from silver-stained polyacrylamide gel: a method for the removal of silver ions to enhance sensitivity. Electrophoresis *20*, 601-605.

Gollin,P.A., Kalaria,R.N., Eikelenboom,P., Rozemuller,A., and Perry,G. (1992). Alpha 1-antitrypsin and alpha 1-antichymotrypsin are in the lesions of Alzheimer's disease. Neuroreport *3*, 201-203.

Gomez-Cabrera,M.C., Borras,C., Pallardo,F.V., Sastre,J., Ji,L.L., and Vina,J. (2005). Decreasing xanthine oxidase-mediated oxidative stress prevents useful cellular adaptations to exercise in rats. J. Physiol *567*, 113-120.

Gomez-Cabrera,M.C., Domenech,E., and Vina,J. (2008). Moderate exercise is an antioxidant: upregulation of antioxidant genes by training. Free Radic. Biol. Med. *44*, 126-131.

Goodman,Y. and Mattson,M.P. (1994). Secreted forms of beta-amyloid precursor protein protect hippocampal neurons against amyloid-beta-peptide induced oxidative injury. Exp. Neurol. *128*, 1-12.

Greilberger,J., Koidl,C., Greilberger,M., Lamprecht,M., Schroecksnadel,K., Leblhuber,F., Fuchs,D., and Oettl,K. (2008). Malondialdehyde, carbonyl proteins and albumin-disulphide as useful oxidative markers in mild cognitive impairment and Alzheimer's disease. Free Radic. Res. *42*, 633-638.

Guidi,I., Galimberti,D., Lonati,S., Novembrino,C., Bamonti,F., Tiriticco,M., Fenoglio,C., Venturelli,E., Baron,P., Bresolin,N., and Scarpini,E. (2006). Oxidative imbalance in patients with mild cognitive impairment and Alzheimer's disease. Neurobiol. Aging *27*, 262-269.

Guntert,A., Campbell,J., Saleem,M., O'Brien,D.P., Thompson,A.J., Byers,H.L., Ward,M.A., and Lovestone,S. (2010). Plasma Gelsolin is Decreased and Correlates with Rate of Decline in Alzheimer's Disease. J. Alzheimers. Dis. *21(2)*, 585-596.

Gustaw-Rothenberg,K., Kowalczuk,K., and Stryjecka-Zimmer,M. (2010). Lipids' peroxidation markers in Alzheimer's disease and vascular dementia. Geriatr Gerontol Int *10*, 161-166.

Halliwell,B. (2006). Oxidative stress and neurodegeneration: where are we now? J. Neurochem. *97*, 1634-1658.

Halliwell,B. and Gutteridge,J.M.C. (1989). Free Radicals in Biology and Medicine. Clarendon Press, Oxford, UK).

Hardy,J. and Selkoe,D.J. (2002). The amyloid hypothesis of Alzheimer's disease: progress and problems on the road to therapeutics. Science *297*, 353-356.

Harman,D. (1956). Aging: a theory based on free radical and radiation chemistry. J. Gerontol *11*, 298-300.

Harrison,D., Griendling,K.K., Landmesser,U., Hornig,B., and Drexler,H. (2003). Role of oxidative stress in atherosclerosis. Am. J. Cardiol. *91*, 7A-11A.

Hellman,U., Wernstedt,C., Gonez,J., and Heldin,C.H. (1995). Improvement of an "In-Gel" digestion procedure for the micropreparation of internal protein fragments for amino acid sequencing. Anal. Biochem. *224*, 451-455.

Hensley,K., Hall,N., Subramaniam,R., Cole,P., Harris,M., Aksenov,M., Aksenova,M., Gabbita,S.P., Wu,J.F., Carney,J.M., and . (1995). Brain regional correspondence between Alzheimer's disease histopathology and biomarkers of protein oxidation. J. Neurochem. *65*, 2146-2156.

Hensley,K., Maidt,M.L., Yu,Z., Sang,H., Markesbery,W.R., and Floyd,R.A. (1998). Electrochemical analysis of protein nitrotyrosine and dityrosine in the Alzheimer brain indicates region-specific accumulation. J. Neurosci. *18*, 8126-8132.

Hensley,K., Williamson,K.S., Maidt,M.L., Gabbita,S.P., Grammas,P., and Floyd,R.A. (1999). Determination of Biological Oxidative Stress Using High Performance Liquid Chromatography with Electrochemical Detection (HPLC-ECD). Journal of high resolution chromatography *22*, 429-437.

Himmelfarb,J. and McMonagle,E. (2001). Albumin is the major plasma protein target of oxidant stress in uremia. Kidney Int. *60*, 358-363.

Hofman,A., Ott,A., Breteler,M.M., Bots,M.L., Slooter,A.J., van,H.F., van Duijn,C.N., Van,B.C., and Grobbee,D.E. (1997). Atherosclerosis, apolipoprotein E, and prevalence of dementia and Alzheimer's disease in the Rotterdam Study. Lancet *349*, 151-154.

Holmes,C. and Lovestone,S. (2003). Long-term cognitive and functional decline in late onset Alzheimer's disease:therapeutic implications. Age Ageing *32*, 200-204.

Holvoet,P., Mertens,A., Verhamme,P., Bogaerts,K., Beyens,G., Verhaeghe,R., Collen,D., Muls,E., and Van de,W.F. (2001). Circulating oxidized LDL is a useful marker for identifying patients with coronary artery disease. Arterioscler. Thromb. Vasc. Biol. *21*, 844-848.

Horgan,G.W. (2007). Sample Size and Replication in 2D Gel Electrophoresis Studies. J. Proteome Res *6*, 2884-2887.

Hughes,S.R., Khorkova,O., Goyal,S., Knaeblein,J., Heroux,J., Riedel,N.G., and Sahasrabudhe,S. (1998). Alpha2-macroglobulin associates with beta-amyloid peptide and prevents fibril formation. Proc. Natl. Acad. Sci. U. S. A *95*, 3275-3280.

Hye,A., Lynham,S., Thambisetty,M., Causevic,M., Campbell,J., Byers,H.L., Hooper,C., Rijsdijk,F., Tabrizi,S.J., Banner,S., Shaw,C.E., Foy,C., Poppe,M., Archer,N., Hamilton,G., Powell,J., Brown,R.G., Sham,P., Ward,M., and Lovestone,S. (2006). Proteome-based plasma biomarkers for Alzheimer's disease. Brain *129*, 3042-3050.

Ishii,T., Tatsuda,E., Kumazawa,S., Nakayama,T., and Uchida,K. (2003). Molecular basis of enzyme inactivation by an endogenous electrophile 4-hydroxy-2-nonenal: identification of modification sites in glyceraldehyde-3-phosphate dehydrogenase. Biochemistry *42*, 3474-3480.

Ji,Y., Neverova,I., Van Eyk,J.E., and Bennett,B.M. (2006). Nitration of tyrosine 92 mediates the activation of rat microsomal glutathione s-transferase by peroxynitrite. J. Biol. Chem. *281*, 1986-1991.

Jones,D.P., Mody,V.C., Jr., Carlson,J.L., Lynn,M.J., and Sternberg,P., Jr. (2002). Redox analysis of human plasma allows separation of pro-oxidant events of aging from decline in antioxidant defenses. Free Radic. Biol. Med. *33*, 1290-1300.

Kalaria,R.N. and Ballard,C. (1999). Overlap between pathology of Alzheimer disease and vascular dementia. Alzheimer Dis. Assoc. Disord. *13 Suppl 3*, S115-S123.

Karp,N.A. and Lilley,K.S. (2007). Design and Analysis issues in Quantitative Proteomics Studies. Pract. Proteomics *7*, 42-50.

Karp,N.A., Spencer,M., Lindsay,H., O'Dell,K., and Lilley,K.S. (2005). Impact of Replicate Types on Proteomic Expression Analysis. J. Proteome Res *4*, 1867-1871.

Kato,G.J. (2009). Haptoglobin halts hemoglobin's havoc. J. Clin. Invest *119*, 2140-2142.

Katzman,R. and Saitoh,T. (1991). Advances in Alzheimer's disease. FASEB J. *5*, 278-286.

Keller,J.N., Schmitt,F.A., Scheff,S.W., Ding,Q., Chen,Q., Butterfield,D.A., and Markesbery,W.R. (2005). Evidence of increased oxidative damage in subjects with mild cognitive impairment. Neurology *64*, 1152-1156.

Khalil,A., Wagner,R.J., Lacombe,G., Dangoisse,V., and Fülöp Jr,T. (1996). Increased susceptibility of low-density lipoprotein (LDL) to oxidation by γ-radiolysis with age. FEBS Lett. *392*, 45-48.

Khatoon,S., Grundke-Iqbal,I., and Iqbal,K. (1992). Brain levels of microtubule-associated protein tau are elevated in Alzheimer's disease: a radioimmuno-slot-blot assay for nanograms of the protein. J. Neurochem. *59*, 750-753.

Kita,T., Kume,N., Minami,M., Hayashida,K., Murayama,T., Sano,H., Moriwaki,H., Kataoka,H., Nishi,E., Horiuchi,H., Arai,H., and Yokode,M. (2001). Role of oxidized LDL in atherosclerosis. Ann. N. Y. Acad. Sci. *947*, 199-205.

Kontush,A. (2001). Amyloid-beta: an antioxidant that becomes a pro-oxidant and critically contributes to Alzheimer's disease. Free Radic. Biol. Med. *31*, 1120-1131.

Korolainen,M.A., Goldsteins,G., Alafuzoff,I., Koistinaho,J., and Pirttila,T. (2002). Proteomic analysis of protein oxidation in Alzheimer's disease brain. Electrophoresis *23*, 3428-3433.

Korolainen,M.A., Nyman,T.A., Nyyssonen,P., Hartikainen,E.S., and Pirttila,T. (2007). Multiplexed proteomic analysis of oxidation and concentrations of cerebrospinal fluid proteins in Alzheimer disease. Clin. Chem. *53*, 657-665.

Korolainen,M.A. and Pirttila,T. (2009). Cerebrospinal fluid, serum and plasma protein oxidation in Alzheimer's disease. Acta Neurol. Scand. *119*, 32-38.

Kuo,Y.M., Emmerling,M.R., Bisgaier,C.L., Essenburg,A.D., Lampert,H.C., Drumm,D., and Roher,A.E. (1998). Elevated low-density lipoprotein in Alzheimer's disease correlates with brain abeta 1-42 levels. Biochem. Biophys. Res. Commun. *252*, 711-715.

Landmesser,U., Dikalov,S., Price,S.R., McCann,L., Fukai,T., Holland,S.M., Mitch,W.E., and Harrison,D.G. (2003). Oxidation of tetrahydrobiopterin leads to uncoupling of endothelial cell nitric oxide synthase in hypertension. J. Clin. Invest *111*, 1201-1209.

Larson,E.B., Wang,L., Bowen,J.D., McCormick,W.C., Teri,L., Crane,P., and Kukull,W. (2006). Exercise is associated with reduced risk for incident dementia among persons 65 years of age and older. Ann. Intern. Med. *144*, 73-81.

Launer,L.J. (2002). Demonstrating the case that AD is a vascular disease: epidemiologic evidence. Ageing Res. Rev. *1*, 61-77.

Levine,R.L., Williams,J.A., Stadtman,E.R., and Shacter,E. (1994). Carbonyl assays for determination of oxidatively modified proteins. Methods Enzymol. *233*, 346-357.

Luth,H.J., Munch,G., and Arendt,T. (2002). Aberrant expression of NOS isoforms in Alzheimer's disease is structurally related to nitrotyrosine formation. Brain Res. *953*, 135-143.

Lyras,L., Cairns,N.J., Jenner,A., Jenner,P., and Halliwell,B. (1997). An assessment of oxidative damage to proteins, lipids, and DNA in brain from patients with Alzheimer's disease. J. Neurochem. *68*, 2061-2069.

Mangialasche,F., Polidori,M.C., Monastero,R., Ercolani,S., Camarda,C., Cecchetti,R., and Mecocci,P. (2009). Biomarkers of oxidative and nitrosative damage in Alzheimer's disease and mild cognitive impairment. Ageing Res. Rev. *8*, 285-305.

Mark,R.J., Lovell,M.A., Markesbery,W.R., Uchida,K., and Mattson,M.P. (1997). A role for 4-hydroxynonenal, an aldehydic product of lipid peroxidation, in disruption of ion homeostasis and neuronal death induced by amyloid beta-peptide. J. Neurochem. *68*, 255-264.

Markesbery,W.R. (1997). Oxidative stress hypothesis in Alzheimer's disease. Free Radic. Biol. Med. *23*, 134-147.

Markesbery,W.R. and Lovell,M.A. (1998). Four-hydroxynonenal, a product of lipid peroxidation, is increased in the brain in Alzheimer's disease. Neurobiol. Aging *19*, 33-36.

Martin-Aragon,S., Bermejo-Bescos,P., Benedi,J., Felici,E., Gil,P., Ribera,J.M., and Villar,A.M. (2009). Metalloproteinase's activity and oxidative stress in mild cognitive impairment and Alzheimer's disease. Neurochem. Res. *34*, 373-378.

Maruyama,W., Hashizume,Y., Matsubara,K., and Naoi,M. (1996). Identification of 3-nitro-L-tyrosine, a product of nitric oxide and superoxide, as an indicator of oxidative stress in the human brain. J. Chromatogr. B Biomed. Appl. *676*, 153-158.

Mattson,M.P. (1997). Cellular Actions of Beta-Amyloid Precursor Protein and Its Soluble and Fibrillogenic Derivatives. Physiol Rev. *77*, 1081-1132.

Mattson,M.P. (2004). Pathways towards and away from Alzheimer's disease. Nature *430*, 631-639.

Maxwell,A.J. (2002). Mechanisms of dysfunction of the nitric oxide pathway in vascular diseases. Nitric. Oxide. *6*, 101-124.

McAnulty,S.R., McAnulty,L.S., Nieman,D.C., Morrow,J.D., Utter,A.C., and Dumke,C.L. (2005). Effect of resistance exercise and carbohydrate ingestion on oxidative stress. Free Radic. Res. *39*, 1219-1224.

McCord,J.M. (2004). Iron,Free Radicals,and Oxidative Injury. J. Nutr. *134*, 3171S-3172S.

McGeer,P.L., Akiyama,H., Itagaki,S., and McGeer,E.G. (1989). Activation of the classical complement pathway in brain tissue of Alzheimer patients. Neurosci. Lett. *107*, 341-346.

McGrath,L.T., McGleenon,B.M., Brennan,S., McColl,D., McILroy,S., and Passmore,A.P. (2001). Increased oxidative stress in Alzheimer's disease as assessed with 4-hydroxynonenal but not malondialdehyde. QJM. *94*, 485-490.

Mecocci,P., Polidori,M.C., Cherubini,A., Ingegni,T., Mattioli,P., Catani,M., Rinaldi,P., Cecchetti,R., Stahl,W., Senin,U., and Beal,M.F. (2002). Lymphocyte oxidative DNA damage and plasma antioxidants in Alzheimer disease. Arch. Neurol. *59*, 794-798.

Michael Kinter and Nicholas E.Sherman (2000). The Preparation of Protein Digests for Mass Spectrometric Sequencing Experiments. In Protein Sequencing and Identification Using Mass Spectrometry, John Wiley & Sons), pp. 160-165.

Migliore,L., Fontana,I., Trippi,F., Colognato,R., Coppede,F., Tognoni,G., Nucciarone,B., and Siciliano,G. (2005). Oxidative DNA damage in peripheral leukocytes of mild cognitive impairment and AD patients. Neurobiol. Aging *26*, 567-573.

Millan-Crow,L.A., Crow,J.P., Kerby,J.D., Beckman,J.S., and Thompson,J.A. (1996). Nitration and inactivation of manganese superoxide dismutase in chronic rejection of human renal allografts. Proc. Natl. Acad. Sci. U. S. A *93*, 11853-11858.

Miranda,K.M., Espey,M.G., and Wink,D.A. (2001). A rapid, simple spectrophotometric method for simultaneous detection of nitrate and nitrite. Nitric. Oxide. *5*, 62-71.

Mitrogianni,Z., Barbouti,A., Galaris,D., and Siamopoulos,K.C. (2004). Tyrosine nitration in plasma proteins from patients undergoing hemodialysis. Am. J. Kidney Dis. *44*, 286-292.

Moraga,F. and Janciauskiene,S. (2000). Activation of primary human monocytes by the oxidized form of alpha 1-antitrypsin. J. Biol. Chem. *275*, 7693-7700.

Moreira,P.I., Akihiko Nunomura, Honda,K., Aliev,G., Casadesus,G., Zhu,X., Smith,M.A., and Perry,G. (2007). The Key Role of Oxidative Stress in Alzheimer's disease. In Oxidative Stress and Neurodegenerative Disorders, G.Ali Qureshi and S.Hassan Parvez, eds. Elsevier), pp. 267-281.

Moshage,H., Kok,B., Huizenga,J.R., and Jansen,P.L. (1995). Nitrite and nitrate determinations in plasma: a critical evaluation. Clin. Chem. *41*, 892-896.

Mutlu-Turkoglu,U., Ilhan,E., Oztezcan,S., Kuru,A., ykac-Toker,G., and Uysal,M. (2003). Age-related increases in plasma malondialdehyde and protein carbonyl levels and lymphocyte DNA damage in elderly subjects. Clin. Biochem. *36*, 397-400.

Navarro,A., Gomez,C., Lopez-Cepero,J.M., and Boveris,A. (2004). Beneficial effects of moderate exercise on mice aging: survival, behavior, oxidative stress, and mitochondrial electron transfer. Am. J. Physiol Regul. Integr. Comp Physiol *286*, R505-R511.

Newman,A.B., Fitzpatrick,A.L., Lopez,O., Jackson,S., Lyketsos,C., Jagust,W., Ives,D., Dekosky,S.T., and Kuller,L.H. (2005). Dementia and Alzheimer's disease incidence in relationship to cardiovascular disease in the Cardiovascular Health Study cohort. J. Am. Geriatr. Soc. *53*, 1101-1107.

Niki,E. (2009). Lipid peroxidation: physiological levels and dual biological effects. Free Radic. Biol. Med. *47*, 469-484.

Nunomura,A., Perry,G., Aliev,G., Hirai,K., Takeda,A., Balraj,E.K., Jones,P.K., Ghanbari,H., Wataya,T., Shimohama,S., Chiba,S., Atwood,C.S., Petersen,R.B., and Smith,M.A. (2001). Oxidative damage is the earliest event in Alzheimer disease. J. Neuropathol. Exp. Neurol. *60*, 759-767.

Nunomura,A., Perry,G., Hirai,K., Aliev,G., Takeda,A., Chiba,S., and Smith,M.A. (1999). Neuronal RNA oxidation in Alzheimer's disease and Down's syndrome. Ann. N. Y. Acad. Sci. *893*, 362-364.

O'Barr,S.A., Oh,J.S., Ma,C., Brent,G.A., and Schultz,J.J. (2006). Thyroid hormone regulates endogenous amyloid-beta precursor protein gene expression and processing in both in vitro and in vivo models. Thyroid *16*, 1207-1213.

Ohshima,H., Friesen,M., Brouet,I., and Bartsch,H. (1990). Nitrotyrosine as a new marker for endogenous nitrosation and nitration of proteins. Food Chem. Toxicol. *28*, 647-652.

Oldreive,C. and Rice-Evans,C. (2001). The mechanisms for nitration and nitrotyrosine formation in vitro and in vivo: impact of diet. Free Radic. Res. *35*, 215-231.

Olsen,J.V., Schwartz,J.C., Griep-Raming,J., Nielsen,M.L., Damoc,E., Denisov,E., Lange,O., Remes,P., Taylor,D., Splendore,M., Wouters,E.R., Senko,M., Makarov,A., Mann,M., and Horning,S. (2009). A dual pressure linear ion trap Orbitrap instrument with very high sequencing speed. Mol. Cell Proteomics. *8*, 2759-2769.

Ott,A., Stolk,R.P., Hofman,A., van,H.F., Grobbee,D.E., and Breteler,M.M. (1996). Association of diabetes mellitus and dementia: the Rotterdam Study. Diabetologia *39*, 1392-1397.

Packer,M.A. and Murphy,M.P. (1994). Peroxynitrite causes calcium efflux from mitochondria which is prevented by Cyclosporin A. FEBS Lett. *345*, 237-240.

Padurariu,M., Ciobica,A., Hritcu,L., Stoica,B., Bild,W., and Stefanescu,C. (2009). Changes of some oxidative stress markers in the serum of patients with mild cognitive impairment and Alzheimer's disease. Neurosci. Lett.

Palleschi,L., Vetta,F., DeGennaro,E., Idone,G., Sottosanti,G., Gianni,W., and Marigliano,V. (1996). Effect of aerobic training on the cognitive performance of elderly patients with senile dementia of Alzheimer type. Archives of Gerontology and Geriatrics 47-50.

Pamplona,R., Dalfo,E., Ayala,V., Bellmunt,M.J., Prat,J., Ferrer,I., and Portero-Otin,M. (2005). Proteins in human brain cortex are modified by oxidation, glycoxidation, and lipoxidation. Effects of Alzheimer disease and identification of lipoxidation targets. J. Biol. Chem. *280*, 21522-21530.

Pandey,A. and Mann,M. (2000). Proteomics to study genes and genomes. Nature *405*, 837-846.

Parkes,T.L., Elia,A.J., Dickinson,D., Hilliker,A.J., Phillips,J.P., and Boulianne,G.K. (1998). Extension of *Drosophila* lifespan by overexpression of human SOD1 in motorneurons. Nat. Genet. *19*, 171-174.

Parthasarathy,S., Quinn,M.T., Schwenke,D.C., Carew,T.E., and Steinberg,D. (1989). Oxidative modification of beta-very low density lipoprotein. Potential role in monocyte recruitment and foam cell formation. Arteriosclerosis *9*, 398-404.

Perez-Gracia,E., Blanco,R., Carmona,M., Carro,E., and Ferrer,I. (2009). Oxidative stress damage and oxidative stress responses in the choroid plexus in Alzheimer's disease. Acta Neuropathol.

Petersen,R.C., Doody,R., Kurz,A., Mohs,R.C., Morris,J.C., Rabins,P.V., Ritchie,K., Rossor,M., Thal,L., and Winblad,B. (2001). Current concepts in mild cognitive impairment. Arch. Neurol. *58*, 1985-1992.

Polidori,M.C., Mattioli,P., Aldred,S., Cecchetti,R., Stahl,W., Griffiths,H., Senin,U., Sies,H., and Mecocci,P. (2004). Plasma antioxidant status, immunoglobulin g oxidation and lipid peroxidation in demented patients: relevance to Alzheimer disease and vascular dementia. Dement. Geriatr. Cogn Disord. *18*, 265-270.

Poulter,N. (2003). Global risk of cardiovascular disease. Heart *89 Suppl 2*, ii2-ii5.

Puchades,M., Hansson,S.F., Nilsson,C.L., Andreasen,N., Blennow,K., and Davidsson,P. (2003). Proteomic studies of potential cerebrospinal fluid protein markers for Alzheimer's disease. Brain Res. Mol. Brain Res. *118*, 140-146.

Pulido,R., Jimenez-Escrig,A., Orensanz,L., Saura-Calixto,F., and Jimenez-Escrig,A. (2005). Study of plasma antioxidant status in Alzheimer's disease. Eur. J. Neurol. *12*, 531-535.

Raitakari,O.T., Pitkanen,O.P., Lehtimaki,T., Lahdenpera,S., Iida,H., Yla-Herttuala,S., Luoma,J., Mattila,K., Nikkari,T., Taskinen,M.R., Viikari,J.S., and Knuuti,J. (1997). In vivo low density lipoprotein oxidation relates to coronary reactivity in young men. J. Am. Coll. Cardiol. *30*, 97-102.

Reed,T.T., Pierce,W.M., Jr., Turner,D.M., Markesbery,W.R., and Butterfield,D.A. (2008). Proteomic identification of nitrated brain proteins in early Alzheimer's disease inferior parietal lobule. J. Cell Mol. Med.

Repetto,M.G., Reides,C.G., Evelson,P., Kohan,S., de Lustig,E.S., and Llesuy,S.F. (1999). Peripheral markers of oxidative stress in probable Alzheimer patients. Eur. J. Clin. Invest *29*, 643-649.

Righetti,P.G., Castagna,A., Antonucci,F., Piubelli,C., Cecconi,D., Campostrini,N., Rustichelli,C., Antonioli,P., Zanusso,G., Monaco,S., Lomas,L., and Boschetti,E. (2005). Proteome analysis in the clinical chemistry laboratory: myth or reality? Clin. Chim. Acta *357*, 123-139.

Rinaldi,P., Polidori,M.C., Metastasio,A., Mariani,E., Mattioli,P., Cherubini,A., Catani,M., Cecchetti,R., Senin,U., and Mecocci,P. (2003). Plasma antioxidants are similarly depleted in mild cognitive impairment and in Alzheimer's disease. Neurobiol. Aging *24*, 915-919.

Roher,A.E., Esh,C., Kokjohn,T.A., Kalback,W., Luehrs,D.C., Seward,J.D., Sue,L.I., and Beach,T.G. (2003). Circle of willis atherosclerosis is a risk factor for sporadic Alzheimer's disease. Arterioscler. Thromb. Vasc. Biol. *23*, 2055-2062.

Roman,G.C. (2003). Vascular dementia: distinguishing characteristics, treatment, and prevention. J. Am. Geriatr. Soc. *51*, S296-S304.

Rosenfeld,J., Capdevielle,J., Guillemot,J.C., and Ferrara,P. (1992). In-gel digestion of proteins for internal sequence analysis after one- or two-dimensional gel electrophoresis. Anal. Biochem. *203*, 173-179.

Ross,P.L., Huang,Y.N., Marchese,J.N., Williamson,B., Parker,K., Hattan,S., Khainovski,N., Pillai,S., Dey,S., Daniels,S., Purkayastha,S., Juhasz,P., Martin,S., Bartlet-Jones,M., He,F., Jacobson,A., and Pappin,D.J. (2004). Multiplexed protein quantitation in Saccharomyces

cerevisiae using amine-reactive isobaric tagging reagents. Mol. Cell Proteomics. *3*, 1154-1169.

Ryberg,H., Soderling,A.S., Davidsson,P., Blennow,K., Caidahl,K., and Persson,L.I. (2004). Cerebrospinal fluid levels of free 3-nitrotyrosine are not elevated in the majority of patients with amyotrophic lateral sclerosis or Alzheimer's disease. Neurochem. Int. *45*, 57-62.

Santana-Sosa,E., Barriopedro,M.I., Lopez-Mojares,L.M., Perez,M., and Lucia,A. (2008). Exercise training is beneficial for Alzheimer's patients. Int. J. Sports Med. *29*, 845-850.

Sayre,L.M., Smith,M.A., and Perry,G. (2001). Chemistry and biochemistry of oxidative stress in neurodegenerative disease. Curr. Med. Chem. *8*, 721-738.

Scacchi,R., Ruggeri,M., Gambina,G., Martini,M.C., and Corbo,R.M. (2002). Alpha2-macroglobulin deletion polymorphism and plasma levels in late onset Alzheimer's disease. Clin. Chem. Lab Med. *40*, 333-336.

Schippling,S., Kontush,A., Arlt,S., Buhmann,C., Sturenburg,H.J., Mann,U., Muller-Thomsen,T., and Beisiegel,U. (2000). Increased lipoprotein oxidation in Alzheimer's disease. Free Radic. Biol. Med. *28*, 351-360.

Schulz,B., Liebisch,G., Grandl,M., Werner,T., Barlage,S., and Schmitz,G. (2007). Beta-amyloid (Abeta40, Abeta42) binding to modified LDL accelerates macrophage foam cell formation. Biochim. Biophys. Acta *1771*, 1335-1344.

Sekler,A., Jimenez,J.M., Rojo,L., Pastene,E., Fuentes,P., Slachevsky,A., and Maccioni,R.B. (2008). Cognitive impairment and Alzheimer's disease: Links with oxidative stress and cholesterol metabolism. Neuropsychiatr. Dis. Treat. *4*, 715-722.

Selkoe,D. (2001). Alzheimer's disease: Genes, Proteins, and Therapy. Physiol Rev. *81*, 741-766.

Selley,M.L. (2003). Increased concentrations of homocysteine and asymmetric dimethylarginine and decreased concentrations of nitric oxide in the plasma of patients with Alzheimer's disease. Neurobiol. Aging *24*, 903-907.

Shacter,E., Williams,J.A., Lim,M., and Levine,R.L. (1994). Differential susceptibility of plasma proteins to oxidative modification: examination by western blot immunoassay. Free Radic. Biol. Med. *17*, 429-437.

Sies,H. (1997). Oxidative stress: oxidants and antioxidants. Exp. Physiol *82*, 291-295.

Sies,H. (1999). Glutathione and its role in cellular functions. Free Radic. Biol. Med. *27*, 916-921.

Sinclair,A.J., Bayer,A.J., Johnston,J., Warner,C., and Maxwell,S.R. (1998). Altered plasma antioxidant status in subjects with Alzheimer's disease and vascular dementia. Int. J. Geriatr. Psychiatry *13*, 840-845.

Smith,C.D., Carney,J.M., Starke-Reed,P.E., Oliver,C.N., Stadtman,E.R., Floyd,R.A., and Markesbery,W.R. (1991). Excess brain protein oxidation and enzyme dysfunction in normal aging and in Alzheimer disease. Proc. Natl. Acad. Sci. U. S. A *88*, 10540-10543.

Smith,M.A., Harris,P.L., Sayre,L.M., and Perry,G. (1997a). Iron accumulation in Alzheimer disease is a source of redox-generated free radicals. Proc. Natl. Acad. Sci. U. S. A *94*, 9866-9868.

Smith,M.A., Richey Harris,P.L., Sayre,L.M., Beckman,J.S., and Perry,G. (1997b). Widespread peroxynitrite-mediated damage in Alzheimer's disease. J. Neurosci. *17*, 2653-2657.

Smith,P.K., Krohn,R.I., Hermanson,G.T., Mallia,A.K., Gartner,F.H., Provenzano,M.D., Fujimoto,E.K., Goeke,N.M., Olson,B.J., and Klenk,D.C. (1985). Measurement of protein using bicinchoninic acid. Anal. Biochem. *150*, 76-85.

Sodergren,E., Nourooz-Zadeh,J., Berglund,L., and Vessby,B. (1998). Re-evaluation of the ferrous oxidation in xylenol orange assay for the measurement of plasma lipid hydroperoxides. J. Biochem. Biophys. Methods *37*, 137-146.

Souza,J.M., Peluffo,G., and Radi,R. (2008). Protein tyrosine nitration--functional alteration or just a biomarker? Free Radic. Biol. Med. *45*, 357-366.

Spickett,C.M., Pitt,A.R., Morrice,N., and Kolch,W. (2006). Proteomic analysis of phosphorylation, oxidation and nitrosylation in signal transduction. Biochim. Biophys. Acta *1764*, 1823-1841.

Steinberg,D., Parthasarathy,S., Carew,T.E., Khoo,J.C., and Witztum,J.L. (1989). Beyond cholesterol. Modifications of low-density lipoprotein that increase its atherogenicity. N. Engl. J. Med. *320*, 915-924.

Strohmeyer,R. and Rogers,J. (2001). Molecular and cellular mediators of Alzheimer's disease inflammation. J. Alzheimers Dis. *3*, 131-157.

Sultana,R., Boyd-Kimball,D., Poon,H.F., Cai,J., Pierce,W.M., Klein,J.B., Markesbery,W.R., Zhou,X.Z., Lu,K.P., and Butterfield,D.A. (2006a). Oxidative modification and down-regulation of Pin1 in Alzheimer's disease hippocampus: A redox proteomics analysis. Neurobiol. Aging *27*, 918-925.

Sultana,R., Boyd-Kimball,D., Poon,H.F., Cai,J., Pierce,W.M., Klein,J.B., Merchant,M., Markesbery,W.R., and Butterfield,D.A. (2006b). Redox proteomics identification of oxidized proteins in Alzheimer's disease hippocampus and cerebellum: an approach to understand pathological and biochemical alterations in AD. Neurobiol. Aging *27*, 1564-1576.

Sultana,R., Perluigi,M., Newman,S.F., Pierce,W.M., Cini,C., Coccia,R., and Butterfield,D.A. (2010). Redox proteomic analysis of carbonylated brain proteins in mild cognitive impairment and early Alzheimer's disease. Antioxid. Redox. Signal. *12*, 327-336.

Sun,J., Folk,D., Bradley,T.J., and Tower,J. (2002). Induced over-expression of mitochondrial Mn-superoxide dismutase extends the lifespan of adult *Drosophila melanogaster*. Genetics *161*, 661-672.

Sun,Y.C., Chang,P.Y., Tsao,K.C., Wu,T.L., Sun,C.F., Wu,L.L., and Wu,J.T. (2007). Establishment of a sandwich ELISA using commercial antibody for plasma or serum 3-nitrotyrosine (3NT). Elevation in inflammatory diseases and complementary between 3NT and myeloperoxidase. Clin. Chim. Acta *378*, 175-180.

Suzuki,Y.J., Forman,H.J., and Sevanian,A. (1997). Oxidants as stimulators of signal transduction. Free Radic. Biol. Med. *22*, 269-285.

Tamagno,E., Bardini,P., Obbili,A., Vitali,A., Borghi,R., Zaccheo,D., Pronzato,M.A., Danni,O., Smith,M.A., Perry,G., and Tabaton,M. (2002). Oxidative stress increases expression and activity of BACE in NT2 neurons. Neurobiol. Dis. *10*, 279-288.

Tamagno,E., Robino,G., Obbili,A., Bardini,P., Aragno,M., Parola,M., and Danni,O. (2003). H2O2 and 4-hydroxynonenal mediate amyloid beta-induced neuronal apoptosis by activating JNKs and p38MAPK. Exp. Neurol. *180*, 144-155.

Taniyama,Y. and Griendling,K.K. (2003). Reactive oxygen species in the vasculature: molecular and cellular mechanisms. Hypertension *42*, 1075-1081.

Taysi,S., Polat,F., Gul,M., Sari,R.A., and Bakan,E. (2002). Lipid peroxidation, some extracellular antioxidants, and antioxidant enzymes in serum of patients with rheumatoid arthritis. Rheumatol. Int. *21*, 200-204.

Telci,A., Cakatay,U., Kayali,R., Erdogan,C., Orhan,Y., Sivas,A., and Akcay,T. (2000). Oxidative protein damage in plasma of type 2 diabetic patients. Horm. Metab Res. *32*, 40-43.

ter Steege,J.C., Koster-Kamphuis,L., van Straaten,E.A., Forget,P.P., and Buurman,W.A. (1998). Nitrotyrosine in plasma of celiac disease patients as detected by a new sandwich ELISA. Free Radic. Biol. Med. *25*, 953-963.

Terni,B., Boada,J., Portero-Otin,M., Pamplona,R., and Ferrer,I. (2009). Mitochondrial ATP-Synthase in the Entorhinal Cortex Is a Target of Oxidative Stress at Stages I/II of Alzheimer's Disease Pathology. Brain Pathol.

Tian,L., Cai,Q., and Wei,H. (1998). Alterations of antioxidant enzymes and oxidative damage to macromolecules in different organs of rats during aging. Free Radic. Biol. Med. *24*, 1477-1484.

Tohgi,H., Abe,T., Yamazaki,K., Murata,T., Ishizaki,E., and Isobe,C. (1999). Alterations of 3-nitrotyrosine concentration in the cerebrospinal fluid during aging and in patients with Alzheimer's disease. Neurosci. Lett. *269*, 52-54.

Tseng,C.F., Lin,C.C., Huang,H.Y., Liu,H.C., and Mao,S.J.T. (2004). Antioxidant role of human haptoglobin. Proteomics *4*, 2221-2228.

Tsikas,D. and Caidahl,K. (2005). Recent methodological advances in the mass spectrometric analysis of free and protein-associated 3-nitrotyrosine in human plasma. J. Chromatogr. B Analyt. Technol. Biomed. Life Sci. *814*, 1-9.

Ueda,M., Mashiba,S., and Uchida,K. (2002). Evaluation of oxidized alpha-1-antitrypsin in blood as an oxidative stress marker using anti-oxidative α1-AT monoclonal antibody. Clin. Chim. Acta *317*, 125-131.

Um,H.S., Kang,E.B., Leem,Y.H., Cho,I.H., Yang,C.H., Chae,K.R., Hwang,D.Y., and Cho,J.Y. (2008). Exercise training acts as a therapeutic strategy for reduction of the pathogenic phenotypes for Alzheimer's disease in an NSE/APPsw-transgenic model. Int. J. Mol. Med. *22*, 529-539.

van,O.M., de Jong,F.J., Witteman,J.C., Hofman,A., Koudstaal,P.J., and Breteler,M.M. (2007). Atherosclerosis and risk for dementia. Ann. Neurol. *61*, 403-410.

Veskoukis,A.S., Nikolaidis,M.G., Kyparos,A., and Kouretas,D. (2009). Blood reflects tissue oxidative stress depending on biomarker and tissue studied. Free Radic. Biol. Med. *47*, 1371-1374.

Vina,J., Gomez-Cabrera,M.C., Lloret,A., Marquez,R., Minana,J.B., Pallardo,F.V., and Sastre,J. (2000). Free radicals in Exhaustive Physical Exercise:Mechanism of Production, and Protection by Antioxidants. IUBMB Life *50*, 271-277.

Voss,T. and Haberl,P. (2000). Observations on the reproducibility and matching efficiency of two-dimensional electrophoresis gels:Consequences for comprehensive data analysis. Electrophoresis *21*, 3345-3350.

Wetterling,T., Kanitz,R.D., and Borgis,K.J. (1996). Comparison of different diagnostic criteria for vascular dementia (ADDTC, DSM-IV, ICD-10, NINDS-AIREN). Stroke *27*, 30-36.

Whiteman,M. and Halliwell,B. (1999). Loss of 3-nitrotyrosine on exposure to hypochlorous acid: implications for the use of 3-nitrotyrosine as a bio-marker in vivo. Biochem. Biophys. Res. Commun. *258*, 168-172.

Witztum,J.L. and Steinberg,D. (1991). Role of oxidized low density lipoprotein in atherogenesis. J. Clin. Invest *88*, 1785-1792.

Wu,S.M., Patel,D.D., and Pizzo,S.V. (1998). Oxidized α_2-Macroglobulin (α2M) Differentially Regulates Receptor Binding by Cytokines/Growth Factors:Implications for Tissue Injury and Repair Mechanisms in Inflammation. J. Immunol. *161*, 4356-4365.

Wu,S.M. and Pizzo,S.V. (1999). Mechanism of Hypochlorite-Mediated Inactivation of Proteinase Inhibition by α_2-Macroglobulin. Biochemistry *38*, 13983-13990.

Wu,S.M. and Pizzo,S.V. (2001). α_2-Macroglobulin from Rheumatoid Arthritis Synovial Fluid:Functional Analysis Defines a Role for Oxidation in Inflammation. Arch. Biochem. Biophys. *391*, 119-126.

Wysocki,V.H., Resing,K.A., Zhang,Q., and Cheng,G. (2005). Mass spectrometry of peptides and proteins. Methods *35*, 211-222.

Yamakura,F. and Ikeda,K. (2006). Modification of tryptophan and tryptophan residues in proteins by reactive nitrogen species. Nitric Oxide *14*, 152-161.

Yan,J.X., Wait,R., Berkelman,T., Harry,R.A., Westbrook,J.A., Wheeler,C.H., and Dunn,M.J. (2000). A modified silver staining protocol for visualization of proteins compatible with matrix-assisted laser desorption/ionization and electrospray ionization-mass spectrometry. Electrophoresis *21*, 3666-3672.

Yu,H.L., Chertkow,H.M., Bergman,H., and Schipper,H.M. (2003). Aberrant profiles of native and oxidized glycoproteins in Alzheimer plasma. Proteomics. *3*, 2240-2248.

Zafrilla,P., Mulero,J., Xandri,J.M., Santo,E., Caravaca,G., and Morillas,J.M. (2006). Oxidative stress in Alzheimer patients in different stages of the disease. Curr. Med. Chem. *13*, 1075-1083.

Zahedi,A.S., Ghasemi,A., and Azizi,F. (2008). Serum nitric oxide metabolites in subjects with metabolic syndrome. Clin. Biochem. *41*, 1342-1347.

Zhang,Y.J., Xu,Y.F., Liu,Y.H., Yin,J., and Wang,J.Z. (2005). Nitric oxide induces tau hyperphosphorylation via glycogen synthase kinase-3beta activation. FEBS Lett. *579*, 6230-6236.

Zini,I., Tomasi,A., Grimaldi,R., Vannini,V., and Agnati,L.F. (1992). Detection of free radicals during brain ischemia and reperfusion by spin trapping and microdialysis. Neurosci. Lett. *138*, 279-282.

Zolg,W. (2006). The Proteomic Search for Diagnostic Biomarkers. Mol. Cell Proteomics. *5*, 1720-1726.

Appendix I

APPENDIX I

Optimizing applied voltage for HPLC-ECD; Thesis Chapter 4.

For detection of 3-nitrotyrosine in plasma from Alzheimer's disease (AD) and age-matched control subjects the present study used a modified HPLC-ECD method from that described by Maruyama et al. (1996). Method development was necessary to establish the optimum applied voltage required to provide the greatest 3-nitrotyrosine signal. A known concentration of synthetic 3-nitrotyrosine (10µM) was manually loaded onto the column and the applied voltage was adjusted by 10mV increments ranging between 900mV and 1040mV. All other conditions were kept standard and each sample was assayed in duplicate. The optimal applied voltage was evident at 990mV.

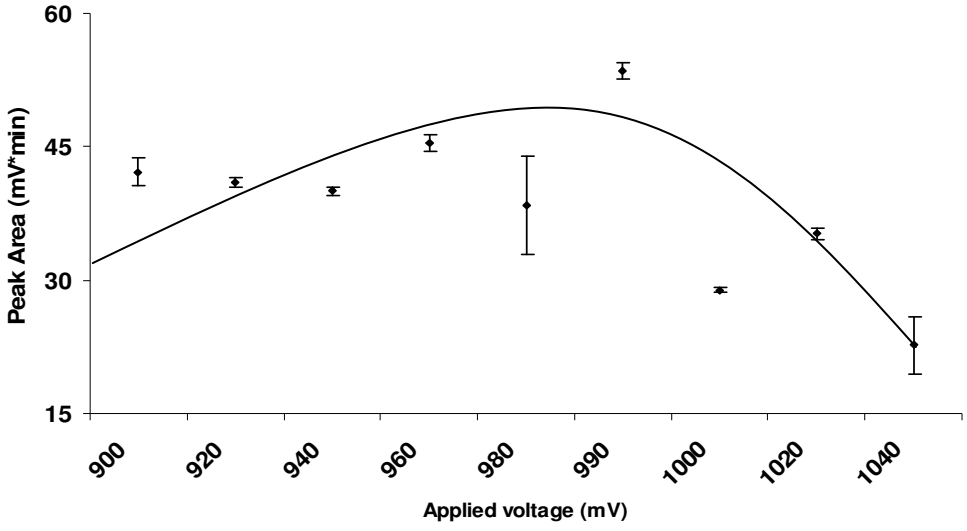

Appendix II

APPENDIX II

Protein summary from OSSMA Browser for excised gel band; Thesis Chapter 5

Protein Summary View for OMSSA file: OMSSA Output Band A.omx

No.	Index	gi#	Accession	Sum log E-Value	Protein Score	%Coverage	#Pep.	#Unique Pep.	Protein Description	MW	Length	Seq ID
1	110	gi|112911	P01023	-266.03	-837.53	28.29	55	34	RecName: Full=Alpha-2-macroglobulin; Short=Alpha-2-M; AltName: Full=C3 and PZP-like alpha-2-macroglobulin domain-containing protein 5; Flags: Precursor	163.3 kDa	1474	933407
2	211	gi|75054706	Q5R4N8	-248.38	-791.5	26.8	50	30	RecName: Full=Alpha-2-macroglobulin; Short=Alpha-2-M; Flags: Precursor	163.3 kDa	1474	1365524
3	44	gi|75054626	Q5NVH5	-166.79	-586.6	45.32	30	26	RecName: Full=Serum albumin; Flags: Precursor	69.4 kDa	609	771862
4	351	gi|158517847	P08603	-115.08	-371.28	21.36	23	22	RecName: Full=Complement factor H; AltName: Full=H factor 1; Flags: Precursor	139.1 kDa	1231	5379492
5	325	gi|238054406	P04264	-90.59	-315.4	27.64	18	17	RecName: Full=Keratin, type II cytoskeletal 1; AltName: Full=Cytokeratin-1; Short=CK-1; AltName: Full=Keratin-1; Short=K1; AltName: Full=67 kDa cytokeratin; AltName: Full=Hair alpha protein	66.0 kDa	644	3991702
6	341	gi|215275331	A5A6M6	-89.01	-314.37	26.37	17	16	RecName: Full=Keratin, type II cytoskeletal 1; AltName: Full=Cytokeratin-1; Short=CK-1; AltName: Full=Keratin-1; Short=K1	65.5 kDa	637	4654833
7	128	gi|24927797	Q28522	-86.63	-296.91	25.33	17	14	RecName: Full=Serum albumin; Flags: Precursor	67.9 kDa	600	988964
8	308	gi|190358749	A2V9Z4	-86.63	-296.58	25	17	14	RecName: Full=Serum albumin; Flags: Precursor	68.9 kDa	608	3389340
9	138	gi|1351907	P02769	-84.74	-286.73	24.55	17	13	RecName: Full=Serum albumin; AltName: Full=BSA; AltName: Allergen=Bos d 6; Flags: Precursor	69.3 kDa	607	1004954
10	283	gi|119370332	P01024	-89.48	-280.1	10.82	17	15	RecName: Full=Complement C3; AltName: Full=C3 and PZP-like alpha-2-macroglobulin domain-containing protein 1; Contains: RecName: Full=Complement C3 beta chain; Contains: RecName: Full=Complement C3 alpha chain; Contains: RecName: Full=C3a anaphylatoxin; Contains: RecName: Full=Complement C3b alpha' chain; Contains: RecName: Full=Complement C3c alpha' chain fragment 1; Contains: RecName: Full=Complement C3dg fragment; Contains: RecName: Full=Complement C3g fragment; Contains: RecName: Full=Complement C3d fragment; Contains: RecName: Full=Complement C3f fragment; Contains: RecName: Full=Complement C3c alpha' chain fragment 2; Flags: Precursor	187.1 kDa	1663	2610664
11	281	gi|239936650	P35908	-65.74	-223.11	23.16	14	14	RecName: Full=Keratin, type II cytoskeletal 2 epidermal; AltName: Full=Cytokeratin-2e; Short=CK 2e; Short=K2e; Short=keratin-2	65.4 kDa	639	2568988
12	344	gi|147744568	P13645	-51.35	-186.77	22.77	10	10	RecName: Full=Keratin, type I cytoskeletal 10; AltName: Full=Cytokeratin-10; Short=CK-10; AltName: Full=Keratin-10; Short=K10	59.5 kDa	593	4658040
13	331	gi|166899089	P20742	-61.51	-181.35	9.65	15	11	RecName: Full=Pregnancy zone protein; AltName: Full=C3 and PZP-like alpha-2-macroglobulin domain-containing protein 6; Flags: Precursor	163.8 kDa	1462	4088341
14	288	gi|239938886	P35527	-41.08	-147.91	16.05	8	7	RecName: Full=Keratin, type I cytoskeletal 9; AltName: Full=Cytokeratin-9; Short=CK-9; AltName: Full=Keratin-9; Short=K9	62.1 kDa	623	2676343
15	26	gi|115646	P02662	-34	-140.26	22.43	5	4	RecName: Full=Alpha-S'-casein; Contains: RecName: Full=Antioxidant peptide; Flags: Precursor	24.5 kDa	214	738260
16	294	gi|75043394	Q6EIZ0	-32.76	-116.17	15.67	7	7	RecName: Full=Keratin, type I cytoskeletal 10; AltName: Full=Cytokeratin-10; AltName: Full=Keratin-10; Short=K10; AltName: Full=Epithelial keratin-10	57.7 kDa	568	2891359
17	102	gi|1351908	P49064	-31.65	-110.16	8.88	6	5	RecName: Full=Serum albumin; AltName: Allergen=Fel d 2; Flags: Precursor	68.7 kDa	608	917585
18	140	gi|75038951	O62823	-24.1	-99.14	15.42	4	3	RecName: Full=Alpha-S'-casein; Flags: Precursor	24.3 kDa	214	1010640
19	141	gi|125074	P06394	-25.4	-86.87	11.79	6	6	RecName: Full=Keratin, type I cytoskeletal 10; AltName: Full=Cytokeratin-10; Short=CK-10; AltName: Full=Keratin-10; Short=K10; AltName: Full=Cytokeratin-8B; AltName: Full=Cytokeratin VIB	54.8 kDa	526	1023361
20	68	gi|113582	P14639	-26.45	-85.51	10.05	6	6	RecName: Full=Serum albumin; Flags: Precursor	69.2 kDa	607	826943
21	201	gi|71152981	P08835	-24.63	-83.08	8.57	5	5	RecName: Full=Serum albumin; Flags: Precursor	69.7 kDa	607	1324074
22	242	gi|75062693	Q6EIY9	-27.69	-82.4	12.6	8	8	RecName: Full=Keratin, type II cytoskeletal 1; AltName: Full=Cytokeratin-1; Short=CK-1; AltName: Full=Keratin-1; Short=K1; AltName: Full=Epithelial keratin-1	63.8 kDa	619	1743526
23	67	gi|116117	P00450	-26.09	-81.3	6.01	6	5	RecName: Full=Ceruloplasmin; AltName: Full=Ferroxidase; Flags: Precursor	122.2 kDa	1065	826637
24	257	gi|119370261	P06238	-34.51	-81.01	5.03	11	5	RecName: Full=Alpha-2-macroglobulin; Short=Alpha-2-M; Flags: Precursor	163.8 kDa	1472	1954555
25	106	gi|44869024	P49065	-22.3	-78.71	3.13	4	3	RecName: Full=Serum albumin; Flags: Precursor	68.9 kDa	608	924112
26	80	gi|93806361	P01860	-23.22	-75.57	13.79	7	4	RecName: Full=Ig gamma-3 chain C region; AltName: Full=Heavy chain disease protein; AltName: Full=HDC	41.3 kDa	377	871346
27	299	gi|81891716	Q6IMF3	-20.52	-71.68	5.76	4	4	RecName: Full=Keratin, type II cytoskeletal 1; AltName: Full=Cytokeratin-1; Short=CK-1; AltName: Full=Keratin-1; Short=K1; AltName: Full=Type II keratin Kb1	64.8 kDa	625	2971878
28	256	gi|123781839	Q4FZU2	-21.02	-68.52	9.42	5	5	RecName: Full=Keratin, type II cytoskeletal 6A; AltName: Full=Cytokeratin-6A; Short=CK 6A; AltName: Full=K6a keratin	59.2 kDa	552	1954546
29	90	gi|136191	P02787	-20.97	-66.28	8.6	5	5	RecName: Full=Serotransferrin; Short=Transferrin; AltName: Full=Siderophilin; AltName: Full=Beta-1 metal-binding globulin; Flags: Precursor	77.1 kDa	698	902357
30	197	gi|45476906	Q86YZ3	-27.89	-65.89	1.93	8	3	RecName: Full=Hornerin	282.4 kDa	2850	1193298
31	244	gi|81892069	Q6NXH9	-15.31	-58.95	4.27	2	2	RecName: Full=Keratin, type II cytoskeletal 73; AltName: Full=Cytokeratin-73; Short=CK-73; AltName: Full=Keratin-73; Short=K73; AltName: Full=Type II keratin-36; AltName: Full=Type I inner root sheath-specific keratin-K6irs3	58.9 kDa	539	1745820
32	253	gi|75062316	Q5XQN5	-15.77	-55.63	5.32	3	3	RecName: Full=Keratin, type II cytoskeletal 5; AltName: Full=Cytokeratin-5; Short=CK-5; AltName: Full=Keratin-5; Short=K5	62.9 kDa	601	1840953
33	324	gi|143811411	P13647	-16.99	-55.6	6.95	4	4	RecName: Full=Keratin, type II cytoskeletal 5; AltName: Full=Cytokeratin-5; Short=CK-5; AltName: Full=Keratin-5; Short=K5; AltName: Full=58 kDa cytokeratin	62.4 kDa	590	3991701
34	343	gi|218526449	A5A6M8	-15.41	-54.02	5.07	3	3	RecName: Full=Keratin, type II cytoskeletal 5; AltName: Full=Cytokeratin-5; Short=CK-5; AltName: Full=Keratin-5; Short=K5	62.5 kDa	592	4654861
35	367	gi|229463044	P02533	-18.46	-53.08	16.1	6	6	RecName: Full=Keratin, type I cytoskeletal 14; AltName: Full=Cytokeratin-14; Short=CK-14; AltName: Full=Keratin-14; Short=K14	51.6 kDa	472	8763417
36	34	gi|547751	Q04695	-16.47	-49.61	9.26	5	5	RecName: Full=Keratin, type I cytoskeletal 17; AltName: Full=Cytokeratin-17; Short=CK-17; AltName: Full=Keratin-17; Short=K17; AltName: Full=39.1	48.1 kDa	432	749734
37	239	gi|1346344	P02538	-16.67	-48.45	9.22	5	5	RecName: Full=Keratin, type II cytoskeletal 6A; AltName: Full=Cytokeratin-6A; Short=CK 6A; AltName: Full=K6a keratin; AltName: Full=Cytokeratin-6D; Short=Ck 6D; AltName: Allergen=Hom s 5	60.0 kDa	564	1658689
38	241	gi|75062694	Q6EIZ1	-16.49	-47.62	6.95	5	5	RecName: Full=Keratin, type II cytoskeletal 2 epidermal; AltName: Full=Cytokeratin-2e; Short=CK 2e; Short=K2e; Short=keratin-2; AltName: Full=Epithelial keratin-2e	64.5 kDa	633	1743515
39	172	gi|2506226	P13635	-14.36	-46.72	3.59	3	3	RecName: Full=Ceruloplasmin; AltName: Full=Ferroxidase; Flags: Precursor	120.8 kDa	1059	1091287
40	275	gi|61784289	Q61147	-14.36	-46.61	3.58	3	3	RecName: Full=Ceruloplasmin; AltName: Full=Ferroxidase; Flags: Precursor	121.2 kDa	1061	2403548

41	230	gi|82654947	P19013	-12.42	-46.17	3.75	2	2	RecName: Full=Keratin, type II cytoskeletal 4; AltName: Full=Cytokeratin-4; Short=CK-4; Short=Keratin-4; Short=K4	57.3 kDa	534	1551602
42	311	gi|126302559	P04104	-13.7	-45.94	3.77	3	3	RecName: Full=Keratin, type II cytoskeletal 1; AltName: Full=Cytokeratin-1; Short=CK-1; AltName: Full=Keratin-1; Short=K1; AltName: Full=67 kDa cytokeratin; AltName: Full=Krt1 protein	65.6 kDa	637	3446472
43	272	gi|81170668	Q922U2	-12.38	-45.66	3.79	2	2	RecName: Full=Keratin, type II cytoskeletal 5; AltName: Full=Cytokeratin-5; Short=CK-5; AltName: Full=Keratin-5; Short=K5	61.8 kDa	580	2380372
44	274	gi|81170669	Q6P6Q2	-12.38	-45.59	3.82	2	2	RecName: Full=Keratin, type II cytoskeletal 5; AltName: Full=Cytokeratin-5; Short=CK-5; AltName: Full=Keratin-5; Short=K5	61.8 kDa	576	2402900
45	112	gi|23396626	Q9QWL7	-14.14	-44.27	7.62	4	4	RecName: Full=Keratin, type I cytoskeletal 17; AltName: Full=Cytokeratin-17; Short=CK-17; AltName: Full=Keratin-17; Short=K17	48.2 kDa	433	934447
46	270	gi|238054404	P04259	-13.14	-43.53	5.14	3	3	RecName: Full=Keratin, type II cytoskeletal 6B; AltName: Full=Cytokeratin-6B; Short=CK 6B; AltName: Full=K6b keratin	60.1 kDa	564	2202161
47	161	gi|61211605	Q7SIH1	-10.36	-42.73	10	3	1	RecName: Full=Alpha-2-macroglobulin; Short=Alpha-2-M	14.5 kDa	130	1060834
48	328	gi|121039	P01857	-11.01	-42.57	9.09	2	2	RecName: Full=Ig gamma-1 chain C region	36.1 kDa	330	4034695
49	342	gi|160358759	A5A6I6	-14.37	-41.84	6.73	4	4	RecName: Full=Serotransferrin; Short=Transferrin; AltName: Full=Siderophilin; AltName: Full=Beta-1 metal-binding globulin; Flags: Precursor	77.1 kDa	698	4654860
50	191	gi|82190775	O93256	-12.14	-40.57	4.73	3	3	RecName: Full=Keratin, type I cytoskeletal 19; AltName: Full=Cytokeratin-19; Short=CK-19; AltName: Full=Keratin-19; Short=K19; AltName: Ful=GK-19	46.1 kDa	423	1125837
51	347	gi|205830697	P85925	-7.22	-39.68	100	2	2	RecName: Full=Unknown protein 18	1.4 kDa	12	5231946
52	180	gi|113583	P20758	-11.7	-39.14	13.6	4	4	RecName: Full=Ig alpha-1 chain C region	37.8 kDa	353	1112550
53	326	gi|113584	P01876	-11.7	-39.14	13.6	4	4	RecName: Full=Ig alpha-1 chain C region	37.7 kDa	353	4034629
54	130	gi|125946	P01842	-9.2	-38.71	23.81	2	2	RecName: Full=Ig lambda chain C regions	11.2 kDa	105	993812
55	127	gi|125079	P05785	-9.38	-38.56	11.83	2	2	RecName: Full=Keratin, type I cytoskeletal 14; AltName: Full=Cytokeratin-14; Short=CK-14; AltName: Full=Keratin-14; Short=K14; AltName: Ful=Cytokeratin-7; AltName: Full=Cytokeratin VII	10.7 kDa	93	987292
56	190	gi|218512041	Q03591	-10.12	-37.97	6.06	2	2	RecName: Full=Complement factor H-related protein 1; Short=FHR-1; AltName: Full=H factor-like protein 1; Short=H-factor-like 1; AltName: Full=H36; Flags: Precursor	37.7 kDa	330	1124222
57	83	gi|125106	P16878	-10.63	-37.79	4.09	2	2	RecName: Full=Keratin, type II cytoskeletal; AltName: Full=XENCK55(5/6)	55.5 kDa	513	884725
58	143	gi|90110027	P05787	-10.63	-37.74	4.35	2	2	RecName: Full=Keratin, type II cytoskeletal 8; AltName: Full=Cytokeratin-8; Short=CK-8; AltName: Full=Keratin-8; Short=K8	53.7 kDa	483	1028452
59	231	gi|1708592	Q10758	-10.63	-37.62	4.35	2	2	RecName: Full=Keratin, type II cytoskeletal 8; AltName: Full=Cytokeratin-8; Short=CK-8; AltName: Full=Keratin-8; Short=K8; AltName: Full=Cytokeratin endo A	54.0 kDa	483	1554875
60	136	gi|124740	P18520	-10.63	-37.57	4.04	2	2	RecName: Full=Intermediate filament protein ON3	57.8 kDa	520	1003988
61	142	gi|56757408	P49822	-11.91	-36.86	4.93	3	3	RecName: Full=Serum albumin; AltName: Allergen=Can f 3; Flags: Precursor	68.6 kDa	608	1027915
62	238	gi|33302628	Q61781	-11.38	-36.3	4.96	3	3	RecName: Full=Keratin, type I cytoskeletal 14; AltName: Full=Cytokeratin-14; Short=CK-14; AltName: Full=Keratin-14; Short=K14	52.9 kDa	484	1656757
63	31	gi|123856	P01777	-8.23	-36.24	15.97	1	1	RecName: Full=Ig heavy chain V-III region TEI	12.6 kDa	119	744988
64	301	gi|81884761	Q6GQT1	-17.17	-36.08	3.19	6	3	RecName: Full=Alpha-2-macroglobulin-P; AltName: Full=Alpha-2-macroglobulin; Flags: Precursor	164.3 kDa	1474	2988840
65	165	gi|123845	P01766	-8.23	-36.08	15.83	1	1	RecName: Full=Ig heavy chain V-III region BRO	13.2 kDa	120	1067648
66	318	gi|118595772	P68082	-8.5	-35.92	9.74	1	1	RecName: Full=Myoglobin	17.1 kDa	154	3927827
67	170	gi|123794	P01786	-8.23	-35.71	16.24	1	1	RecName: Full=Ig heavy chain V region MOPC 47A	12.4 kDa	117	1088592
68	58	gi|123814	P01794	-8.23	-35.58	15.45	1	1	RecName: Full=Ig heavy chain V region HPCG14	13.8 kDa	123	802681
69	144	gi|123811	P01791	-8.23	-35.58	15.45	1	1	RecName: Full=Ig heavy chain V region HPCM6	13.9 kDa	123	1030372
70	94	gi|123813	P01793	-8.23	-35.58	15.45	1	1	RecName: Full=Ig heavy chain V region HPCG13	13.8 kDa	123	905712
71	189	gi|123795	P01787	-8.23	-35.58	15.45	1	1	RecName: Full=Ig heavy chain V regions TEPC 15/S107/HPCM1/HPCM2/HPCM3	13.8 kDa	123	1123320
72	78	gi|123810	P01790	-8.23	-35.58	15.57	1	1	RecName: Full=Ig heavy chain V region M511	13.7 kDa	122	869122
73	363	gi|218512079	P01859	-12.01	-35.56	12.88	5	3	RecName: Full=Ig gamma-2 chain C region	35.9 kDa	326	7474819
74	157	gi|123809	P01789	-8.23	-35.46	15.57	1	1	RecName: Full=Ig heavy chain V region M603	13.6 kDa	122	1054882
75	33	gi|123812	P01792	-8.23	-35.4	15.45	1	1	RecName: Full=Ig heavy chain V region HPCG8	13.9 kDa	123	748636
76	147	gi|81906177	Q9DCV7	-8.83	-35.14	2.41	1	1	RecName: Full=Keratin, type II cytoskeletal 7; AltName: Full=Cytokeratin-7; Short=CK-7; Short=Keratin 7; Short=K7	50.7 kDa	457	1039159
77	137	gi|125112	P08776	-8.83	-35.09	2.19	1	1	RecName: Full=Keratin, type II cytoskeletal 8; AltName: Full=Cytokeratin-8; Short=CK-8; AltName: Full=Keratin-8; Short=K8	55.7 kDa	502	1004295
78	116	gi|121135	P14136	-8.83	-34.97	2.55	1	1	RecName: Full=Glial fibrilary acidic protein; Short=GFAP	49.9 kDa	432	949293

79	212	gi|75061841	Q5RA72	-8.83	-34.97	2.55	1	1	RecName: Full=Glial fibrillary acidic protein; Short=GFAP	49.9 kDa	432	1365837
80	56	gi|60416436	P50446	-11.27	-34.94	5.97	3	3	RecName: Full=Keratin, type II cytoskeletal 6A; AltName: Full=Cytokeratin-6A; Short=CK 6A; AltName: Full=K6a keratin; AltName: Full=Keratin-6 alpha; Short=mK6-alpha	59.3 kDa	553	801795
81	111	gi|59798479	Q9Z331	-11.27	-34.8	5.87	3	3	RecName: Full=Keratin, type II cytoskeletal 6B; AltName: Full=Cytokeratin-6B; Short=CK 6B; AltName: Full=K6b keratin; AltName: Full=Keratin-6 beta; Short=mK6-beta	60.3 kDa	562	934090
82	171	gi|56404987	P68293	-8.47	-34.43	4.49	1	1	RecName: Full=Apolipoprotein A-I; Short=Apo-AI; Short=ApoA-I; Flags: Precursor	30.7 kDa	267	1090052
83	105	gi|113992	P02647	-8.47	-34.43	4.49	1	1	RecName: Full=Apolipoprotein A-I; Short=Apo-AI; Short=ApoA-I; Contains: RecName: Full=Apolipoprotein A-I(1-242); Flags: Precursor	30.8 kDa	267	920947
84	114	gi|125086	P08728	-9.38	-33.24	2.76	2	2	RecName: Full=Keratin, type I cytoskeletal 19; AltName: Full=Cytokeratin-19; Short=CK-19; AltName: Full=Keratin-19; Short=K19	43.9 kDa	399	939182
85	131	gi|5915682	P07724	-8.46	-33.13	2.14	1	1	RecName: Full=Serum albumin; Flags: Precursor	68.7 kDa	608	993949
86	135	gi|1708588	P08730	-9.34	-33.08	4.58	2	2	RecName: Full=Keratin, type I cytoskeletal 13; AltName: Full=Cytokeratin-13; Short=CK-13; AltName: Full=Keratin-13; Short=K13; AltName: Full=47 kDa cytokeratin	47.8 kDa	437	1002993
87	321	gi|118595800	P02166	-7.87	-33	9.74	1	1	RecName: Full=Myoglobin	17.1 kDa	154	3929976
88	320	gi|118595791	P02167	-7.87	-33	9.74	1	1	RecName: Full=Myoglobin	17.0 kDa	154	3929861
89	309	gi|118595784	P02150	-7.87	-32.93	9.74	1	1	RecName: Full=Myoglobin	17.2 kDa	154	3396537
90	322	gi|118595765	P02168	-7.87	-32.93	9.74	1	1	RecName: Full=Myoglobin	17.1 kDa	154	3930012
91	315	gi|116247696	P02152	-7.87	-32.85	9.74	1	1	RecName: Full=Myoglobin	17.2 kDa	154	3781138
92	323	gi|118595742	P02151	-7.87	-32.85	9.74	1	1	RecName: Full=Myoglobin	17.2 kDa	154	3930014
93	319	gi|118595778	P02154	-7.87	-32.85	9.74	1	1	RecName: Full=Myoglobin	17.2 kDa	154	3929811
94	265	gi|109892943	Q3AHU2	-8.52	-32.81	11.2	2	1	RecName: Full=Orotidine 5'-phosphate decarboxylase; AltName: Full=OMP decarboxylase; Short=OMPdecase; Short=OMPDCase; Short=OMPdecase	24.7 kDa	241	2082534
95	61	gi|547750	P35900	-9.38	-32.54	2.59	2	2	RecName: Full=Keratin, type I cytoskeletal 20; AltName: Full=Cytokeratin-20; Short=CK-20; AltName: Full=Keratin-20; Short=K20; AltName: Full=Protein IT	48.5 kDa	424	809150
96	313	gi|122132186	Q08D91	-9.39	-32	4.05	2	2	RecName: Full=Keratin, type II cytoskeletal 75; AltName: Full=Cytokeratin-75; Short=CK-75; AltName: Full=Keratin-75; Short=K75; AltName: Full=Type II keratin-K6hf; AltName: Full=Keratin-6 hair follicle	59.0 kDa	543	3701717
97	224	gi|81175167	P0C0L5	-10.04	-31.13	1.38	2	2	RecName: Full=Complement C4-B; AltName: Full=Basic complement C4; AltName: Full=C3 and PZP-like alpha-2-macroglobulin domain-containing proten 3; Contains: RecName: Full=Complement C4 beta chain; Contains: RecName: Full=Complement C4-B alpha chain; Contains: RecName: Full=C4a anaphylatoxin; Contains: RecName: Full=C4b-B; Contains: RecName: Full=C4d-B; Contains: RecName: Full=Complement C4 gamma chain; Flags: Precursor	192.8 kDa	1744	1489306
98	150	gi|81175238	P0C0L4	-10.04	-31.13	1.38	2	2	RecName: Full=Complement C4-A; AltName: Full=Acidic complement C4; AltName: Full=C3 and PZP-like alpha-2-macroglobulin domain-containing proten 2; Contains: RecName: Full=Complement C4 beta chain; Contains: RecName: Full=Complement C4-A alpha chain; Contains: RecName: Full=C4a anaphylatoxin; Contains: RecName: Full=C4b-A; Contains: RecName: Full=C4d-A; Contains: RecName: Full=Complement C4 gamma chain; Flags: Precursor	192.8 kDa	1744	1043573
99	327	gi|121047	P01861	-9.3	-31.05	12.84	3	3	RecName: Full=Ig gamma-4 chain C region	35.9 kDa	327	4034648
100	64	gi|13431311	O75882	-10.88	-29.29	3.08	3	3	RecName: Full=Attractin; AltName: Full=Mahogany homolog; AltName: Full=DPPT-L; Flags: Precursor	158.5 kDa	1429	813401
101	250	gi|81170667	Q6IFV1	-8.58	-28.86	4.95	2	2	RecName: Full=Keratin, type I cytoskeletal 14; AltName: Full=Cytokeratin-14; Short=CK-14; AltName: Full=Keratin-14; Short=K14; AltName: Full=Type I keratin Ka14	52.7 kDa	485	1801922
102	21	gi|1703025	P01009	-8.16	-28.23	6.94	2	2	RecName: Full=Alpha-1-antitrypsin; AltName: Full=Alpha-1 protease inhibitor; AltName: Full=Alpha-1-antiproteinase; Contains: RecName: Full=Short peptide from AAT; Short=SPAAT; Flags: Precursor	46.7 kDa	418	729287
103	208	gi|68052067	Q5RCW5	-8.16	-28.15	6.94	2	2	RecName: Full=Alpha-1-antitrypsin; AltName: Full=Alpha-1 protease inhibitor; AltName: Full=Alpha-1-antiproteinase; Flags: Precursor	46.9 kDa	418	1363297
104	300	gi|81891691	Q6IFX2	-8.41	-28.04	4.87	2	2	RecName: Full=Keratin, type I cytoskeletal 42; AltName: Full=Cytokeratin-42; Short=CK-42; AltName: Full=Keratin-42; Short=K42; AltName: Full=Type I keratin Ka22; AltName: Full=Keratin-17n	50.1 kDa	452	2973373
105	113	gi|75075054	Q9XT27	-8.83	-27.73	0.95	2	1	RecName: Full=Ceruloplasmin; AltName: Full=Ferroxidase; Flags: Precursor	119.1 kDa	1048	935572
106	77	gi|112688	P01010	-7	-27.63	3.67	1	1	RecName: Full=Alpha-1-antitrypsin; Short=AAT; AltName: Full=Alpha-1 protease inhibitor; AltName: Full=Alpha-1-antiproteinase; Flags: Precursor	45.7 kDa	409	867648
107	145	gi|68051994	O00394	-7	-27.59	3.79	1	1	RecName: Full=Alpha-1-antitrypsin; AltName: Full=Alpha-1 protease inhibitor; AltName: Full=Alpha-1-antiproteinase; Flags: Precursor	44.6 kDa	396	1036117
108	162	gi|30024068	Q61703	-8.69	-27.33	2.75	2	2	RecName: Full=Inter-alpha-trypsin inhibitor heavy chain H2; Short=Inter-alpha-inhibitor heavy chain 2; Short=ITI heavy chain H2; Flags: Precursor	105.9 kDa	946	1062455
109	287	gi|229462889	P19823	-8.69	-27.23	2.75	2	2	RecName: Full=Inter-alpha-trypsin inhibitor heavy chain H2; Short=Inter-alpha-inhibitor heavy chain 2; Short=ITI heavy chain H2; AltName: Full=Inter-alpha-trypsin inhibitor complex component II; AltName: Full=Serum-derived hyaluronan-associated protein; Short=SHAP; Flags: Precursor	106.5 kDa	946	2643994
110	52	gi|30024062	P97279	-8.69	-27.2	2.75	2	2	RecName: Full=Inter-alpha-trypsin inhibitor heavy chain H2; Short=Inter-alpha-inhibitor heavy chain 2; Short=ITI heavy chain H2; Short=HC2; Flags: Precursor	106.6 kDa	946	794353
111	174	gi|30024050	O02668	-8.69	-27.15	2.78	2	2	RecName: Full=Inter-alpha-trypsin inhibitor heavy chain H2; Short=Inter-alpha-inhibitor heavy chain 2; Short=ITI heavy chain H2; Flags: Precursor	104.6 kDa	935	1097442
112	215	gi|57015287	P04653	-6.53	-26.78	4.67	1	1	RecName: Full=Alpha-S1-casein; Flags: Precursor	24.3 kDa	214	1409496

113	178	gi	416750	P18626	-6.53	-26.75	4.67	1	1	RecName: Full=Alpha-S1-casein; Short=Alpha-S1-CN; Flags: Precursor	24.3 kDa	214	1110042
114	280	gi	13431313	Q9MU60	-8.63	-25.86	2.17	2	2	RecName: Full=Attractin; AltName: Full=Protein mahogany; Flags: Precursor	158.1 kDa	1428	2559818
115	247	gi	81891678	Q6IFV4	-6.58	-25.35	2.51	1	1	RecName: Full=Keratin, type I cytoskeletal 13; AltName: Full=Cytokeratin-13; Short=CK-13; AltName: Full=Keratin-13; Short=K13; AltName: Full=Type I keratin Ka13	47.7 kDa	438	1801907
116	177	gi	20178290	P02755	-7.51	-25.16	13.33	3	3	RecName: Full=Beta-lactoglobulin; Short=Beta-LG; Flags: Precursor	20.0 kDa	180	1107923
117	168	gi	125910	P02754	-7.51	-25.16	13.48	3	3	RecName: Full=Beta-lactoglobulin; Short=Beta-LG; AltName: Allergen=Bos d 5; Flags: Precursor	19.9 kDa	178	1085991
118	57	gi	75059267	Q29426	-7.88	-25.05	3.66	2	2	RecName: Full=Keratin, type II cytoskeletal 3; AltName: Full=Cytokeratin-3; Short=CK-3; Short=Keratin-3; Short=K3	64.3 kDa	629	802106
119	232	gi	5477752	Q01546	-7.88	-24.91	3.61	2	2	RecName: Full=Keratin, type II cytoskeletal 2 oral; AltName: Full=Cytokeratin-2P; Short=CK 2P; Short=K2P; AltName: Full=Keratin-76; Short=K76	65.9 kDa	638	1579557
120	298	gi	81891690	Q6IFW6	-8.78	-24.71	5.7	3	3	RecName: Full=Keratin, type I cytoskeletal 10; AltName: Full=Cytokeratin-10; Short=CK-10; AltName: Full=Keratin-10; Short=K10; AltName: Full=Type I keratin Ka10	56.5 kDa	526	2971877
121	251	gi	81891697	Q6IFZ9	-6.48	-24.34	2.42	1	1	RecName: Full=Keratin, type II cytoskeletal 74; AltName: Full=Keratin-74; Short=K74; AltName: Full=Type II keratin Kb37	54.7 kDa	495	1801923
122	289	gi	81891673	Q6IFU7	-6.45	-24.34	2.21	1	1	RecName: Full=Keratin, type I cytoskeletal 42; AltName: Full=Cytokeratin-42; Short=CK-42; AltName: Full=Keratin-42; Short=K42; AltName: Full=Type I keratin Ka22	50.2 kDa	452	2692146
123	99	gi	74750553	Q86Y46	-7.72	-24.16	3.89	2	2	RecName: Full=Keratin, type II cytoskeletal 73; AltName: Full=Cytokeratin-73; Short=CK-73; AltName: Full=Keratin-73; Short=K73; AltName: Full=Type II keratin-36; AltName: Full=Type II inner root sheath-specific keratin-K6irs3	58.9 kDa	540	913752
124	249	gi	66773987	Q6IFZ6	-6.48	-24.15	2.1	1	1	RecName: Full=Keratin, type II cytoskeletal 1b; AltName: Full=Cytokeratin-1B; Short=CK-1B; AltName: Full=Keratin-77; Short=K77; AltName: Full=Type II keratin Kb39; AltName: Full=Embryonic type II keratin-1	61.4 kDa	572	1801921
125	153	gi	60390219	Q9R0H5	-6.48	-24.15	2.29	1	1	RecName: Full=Keratin, type II cytoskeletal 71; AltName: Full=Cytokeratin-71; Short=CK-71; AltName: Full=Keratin-71; Short=K71; AltName: Full=Type II keratin-34; AltName: Full=Type II inner root sheath-specific keratin-K6irs1; Short=mK6irs1/Krt2-6g; Short=mK6irs; AltName: Full=Cytokeratin-6G; Short=CK 6G; AltName: Full=K6g keratin	57.4 kDa	524	1046847
126	297	gi	81891700	Q6IG03	-6.48	-24.02	2.17	1	1	RecName: Full=Keratin, type II cytoskeletal 73; AltName: Full=Cytokeratin-73; Short=CK-73; AltName: Full=Keratin-73; Short=K73; AltName: Full=Type II keratin-36; AltName: Full=Type II inner root sheath-specific keratin-K6irs3	60.4 kDa	553	2971875
127	364	gi	21851208	P01877	-6.76	-23.97	7.94	2	2	RecName: Full=Ig alpha-2 chain C region	36.5 kDa	340	7474820
128	357	gi	2053711736	P85295	-6.05	-23.63	23.33	2	2	RecName: Full=Serum albumin	9.7 kDa	90	6930585
129	306	gi	117949802	P07996	-6.23	-21.95	0.77	1	1	RecName: Full=Thrombospondin-1; Flags: Precursor	129.4 kDa	1170	3195141
130	93	gi	12644428	Q28178	-6.23	-21.89	0.77	1	1	RecName: Full=Thrombospondin-1; Flags: Precursor	129.5 kDa	1170	904312
131	237	gi	59803089	P48668	-8.4	-21.7	5.32	3	3	RecName: Full=Keratin, type II cytoskeletal 6C; AltName: Full=Cytokeratin-6C; Short=CK 6C; AltName: Full=K6c keratin; AltName: Full=Cytokeratin-6E; Short=CK 6E; AltName: Full=Keratin K6h	60.0 kDa	564	1616820
132	158	gi	1706799	P02671	-8.79	-21.62	4.5	3	3	RecName: Full=Fibrinogen alpha chain; Contains: RecName: Full=Fibrinopeptide A; Flags: Precursor	95.0 kDa	866	1057378
133	314	gi	116242600	P02535	-6.87	-21.61	4.39	2	2	RecName: Full=Keratin, type I cytoskeletal 10; AltName: Full=Cytokeratin-10; Short=CK-10; AltName: Full=Keratin-10; Short=K10; AltName: Full=56 kDa cytokeratin; AltName: Full=Keratin, type I cytoskeletal 59 kDa	57.8 kDa	570	3781067
134	185	gi	123510	P00739	-5.59	-21.32	3.45	1	1	RecName: Full=Haptoglobin-related protein; Flags: Precursor	39.0 kDa	348	1121035
135	209	gi	68565358	Q5R5F6	-5.59	-21.32	3.46	1	1	RecName: Full=Haptoglobin; Contains: RecName: Full=Haptoglobin alpha chain; Contains: RecName: Full=Haptoglobin beta chain; Flags: Precursor	38.5 kDa	347	1364304
136	101	gi	68565391	Q28801	-5.59	-21.21	3.47	1	1	RecName: Full=Haptoglobin-related protein; Flags: Precursor	38.9 kDa	346	915896
137	41	gi	123508	P00738	-5.59	-20.98	2.96	1	1	RecName: Full=Haptoglobin; Contains: RecName: Full=Haptoglobin alpha chain; Contains: RecName: Full=Haptoglobin beta chain; Flags: Precursor	45.2 kDa	406	758523
138	359	gi	226709030	B6E141	-5.59	-20.75	2.99	1	1	RecName: Full=Haptoglobin; Contains: RecName: Full=Haptoglobin alpha chain; Contains: RecName: Full=Haptoglobin beta chain; Flags: Precursor	44.6 kDa	401	7003521
139	360	gi	226704449	B6D985	-5.59	-20.74	3	1	1	RecName: Full=Haptoglobin; Contains: RecName: Full=Haptoglobin alpha chain; Contains: RecName: Full=Haptoglobin beta chain; Flags: Precursor	44.7 kDa	400	7005839
140	262	gi	122137096	Q2TBU0	-5.59	-20.72	2.99	1	1	RecName: Full=Haptoglobin; Contains: RecName: Full=Haptoglobin alpha chain; Contains: RecName: Full=Haptoglobin beta chain; Flags: Precursor	44.9 kDa	401	2048176
141	240	gi	123797712	Q8WED5	-6.68	-19.49	4.14	2	2	RecName: Full=Keratin, type II cytoskeletal 79; AltName: Full=Cytokeratin-79; Short=CK-79; AltName: Full=Keratin-79; Short=K79; AltName: Full=Type II keratin-38	57.6 kDa	531	1689111
142	70	gi	59799796	P69185	-7.99	-19.06	7.1	4	1	RecName: Full=Thymidine kinase	38.8 kDa	352	835497
143	65	gi	125097	P04266	-4.88	-17.28	2.82	1	1	RecName: Full=Keratin, type II cytoskeletal I; AltName: Full=Clone PUF23	45.7 kDa	425	816428
144	261	gi	122143589	Q148H7	-4.88	-16.86	2.24	1	1	RecName: Full=Keratin, type II cytoskeletal 79; AltName: Full=Cytokeratin-79; Short=CK-79; AltName: Full=Keratin-79; Short=K79	57.7 kDa	535	2047188
145	285	gi	81896062	Q8BGZ7	-4.87	-16.72	2.18	1	1	RecName: Full=Keratin, type II cytoskeletal 75; AltName: Full=Cytokeratin-75; Short=CK-75; AltName: Full=Keratin-75; Short=K75; AltName: Full=Type II keratin-18; AltName: Full=Type II keratin-K6hf; AltName: Full=Keratin-6 hair follicle; Short=mK6hf	59.7 kDa	551	2639418
146	243	gi	81891714	Q6IME9	-4.78	-16.41	2.31	1	1	RecName: Full=Keratin, type II cytoskeletal 72; AltName: Full=Cytokeratin-72; Short=CK-72; AltName: Full=Keratin-72; Short=K72; AltName: Full=Type-II keratin-35; AltName: Full=Type II inner root sheath-specific keratin-K6irs2	56.8 kDa	520	1745652
147	229	gi	166218813	Q14CN4	-4.78	-16.34	2.35	1	1	RecName: Full=Keratin, type II cytoskeletal 72; AltName: Full=Cytokeratin-72; Short=CK-72; AltName: Full=Keratin-72; Short=K72; AltName: Full=Type-II keratin-35; AltName: Full=Type II inner root sheath-specific keratin-K6irs2	55.9 kDa	511	1548680
148	271	gi	23503075	P08779	-6.89	-16.32	8.03	3	3	RecName: Full=Keratin, type I cytoskeletal 16; AltName: Full=Cytokeratin-16; Short=CK-16; AltName: Full=Keratin-16; Short=K16	51.3 kDa	473	2321437

149	207	gil	166218815	Q3SY84	-4.78	-16.31	2.29	1	1	Short=K71; AltName: Full=Type II keratin-34; AltName: Full=Type II inner root sheath-specific keratin-K6irs1; Short=Keratin 6 irs; Short=hK6irs; Short=hK6irs1	57.2 kDa	523	1363079
150	248	gil	81891698	Q6IG00	-5.95	-16.11	3.73	2	2	RecName: Full=Keratin, type II cytoskeletal 4; AltName: Full=Cytokeratin-4; Short=Ck-4; Short=Keratin-4; Short=K4; AltName: Full=Type II keratin Kb4	57.7 kDa	536	1801909
151	206	gil	76363596	Q5XLE4	-5.9	-15.06	2.8	2	2	RecName: Full=Serum albumin; Flags: Precursor	68.5 kDa	607	1357522
152	23	gil	543794	P35747	-5.9	-15.02	2.8	2	2	RecName: Full=Serum albumin; AltName: Allergen=Equ c 3; Flags: Precursor	68.6 kDa	607	731698
153	220	gil	88909208	Q4FPN5	-4.33	-14.79	3.57	1	1	RecName: Full=S-adenosyl-L-methionine-dependent methyltransferase mraW	38.8 kDa	336	1447861
154	29	gil	127506	P04220	-5.08	-14.49	6.65	2	2	RecName: Full=Ig mu heavy chain disease protein; AltName: Full=BOT	43.1 kDa	391	741484
155	233	gil	233966632	Q9Z2K1	-5.41	-14.3	4.26	2	2	RecName: Full=Keratin, type I cytoskeletal 16; AltName: Full=Cytokeratin-16; Short=CK-16; AltName: Full=Keratin-16; Short=K16	51.6 kDa	469	1596627
156	104	gil	124096	P05155	-5.19	-14.09	4.4	2	2	RecName: Full=Plasma protease C1 inhibitor; Short=C1 Inh; Short=C1Inh; AltName: Full=C1 esterase inhibitor; AltName: Full=C1-inhibiting factor; Flags: Precursor	55.2 kDa	500	919283
157	356	gil	193806374	P01871	-5.08	-14.04	5.75	2	2	RecName: Full=Ig mu chain C region	49.3 kDa	452	6506548
158	36	gil	3183048	Q28706	-5.1	-13.63	3.89	2	2	RecName: Full=Keratin, type I cytoskeletal 12; AltName: Full=Cytokeratin-12; Short=CK-12; AltName: Full=Keratin-12; Short=K12	45.7 kDa	411	754832
159	183	gil	136429	P00761	-4.14	-13.51	8.66	2	2	RecName: Full=Trypsin; Flags: Precursor	24.4 kDa	231	1114697
160	338	gil	187668015	A5H447	-3.86	-12.73	2.87	1	1	RecName: Full=Zyxin	70.7 kDa	663	4613410
161	22	gil	77416709	P0AAP1	-3.69	-12.57	3.5	1	1	RecName: Full=Protein adrA	41.5 kDa	371	731613
162	79	gil	75058787	O77727	-4.85	-12.21	4.64	2	2	RecName: Full=Keratin, type I cytoskeletal 15; AltName: Full=Cytokeratin-15; Short=CK-15; AltName: Full=Keratin-15; Short=K15	48.8 kDa	453	871196
163	81	gil	29337194	P08649	-4.26	-11.97	0.52	1	1	RecName: Full=Complement C4; Contains: RecName: Full=Complement C4 beta chain; Contains: RecName: Full=Complement C4 alpha chain; Contains: RecName: Full=C4a anaphylatoxin; Contains: RecName: Full=Complement C4 gamma chain; Flags: Precursor	192.2 kDa	1737	871450
164	335	gil	126302537	P01029	-4.26	-11.94	0.52	1	1	RecName: Full=Complement C4-B; Contains: RecName: Full=Complement C4 beta chain; Contains: RecName: Full=Complement C4 alpha chain; Contains: RecName: Full=C4a anaphylatoxin; Contains: RecName: Full=Complement C4 gamma chain; Flags: Precursor	192.9 kDa	1738	4374985
165	132	gil	1708590	P51856	-4.72	-11.88	5.24	2	2	RecName: Full=Keratin, type I cytoskeletal 19; AltName: Full=Cytokeratin-19; Short=CK-19; AltName: Full=Keratin-19; Short=K19	43.8 kDa	401	996741
166	82	gil	81725314	Q87G42	-3.22	-11.22	5.51	1	1	RecName: Full=Purine nucleoside phosphorylase deoD-type 2; Short=PNP 2	25.7 kDa	236	874943
167	13	gil	85681036	Q9KNB2	-3.22	-11.19	5.51	1	1	RecName: Full=Purine nucleoside phosphorylase deoD-type 2; Short=PNP 2	25.6 kDa	236	407441
168	3	gil	2499702	P71198	-3.11	-11.18	7.53	1	1	RecName: Full=Protein traM	15.6 kDa	146	17631
169	96	gil	85540976	Q7MFQ6	-3.22	-11.16	5.51	1	1	RecName: Full=Purine nucleoside phosphorylase deoD-type 2; Short=PNP 2	25.7 kDa	236	909790
170	100	gil	115654	P02663	-4.15	-11.07	9.46	2	2	RecName: Full=Alpha-S2-casein; Contains: RecName: Full=Casocidin-1; AltName: Full=Casocidin-I; Flags: Precursor	26.0 kDa	222	913994
171	24	gil	115658	P04654	-4.15	-10.91	9.42	2	2	RecName: Full=Alpha-S2-casein; Flags: Precursor	26.3 kDa	223	737422
172	117	gil	416751	P33049	-4.15	-10.91	9.42	2	2	RecName: Full=Alpha-S2-casein; Short=Alpha-S2-CN; Flags: Precursor	26.4 kDa	223	949345
173	8	gil	74595791	Q5B4D1	-5.01	-10.85	2.21	2	1	RecName: Full=Protein grc3	90.0 kDa	816	98744
174	89	gil	3121749	O35090	-4.96	-10.8	2.79	2	1	RecName: Full=Serum albumin; Flags: Precursor	68.9 kDa	609	902155
175	35	gil	123523	P04196	-4.47	-10.69	3.81	2	2	RecName: Full=Histidine-rich glycoprotein; AltName: Full=Histidine-proline-rich glycoprotein; Short=HPRG; Flags: Precursor	59.6 kDa	525	752799
176	11	gil	74996492	Q54DC8	-3.73	-10.38	0.9	1	1	RecName: Full=Probable serine/threonine-protein kinase DDB_G0292350	139.0 kDa	1224	232943
177	54	gil	141451	P20188	-3.38	-10.21	3.8	1	1	RecName: Full=Uncharacterized 44.4 kDa protein in transposon Tn4556	44.4 kDa	395	799642
178	92	gil	13124752	Q02985	-3	-9.86	3.03	1	1	RecName: Full=Complement factor H-related protein 3; Short=FHR-3; AltName: Full=H factor-like protein 3; AltName: Full=DOWN16; Flags: Precursor	37.3 kDa	330	903841
179	139	gil	59797484	Q99J86	-3.63	-9.82	1.12	1	1	RecName: Full=Attractin; AltName: Full=Protein zitter; Flags: Precursor	158.7 kDa	1432	1006713
180	216	gil	62510978	Q5JHM9	-3.14	-9.77	3.55	1	1	RecName: Full=Aspartate carbamoyltransferase; AltName: Full=Aspartate transcarbamylase; Short=ATCase	34.7 kDa	310	1411318
181	129	gil	22256985	Q8U373	-3.14	-9.75	3.57	1	1	RecName: Full=Aspartate carbamoyltransferase; AltName: Full=Aspartate transcarbamylase; Short=ATCase	34.7 kDa	308	991289
182	6	gil	74638644	Q9P3T4	-2.89	-9.73	11.23	1	1	RecName: Full=Translation machinery-associated protein 22	20.8 kDa	187	33147
183	19	gil	2499404	P77918	-3.14	-9.62	3.57	1	1	RecName: Full=Aspartate carbamoyltransferase; AltName: Full=Aspartate transcarbamylase; Short=ATCase	34.9 kDa	308	724928
184	91	gil	130509	P29152	-3.98	-9.07	0.37	1	1	RecName: Full=Genome polyprotein; Contains: RecName: Full=P1 proteinase; AltName: Full=N-terminal protein; Contains: RecName: Full=Helper component proteinase; Short=HC-pro; Contains: RecName: Full=Protein P3; Contains: RecName: Full=6 kDa protein 1; Short=6K1; Contains: RecName: Full=Cytoplasmic inclusion protein; Short=CI; Contains: RecName: Full=6 kDa protein 2; Short=6K2; Contains: RecName: Full=Viral genome-linked protein; AltName: Full=VPg; Contains: RecName: Full=Nuclear inclusion protein A; Short=NI-a; Short=NIa; AltName: Full=NIa-pro; AltName: Full=49 kDa proteinase; Short=49 kDa-Pro; Contains: RecName: Full=Nuclear inclusion protein B; Short=NI-b; Short=NIb; AltName: Full=RNA-directed RNA polymerase; Contains: RecName: Full=Coat protein; Short=CP	364.3 kDa	3206	902732

185	307	gi|166229928	A8F062	-3.18	-8.9	4.98	1	1	RecName: Full=Trigger factor; Short=TF	50.8 kDa	442	3320674
186	16	gi|116144	P23013	-2.87	-8.84	3.79	1	1	RecName: Full=Protein cfxQ	35.1 kDa	317	721529
187	188	gi|28558077	Q9XF89	-2.75	-8.79	7.5	1	1	RecName: Full=Chlorophyll a-b binding protein CP26, chloroplastic; AltName: Full=Light-harvesting complex II protein 5; AltName: Full=LHCB5; AltName: Full=LHCIIc; Flags: Precursor	30.2 kDa	280	1122911
188	235	gi|74750885	Q8N1A0	-2.8	-8.31	3.05	1	1	RecName: Full=Keratin-like protein KRT222; AltName: Full=Keratin-222; AltName: Full=Keratin-222 pseudogene	34.2 kDa	295	1603893
189	66	gi|1350848	P47767	-4.99	-8.2	0.69	2	1	RecName: Full=DNA-directed RNA polymerase subunit beta; Short=RNAP subunit beta; AltName: Full=Transcriptase subunit beta; AltName: Full=RNA polymerase subunit beta	146.5 kDa	1302	825847
190	51	gi|20178281	P02747	-2.47	-8.18	4.9	1	1	RecName: Full=Complement C1q subcomponent subunit C; Flags: Precursor	25.8 kDa	245	794335
191	246	gi|81891699	Q6IG02	-3.01	-8.03	1.61	1	1	RecName: Full=Keratin, type II cytoskeletal 2 epidermal; AltName: Full=Cytokeratin-2e; Short=CK 2e; Short=K2e; Short=keratin-2; AltName: Full=Type II keratin Kb2	69.1 kDa	685	1801906
192	210	gi|75041620	Q5R8S9	-2.8	-7.84	2.25	1	1	RecName: Full=Keratin, type I cytoskeletal 19; AltName: Full=Cytokeratin-19; Short=CK-19; AltName: Full=Keratin-19; Short=K19	44.1 kDa	400	1365161
193	358	gi|206558253	Q3TD16	-2.94	-7.84	1.85	1	1	RecName: Full=Uncharacterized protein C13orf18 homolog	72.3 kDa	648	6937339
194	15	gi|189043559	A1VK39	-2.32	-7.81	8.25	1	1	RecName: Full=Imidazoleglycerol-phosphate dehydratase; Short=IGPD	22.2 kDa	206	557334
195	176	gi|464693	P33395	-2.33	-7.66	12.67	1	1	RecName: Full=Protein rrf2	16.7 kDa	150	1105534
196	234	gi|75246487	Q8LPF1	-2.99	-7.62	2.4	1	1	RecName: Full=Pentatricopeptide repeat-containing protein At5g15980, mitochondrial; Flags: Precursor	75.3 kDa	668	1603116
197	151	gi|2497269	Q99456	-2.76	-7.56	1.82	1	1	RecName: Full=Keratin, type I cytoskeletal 12; AltName: Full=Cytokeratin-12; Short=CK-12; AltName: Full=Keratin-12; Short=K12	53.5 kDa	494	1044884
198	217	gi|82195557	Q5K2P2	-2.76	-7.47	2.04	1	1	RecName: Full=Keratin, type I cytoskeletal 15; AltName: Full=Cytokeratin-15; Short=CK-15; AltName: Full=Keratin-15; Short=K15	48.9 kDa	441	1413126
199	366	gi|226706245	Q54QG5	-3.76	-7.44	0.17	1	1	RecName: Full=Probable E3 ubiquitin-protein ligase DDB_G0283893	658.2 kDa	5875	8211650
200	266	gi|123555922	Q31IH6	-2.51	-7.27	4	1	1	RecName: Full=Erythronate-4-phosphate dehydrogenase	42.2 kDa	375	2086038
201	1	gi|88942920	P0AA30	-1.96	-6.83	11.01	1	1	RecName: Full=Thioredoxin-1; Short=Trx-1	11.8 kDa	109	2985
202	282	gi|81916943	Q9D1G5	-2.33	-6.79	3.77	1	1	RecName: Full=Leucine-rich repeat-containing protein 57	26.8 kDa	239	2599340
203	223	gi|123728636	Q38W64	-2.38	-6.66	3.79	1	1	RecName: Full=30S ribosomal protein S2	29.9 kDa	264	1487180
204	361	gi|229470721	B6YQ95	-2.79	-6.55	1.85	1	1	RecName: Full=Threonyl-tRNA synthetase; AltName: Full=Threonine--tRNA ligase; Short=ThrRS	75.2 kDa	648	7200454
205	304	gi|81910015	Q5RJ54	-2.62	-6.43	2.79	1	1	RecName: Full=Zinc finger protein 187; AltName: Full=Zinc finger and SCAN domain-containing protein 26	53.5 kDa	466	3057847
206	200	gi|74610271	Q6FU05	-2.52	-6.41	4.36	1	1	RecName: Full=Ribosome biogenesis protein NSA1	49.4 kDa	436	1298105
207	62	gi|3024799	Q80910	-2.56	-6.31	3.17	1	1	RecName: Full=Regulatory protein E2	49.7 kDa	441	809480
208	352	gi|226707753	B0BUE2	-1.54	-6.05	26.03	1	1	RecName: Full=UPF0352 protein APJL_0577	8.0 kDa	73	5675779
209	7	gi|167016716	A3MZV0	-1.54	-6.05	26.03	1	1	RecName: Full=UPF0352 protein APL_0584	7.9 kDa	73	91999
210	95	gi|6686299	Q14525	-2.34	-6	1.73	1	1	RecName: Full=Keratin, type I cuticular Ha3-II; AltName: Full=Hair keratin, type I Ha3-II; AltName: Full=Keratin-33B; Short=K33B	46.2 kDa	404	909197
211	88	gi|46397807	O76014	-2.34	-5.93	1.56	1	1	RecName: Full=Keratin, type I cuticular Ha7; AltName: Full=Hair keratin, type I Ha7; AltName: Full=Keratin-37; Short=K37	49.7 kDa	449	899973
212	59	gi|3183065	Q62168	-2.34	-5.93	1.72	1	1	RecName: Full=Keratin, type I cuticular Ha2; AltName: Full=Hair keratin, type I Ha2; AltName: Full=Keratin-32; Short=K32	46.4 kDa	407	807100
213	76	gi|125090	P02534	-2.34	-5.84	1.7	1	1	RecName: Full=Keratin, type I microfibrillar 48 kDa, component 8C-1; AltName: Full=Low-sulfur keratin	46.7 kDa	412	859786
214	125	gi|57012974	Q9JL16	-2.11	-5.83	6.67	1	1	RecName: Full=Interferon-stimulated gene 20 kDa protein; AltName: Full=Promyelocytic leukemia nuclear body-associated protein ISG20; AltName: Full=DnaQL protein	32.5 kDa	300	983676
215	86	gi|125070	P08777	-2.34	-5.66	1.63	1	1	RecName: Full=Keratin, type I cytoskeletal 47 kDa	47.2 kDa	429	894783
216	49	gi|125072	P05781	-2.34	-5.63	1.67	1	1	RecName: Full=Keratin, type I cytoskeletal 47 kDa	45.7 kDa	419	789292
217	87	gi|125083	P05783	-2.34	-5.41	1.63	1	1	RecName: Full=Keratin, type I cytoskeletal 18; AltName: Full=Cytokeratin-18; Short=CK-18; AltName: Full=Keratin-18; Short=K18; AltName: Full=Cell proliferation-inducing gene 46 protein	48.1 kDa	430	896230
218	85	gi|148886614	P05784	-2.34	-5.39	1.65	1	1	RecName: Full=Keratin, type I cytoskeletal 18; AltName: Full=Cytokeratin-18; Short=CK-18; AltName: Full=Keratin-18; Short=K18; AltName: Full=Cytokeratin endo B; Short=Keratin D	47.5 kDa	423	894113
219	38	gi|2506872	P02751	-2.77	-5.06	0.54	1	1	RecName: Full=Fibronectin; Short=FN; AltName: Full=Cold-insoluble globulin; Short=CIG; Contains: RecName: Full=Ugl-Y1; Contains: RecName: Full=Ugl-Y2; Contains: RecName: Full=Ugl-Y3; Flags: Precursor	262.6 kDa	2386	756068
220	365	gi|218512156	P07589	-2.77	-4.99	0.52	1	1	RecName: Full=Fibronectin; Short=FN; Flags: Precursor	272.2 kDa	2478	7474835
221	5	gi|73622062	Q5HWB9	-2.14	-4.97	5.61	1	1	RecName: Full=Tryptophan synthase beta chain	42.9 kDa	392	29863
222	198	gi|38372875	P11276	-2.77	-4.93	0.52	1	1	RecName: Full=Fibronectin; Short=FN; Flags: Precursor	272.5 kDa	2477	1200482
223	149	gi|120178	P04937	-2.77	-4.92	0.52	1	1	RecName: Full=Fibronectin; Short=FN; Flags: Precursor	272.5 kDa	2477	1042187
224	48	gi|3334344	O42816	-2.2	-4.73	3.6	1	1	RecName: Full=Signal recognition particle 54 kDa protein homolog	60.7 kDa	556	783826
225	348	gi|189046141	A8AYT8	-2.62	-4.59	4.72	2	1	RecName: Full=Segregation and condensation protein A	27.4 kDa	233	5238110

226	316	gi|189083578	A4SWP6	-2.08	-4.46	6.19	1	1	RecName: Full=Seryl-tRNA synthetase; AltName: Full=Seryl-tRNA(Ser/Sec) synthetase; AltName: Full=Serine--tRNA ligase; Short=SerRS	48.3 kDa	436	3782228
227	25	gi|42558855	Q8JH64	-3.56	-4.37	1.83	2	1	RecName: Full=Tyrosine-protein kinase BTK; AltName: Full=Bruton tyrosine kinase	75.9 kDa	657	737591
228	50	gi|75309179	Q9FLF0	-1.89	-4.33	8.12	1	1	RecName: Full=40S ribosomal protein S9-2	23.2 kDa	197	792124
229	166	gi|1168777	P42155	-1.19	-4.31	8.09	1	1	RecName: Full=Kappa-casein	14.9 kDa	136	1071523
230	317	gi|166198471	A0KXW8	-1.81	-4.26	3.04	1	1	RecName: Full=D-alanine--D-alanine ligase; AltName: Full=D-alanylalanine synthetase; AltName: Full=D-Ala-D-Ala ligase	36.3 kDa	329	3823711
231	163	gi|2493503	Q95146	-1.19	-4.2	8.94	1	1	RecName: Full=Kappa-casein	13.3 kDa	123	1063151
232	146	gi|2493504	Q95147	-1.19	-4.2	9.02	1	1	RecName: Full=Kappa-casein	13.2 kDa	122	1037037
233	196	gi|41018298	Q7VBX6	-2.29	-4.2	1.43	1	1	RecName: Full=Phenylalanyl-tRNA synthetase beta chain; AltName: Full=Phenylalanine--tRNA ligase beta chain; Short=PheRS	93.7 kDa	837	1156056
234	273	gi|215274016	P19012	-1.96	-4.05	2.63	1	1	RecName: Full=Keratin, type I cytoskeletal 15; AltName: Full=Cytokeratin-15; Short=CK-15; AltName: Full=Keratin-15; Short=K15	49.2 kDa	456	2388799
235	254	gi|81680610	Q601F2	-1.51	-4	14.14	1	1	RecName: Full=50S ribosomal protein L21	11.3 kDa	99	1841180
236	258	gi|122064997	Q4AAK2	-1.51	-4	14.14	1	1	RecName: Full=50S ribosomal protein L21	11.2 kDa	99	1975632
237	293	gi|81691674	Q6IFU8	-1.99	-3.98	3	1	1	RecName: Full=Keratin, type I cytoskeletal 17; AltName: Full=Cytokeratin-17; Short=CK-17; AltName: Full=Keratin-17; AltName: Full=Type I keratin Ka17	48.1 kDa	433	2890711
238	278	gi|6016411	P13646	-1.96	-3.97	2.62	1	1	RecName: Full=Keratin, type I cytoskeletal 13; AltName: Full=Cytokeratin-13; Short=CK-13; AltName: Full=Keratin-13; Short=K13	49.6 kDa	458	2507778
239	264	gi|160395544	A1L595	-1.99	-3.92	2.95	1	1	RecName: Full=Keratin, type I cytoskeletal 17; AltName: Full=Cytokeratin-17; Short=CK-17; AltName: Full=Keratin-17; Short=K17	48.7 kDa	441	2048502
240	192	gi|116596	P12247	-2.13	-3.82	1.65	1	1	RecName: Full=Complement C3 alpha chain	81.8 kDa	726	1126269
241	72	gi|13431670	Q62774	-3.75	-3.77	2.49	2	1	RecName: Full=Myosin-Ia; AltName: Full=Brush border myosin I; Short=BBM-I; Short=BBMI; AltName: Full=Myosin I heavy chain; Short=MIHC	97.2 kDa	842	848011
242	103	gi|22095702	P58962	-1.82	-3.61	2.53	1	1	RecName: Full=Putative gustatory receptor 58a	46.3 kDa	395	918179
243	107	gi|48428497	Q9VEZ5	-2.14	-3.56	1.6	1	1	RecName: Full=Inhibitor of nuclear factor kappa-B kinase subunit beta; Short=DmIKK-beta; AltName: Full=Immune response deficient protein 5; AltName: Full=IKK-like protein; AltName: Full=Lipopolysaccharide-activated kinase; Short=DLAK; AltName: Full=Cactus kinase IKK	86.4 kDa	751	924279
244	32	gi|2497229	Q04898	-1.15	-3.48	10.48	1	1	RecName: Full=Putative uncharacterized protein YMR321C	11.6 kDa	105	748293
245	4	gi|74860359	Q86A05	-1.46	-3.47	10.71	1	1	RecName: Full=Putative acetyltransferase DDB_G0275507	21.5 kDa	196	19750
246	277	gi|146886594	Q9HG11	-1.63	-3.39	2.41	1	1	RecName: Full=Mitogen-activated protein kinase mpkC; Short=MAP kinase C	47.0 kDa	415	2504350
247	194	gi|47117453	Q7UA73	-1.04	-3.29	15.04	1	1	RecName: Full=UPF0133 protein SYNW0027	12.0 kDa	113	1129996
248	37	gi|2493509	Q28417	-1.19	-3.28	7.19	1	1	RecName: Full=Kappa-casein	17.1 kDa	153	755486
249	225	gi|82592668	Q9JM01	-1.98	-3.23	2.87	1	1	RecName: Full=Cyclin-dependent kinase-like 3; AltName: Full=Serine/threonine protein kinase NKIATRE	67.6 kDa	593	1490818
250	336	gi|193805956	A4GGB9	-1.62	-3.2	4.38	1	1	RecName: Full=Apocytochrome f; Flags: Precursor	35.4 kDa	320	4455502
251	74	gi|13432029	P47807	-3.75	-3.13	2.01	2	1	RecName: Full=Myosin-Ia; AltName: Full=Brush border myosin I; Short=BBM-I; Short=BBMI; AltName: Full=Myosin I heavy chain; Short=MIHC	119.3 kDa	1045	855376
252	69	gi|60416426	Q9UKT5	-1.61	-3.1	2.33	1	1	RecName: Full=F-box only protein 4	44.1 kDa	387	827164
253	184	gi|115667	P02668	-1.19	-3.09	5.79	1	1	RecName: Full=Kappa-casein; Contains: RecName: Full=Casoxin-C; Contains: RecName: Full=Casoxin-6; Contains: RecName: Full=Casoxin-A; Contains: RecName: Full=Casoxin-B; Contains: RecName: Full=Casoplatelin; Flags: Precursor	21.3 kDa	190	1121002
254	186	gi|127757	P10568	-3.75	-3.06	2.01	2	1	RecName: Full=Myosin-Ia; AltName: Full=Brush border myosin I; Short=BBM-I; Short=BBMI; AltName: Full=Myosin I heavy chain; Short=MIHC; AltName: Full=Brush border 110 kDa protein	118.9 kDa	1043	1121436
255	305	gi|93140695	Q2UB3	-2.02	-3.02	1.75	1	1	RecName: Full=Phenylalanyl-tRNA synthetase beta chain; AltName: Full=Phenylalanine--tRNA ligase beta chain; Short=PheRS	84.2 kDa	800	3109886
256	252	gi|152031641	O88329	-3.75	-2.95	2.01	2	1	RecName: Full=Myosin-Ia; AltName: Full=Brush border myosin I; Short=BBM-I; Short=BBMI; AltName: Full=Myosin I heavy chain; Short=MIHC	118.7 kDa	1043	1819768
257	63	gi|73619730	Q9V302	-1.54	-2.94	4.05	1	1	RecName: Full=CCA-adding enzyme; AltName: Full=tRNA nucleotidyltransferase; AltName: Full=tRNA adenylyl-/cytidylyl-transferase; AltName: Full=tRNA CCA-pyrophosphorylase; AltName: Full=tRNA-NT	25.5 kDa	222	812283
258	84	gi|13525213	P35228	-2.14	-2.88	1.39	1	1	RecName: Full=Nitric oxide synthase, inducible; AltName: Full=Inducible NO synthase; Short=Inducible NOS; Short=iNOS; AltName: Full=NOS type II; AltName: Full=Hepatocyte NOS; Short=HEP-NOS	131.1 kDa	1153	893424
259	227	gi|85542913	O62689	-2.14	-2.85	1.39	1	1	RecName: Full=Nitric oxide synthase, inducible; AltName: Full=Inducible NO synthase; Short=Inducible NOS; Short=iNOS; AltName: Full=NOS type II	131.8 kDa	1154	1517347
260	97	gi|39314012	O51568	-2.25	-2.79	1.33	1	1	RecName: Full=Transcription-repair-coupling factor; Short=TRCF; AltName: Full=ATP-dependent helicase mfd	130.7 kDa	1125	910879
261	349	gi|167016444	A8G7J6	-1.43	-2.71	8.48	1	1	RecName: Full=Queuosine biosynthesis protein queC	25.2 kDa	224	5286480
262	332	gi|167016446	A2BTS3	-1.43	-2.71	8.48	1	1	RecName: Full=Queuosine biosynthesis protein queC	25.0 kDa	224	4212322

268	284	gi|145559451	P48758	-1.48	-2.38	5.42	1	1	RecName: Full=Carbonyl reductase [NADPH] 1; AltName: Full=NADPH-dependent carbonyl reductase 1	30.6 kDa	277	2612683
269	71	gi|54037713	P67976	-1.19	-2.35	5.56	1	1	RecName: Full=Beta-lactoglobulin-1/B; Short=Beta-LG; Flags: Precursor	19.9 kDa	180	839491
270	312	gi|122142424	Q0VCM5	-1.89	-2.35	1.32	1	1	RecName: Full=Inter-alpha-trypsin inhibitor heavy chain H1; Short=Inter-alpha-inhibitor heavy chain 1; Short=ITI heavy chain H1; Flags: Precursor	101.2 kDa	906	3539428
271	12	gi|166982881	A0LIV4	-1.26	-2.28	6.34	1	1	RecName: Full=50S ribosomal protein L13	16.1 kDa	142	375031
272	290	gi|82190152	O57611	-1.64	-2.27	2.17	1	1	RecName: Full=Keratin, type I cytoskeletal 18; AltName: Full=Cytokeratin-18; Short=CK-18; AltName: Full=Keratin-18; Short=K18	46.8 kDa	415	2816616
273	334	gi|189028689	A6US67	-1.56	-2.26	4.04	1	1	RecName: Full=Probable molybdenum cofactor biosynthesis protein A	34.1 kDa	297	4303162
274	154	gi|125912	P02756	-1.19	-2.23	5.56	1	1	RecName: Full=Beta-lactoglobulin; Short=Beta-LG; Flags: Precursor	20.0 kDa	180	1049037
275	362	gi|215274954	B3NKZ6	-1.16	-2.2	11.03	1	1	RecName: Full=Protein Turandot E; AltName: Full=Protein Victoria; Flags: Precursor	16.1 kDa	145	7303285
276	339	gi|158514297	A4YQD3	-1.58	-2.14	2.3	1	1	RecName: Full=Ribulose bisphosphate carboxylase large chain 2; Short=RuBisCO large subunit 2	53.3 kDa	479	4617321
277	14	gi|158513273	A5EF40	-1.58	-2.14	2.3	1	1	RecName: Full=Ribulose bisphosphate carboxylase large chain 2; Short=RuBisCO large subunit 2	53.3 kDa	479	475071
278	269	gi|75056016	Q9BGM5	-1.53	-2.07	2	1	1	RecName: Full=Keratin, type I cytoskeletal 25; AltName: Full=Cytokeratin-25; Short=CK-25; AltName: Full=Keratin-25; Short=K25; AltName: Full=Type I inner root sheath-specific keratin-K25irs1; AltName: Full=Type I keratin intermediate filament IRSa1	49.3 kDa	450	2174934
279	291	gi|74723316	Q7Z3Z0	-1.53	-2.07	2	1	1	RecName: Full=Keratin, type I cytoskeletal 25; AltName: Full=Cytokeratin-25; Short=CK-25; AltName: Full=Keratin-25; Short=K25; AltName: Full=Type I inner root sheath-specific keratin-K25irs1; AltName: Full=Keratin 25A	49.3 kDa	450	2840099
280	295	gi|75052973	Q6R650	-1.53	-2.07	2	1	1	RecName: Full=Keratin, type I cytoskeletal 25; AltName: Full=Cytokeratin-25; Short=CK-25; AltName: Full=Keratin-25; Short=K25; AltName: Full=Type I inner root sheath-specific keratin-K25irs1; AltName: Full=Type I keratin intermediate filament IRSa1	49.4 kDa	450	2944904
281	263	gi|122143245	Q0P5J4	-1.53	-2.07	2	1	1	RecName: Full=Keratin, type I cytoskeletal 25; AltName: Full=Cytokeratin-25; Short=CK-25; AltName: Full=Keratin-25; Short=K25; AltName: Full=Type I inner root sheath-specific keratin-K25irs1	49.3 kDa	450	2048273
282	182	gi|1352536	P48897	-1.06	-2.02	3.01	1	1	RecName: Full=NADH-ubiquinone oxidoreductase chain 1; AltName: Full=NADH dehydrogenase subunit 1	34.4 kDa	299	1114614
283	355	gi|229488129	B3QNZ9	-1.08	-2	5.42	1	1	RecName: Full=Phosphopantetheine adenylyltransferase; AltName: Full=Pantetheine-phosphate adenylyltransferase; Short=PPAT; AltName: Full=Dephospho-CoA pyrophosphorylase	18.9 kDa	166	6477252
284	292	gi|74723314	Q7Z3Y8	-1.53	-1.99	1.96	1	1	RecName: Full=Keratin, type I cytoskeletal 27; AltName: Full=Cytokeratin-27; Short=CK-27; AltName: Full=Keratin-27; Short=K27; AltName: Full=Type I inner root sheath-specific keratin-K25irs3	49.8 kDa	459	2840120
285	296	gi|75052972	Q6R649	-1.53	-1.96	1.96	1	1	RecName: Full=Keratin, type I cytoskeletal 27; AltName: Full=Cytokeratin-27; Short=CK-27; AltName: Full=Keratin-27; Short=K27; AltName: Full=Type I inner root sheath-specific keratin-K25irs3; AltName: Full=Type I keratin intermediate filament C29	50.0 kDa	460	2944922
286	310	gi|122142499	Q148H6	-1.53	-1.93	1.94	1	1	RecName: Full=Keratin, type I cytoskeletal 28; AltName: Full=Cytokeratin-28; Short=CK-28; AltName: Full=Keratin-28; Short=K28; AltName: Full=Type I inner root sheath-specific keratin-K25irs4	50.8 kDa	464	3444953
287	255	gi|75536599	Q4UM01	-1.37	-1.88	4.9	1	1	RecName: Full=Tyrosine recombinase xerD	34.8 kDa	306	1929000
288	167	gi|61216729	Q9CJH4	-1.57	-1.86	2.36	1	1	RecName: Full=tRNA(Ile)-lysidine synthase; AltName: Full=tRNA(Ile)-lysidine synthetase; AltName: Full=tRNA(Ile)-2-lysyl-cytidine synthase	49.6 kDa	423	1076738
289	43	gi|416672	P26854	-1.55	-1.85	4.09	1	1	RecName: Full=ATP synthase subunit alpha, mitochondrial	55.4 kDa	513	768935
290	155	gi|1345987	P49066	-1.61	-1.85	1.15	1	1	RecName: Full=Alpha-fetoprotein; AltName: Full=Alpha-1-fetoprotein; AltName: Full=Alpha-fetoglobulin; Flags: Precursor	68.4 kDa	609	1050915
291	27	gi|114407	P05495	-1.55	-1.84	4.13	1	1	RecName: Full=ATP synthase subunit alpha, mitochondrial	55.2 kDa	509	738741
292	55	gi|55976783	P68542	-1.55	-1.84	4.14	1	1	RecName: Full=ATP synthase subunit alpha, mitochondrial	55.1 kDa	507	801111
293	121	gi|114403	P22201	-1.55	-1.83	4.14	1	1	RecName: Full=ATP synthase subunit alpha, mitochondrial	55.1 kDa	507	966713
294	236	gi|75054076	Q8MJ76	-1.61	-1.81	1.15	1	1	RecName: Full=Alpha-fetoprotein; AltName: Full=Alpha-1-fetoprotein; AltName: Full=Alpha-fetoglobulin; Flags: Precursor	68.6 kDa	610	1613114
295	18	gi|114419	P12862	-1.55	-1.8	4.13	1	1	RecName: Full=ATP synthase subunit alpha, mitochondrial	55.3 kDa	509	723537
296	122	gi|114404	P18260	-1.55	-1.78	4.12	1	1	RecName: Full=ATP synthase subunit alpha, mitochondrial	55.5 kDa	510	968047
297	42	gi|231585	Q01915	-1.55	-1.78	4.13	1	1	RecName: Full=ATP synthase subunit alpha, mitochondrial	55.3 kDa	508	760743
298	115	gi|114408	P05492	-1.55	-1.77	4.11	1	1	RecName: Full=ATP synthase subunit alpha, mitochondrial	55.6 kDa	511	939843
299	156	gi|543866	P05493	-1.55	-1.77	4.14	1	1	RecName: Full=ATP synthase subunit alpha, mitochondrial	55.0 kDa	507	1051806
300	40	gi|114405	P05494	-1.55	-1.76	4.13	1	1	RecName: Full=ATP synthase subunit alpha, mitochondrial	55.2 kDa	508	757017
301	260	gi|110278951	Q3SZ57	-1.61	-1.74	1.15	1	1	RecName: Full=Alpha-fetoprotein; AltName: Full=Alpha-1-fetoprotein; AltName: Full=Alpha-fetoglobulin; Flags: Precursor	68.6 kDa	610	2027266
302	173	gi|73619728	Q9HI95	-1.54	-1.71	2.09	1	1	RecName: Full=CCA-adding enzyme; AltName: Full=tRNA nucleotidyltransferase; AltName: Full=tRNA adenylyl-/cytidylyl-transferase; AltName: Full=tRNA CCA-pyrophosphorylase; AltName: Full=tRNA-NT	49.4 kDa	431	1094423
303	123	gi|75054113	Q8MJU5	-1.61	-1.71	1.15	1	1	RecName: Full=Alpha-fetoprotein; AltName: Full=Alpha-1-fetoprotein; AltName: Full=Alpha-fetoglobulin; Flags: Precursor	68.8 kDa	609	970514
304	193	gi|136406	P06871	-1.05	-1.69	4.07	1	1	RecName: Full=Cationic trypsin; Flags: Precursor	26.2 kDa	246	1127279

305	75	gi|13431984	Q83981	-1.63	-1.61	1.98	1	1	RecName: Full=2',3'-cyclic-nucleotide 2'-phosphodiesterase	57.1 kDa	504	859062			
306	159	gi|2851501	P19827	-3.02	-1.61	2.41	2	2	RecName: Full=Inter-alpha-trypsin inhibitor heavy chain H1; Short=ITI heavy chain H1; AltName: Full=Inter-alpha-trypsin inhibitor complex component III; AltName: Full=Serum-derived hyaluronan-associated protein; Short=SHAP; Flags: Precursor	101.4 kDa	911	1059516			
307	276	gi|818263B9	Q6A6M6	-1.23	-1.55	8.97	1	1	RecName: Full=50S ribosomal protein L3	23.5 kDa	223	2423366			
308	195	gi|33301608	Q821V0	-1.07	-1.47	10.07	1	1	RecName: Full=Ribonuclease P protein component; Short=RNaseP protein; Short=RNase P protein; AltName: Full=Protein C5	15.9 kDa	139	1135596			
309	152	gi|1114014	P04114	-2.41	-1.38	0.31	1	1	RecName: Full=Apolipoprotein B-100; Short=Apo B-100; Contains: RecName: Full=Apolipoprotein B-48; Short=Apo B-48; Flags: Precursor	515.6 kDa	4563	1045567			
310	350	gi|23397341	P33433	-1.23	-1.35	2.27	1	1	RecName: Full=Histidine-rich glycoprotein; AltName: Full=Histidine-proline-rich glycoprotein; Short=HPRG	44.5 kDa	396	5378998			
311	60	gi|1723702	P53270	-1.38	-1.35	3.57	1	1	RecName: Full=Uncharacterized protein YGR117C	53.4 kDa	476	808231			
312	345	gi|2058292252	A6TB47	-1.43	-1.3	2.32	1	1	RecName: Full=Alpha,alpha-trehalose-phosphate synthase [UDP-forming]; AltName: Full=Trehalose-6-phosphate synthase; AltName: Full=UDP-glucose-glucosephosphate glucosyltransferase; AltName: Full=Osmoregulatory trehalose synthesis protein A	53.8 kDa	474	5002186			
313	228	gi|123483805	Q255T8	-1.07	-1.3	10.07	1	1	RecName: Full=Ribonuclease P protein component; Short=RNaseP protein; Short=RNase P protein; AltName: Full=Protein C5	16.1 kDa	139	1528841			
314	10	gi|148841243	A2SEL8	-1.06	-1.28	6.67	1	1	RecName: Full=Undecaprenyl-diphosphatase; AltName: Full=Undecaprenyl pyrophosphate phosphatase; AltName: Full=Bacitracin resistance protein	31.0 kDa	285	175553			
315	39	gi|74583784	Q08985	-1.15	-1.23	3.38	1	1	RecName: Full=Homocysteine S-methyltransferase 2; AltName: Full=S-methylmethionine:homocysteine methyltransferase 2; Short=SMM:Hcy S-methyltransferase 2; AltName: Full=S-adenosylmethionine metabolism protein 4	36.7 kDa	325	756170			
316	204	gi|73621501	Q5Z354	-1.02	-1.17	4.46	1	1	RecName: Full=Recombination protein recR	22.0 kDa	202	1356499			
317	203	gi|75114661	Q653Z5	-1.15	-1.14	2.62	1	1	RecName: Full=Squamosa promoter-binding-like protein 11	37.3 kDa	343	1333389			
318	124	gi|55584014	Q9Y6Y8	-1.58	-1.12	1.2	1	1	RecName: Full=SEC23-interacting protein; AltName: Full=p125	111.1 kDa	1000	975637			
319	214	gi|71152402	Q5NVM5	-1.49	-1.09	2.97	1	1	RecName: Full=60 kDa heat shock protein, mitochondrial; AltName: Full=Heat shock protein 60; Short=HSP-60; Short=Hsp60; AltName: Full=60 kDa chaperonin; AltName: Full=Chaperonin 60; Short=CPN60; Flags: Precursor	61.0 kDa	573	1378116			
320	219	gi|123650055	Q4JSL5	-1.02	-1.04	3.6	1	1	RecName: Full=Recombination protein recR	26.6 kDa	250	1444935			
321	133	gi|137441	P25051	-1.17	-0.97	2.33	1	1	RecName: Full=Vancomycin/teicoplanin A-type resistance protein vanA; AltName: Full=VanA ligase; AltName: Full=D-alanine--D-lactate ligase	37.4 kDa	343	1001199			
322	160	gi|81861573	O89000	-3.02	-0.9	1.56	2	1	RecName: Full=Dihydropyrimidine dehydrogenase [NADP+]; Short=DHPDHase; Short=DPD; AltName: Full=Dihydrouracil dehydrogenase; AltName: Full=Dihydrothymine dehydrogenase	111.5 kDa	1025	1060724			
323	259	gi|123620503	Q46HM4	-1.1	-0.86	2.42	1	1	RecName: Full=NAD(P)H-quinone oxidoreductase chain 4; AltName: Full=NAD(P)H dehydrogenase I, chain 4; AltName: Full=NDH-1, chain 4	58.8 kDa	538	1979605			
324	333	gi|193806228	A2BZX6	-1.1	-0.82	2.42	1	1	RecName: Full=NAD(P)H-quinone oxidoreductase chain 4; AltName: Full=NAD(P)H dehydrogenase I, chain 4; AltName: Full=NDH-1, chain 4	58.8 kDa	538	4223862			
325	245	gi|81567070	Q72E02	-1.31	-0.77	2.19	1	1	RecName: Full=ATP synthase subunit alpha; AltName: Full=F-ATPase subunit alpha; AltName: Full=ATP synthase F1 sector subunit alpha	54.6 kDa	502	1799090			
326	337	gi|166973704	A4WNC4	-1.19	-0.68	2.6	1	1	RecName: Full=Flap structure-specific endonuclease	39.0 kDa	346	4581033			
327	73	gi|2494026	Q28640	-1.23	-0.64	1.71	1	1	RecName: Full=Histidine-rich glycoprotein; AltName: Full=Histidine-proline-rich glycoprotein; Short=HPRG; Flags: Precursor	58.9 kDa	526	852348			
328	108	gi|28380018	Q8ZYN2	-1.19	-0.62	2.6	1	1	RecName: Full=Flap structure-specific endonuclease	39.1 kDa	346	924784			
329	164	gi|29336906	Q9B5P3	-1.23	-0.61	5.23	1	1	RecName: Full=Glucose-1-phosphate adenylyltransferase; AltName: Full=ADP-glucose synthase; AltName: Full=ADP-glucose pyrophosphorylase; Short=ADPGlc PPase	47.0 kDa	421	1067217			
330	330	gi|166973706	A1RSC7	-1.19	-0.61	2.6	1	1	RecName: Full=Flap structure-specific endonuclease	39.3 kDa	346	4063083			
331	268	gi|401244	Q01477	-1.54	-0.6	1.21	1	1	RecName: Full=Ubiquitin carboxyl-terminal hydrolase 3; AltName: Full=Ubiquitin thioesterase 3; AltName: Full=Ubiquitin-specific-processing protease 3; AltName: Full=Deubiquitinating enzyme 3	101.9 kDa	912	2168525			
332	2	gi|74660417	Q86AC8	-1.99	-0.57	0.46	1	1	RecName: Full=Myosin-G heavy chain	386.9 kDa	3446	4762			
333	9	gi|74702478	Q4PB56	-1.39	-0.48	2.41	1	1	RecName: Full=Glycylpeptide N-tetradecanoyltransferase; AltName: Full=Peptide N-myristoyltransferase; AltName: Full=Myristoyl-CoA:protein N-myristoyltransferase; Short=NMT	77.6 kDa	706	131814			
334	199	gi|57012654	Q60G85	-1.14	-0.26	1.43	1	1	RecName: Full=Dihydropyrimidinase 1	53.5 kDa	489	1209437			
335	20	gi|74733576	Q9H3R5	-1.02	-0.22	4.05	1	1	RecName: Full=Centromere protein H; Short=CENP-H; AltName: Full=Interphase centromere complex protein 35	28.5 kDa	247	727128			
336	202	gi|57015267	Q63150	-1.14	0.04	1.35	1	1	RecName: Full=Dihydropyrimidinase; Short=DHPase; Short=DHP; AltName: Full=Dihydropyrimidine amidohydrolase; AltName: Full=Hydantoinase	56.8 kDa	519	1332805			
337	30	gi|21362535	Q9EQF5	-1.14	0.06	1.35	1	1	RecName: Full=Dihydropyrimidinase; Short=DHPase; Short=DHP; AltName: Full=Dihydropyrimidine amidohydrolase; AltName: Full=Hydantoinase	56.7 kDa	519	742679			
338	302	gi|75253365	Q65X23	-1.2	0.06	1.61	1	1	RecName: Full=Probable serine/threonine-protein kinase WNK2; Short=OsWNK2; AltName: Full=Protein kinase with no lysine 2; AltName: Full=Protein DISEASE RELATIVE SIGNAL 1	70.1 kDa	621	3028679			

339	329	gi|116248529	Q5VUJ6	-1.31	0.09	1.31	1	1	RecName: Full=Leucine-rich repeat and calponin homology domain-containing protein 2	84.6 kDa	765	4034887
340	286	gi|75174149	Q9LFM6	-1.25	0.11	2.16	1	1	RecName: Full=Pentatricopeptide repeat-containing protein At5g11310, mitochondrial; Flags: Precursor	68.3 kDa	602	2642665
341	175	gi|1352384	P11598	-1.19	0.18	3.37	1	1	RecName: Full=Protein disulfide-isomerase A3; AltName: Full=Disulfide isomerase ER-60; AltName: Full=ERp60; AltName: Full=58 kDa microsomal protein; AltName: Full=p58; AltName: Full=ERp57; AltName: Full=HIP-70; AltName: Full=Q-2; Flags: Precursor	56.6 kDa	505	1103394
342	279	gi|119367677	Q1QIR5	-1.28	0.21	1.74	1	1	RecName: Full=UvrABC system protein C; Short=Protein uvrC; AltName: Full=Excinuclease ABC subunit C	75.9 kDa	690	2527581
343	45	gi|6225816	O04015	-1.25	0.29	1.67	1	1	RecName: Full=Delta-1-pyrroline-5-carboxylate synthetase; Short=P5CS; Includes: RecName: Full=Glutamate 5-kinase; Short=GK; AltName: Full=Gamma-glutamyl kinase; Includes: RecName: Full=Gamma-glutamyl phosphate reductase; Short=GPR; AltName: Full=Glutamate-5-semialdehyde dehydrogenase; AltName: Full=Glutamyl-gamma-semialdehyde dehydrogenase	77.4 kDa	717	778656
344	187	gi|6226296	Q9ZDW2	-1.25	0.31	2.27	1	1	RecName: Full=UvrABC system protein B; Short=Protein uvrB; AltName: Full=Excinuclease ABC subunit B	75.9 kDa	662	1121828
345	148	gi|12644629	P75493	-1.35	0.35	2.64	1	1	RecName: Full=Uncharacterized lipoprotein MPN_284; Flags: Precursor	87.2 kDa	794	1041765
346	179	gi|62900709	Q9H6R4	-1.34	0.46	1.05	1	1	RecName: Full=Nucleolar protein 6; AltName: Full=Nucleolar RNA-associated protein; Short=Nrap	127.6 kDa	1146	1110821
347	119	gi|123687	P10961	-1.19	0.47	3.12	1	1	RecName: Full=Heat shock factor protein; Short=HSF; AltName: Full=Heat shock transcription factor; Short=HSTF	93.3 kDa	833	960135
348	53	gi|229463048	Q14624	-1.23	0.62	1.29	1	1	RecName: Full=Inter-alpha-trypsin inhibitor heavy chain H4; Short=Inter-alpha-inhibitor heavy chain 4; Short=ITI heavy chain H4; AltName: Full=Inter-alpha-trypsin inhibitor family heavy chain-related protein; Short=IHRP; AltName: Full=Plasma kallikrein sensitive glycoprotein 120; Short=PK-120; Short=GP120; Contains: RecName: Full=70 kDa inter-alpha-trypsin inhibitor heavy chain H4; Contains: RecName: Full=35 kDa inter-alpha-trypsin inhibitor heavy chain H4; Flags: Precursor	103.4 kDa	930	799573
349	120	gi|1351266	P16154	-1.71	0.66	0.74	1	1	RecName: Full=Toxin A	308.1 kDa	2710	964061
350	218	gi|81305979	Q4UVY7	-1.15	0.69	1.74	1	1	RecName: Full=Chaperone protein htpG; AltName: Full=Heat shock protein htpG; AltName: Full=High temperature protein G	70.8 kDa	634	1430030
351	221	gi|88909155	Q3BS21	-1.15	0.69	1.74	1	1	RecName: Full=Chaperone protein htpG; AltName: Full=Heat shock protein htpG; AltName: Full=High temperature protein G	70.9 kDa	634	1484324
352	98	gi|23821706	Q8P855	-1.15	0.69	1.74	1	1	RecName: Full=Chaperone protein htpG; AltName: Full=Heat shock protein htpG; AltName: Full=High temperature protein G	70.8 kDa	634	910954
353	118	gi|23821708	Q8PJK3	-1.15	0.69	1.74	1	1	RecName: Full=Chaperone protein htpG; AltName: Full=Heat shock protein htpG; AltName: Full=High temperature protein G	70.8 kDa	634	951596
354	226	gi|116256803	Q2P2U8	-1.15	0.69	1.74	1	1	RecName: Full=Chaperone protein htpG; AltName: Full=Heat shock protein htpG; AltName: Full=High temperature protein G	70.9 kDa	634	1510876
355	353	gi|229553902	B1MTG4	-1.49	0.81	1	1	1	RecName: Full=Cingulin	135.6 kDa	1198	6053303
356	205	gi|62906865	P32744	-1.34	0.81	1.18	1	1	RecName: Full=Protein CLASP-2	112.3 kDa	1020	1357363
357	267	gi|94730430	P47264	-1.37	0.91	1.16	1	1	RecName: Full=Uncharacterized ATP-dependent helicase MG018	119.7 kDa	1031	2133961
358	28	gi|134083	P21328	-1.22	1.01	1.2	1	1	RecName: Full=RNA-directed DNA polymerase from mobile element jockey; AltName: Full=Reverse transcriptase	103.4 kDa	916	739865
359	109	gi|134082	P21329	-1.22	1.04	1.2	1	1	RecName: Full=RNA-directed DNA polymerase from mobile element jockey; AltName: Full=Reverse transcriptase	103.5 kDa	916	929207
360	303	gi|74744048	Q5SY80	-1.08	1.08	2	1	1	RecName: Full=Uncharacterized protein C1orf101; Flags: Precursor	109.7 kDa	951	3053168
361	346	gi|152013456	Q1MSJ5	-1.33	1.39	0.74	1	1	RecName: Full=Centrosome and spindle pole-associated protein 1	141.8 kDa	1221	5043817
362	222	gi|78099779	P49194	-1.06	1.4	1.05	1	1	RecName: Full=Retinol-binding protein 3; AltName: Full=Interphotoreceptor retinoid-binding protein; Short=IRBP; AltName: Full=Interstitial retinol-binding protein; Flags: Precursor	134.5 kDa	1234	1485871
363	47	gi|136925	P16785	-1.17	2.71	0.54	1	1	RecName: Full=Large tegument protein	253.2 kDa	2241	783152
364	169	gi|56404951	Q9BX84	-1.04	3.3	0.54	1	1	RecName: Full=Transient receptor potential cation channel subfamily M member 6; AltName: Full=Channel kinase 2; AltName: Full=Melastatin-related TRP cation channel 6	231.7 kDa	2022	1087818
365	46	gi|13431706	Q27991	-1.14	3.41	1.01	1	1	RecName: Full=Myosin-10; AltName: Full=Myosin heavy chain 10; AltName: Full=Myosin heavy chain, non-muscle IIb; AltName: Full=Non-muscle myosin heavy chain IIb; Short=NMMHC II-b; Short=NMMHC-IIB; AltName: Full=Cellular myosin heavy chain, type B; AltName: Full=Non-muscle myosin heavy chain B; Short=NMMHC-B	229.1 kDa	1976	780878
366	354	gi|182637564	Q8NCM8	-1.07	4.81	0.63	1	1	RecName: Full=Cytoplasmic dynein 2 heavy chain 1; AltName: Full=Cytoplasmic dynein 2 heavy chain; AltName: Full=Dynein cytoplasmic heavy chain 2; AltName: Full=Dynein heavy chain isotype 1B; AltName: Full=Dynein heavy chain 11; Short=hDHC11	492.6 kDa	4307	6210494
367	213	gi|90111013	Q3ZJ90	-2.34	8.52	0.43	2	1	RecName: Full=DNA-directed RNA polymerase subunit beta"; AltName: Full=PEP; AltName: Full=Plastid-encoded RNA polymerase subunit beta"; Short=RNA polymerase subunit beta"	400.7 kDa	3462	1368714

Appendix III

APPENDIX III

Protein summary from OSSMA Browser for one excised gel spot from one wide range gel; Thesis Chapter 6

Protein Summary View for OMSSA file: Sample 2 OMSSA Output.omx

No.	Index	gi#	Accession	Sum log E-Value	Protein Score	%Coverage	#Pep	#Unique Pep	Protein Description	MW	Length	Seq ID
1	36	gi|136429	P00761	-76.14	-328.47	21.65	8	4	RecName: Full=Trypsin; Flags: Precursor	24.4 kDa	231	1114697
									RecName: Full=Anionic trypsin-1; AltName: Full=Anionic trypsin I; AltName: Full=Pretrypsinogen I; AltName: Full=Serine protease 1; Flags: Precursor	26.0 kDa	246	833996
2	19	gi|136409	P00762	-16.5	-69.79	8.13	3	1				
3	31	gi|1351907	P02769	-17.02	-60.12	5.93	3	3	RecName: Full=Serum albumin; AltName: Full=BSA; AltName: Allergen=Bos d 6; Flags: Precursor	69.3 kDa	607	1004954
4	26	gi|1351908	P49064	-14.08	-53	4.11	2	2	RecName: Full=Serum albumin; AltName: Allergen=Fel d 2; Flags: Precursor	68.7 kDa	608	917585
5	29	gi|2492797	Q28522	-14.08	-52.85	4.17	2	2	RecName: Full=Serum albumin; Flags: Precursor	67.9 kDa	600	988964
6	73	gi|190356749	A2V9Z4	-14.08	-52.81	4.11	2	2	RecName: Full=Serum albumin; Flags: Precursor	68.9 kDa	608	3388340
7	12	gi|75064626	Q5NVH5	-14.08	-52.76	4.11	2	2	RecName: Full=Serum albumin; Flags: Precursor	69.4 kDa	609	771862
8	43	gi|59803089	P48668	-12.4	-40.1	5.5	3	3	RecName: Full=Keratin, type II cytoskeletal 6C; AltName: Full=Cytokeratin-6C; Short=CK-6C; AltName: Full=K6c keratin; AltName: Full=Cytokeratin-6E; Short=CK-6E; AltName: Full=Keratin K6h	60.0 kDa	564	1616820
9	44	gi|1346344	P02538	-12.4	-40.1	5.5	3	3	RecName: Full=Keratin, type II cytoskeletal 6A; AltName: Full=Cytokeratin-6A; Short=CK-6A; AltName: Full=K6a keratin; AltName: Full=Cytokeratin-6D; Short=CK-6D; AltName: Allergen=Hom s 5	60.0 kDa	564	1659689
10	55	gi|123781839	Q4FZU2	-10.99	-39.32	3.8	2	2	RecName: Full=Keratin, type II cytoskeletal 6A; AltName: Full=Cytokeratin-6A; Short=CK-6A; AltName: Full=K6a keratin	59.2 kDa	552	1954546
11	68	gi|23993865O	P35908	-10.87	-38.7	3.29	2	2	RecName: Full=Keratin, type II cytoskeletal 2 epidermal; AltName: Full=Cytokeratin-2e; Short=CK-2e; Short=K2e; Short=keratin-2	65.4 kDa	639	2566968
12	32	gi|75038951	O62823	-7.8	-30	10.28	2	2	RecName: Full=Alpha-S1-casein; Flags: Precursor	24.3 kDa	214	1010640
13	11	gi|115646	P02662	-7.8	-29.41	10.28	2	2	RecName: Full=Alpha-S1-casein; Contains: RecName: Full=Antioxidant peptide; Flags: Precursor	24.5 kDa	214	738260
14	46	gi|123797712	Q8VED5	-8.48	-27.8	4.14	2	2	RecName: Full=Keratin, type II cytoskeletal 79; AltName: Full=Cytokeratin-79; Short=CK-79; AltName: Full=Keratin-79; Short=K79; AltName: Full=Type II keratin-38	57.6 kDa	531	1689111
15	58	gi|122135340	Q29521	-7.07	-27.08	2.58	1	1	RecName: Full=Keratin, type II cytoskeletal 7; AltName: Full=Cytokeratin-7; Short=CK-7; Short=Keratin 7; Short=K7	51.6 kDa	466	2049513
16	80	gi|2152753331	A5A6M6	-7.07	-26.96	1.88	1	1	RecName: Full=Keratin, type II cytoskeletal 1; AltName: Full=Cytokeratin-1; Short=CK-1; AltName: Full=Keratin-1; Short=K1	65.5 kDa	637	4654833
17	78	gi|23805406	P04264	-7.07	-26.92	1.86	1	1	RecName: Full=Keratin, type II cytoskeletal 1; AltName: Full=Cytokeratin-1; Short=CK-1; AltName: Full=Keratin-1; Short=K1; AltName: Full=67 kDa cytokeratin; AltName: Full=Hair alpha protein	66.0 kDa	644	3991702
18	16	gi|60416436	P50446	-7.07	-26.92	2.17	1	1	RecName: Full=Keratin, type II cytoskeletal 6A; AltName: Full=Cytokeratin-6A; Short=CK-6A; AltName: Full=K6a keratin; AltName: Full=Keratin-6 alpha; Short=mK6-alpha	59.3 kDa	553	801795
19	54	gi|75062316	Q5XQN5	-7.07	-26.91	2	1	1	RecName: Full=Keratin, type II cytoskeletal 5; AltName: Full=Cytokeratin-5; Short=CK-5; AltName: Full=Keratin-5; Short=K5	62.9 kDa	601	1840953
20	64	gi|81170668	Q922U2	-7.07	-26.91	2.07	1	1	RecName: Full=Keratin, type II cytoskeletal 5; AltName: Full=Cytokeratin-5; Short=CK-5; AltName: Full=Keratin-5; Short=K5	61.8 kDa	580	2380372
21	69	gi|81896062	Q8BGZ7	-7.07	-26.89	2.18	1	1	RecName: Full=Keratin, type II cytoskeletal 75; AltName: Full=Cytokeratin-75; Short=CK-75; AltName: Full=Keratin-75; Short=K75; AltName: Full=Type II keratin-18; AltName: Full=Type II keratin-KBhf; AltName: Full=Keratin-6 hair follicle; Short=hK6hf	59.7 kDa	551	2639418
22	66	gi|81170689	Q6P6Q2	-7.07	-26.88	2.08	1	1	RecName: Full=Keratin, type II cytoskeletal 5; AltName: Full=Cytokeratin-5; Short=CK-5; AltName: Full=Keratin-5; Short=K5	61.8 kDa	576	2402900
23	27	gi|59798479	Q9Z331	-7.07	-26.88	2.14	1	1	RecName: Full=Keratin, type II cytoskeletal 6B; AltName: Full=Cytokeratin-6B; Short=CK-6B; AltName: Full=K6b keratin; AltName: Full=Keratin-6 beta; Short=mK6-beta	60.3 kDa	562	934090
24	57	gi|122143589	Q148H7	-6.96	-26.44	2.24	1	1	RecName: Full=Keratin, type II cytoskeletal 79; AltName: Full=Cytokeratin-79; Short=CK-79; AltName: Full=Keratin-79; Short=K79	57.7 kDa	536	2047188
25	60	gi|34922442	Q93532	-6.96	-26.44	2.44	1	1	RecName: Full=Keratin, type II cytoskeletal cochlear; AltName: Full=Cytokeratin otokeratin	53.8 kDa	492	2171329
26	71	gi|74748078	Q5XKE5	-6.96	-26.43	2.24	1	1	RecName: Full=Keratin, type II cytoskeletal 79; AltName: Full=Cytokeratin-79; Short=CK-79; AltName: Full=Keratin-79; Short=K79; AltName: Full=Type II keratin-38; AltName: Full=Keratin-6-like; Short=Keratin-6L	57.8 kDa	535	2956853
27	81	gi|21626449	A5A6M8	-6.96	-26.39	2.03	1	1	RecName: Full=Keratin, type II cytoskeletal 5; AltName: Full=Cytokeratin-5; Short=CK-5; AltName: Full=Keratin-5; Short=K5	62.5 kDa	592	4654861
28	77	gi|143811411	P13647	-6.96	-26.37	2.03	1	1	RecName: Full=Keratin, type II cytoskeletal 5; AltName: Full=Cytokeratin-5; Short=CK-5; AltName: Full=Keratin-5; Short=K5; AltName: Full=58 kDa cytokeratin	62.4 kDa	590	3991701
29	79	gi|23993865I	O95678	-6.96	-26.35	2.18	1	1	RecName: Full=Keratin, type II cytoskeletal 75; AltName: Full=Cytokeratin-75; Short=CK-75; AltName: Full=Keratin-75; Short=K75; AltName: Full=Type II keratin-18; AltName: Full=Type II keratin-KBhf; AltName: Full=Keratin-6 hair follicle; Short=hK6hf	59.6 kDa	551	4082971
30	40	gi|57015267	P04653	-6.35	-25.96	4.67	1	1	RecName: Full=Alpha-S1-casein; Flags: Precursor	24.3 kDa	214	1405496
31	35	gi|416750	P18626	-6.35	-25.93	4.67	1	1	RecName: Full=Alpha-S1-casein; Short=Alpha-S1-CN; Flags: Precursor	24.3 kDa	214	1110042
32	30	gi|1708590	P51856	-5.43	-20.07	2.99	1	1	RecName: Full=Keratin, type I cytoskeletal 19; AltName: Full=Cytokeratin-19; Short=CK-19; AltName: Full=Keratin-19; Short=K19	43.8 kDa	401	996741
33	65	gi|215274016	P19012	-5.43	-20.01	2.63	1	1	RecName: Full=Keratin, type I cytoskeletal 15; AltName: Full=Cytokeratin-15; Short=CK-15; AltName: Full=Keratin-15; Short=K15	49.2 kDa	456	2388799
34	20	gi|75068787	O77727	-5.43	-19.94	2.65	1	1	RecName: Full=Keratin, type I cytoskeletal 15; AltName: Full=Cytokeratin-15; Short=CK-15; AltName: Full=Keratin-15; Short=K15	48.8 kDa	453	871196
35	67	gi|60116411	P13646	-5.43	-19.93	2.62	1	1	RecName: Full=Keratin, type I cytoskeletal 13; AltName: Full=Cytokeratin-13; Short=CK-13; AltName: Full=Keratin-13; Short=K13	49.6 kDa	468	2507778
36	63	gi|2350075	P08779	-5.43	-19.86	2.54	1	1	RecName: Full=Keratin, type I cytoskeletal 16; AltName: Full=Cytokeratin-16; Short=CK-16; AltName: Full=Keratin-16; Short=K16	51.3 kDa	473	2321437
37	39	gi|76363696	Q5XLE4	-5.6	-19.75	1.65	1	1	RecName: Full=Serum albumin; Flags: Precursor	68.5 kDa	607	1357522
38	10	gi|643794	P35747	-5.6	-19.73	1.65	1	1	RecName: Full=Serum albumin; AltName: Allergen=Equ c 3; Flags: Precursor	68.6 kDa	607	731698
39	84	gi|229463044	P02533	-5.43	-19.69	2.54	1	1	RecName: Full=Keratin, type I cytoskeletal 14; AltName: Full=Cytokeratin-14; Short=CK-14; AltName: Full=Keratin-14; Short=K14	51.6 kDa	472	8763417
40	72	gi|81891691	O61FX2	-5.43	-19.66	2.65	1	1	RecName: Full=Keratin, type I cytoskeletal 42; AltName: Full=Cytokeratin-42; Short=CK-42; AltName: Full=Keratin-42; Short=K42; AltName: Full=Type I keratin Ka22; AltName: Full=Keratin-17n	50.1 kDa	452	2973373

41	83	gi|205371736	P85295	-4.58	-18.97	12.22	1	1	RecName: Full=Serum albumin	9.7 kDa	90	6930585
42	4	gi|74585209	Q59WK2	-4.19	-18.49	20.79	1	1	RecName: Full=Ubiquitin-related modifier 1 1	11.1 kDa	101	161462
43	23	gi|2495861	Q57677	-4.58	-17.7	11.83	1	1	RecName: Full=Uncharacterized protein MJ0224	19.3 kDa	169	904465
44	18	gi|113582	P14639	-4.58	-15.05	1.81	1	1	RecName: Full=Serum albumin; Flags: Precursor	69.2 kDa	607	826943
45	70	gi|239938886	P35527	-3.86	-12.61	2.57	1	1	RecName: Full=Keratin, type I cytoskeletal 9; AltName: Full=Cytokeratin-9; Short=CK-9; AltName: Full=Keratin-9; Short=K9	62.1 kDa	623	2676343
46	41	gi|82654947	P19013	-3.92	-12.54	1.69	1	1	RecName: Full=Keratin, type II cytoskeletal 4; AltName: Full=Cytokeratin-4; Short=CK-4; Short=Keratin-4; Short=K4	57.3 kDa	534	1551602
47	61	gi|238054404	P04259	-3.92	-12.38	1.6	1	1	RecName: Full=Keratin, type II cytoskeletal 6B; AltName: Full=Cytokeratin-6B; Short=CK 6B; AltName: Full=K6b keratin	60.1 kDa	564	2202161
48	6	gi|166224506	A1ARG8	-3.57	-10.78	3.18	1	1	RecName: Full=GTP-binding protein lepA	67.2 kDa	598	381604
49	76	gi|238692140	B3E9R0	-3.57	-10.74	3.17	1	1	RecName: Full=GTP-binding protein lepA	67.2 kDa	600	3962996
50	37	gi|136406	P06871	-3.67	-10.64	4.07	2	1	RecName: Full=Cationic trypsin; Flags: Precursor	26.2 kDa	246	1127279
51	56	gi|93204556	Q3SYU6	-4.98	-10.52	6.47	3	1	RecName: Full=Calponin-2; AltName: Full=Calponin H2, smooth muscle; AltName: Full=Neutral calponin	33.4 kDa	309	2028110
52	14	gi|75055290	Q5RFN6	-4.98	-10.52	6.47	3	1	RecName: Full=Calponin-2; AltName: Full=Calponin H2, smooth muscle; AltName: Full=Neutral calponin	33.7 kDa	309	790280
53	38	gi|54036231	Q7MPS7	-3.78	-9.78	8.48	2	1	RecName: Full=DNA repair protein radC homolog	25.3 kDa	224	1144521
54	13	gi|68566154	O75365	-2.75	-9.17	11.56	1	1	RecName: Full=Protein tyrosine phosphatase type IVA 3; AltName: Full=Protein-tyrosine phosphatase 4a3; AltName: Full=Protein-tyrosine phosphatase of regenerating liver 3; Short=PRL-3; Short=PRL-R	19.5 kDa	173	786533
55	75	gi|166198471	A0KKW8	-2.73	-8.47	3.04	1	1	RecName: Full=D-alanine--D-alanine ligase; AltName: Full=D-alanylalanine synthetase; AltName: Full=D-Ala-D-Ala ligase	36.3 kDa	329	3823711
56	49	gi|123623989	Q46WU7	-3.34	-7.23	7.49	2	1	RecName: Full=Indole-3-glycerol phosphate synthase; Short=IGPS	29.0 kDa	267	1781194
57	2	gi|123749610	Q2FGJ3	-2.04	-6.36	10.81	1	1	RecName: Full=Elongation factor P; Short=EF-P	20.6 kDa	185	22838
58	15	gi|584955	Q08094	-3.03	-5.7	6.76	2	1	RecName: Full=Calponin-2; AltName: Full=Calponin H2, smooth muscle; AltName: Full=Neutral calponin	32.0 kDa	296	798886
59	5	gi|122299208	Q07ZL7	-1.66	-4.66	4.6	1	1	RecName: Full=Serine/threonine transporter sstT; AltName: Full=Na(+)/serine-threonine symporter	42.8 kDa	413	305434
60	51	gi|81891698	Q6IG00	-2.21	-4.52	1.68	1	1	RecName: Full=Keratin, type II cytoskeletal 4; AltName: Full=Cytokeratin-4; Short=CK-4; Short=Keratin-4; Short=K4; AltName: Full=Type II keratin Kb4	57.7 kDa	536	1801909
61	24	gi|74750553	Q86Y46	-2.21	-4.47	1.67	1	1	RecName: Full=Keratin, type II cytoskeletal 73; AltName: Full=Cytokeratin-73; Short=CK-73; AltName: Full=Keratin-73; Short=K73; AltName: Full=Type II keratin-36; AltName: Full=Type II inner root sheath-specific keratin-K6irs3	58.9 kDa	540	913752
62	74	gi|166198591	A1TNR1	-1.97	-3.89	3.7	1	1	RecName: Full=1-deoxy-D-xylulose-5-phosphate synthase; AltName: Full=1-deoxyxylulose-5-phosphate synthase; Short=DXP synthase; Short=DXPS	66.3 kDa	622	3537770
63	1	gi|122057634	Q556K3	-1.97	-3.79	3.82	1	1	RecName: Full=Probable flavin-containing monoamine oxidase B	53.6 kDa	471	14172
64	3	gi|122057635	Q556K4	-1.97	-3.68	3.85	1	1	RecName: Full=Probable flavin-containing monoamine oxidase C	53.1 kDa	467	24823
65	59	gi|123293234	Q2J2Q3	-1.36	-3.41	19.8	1	1	RecName: Full=50S ribosomal protein L28	10.8 kDa	101	2145981
66	7	gi|123722228	Q13EG6	-1.36	-3.41	19.8	1	1	RecName: Full=50S ribosomal protein L28	10.8 kDa	101	431563
67	8	gi|122477466	Q21BW8	-1.36	-3.31	19.8	1	1	RecName: Full=50S ribosomal protein L28	11.1 kDa	101	463883
68	45	gi|1345813	P16389	-1.72	-3.31	4.01	1	1	RecName: Full=Potassium voltage-gated channel subfamily A member 2; AltName: Full=Voltage-gated potassium channel subunit Kv1.2; AltName: Full=HBK5; AltName: Full=NGK1; AltName: Full=HUKIV	56.7 kDa	499	1678916
69	28	gi|52000925	P63141	-1.72	-3.31	4.01	1	1	RecName: Full=Potassium voltage-gated channel subfamily A member 2; AltName: Full=Voltage-gated potassium channel subunit Kv1.2; Short=MK2	56.7 kDa	499	974842
70	62	gi|66773953	Q28293	-1.72	-3.31	4.01	1	1	RecName: Full=Potassium voltage-gated channel subfamily A member 2; AltName: Full=Voltage-gated potassium channel subunit Kv1.2; AltName: Full=CSMK1	56.6 kDa	499	2207820
71	48	gi|123760553	Q47FN9	-1.3	-2.63	12.84	1	1	RecName: Full=Ribonuclease H; Short=RNase H	16.6 kDa	148	1759770
72	34	gi|29427843	Q8R0G9	-1.94	-2.19	1.82	1	1	RecName: Full=Nuclear pore complex protein Nup133; AltName: Full=Nucleoporin Nup133; AltName: Full=133 kDa nucleoporin	128.7 kDa	1155	1073812
73	82	gi|224493058	A7E8H8	-1.41	-2.07	7.64	1	1	RecName: Full=Adenylate kinase 1; Short=AK 1; AltName: Full=ATP-AMP transphosphorylase 1; AltName: Full=Adenylate kinase cytosolic and mitochondrial	29.7 kDa	275	5098223
74	25	gi|46576384	Q19289	-1.78	-1.94	3.23	1	1	RecName: Full=Intermediate filament protein ifb-1; AltName: Full=Intermediate filament protein B1; Short=IF-B1; AltName: Full=Cel IF B1	67.1 kDa	589	916658
75	21	gi|124235	P23731	-1.78	-1.93	3.23	1	1	RecName: Full=Intermediate filament protein B; Short=IF-B	67.7 kDa	589	883826
76	50	gi|91207059	Q2RGV8	-1.43	-1.68	5.19	1	1	RecName: Full=Histidinol dehydrogenase; Short=HDH	45.0 kDa	424	1785621
77	53	gi|66773802	Q6IG01	-1.53	-1.52	1.93	1	1	RecName: Full=Keratin, type II cytoskeletal 1b; AltName: Full=Cytokeratin-1B; Short=CK-1B; AltName: Full=Keratin-77; Short=K77; AltName: Full=Type II keratin Kb39	57.3 kDa	519	1801924
78	22	gi|125106	P16878	-1.53	-1.44	1.95	1	1	RecName: Full=Keratin, type II cytoskeletal; AltName: Full=XENCK55(5/6)	55.5 kDa	513	884725
79	33	gi|90110027	P05787	-1.53	-1.42	2.07	1	1	RecName: Full=Keratin, type II cytoskeletal 8; AltName: Full=Cytokeratin-8; Short=CK-8; AltName: Full=Keratin-8; Short=K8	53.7 kDa	483	1028452
80	9	gi|90110028	P11679	-1.53	-1.39	2.04	1	1	RecName: Full=Keratin, type II cytoskeletal 8; AltName: Full=Cytokeratin-8; Short=CK-8; AltName: Full=Keratin-8; Short=K8; AltName: Full=Cytokeratin endo A	54.6 kDa	490	722912
81	47	gi|75062693	Q6EIY9	-1.53	-1.38	1.62	1	1	RecName: Full=Keratin, type II cytoskeletal 1; AltName: Full=Cytokeratin-1; Short=CK-1; AltName: Full=Keratin-1; Short=K1; AltName: Full=Epithelial keratin-1	63.8 kDa	619	1743526
82	42	gi|1708592	Q10758	-1.53	-1.36	2.07	1	1	RecName: Full=Keratin, type II cytoskeletal 8; AltName: Full=Cytokeratin-8; Short=CK-8; AltName: Full=Keratin-8; Short=K8; AltName: Full=Cytokeratin endo A	54.0 kDa	483	1554875
83	52	gi|66773987	Q6IFZ6	-1.53	-1.33	1.75	1	1	RecName: Full=Keratin, type II cytoskeletal 1b; AltName: Full=Cytokeratin-1B; Short=CK-1B; AltName: Full=Keratin-77; Short=K77; AltName: Full=Type II keratin Kb39; AltName: Full=Embryonic type II keratin-1	61.4 kDa	572	1801921
84	17	gi|135838	P01267	-1.8	-0.03	0.72	1	1	RecName: Full=Thyroglobulin; Short=Tg; Flags: Precursor	303.2 kDa	2769	816716

Protein summary from OSSMA Browser for two excised gel spots pooled from two wide range gels; Thesis Chapter 6

Protein Summary View for OMSSA file: Sample_1_OMSSA_Output.omx

No.	Index	gi#	Accession	log E-Value	Protein Score	%Coverage	#Pep.	Unique Peptides	Protein Description	MW	Length	Seq ID
1	54	gi|136429	P00761	-29.97	-129.69	17.32	3	2	RecName: Full=Trypsin; Flags: Precursor	24.4 kDa	231	1114697
2	3	gi|113258	P10981	-20.73	-82.03	11.97	3	3	RecName: Full=Actin-87E	41.8 kDa	376	4237
3	4	gi|674621 13	P84183	-20.73	-82.03	11.97	3	3	RecName: Full=Actin, cytoplasmic A4	41.8 kDa	376	5088
4	7	gi|113263	P07830	-20.73	-82.03	11.97	3	3	RecName: Full=Major actin; AltName: Full=Actin-1; AltName: Full=Actin-2; AltName: Full=Actin-2-sub 1; AltName: Full=Actin-4; AltName: Full=Actin-5; AltName: Full=Actin-6; AltName: Full=Actin-7; AltName: Full=Actin-8; AltName: Full=Actin A8; AltName: Full=Actin-IEL1; AltName: Full=Actin-9; AltName: Full=Actin-11; AltName: Full=Actin-12; AltName: Full=Actin A12; AltName: Full=Actin-13; AltName: Full=Actin-14; AltName: Full=Actin-15; AltName: Full=Actin A1; AltName: Full=Actin III; AltName: Full=Actin-3a; AltName: Full=Actin-16; AltName: Full=Actin M6; AltName: Full=Actin-19; AltName: Full=Actin-20; AltName: Full=Actin-21	41.7 kDa	376	27157
5	8	gi|1703156	P49871	-20.73	-82.03	11.97	3	3	RecName: Full=Actin, muscle	41.8 kDa	376	31148
6	13	gi|7489746 6	Q55EU6	-17.07	-69.8	9.5	2	2	RecName: Full=Putative actin-23	40.0 kDa	368	236560
7	10	gi|166227347	P07829	-17.07	-69.63	9.04	2	2	RecName: Full=Actin-3; AltName: Full=Actin-3-sub 1	41.8 kDa	376	231074
8	2	gi|122057287	Q553U6	-17.07	-69.63	9.04	2	2	RecName: Full=Putative actin-22	41.7 kDa	376	4117
9	11	gi|748968847	Q54GX7	-12.44	-48.31	7.71	2	2	RecName: Full=Actin-10	41.7 kDa	376	232436
10	16	gi|1168323	P45886	-12.44	-48.31	7.71	2	2	RecName: Full=Actin-3, muscle-specific	41.8 kDa	376	720380
11	15	gi|399003	P30161	-8.77	-35.93	5.44	1	1	RecName: Full=Actin	37.2 kDa	331	719957
12	24	gi|81871239	Q8CGP6	-8.33	-35.22	14.84	1	1	RecName: Full=Histone H2A type 1-H	14.0 kDa	128	762838
13	32	gi|90101450	P0C170	-8.33	-35.18	14.62	1	1	RecName: Full=Histone H2A type 1-E	14.1 kDa	130	867331
14	30	gi|124028536	P04908	-8.33	-35.18	14.62	1	1	RecName: Full=Histone H2A type 1-B/E; AltName: Full=H2A/m; AltName: Full=H2A.2; AltName: Full=H2A/a	14.1 kDa	130	853088
15	41	gi|83268406	P0C0S8	-8.33	-35.18	14.62	1	1	RecName: Full=Histone H2A type 1; Short=H2A.1; Short=H2A/p	14.1 kDa	130	933964
16	40	gi|121978	P20671	-8.33	-35.18	14.62	1	1	RecName: Full=Histone H2A type 1-D; AltName: Full=H2A.3; AltName: Full=H2A/g	14.1 kDa	130	919712
17	33	gi|81910974	Q6GSS7	-8.33	-35.18	14.62	1	1	RecName: Full=Histone H2A type 2-A; Short=H2A.2; AltName: Full=H2a-614; AltName: Full=H2a-615	14.1 kDa	130	869790
18	27	gi|462231	P35062	-8.33	-35.18	14.73	1	1	RecName: Full=Histone H2A-III	14.0 kDa	129	790324
19	31	gi|81878911	Q8R1M2	-8.33	-35.18	14.73	1	1	RecName: Full=Histone H2A.J; Short=H2a/j	14.0 kDa	129	861362
20	25	gi|121999	P13912	-8.33	-35.18	14.73	1	1	RecName: Full=Histone H2A	14.0 kDa	129	766652
21	17	gi|122000	P02263	-8.33	-35.18	14.73	1	1	RecName: Full=Histone H2A-IV	13.9 kDa	129	721195
22	6	gi|13124683	P02574	-8.3	-33.72	4.26	1	1	RecName: Full=Actin, larval muscle; AltName: Full=Actin-79B	41.8 kDa	376	10549
23	5	gi|166227347	P07828	-8.3	-33.62	4.21	1	1	RecName: Full=Actin-18; AltName: Full=Actin-3-sub 2	42.5 kDa	380	8565
24	12	gi|748968937	Q54HF0	-8.3	-33.56	4.16	1	1	RecName: Full=Putative actin-25	43.2 kDa	385	234430
25	43	gi|25091551	Q9MZA9	-7.67	-32.04	6.49	1	1	RecName: Full=Vimentin	17.2 kDa	154	946255
26	29	gi|136409	P00762	-7.58	-30.77	8.13	2	1	RecName: Full=Anionic trypsin-1; AltName: Full=Anionic trypsin I; AltName: Full=Pretrypsinogen I; AltName: Full=Serine protease 1; Flags: Precursor	26.0 kDa	246	833996
27	22	gi|1353212	P48670	-7.67	-29.84	2.23	1	1	RecName: Full=Vimentin	51.8 kDa	448	750274
28	36	gi|136533	P09654	-7.67	-29.8	2.17	1	1	RecName: Full=Vimentin	53.1 kDa	460	892524
29	39	gi|55977767	P08670	-7.67	-29.78	2.15	1	1	RecName: Full=Vimentin	53.7 kDa	466	907032
30	51	gi|401365	P31000	-7.67	-29.78	2.15	1	1	RecName: Full=Vimentin	53.7 kDa	466	1035826
31	53	gi|136536	P20152	-7.67	-29.78	2.15	1	1	RecName: Full=Vimentin	53.7 kDa	466	1114242
32	56	gi|9753761 4	P84198	-7.67	-29.78	2.15	1	1	RecName: Full=Vimentin	53.7 kDa	466	1430952
33	73	gi|158962 63	Q5R1W8	-7.67	-29.78	2.15	1	1	RecName: Full=Vimentin	53.7 kDa	466	4654858
34	34	gi|1353213	P48674	-7.67	-29.75	2.17	1	1	RecName: Full=Vimentin	53.3 kDa	461	870302
35	48	gi|136535	P02544	-7.67	-29.74	2.15	1	1	RecName: Full=Vimentin	53.7 kDa	465	1007156
36	62	gi|912070 94	Q49135	-6.22	-26.37	13.33	1	1	RecName: Full=Galectin-1; AltName: Full=Lectin galactoside-binding soluble 1	14.7 kDa	135	1905315
37	35	gi|126177	P11762	-6.22	-26.24	13.33	1	1	RecName: Full=Galectin-1; AltName: Full=Lectin galactoside-binding soluble 1; AltName: Full=Beta-galactoside-binding lectin L-14-I; Short=Lactose-binding lectin 1; AltName: Full=S-Lac lectin 1; AltName: Full=Galaptin; AltName: Full=14 kDa lectin; AltName: Full=RL 14.5	14.9 kDa	135	871682
38	37	gi|134642 7	P48538	-6.22	-26.24	13.33	1	1	RecName: Full=Galectin-1; AltName: Full=Lectin galactoside-binding soluble 1; AltName: Full=Beta-galactoside-binding lectin L-14-I; Short=Lactose-binding lectin 1; AltName: Full=S-Lac lectin 1; AltName: Full=Galaptin; AltName: Full=14 kDa lectin	14.8 kDa	135	897438
39	50	gi|126172	P16045	-6.22	-26.24	13.33	1	1	RecName: Full=Galectin-1; AltName: Full=Lectin galactoside-binding soluble 1; AltName: Full=Beta-galactoside-binding lectin L-14-I; Short=Lactose-binding lectin 1; AltName: Full=S-Lac lectin 1; AltName: Full=Galaptin; AltName: Full=14 kDa lectin	14.9 kDa	135	1031291
40	71	gi|215274005	P13612	-5.84	-20.45	1.84	1	1	RecName: Full=Integrin alpha-4; AltName: Full=Integrin alpha-IV; AltName: Full=VLA-4; AltName: Full=CD49 antigen-like family membe D; AltName: CD antigen=CD49d; Flags: Precursor	114.9 kDa	1032	4097733

40	71	ii21527400(	P13612	-5.84	-20.45	1.84	1	1	RecName: Full=Integrin alpha-4; AltName: Full=Integrin alpha-IV; AltName: Full=VLA-4; AltName: Full=CD49 antigen-like family membe' D; AltName: CD_antigen=CD49d; Flags: Precursor	114.9 kDa	1032	4097733
41	64	ii12213534(	Q29S21	-5.17	-18.32	2.58	1	1	RecName: Full=Keratin, type II cytoskeletal 7; AltName: Full=Cytokeratin-7; Short=CK-7; Short=Keratin 7; Short=K7	51.6 kDa	466	2049513
42	72	ii21527533	A5A6M6	-5.17	-18.19	1.88	1	1	RecName: Full=Keratin, type II cytoskeletal 1; AltName: Full=Cytokeratin-1; Short=CK-1; AltName: Full=Keratin-1; Short=K1	65.5 kDa	637	4654833
43	67	ii12213218(	Q08D91	-5.17	-18.19	2.21	1	1	RecName: Full=Keratin, type II cytoskeletal 75; AltName: Full=Cytokeratin-75; Short=CK-75; AltName: Full=Keratin-75; Short=K75; AltName: Full=Type II keratin-K6hf; AltName: Full=Keratin-6 hair follicle	59.0 kDa	543	3701717
44	70	ii23805440(	P04264	-5.17	-18.16	1.86	1	1	RecName: Full=Keratin, type II cytoskeletal 1; AltName: Full=Cytokeratin-1; Short=CK-1; AltName: Full=Keratin-1; Short=K1; AltName: Full=67 kDa cytokeratin; AltName: Full=Hair alpha protein	66.0 kDa	644	3991702
45	28	ii60416436	P50446	-5.17	-18.16	2.17	1	1	RecName: Full=Keratin, type II cytoskeletal 6A; AltName: Full=Cytokeratin-6A; Short=CK-6A; AltName: Full=K6a keratin; AltName: Full=Keratin-6 alpha; Short=mK6-alpha	59.3 kDa	553	801795
46	63	ii12378183(	Q4FZU2	-5.17	-18.16	2.17	1	1	RecName: Full=Keratin, type II cytoskeletal 6A; AltName: Full=Cytokeratin-6A; Short=CK-6A; AltName: Full=K6a keratin	59.2 kDa	552	1954546
47	61	ii75062316	Q5XQN5	-5.17	-18.14	2	1	1	RecName: Full=Keratin, type II cytoskeletal 5; AltName: Full=Cytokeratin-5; Short=CK-5; AltName: Full=Keratin-5; Short=K5	62.9 kDa	601	1840953
48	66	ii81896062	Q8BGZ7	-5.17	-18.12	2.18	1	1	RecName: Full=Keratin, type II cytoskeletal 75; AltName: Full=Cytokeratin-75; Short=CK-75; AltName: Full=Keratin-75; Short=K75; AltName: Full=Type II keratin-18; AltName: Full=Type II keratin-K6hf; AltName: Full=Keratin-6 hair follicle; Short=mK6hf	59.7 kDa	551	2639418
49	65	ii81170669	Q6P6Q2	-5.17	-18.11	2.08	1	1	RecName: Full=Keratin, type II cytoskeletal 5; AltName: Full=Cytokeratin-5; Short=CK-5; AltName: Full=Keratin-5; Short=K5	61.8 kDa	576	2402900
50	42	ii59796479	Q92331	-5.17	-18.11	2.14	1	1	RecName: Full=Keratin, type II cytoskeletal 6B; AltName: Full=Cytokeratin-6B; Short=CK-6B; AltName: Full=K6b keratin; AltName: Full=Keratin-6 beta; Short=mK6-beta	60.3 kDa	562	934090
51	58	ii82654947	P19013	-5.04	-17.71	2.06	1	1	RecName: Full=Keratin, type II cytoskeletal 4; AltName: Full=Cytokeratin-4; Short=CK-4; Short=Keratin-4; Short=K4	57.3 kDa	534	1551602
52	52	ii81906177	Q9DCV7	-5.04	-17.71	2.41	1	1	RecName: Full=Keratin, type II cytoskeletal 7; AltName: Full=Cytokeratin-7; Short=CK-7; Short=Keratin 7; Short=K7	50.7 kDa	457	1039159
53	47	gi|125112	P06776	-5.04	-17.66	2.19	1	1	RecName: Full=Keratin, type II cytoskeletal 8; AltName: Full=Cytokeratin-8; Short=CK-8; AltName: Full=Keratin-8; Short=K8	55.7 kDa	502	1004295
54	49	ii90110027	P05787	-5.04	-17.61	2.28	1	1	RecName: Full=Keratin, type II cytoskeletal 8; AltName: Full=Cytokeratin-8; Short=CK-8; AltName: Full=Keratin-8; Short=K8	53.7 kDa	483	1028452
55	59	gi|1708592	Q10758	-5.04	-17.55	2.28	1	1	RecName: Full=Keratin, type II cytoskeletal 8; AltName: Full=Cytokeratin-8; Short=CK-8; AltName: Full=Keratin-8; Short=K8; AltName: Full=Cytokeratin endo A	54.0 kDa	483	1554875
56	21	ii48475043	Q9Z2T6	-5.04	-17.54	2.17	1	1	RecName: Full=Keratin, type II cuticular Hb5; AltName: Full=Type II hair keratin Hb5; AltName: Full=Keratin-85; Short=K85	55.8 kDa	507	736387
57	44	gi|121135	P14136	-5.04	-17.54	2.55	1	1	RecName: Full=Glial fibrillary acidic protein; Short=GFAP	49.9 kDa	432	949293
58	55	ii75061841	Q5RAY2	-5.04	-17.54	2.55	1	1	RecName: Full=Glial fibrillary acidic protein; Short=GFAP	49.9 kDa	432	1365837
59	46	gi|124740	P18520	-5.04	-17.53	2.12	1	1	RecName: Full=Intermediate filament protein ON3	57.8 kDa	520	1003988
60	60	ii81892069	Q6NXH9	-5.04	-17.45	2.04	1	1	RecName: Full=Keratin, type II cytoskeletal 73; AltName: Full=Cytokeratin-73; Short=CK-73; AltName: Full=Keratin-73; Short=K73; AltName: Full=Type II keratin-36; AltName: Full=Type II inner root sheath-specific keratin-K6irs3	58.9 kDa	539	1745820
61	69	ii11937136(	Q2RNY6	-4.02	-12.88	3.16	1	1	RecName: Full=GTP-binding protein lepA	66.4 kDa	601	3989128
62	20	gi|113284	Q00214	-3.67	-12.4	2.9	1	1	RecName: Full=Actin, muscle	42.4 kDa	379	734706
63	18	gi|1168320	P45885	-3.67	-12.4	2.93	1	1	RecName: Full=Actin-2, muscle-specific	41.8 kDa	376	723646
64	1	ii12205740(	Q55458	-3.67	-12.35	2.94	1	1	RecName: Full=Actin-17; AltName: Full=Actin-2-sub 2	41.6 kDa	374	2341
65	19	gi|113216	P07836	-3.67	-12.33	2.93	1	1	RecName: Full=Actin, muscle-type A1	41.9 kDa	376	725870
66	38	gi|113803	P04746	-3.45	-10.72	3.13	1	1	RecName: Full=Pancreatic alpha-amylase; Short=PA; AltName: Full=1,4-alpha-D-glucan glucanohydrolase, Flags: Precursor	57.7 kDa	511	905224
67	45	gi|113789	P19961	-3.45	-10.72	3.13	1	1	RecName: Full=Alpha-amylase 2B; AltName: Full=1,4-alpha-D-glucan glucanohydrolase 2B; AltName: Full=Carcinoid alpha-amylase; Flags: Precursor	57.7 kDa	511	964284
68	23	gi|1351933	P04745	-3.45	-10.68	3.13	1	1	RecName: Full=Alpha-amylase 1; AltName: Full=1,4-alpha-D-glucan glucanohydrolase 1; AltName: Full=Salivary alpha-amylase; Flags: Precursor	57.8 kDa	511	751779
69	26	gi|3183326	O14186	-2.89	-7.32	2.25	1	1	RecName: Full=Uncharacterized WD repeat-containing protein C4F8.11	93.2 kDa	846	783922
70	14	ii16622450(	A1ARG8	-2.42	-5.45	3.18	1	1	RecName: Full=GTP-binding protein lepA	67.2 kDa	598	381604
71	68	ii23869214(	B3E9R0	-2.42	-5.41	3.17	1	1	RecName: Full=GTP-binding protein lepA	67.2 kDa	600	3962996
72	9	ii74585209	Q59WK2	-1.17	-4.6	20.79	1	1	RecName: Full=Ubiquitin-related modifier 1 1	11.1 kDa	101	161462
73	57	ii12368750(	Q3IES7	-1.08	-2.43	14.94	1	1	RecName: Full=Methylglyoxal synthase; Short=MGS	17.0 kDa	154	1477526

Protein summary from OSSMA Browser for excised gel spots pooled from three narrow range gels; Thesis Chapter 6

Protein Summary View for OMSSA file: Spot B OMSSA Output.omx

No.	Index	gi#	Accession	Sum log E-Value	protein Scor	%Coverage	#Pep.	#Unique Pep.	Protein Description	MW	Length	Seq ID
1	4	gi|75054626	Q5NVH5	-74.43	-288.31	12.81	9	5	RecName: Full=Serum albumin; Flags: Precursor	69.4 kDa	609	771862
2	15	gi|2492797	Q28522	-39.38	-145.36	4.67	6	2	RecName: Full=Serum albumin; Flags: Precursor	67.9 kDa	600	988964
3	29	gi|190356749	A2V924	-39.38	-145.24	4.61	6	2	RecName: Full=Serum albumin; Flags: Precursor	68.9 kDa	608	3389340
4	21	gi|71152981	P08835	-36.63	-138.33	2.14	5	1	RecName: Full=Serum albumin; Flags: Precursor	69.7 kDa	607	1324074
5	20	gi|136429	P00761	-23.61	-103.18	8.66	2	1	RecName: Full=Trypsin; Flags: Precursor	24.4 kDa	231	1114697
6	13	gi|44889024	P49065	-12.05	-49.51	1.97	1	1	RecName: Full=Serum albumin; Flags: Precursor	68.9 kDa	608	924112
7	32	gi|121039	P01857	-12.11	-47.64	10	2	2	RecName: Full=Ig gamma-1 chain C region	36.1 kDa	330	4034695
8	8	gi|136409	P00762	-10.62	-44.77	8.13	2	1	RecName: Full=Anionic trypsin-1; AltName: Full=Anionic trypsin I; AltName: Full=Pretrypsinogen I; AltName: Full=Serine protease 1; Flags: Precursor	26.0 kDa	246	833996
9	33	gi|215274002	P13612	-11.99	-42.31	1.84	2	1	RecName: Full=Integrin alpha-4; AltName: Full=Integrin alpha-IV; AltName: Full=VLA-4; AltName: Full=CD49 antigen-like family member D; AltName: CD_antigen=CD49d; Flags: Precursor	114.9 kDa	1032	4097733
10	16	gi|1351907	P02769	-10.71	-37.13	5.11	2	2	RecName: Full=Serum albumin; AltName: Full=BSA; AltName: Allergen=Bos d 6; Flags: Precursor	69.3 kDa	607	1004954
11	2	gi|77416709	P0AAP1	-4.25	-15.14	3.5	1	1	RecName: Full=Protein adrA	41.5 kDa	371	731613
12	3	gi|232227	P29627	-2.95	-11.66	20.59	1	1	RecName: Full=Hemoglobin subunit beta-Z; AltName: Full=Hemoglobin beta-Z chain; AltName: Full=Beta-Z-globin	11.2 kDa	102	769641
13	10	gi|81725314	Q87G42	-3.21	-11.18	5.51	1	1	RecName: Full=Purine nucleoside phosphorylase deoD-type 2; Short=PNP 2	25.7 kDa	236	874943
14	1	gi|85681036	Q9KNB2	-3.21	-11.15	5.51	1	1	RecName: Full=Purine nucleoside phosphorylase deoD-type 2; Short=PNP 2	25.6 kDa	236	407441
15	11	gi|85540976	Q7MFG6	-3.21	-11.12	5.51	1	1	RecName: Full=Purine nucleoside phosphorylase deoD-type 2; Short=PNP 2	25.7 kDa	236	909790
16	18	gi|37538291	P24547	-3.09	-9.01	2.72	1	1	RecName: Full=Inosine-5'-monophosphate dehydrogenase 2; Short=IMP dehydrogenase 2; AltName: Full=IMPDH-II; AltName: Full=IMPD 2	55.8 kDa	514	1079826
17	12	gi|1351908	P49064	-2.76	-6.76	2.47	1	1	RecName: Full=Serum albumin; AltName: Allergen=Fel d 2; Flags: Precursor	68.7 kDa	608	917585
18	19	gi|75162308	Q8WQM6	-2.3	-6.23	4.71	1	1	RecName: Full=Ubiquitin-like domain-containing CTD phosphatase	39.0 kDa	340	1102416
19	17	gi|115311702	Q923B1	-1.83	-3.16	3.64	1	1	RecName: Full=Lariat debranching enzyme	62.3 kDa	550	1053868
20	27	gi|122138783	Q32LI2	-1.34	-2.91	6.2	1	1	RecName: Full=Probable inactive trypsin-X3; Flags: Precursor	27.4 kDa	242	2488946
21	5	gi|75055290	Q5RFN6	-1.49	-2.73	6.47	1	1	RecName: Full=Calponin-2; AltName: Full=Calponin H2, smooth muscle; AltName: Full=Neutral calponin	33.7 kDa	309	790280
22	23	gi|93204556	Q3SYU6	-1.49	-2.73	6.47	1	1	RecName: Full=Calponin-2; AltName: Full=Calponin H2, smooth muscle; AltName: Full=Neutral calponin	33.4 kDa	309	2028110
23	6	gi|584955	Q08094	-1.49	-2.73	6.76	1	1	RecName: Full=Calponin-2; AltName: Full=Calponin H2, smooth muscle; AltName: Full=Neutral calponin	32.0 kDa	296	798886
24	24	gi|122135340	Q29S21	-1.74	-2.53	2.58	1	1	RecName: Full=Keratin, type II cytoskeletal 7; AltName: Full=Cytokeratin-7; Short=CK-7; Short=Keratin 7; Short=K7	51.6 kDa	466	2049513
25	34	gi|215275331	A5A6M6	-1.74	-2.4	1.88	1	1	RecName: Full=Keratin, type II cytoskeletal 1; AltName: Full=Cytokeratin-1; Short=CK-1; AltName: Full=Keratin-1; Short=K1	65.5 kDa	637	4654833
26	30	gi|122132186	Q08D91	-1.74	-2.4	2.21	1	1	RecName: Full=Keratin, type II cytoskeletal 75; AltName: Full=Cytokeratin-75; Short=CK-75; AltName: Full=Keratin-75; Short=K75; AltName: Full=Type II keratin-6hf; AltName: Full=Keratin-6 hair follicle	59.0 kDa	543	3701717
27	31	gi|238054406	P04264	-1.74	-2.37	1.86	1	1	RecName: Full=Keratin, type II cytoskeletal 1; AltName: Full=Cytokeratin-1; Short=CK-1; AltName: Full=Keratin-1; Short=K1; AltName: Full=67 kDa cytokeratin; AltName: Full=Hair alpha protein	66.0 kDa	644	3991702
28	7	gi|60416436	P50446	-1.74	-2.37	2.17	1	1	RecName: Full=Keratin, type II cytoskeletal 6A; AltName: Full=Cytokeratin-6A; Short=CK-6A; AltName: Full=K6a keratin; AltName: Full=Keratin-6 alpha; Short=mK6-alpha	59.3 kDa	553	801795
29	22	gi|123781839	Q4FZU2	-1.74	-2.37	2.17	1	1	RecName: Full=Keratin, type II cytoskeletal 6A; AltName: Full=Cytokeratin-6A; Short=CK-6A; AltName: Full=K6a keratin	59.2 kDa	552	1954546
30	25	gi|81170668	Q922U2	-1.74	-2.35	2.07	1	1	RecName: Full=Keratin, type II cytoskeletal 5; AltName: Full=Cytokeratin-5; Short=CK-5; AltName: Full=Keratin-5; Short=K5	61.8 kDa	580	2380372
31	28	gi|81896062	Q8BGZ7	-1.74	-2.33	2.18	1	1	RecName: Full=Keratin, type II cytoskeletal 75; AltName: Full=Cytokeratin-75; Short=CK-75; AltName: Full=Keratin-75; Short=K75; AltName: Full=Type II keratin-18; AltName: Full=Type II keratin-K6hf; AltName: Full=Keratin-6 hair follicle; Short=mK6hf	59.7 kDa	551	2639418
32	26	gi|81170669	Q6P6Q2	-1.74	-2.32	2.08	1	1	RecName: Full=Keratin, type II cytoskeletal 5; AltName: Full=Cytokeratin-5; Short=CK-5; AltName: Full=Keratin-5; Short=K5	61.8 kDa	576	2402900
33	14	gi|59796479	Q9Z331	-1.74	-2.32	2.14	1	1	RecName: Full=Keratin, type II cytoskeletal 6B; AltName: Full=Cytokeratin-6B; Short=CK 6B; AltName: Full=K6b keratin; AltName: Full=Keratin-6 beta; Short=mK6-beta	60.3 kDa	562	934090
34	9	gi|193806361	P01860	-1.15	-0.82	3.71	1	1	RecName: Full=Ig gamma-3 chain C region; AltName: Full=Heavy chain disease protein; AltName: Full=HDC	41.3 kDa	377	871346